LBL-8739 c. 2

THE ULTRAVIOLET SPECTROSCOPY OF NITROUS OXIDE (N_2O): A TEMPERATURE-RESOLVED STUDY

RECEIVED
LAWRENCE
BERKELEY LABORATORY

JUL 9 1979

LIBRARY AND
DOCUMENTS SECTION

Gary Stewart Selwyn
(Ph. D. thesis)

March 1979

Prepared for the U. S. Department of Energy
under Contract W-7405-ENG-48

TWO-WEEK LOAN COPY

This is a Library Circulating Copy
which may be borrowed for two weeks.
For a personal retention copy, call
Tech. Info. Division, Ext. 6782

LAWRENCE BERKELEY LABORATORY
UNIVERSITY OF CALIFORNIA
BERKELEY

LBL-8739 c. 2

DISCLAIMER

This document was prepared as an account of work sponsored by the United States Government. While this document is believed to contain correct information, neither the United States Government nor any agency thereof, nor the Regents of the University of California, nor any of their employees, makes any warranty, express or implied, or assumes any legal responsibility for the accuracy, completeness, or usefulness of any information, apparatus, product, or process disclosed, or represents that its use would not infringe privately owned rights. Reference herein to any specific commercial product, process, or service by its trade name, trademark, manufacturer, or otherwise, does not necessarily constitute or imply its endorsement, recommendation, or favoring by the United States Government or any agency thereof, or the Regents of the University of California. The views and opinions of authors expressed herein do not necessarily state or reflect those of the United States Government or any agency thereof or the Regents of the University of California.

THE ULTRAVIOLET SPECTROSCOPY OF NITROUS OXIDE (N_2O): A TEMPERATURE-RESOLVED STUDY

by

Gary Stewart Selwyn

Materials and Molecular Research Division,
Lawrence Berkeley Laboratory
and Department of Chemistry, University of California
Berkeley, California 94720

Contents

Abstract vii

I. Introduction 1

A. History of Spectroscopic Studies of Nitrous Oxide in the Near and Middle Ultraviolet 1

B. Photochemical Process of Nitrous Oxide 5

C. Atmosphere Nitrous Oxide 6

II. Long Wavelength Absorption of Nitrous Oxide 8

A. Introduction 8

1. The Bates and Hays Model 8

2. Experimental Indications 8

B. Experimental 11

1. The Cary 118C Spectrometer 11

2. Optics and the Quartz Cell 11

3. Procedures 13

4. Data Collection 15

C. Results 17

1. Absorption Cross Sections, 240-320 nm 17

2. Atmospheric Implications 20

III. Temperature Effect on the U.V. Absorption of N_2O 27

A. Introduction 27

B. Cell Construction and Temperature Control 29

1. Quartz Cell Construction 29

2. Long Pass Stainless Steel Cell Construction 29

C. Experimental Procedures 34

1. Data Collection 34

2. Nitrogen Purging 36

D. Results 38

1. Reliability of Data 38

2. Continuous Absorption 40

3. Structured Spectrum 42

IV. Temperature Effect of Nitrous Oxide Vibronic Structuring at 6.8 eV 46

A. Introduction 46

1. Previous Studies 46

2. Definition of the Vibrational State Spectrum . . . 46

3. Statistical Populations of Normal Vibrational Modes 49

B. Theoretical Aspects of Electronic Spectra of Polyatomic Molecules 53

1. Vibrational State Spectra 53

2. Allowed Electronic Transitions 55

3. "Forbidden" Electronic Transitions 57

4. Rotational Structuring of Electronic Transitions . 60

5. Change of Symmetry during Transition 65

6. Intensities of Continuous Absorptions 68

7. Intersection of Potential Curves 69

C. Experimental 70

1. Instrumental Procedures 70

2. Quartz Cell Design 71

3. Temperature, Pressure and Wavelength Measurement. . 73

4. Three Meter Vacuum Spectrograph 75

D. Data Processing and Graphics 76

1. Data Processing Techniques 76

2. Graphics 76

3. Scale of Figures 77

E. Results 79

1. Temperature Effect on the Structured and Continuous Absorption 79

2. Three Meter Spectrograph 79

F. Discussion 82

1. Contribution of Cold and Hot Bands of $X^1\Sigma^+$ 82

2. Second Order Approximation to the Hot Bands 89

3. Energy Levels of the Upper Electronic State 98

4. Vibrational Selection Pattern 119

G. Photodynamics 125

1. Continuous Absorption 125

2. Structured Absorption 127

3. Vibronic Enhancement of Transition 132

H. Conclusions 134

1. Experimentally Deduced Conclusions 134

2. A Proposed Mechanism of Predissociation 136

Acknowledgments 137

Appendices 139

A. ^{15}N Isotopic Substitution Results 139

1. Temperature Effect - Raw Data 139

2. Deconvolution and Isotope Shift 144

B. An Anomalous Result 156

C. Computer Programs 161

1. Deconvolution and Comparison of Observed and Predicted Spectrum 161

2. Computation of Difference Spectra and Energy Levels in the Upper Electronic State 169

D. Listing of Data 180

1. Cross Sections from 190-172 nm for Eleven Temperatures 180

2. Cross Sections of First Order and Second Order Deconvolutions, 190-172 nm 199

References 218

THE ULTRAVIOLET SPECTROSCOPY OF NITROUS OXIDE (N_2O): A TEMPERATURE-RESOLVED STUDY

Gary Stewart Selwyn

Materials and Molecular Research Division,
Lawrence Berkeley Laboratory
and Department of Chemistry, University of California
Berkeley, California 94720

ABSTRACT

The absorption spectra of nitrous oxide and its ^{15}N isotopes have been studied from 172 to 330 nm. The long wavelength absorption above 265 nm is shown to be almost entirely due to Rayleigh scattering, contrary to previous accounts. This correspondingly reduces the calculated rate of nitrous oxide photolysis in the troposphere to a very small value. The temperature dependence of the absorption from 173 to 240 nm has been measured for use in atmospheric modeling of the photolysis of nitrous oxide. At shorter wavelengths, previous investigators have noted the presence of very weak, diffuse banding of nitrous oxide superimposed on its continuous absorption. Spectra obtained in this study over the wavelength range 172 to 190 nm demonstrate that these diffuse bands are in fact a separate pronounced absorption of nitrous oxide which is strongly affected by temperature. This banding is the result of transitions to discrete vibronic levels in an upper electronic state. No rotational structure can be observed. From the temperature dependence of the observed structure it is shown that the transition results through vibronic coupling of the ν_2 bending mode. The energy spacing of the upper state is measured to be ~ 480 cm^{-1} and this with the available knowledge of the vibrational frequencies of the ground state, permits a partial assignment of the

spectrum. Using the large temperature effect observed, the spectra are deconvoluted into the individual absorption spectra of the (000) and (010) vibrational modes of the ground electronic state. This deconvolution reveals a (000) state absorption spectrum which is weakly structured on top of a continuum and a (010) state absorption spectrum which is strongly structured on top of an enhanced continuum. Using this deconvolution it is then shown that the pronounced structure at higher temperatures is primarily due to the presence of vibrationally "hot" molecules. Substitution of isotopically labeled nitrous oxide indicates a unique isotope shift for these vibronic features which increases in the order: NNO - $N^{15}NO$ - ^{15}NNO - $^{15}N^{15}NO$. The extent of the observed isotope shift is greatest at short wavelengths and has been observed to be as large as 130 cm^{-1}. Using the results of published theoretical studies of N_2O, it is deduced that the structure results from the transition $^1\Sigma^- \leftarrow X^1\Sigma^+$ while the continuous absorption results from the transition $^1\Delta \leftarrow {}^1X\Sigma^+$. Both of these are normally forbidden transitions but are allowed by bending. It is further proposed that in the bent equilibrium geometry, an avoided crossing results from the perturbation of the $^1A''$ components of $^1\Sigma^-$ and $^1\Delta$ in C_s symmetry. Evidence for this bent configuration of $^1\Sigma^-$ is offered and a mechanism of predissociation is proposed. Finally an anomalous result is briefly discussed. In one sample of isotopic nitrous oxide an extremely strong, sharp absorption (FWHM = 0.2Å) is observed which is presumably due to an impurity. By IR, UV and mass spectrometry it was not possible to assign this absorption to any likely molecular or atomic species.

I. INTRODUCTION

This work covers two aspects of study on nitrous oxide: its role in atmospheric photochemistry and the basic ultraviolet spectroscopy of nitrous oxide which partially determines this photochemistry. This work began as a short study to evaluate the rate of tropospheric photolysis of nitrous oxide, but in the initial stages of this study inconsistencies in the near ultraviolet absorption spectrum of nitrous oxide became apparent. In the course of checking these inconsistencies other inconsistencies were noted between the literature and the new experimental evidence presented in this study. Eventually, a different absorption spectrum resulted along with a different theoretical interpretation of the ultraviolet absorption processes of nitrous oxide. The explanation of this absorption process offered here is consistent with all experimental evidence on nitrous oxide to date.

This section, I, covers the background of the two areas of study covered in this work. Sections II and III deal with the atmospheric photolysis of nitrous oxide and Section IV covers the basic spectroscopy of nitrous oxide.

A. History of Spectroscopic Studies of Nitrous Oxide in the Near and Middle Ultraviolet

Leifson[1] in 1926, was the first to study the ultraviolet absorption of nitrous oxide and reported a continuous absorption, from 200 to 168 nm, and a stronger continuum from 155 nm to shorter wavelengths. Dutta[2] in 1932, showed that the first absorption of nitrous oxide actually extended weakly to 275 nm and was unable to trace any banded absorption between 210 and 275 nm. In a broad range study of the nitrous oxide absorption spectrum from 220 to 85 nm, Duncan[4] discovered

discrete structure near 155 nm with a vibrational spacing of 621 cm^{-1} but found only continuous absorption elsewhere.

NO was detected as a product of UV photolysis by Wulf and Melvin[3] and Sen-Gupta[5]. Henry[6] noted these findings and tried to associate them to dissociation products of N_2O.

In an effort to find the long wavelength limit of the dissociation of nitrous oxide, Sponer and Bonner[7] in 1940 used a steel pipe 105 feet long as an absorption cell and filled it with nitrous oxide at pressures up to five atmospheres. At this pressure, the absorption extended weakly up to limit of observation, 306 nm, with two extremely weak continua noted above 275 nm.

In that same year, a study by Nicolle and Vodar[8] reported on the difference in the absorption spectrum at 293 K and 183 K and found that at the lower temperature the absorption is uniformly decreased over the wavelength range studied, 215 to 235 nm.

Romand and Mayence[9] in 1949, also noted banding in the second absorption at 145 nm, and reported a purely continuous absorption in the region about 184 nm. A more detailed study, using photomultipliers and with higher resolution, by Zelikoff, Watanabe and Inn[10] in 1953, studied the absorption of N_2O from 210 nm to the LiF cutoff at 108 nm. Above 138 nm they found strong vibrational structure in the second absorption centered about 145 nm, as did Romand and Mayence, but unlike the previous studies, they noted very weak, diffuse bulges on the continuum centered at 180 nm. Because of the weak nature of these bulges, they could not be measured accurately or further analyzed. These bulges are a major concern of this work and are discussed in

Section IV. Extending to longer wavelengths than the Zelikoff, Watanabe and Inn study, the results of Thompson, Hartreck and Reeves[11] (1963) agreed quantitatively with Zelikoff and workers but found only a continuous absorption with no superimposed features between 150 and 239 nm.

In a study primarily concerning the atmospheric role of nitrous oxide, Bates and Hays[12] (1967) presented the N_2O absorption spectrum from 170 to 320 nm based upon unpublished sources. Their spectrum shows a second absorption above 260 nm. More will be said about this in Section II.

Studying the temperature dependence of the near UV absorption of nitrous oxide between 293 and 953 K, Holliday and Reuben[13] reported in 1968 a very large temperature effect, primarily affecting the longer wavelengths although increasing temperature strengthened the absorption over the entire continuum above 200 nm. More will be said of this temperature dependence in Sections III and IV.

A comprehensive review article on the electronic spectroscopy of nitrous oxide and other molecules isoelectronic with it by Rabalais and coworkers[14] presented new spectra of N_2O from 110 to 215 nm. Their spectrum of the first absorption of N_2O showed only a purely continuous absorption although they refer to the weak absorption bulges of Zelikoff et al. They also presented a review of the theoretical basis of this absorption of nitrous oxide and its related isoelectronic molecules.

Most recently, Monahan and Walker[15] in 1975 compared the absorption of gaseous N_2O at 298 K with the absorption of a thin solid film of N_2O at 53 K. In the gas phase at 180 nm they also observed the very

weak, diffuse bands superimposed on the continuous absorption, but like the Zelikoff study, were unable to analyze them or observe any detailed structuring.

B. Photochemical Processes of Nitrous Oxide

The following products of photolysis of N_2O are energetically possible in the near ultraviolet:

(1) $N_2O + h\nu \rightarrow N_2 + O\ (^1D)$ $\lambda < 340.6$ nm

(2) $\rightarrow N_2 + O\ (^1S)$ $\lambda < 211.6$ nm

(3) $\rightarrow NO + N\ (^2D)$ $\lambda < 169.5$ nm

along with the spin-forbidden product of photolysis:

(4) $N_2O + h\nu \rightarrow N_2 + O\ (^3P)$ $\lambda < 742.4$

(5) $\rightarrow NO + N\ (^4S)$ $\lambda < 251.5$

Originally, the NO produced in the early photochemical decomposition studies of N_2O in the near UV was thought to result from the direct photolysis into NO + N. Studies by Doering and Mahan[16] indicated that channel (5) occurred in about 20% of the products, however more definitive studies have since indicated that production of O (^1D) through (1) is the primary one reached.[17-21]

NO is produced indirectly through the reaction sequence for the photolysis of pure nitrous oxide:

(1) $N_2O + h\nu \rightarrow N_2 + O\ (^1D)$

(7) $N_2O + O\ (^1D) \rightarrow N_2 + O_2$

(8) $\rightarrow 2\ NO$

Davidson[22] has found that the rate constants for (7) and (8) can be fit by the equation:

(9) $$\frac{k_7}{k_8} = (0.72 \pm 0.11) + \frac{21.6 \pm 7.0}{T}$$

$$170 < T < 434\ K$$

with other products constituting less than 4 per cent of the total yield.

C. Atmospheric Nitrous Oxide

Since nitrous oxide was discovered as a trace gas in the atmosphere by Adel[23] in 1938, its atmospheric concentration has been measured by ground based means[23-29], and with air-borne methods to measure the variation in concentration with altitude[30-35,41]. Current estimates indicate a concentration of about 0.32 ppmv in the troposphere[38-40].

Atmospheric nitrous oxide is produced by bacterial action on nitrogenous compounds during the nitrogen cycle[36-37], although a small contribution from combustion[42,43] has also been proposed. The role of the ocean as a source or sink for nitrous oxide has also been debated[49-52], and fresh water bodies have also been proposed as a source of N_2O[44-48].

While unreactive with atmospheric molecules in the lower atmosphere, in the stratosphere nitrous oxide is destroyed by photolysis, (1) or may react with O (^1D) through (7) and (8). The NO produced by (8) then influences stratospheric ozone[53-55] by the NO_x catalytic oxidation cycle:

$$
\begin{array}{lll}
 & NO + O_3 \rightarrow NO_2 + O_2 & \\
(9) & \underline{NO_2 + O \rightarrow NO + O_2} & \\
\text{net:} & O + O_3 \rightarrow 2\,O_2 &
\end{array}
$$

Recognizing that increased man-made fertilizer production may ultimately increase stratospheric nitrous oxide, Crutzen in 1974 estimated

a four percent decrease in stratospheric ozone resulting from a twenty percent increase in atmospheric N_2O concentration.[56]

Estimates by other workers have since proposed both larger and smaller effects on stratospheric ozone.[48,51,52,57-61] Complicating the situation further is evidence that bacterial action may also provide an additional significant sink for N_2O[62] and the possibility has also been raised that non-homogeneous chemistry may be important.[63]

Free radicals other than NO_x vitally affect stratospheric ozone, such as ClO_x and HO_x.[64,65] The degree and nature of the interactions between the NO_x, HO_x and ClO_x families of reactions are currently under investigation and thus it is difficult at this time to predict the effect of increasing N_2O on stratospheric ozone.

II. Long Wavelength Absorption of Nitrous Oxide[67]

A. Introduction

1. The Bates and Hays Model

In an early review of atmospheric nitrous oxide, Bates and Hays[12] presented the photodissociation cross sections of nitrous oxide from 170 to 320 nm. They reported a moderately strong absorption with a maximum at about 180 nm, and a weak absorption at longer wavelengths with maxima at 280 and 295 nm. This weak absorption extended slightly beyond 320 nm, which is above the ozone cut-off of sunlight, and so this portion of the spectrum leads to a slow but significant rate of photolysis of nitrous oxide in the troposphere. On the basis of the observed mixing ratio of troposphere N_2O, the indicated absorption cross sections for dissociation, and an estimated constant vertical exchange coefficient (K_z) of 10^5 cm^{-1} sec^{-1} in the stratosphere. Bates and Hays[12] calculated the flux of nitrous oxide necessary to maintain the troposphere concentration and corresponding 70 year average atmospheric residence time. The error in this type of calculation is large, but should provide an approximate result ($\sim \pm 50\%$).

2. Experimental Indications

At the time of this experiment (1975), there were two arguments that pointed to the belief that the atmosphere residence time was much less than 70 years: (1) Schutz et al.[66] studied the seasonal, geographical and vertical variations in atmospheric nitrous oxide over a two year period and concluded on the basis of their experimental measurements that nitrous oxide is destroyed much faster than by the rate of photolysis as given by Bates and Hays[12]; (2) Junge and Hahn[68]

and Hahn[49] estimated the source of nitrous oxide from bacterial reduction of nitrates and nitrites in the ocean and from soils; although there is a substantial uncertainty in extrapolating those observations to the entire globe, the results strongly implied a source strength such that the atmospheric residence time is about 12 years. Comparing this short residence with the calculated lifetime of 70 years based on the Bates and Hayes model of photolysis in the atmosphere, Junge and coworkers thus argued that there was a large unknown process that removes or destroys N_2O in the troposphere. By stretching every uncertainty to its utmost limit in the direction of minimizing the source's strength of nitrous oxide (i.e. increasing its residence time), it could be argued that such maximum "experimental" lifetimes might be balanced by the photolysis of nitrous oxide using the Bates and Hays cross sections in their model.

The purpose of this experiment was to study the near ultraviolet absorption of nitrous oxide at wavelengths above 260 nm in more depth, so that atmospheric models may more accurately assess the photolysis rate of atmospheric nitrous oxide. The results of this study indicate that this weak absorption does not exist, and so in its absence the rate of photolysis of tropospheric nitrous oxide is negligibly small and thus its atmospheric lifetime based upon photolysis and chemical reaction must be increased more than the 70 years postulated by Bates and Hays.

As stated in Section I, evidence compiled after the completion of this experimental section indicates that other processes, possibly

bacteriological in nature, may play an important role in the destruction rates of atmospheric nitrous oxide. This does not preclude the findings offered here of a large discrepancy between the chemical and photochemical rates of nitrous oxide destruction and the necessary rate to maintain steady state concentration, but instead these non-homogeneous mechanisms may help explain the difference.

B. Experimental

1. The Cary 118C Spectrometer

The Cary 118C spectrometer is manufactured by Varian Associates and the model purchased is equipped with a photomultiplier suitable for use down to 165 nm. It has a double prism monochromator which provides greatest resolution at short wavelengths. A deuterium discharge lamp provides a continuous light supply free from strong emission lines from 480 to 160 nm. A tungsten lamp is also provided for wavelengths greater than 350 nm. The instrument may be operated in the single or double beam mode and provisions are made for purging all light paths. Since the light is dispersed by the monochromator before passage through the sample compartment, photolysis due to the beam is not usually a problem.

2. Optics and the Quartz Cell

The spectra taken in this section used an existing optical system and quartz cell built by my predecessors. The optical system, shown in figure 1, consisted of a plane mirror located within the Cary sample compartment which reflected the beam out through a tube into a double sided trapezoidal mirror housing. In the housing the beam was collected by a three inch concave mirror opposite the Cary and after reflection by a second plane mirror, was sent down the long cell passing through the two suprasil windows of the quartz cell. Beyond the cell, on an optical rail a large concave mirror collected the beam and reflected it back for a nearly identical return trip. Focal lengths of the concave mirrors and their placement were chosen so that the beam was focused at the end mirror.

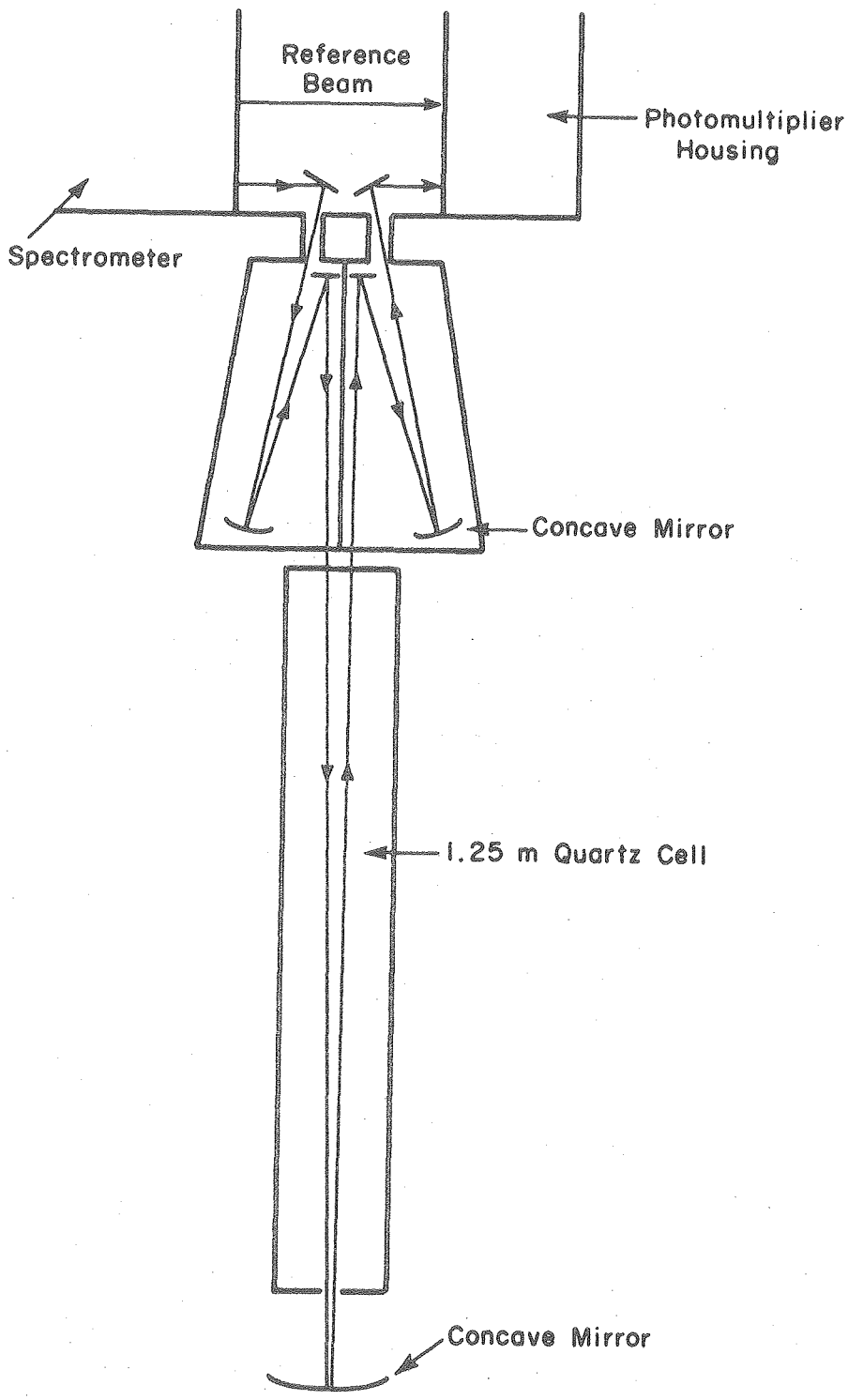

XBL 792-8345

Figure 1

Only a very small percentage of the transmitted light was lost due to overfilling of mirrors or windows; typically the optical arrangement passed 15% of the light at 300 nm with the loss primarily due to inefficiency of the mirrors at each of the seven reflections. To minimize photometric errors arising from a "short-trip" of scattered light in the entrance section being picked up by the mirrors in the exit section, the mirror housing was painted black and the two sections were divided with a partition. This was checked by blocking the beam at any point past the housing; the transmitted light indicated was less than 0.02%.

The cell was constructed entirely of fused silica and had two fused suprasil windows (1/4'' thick). With the double pass optics, a path length of 252 cm resulted. For all experiments it was necessary to blacken the length of the cell and darken the room to avoid light leakage into the spectrometer.

Initial experiments indicated that with the evacuated cell, the beam would be totally absorbed at wavelengths less than 260 nm. Upon tracing the beam path, I soon discovered that one front surface plane mirror had been mounted backwards by my predecessors so that the beam would pass through the pyrex backing before reflecting off the mirror thus resulting in total absorption at the shorter wavelengths. The problem was easily remedied and with proper alignment it was possible to work down to 205 nm with 1% of the transmitted light.

3. Procedures

In all experiments of this section, the spectrometer was used in the double beam mode with the reference path containing an unmodified 15 cm of air in the sample compartment. Due to distortions in

the cell when it was evacuated, there was a small systematic decrease in absorption when the evacuated cell was filled with helium or nitrogen. For this reason, the cell was filled with helium or nitrogen as a reference for N_2O, rather than the evacuated cell. This equal pressure background spectrum was repeated before and after each experiment and was subtracted from the observed spectra obtained with nitrous oxide. Reversing the procedure and measuring the nitrous oxide first and last and the reference spectrum second was occasionally tested and yielded identical results.

Since the object of this study was to measure extremely small absorptions, instrumental drift was an important factor. For this reason, three or four runs over the wavelength interval were repeated for both the reference and sample spectra to test for reproducibility. If a small variation was noted, more runs were repeated until reliability was insured. Occasionally a larger drift was found, and the entire measurement was discarded. The procedure reference-nitrous oxide-reference also served to check on instrumental drift.

Noise was another limiting problem. The most that could be done to improve signal/noise was using larger time constants and slower scan speeds. Most experimentation was done at night when the house current was cleaner. Especially bad results were had at 1-2 PM, 5 PM and 11 PM, the latter probably caused by switching of the compressors at Gaique Laboratory. During this time the Cary also suffered from an intermittent noise problem which was later traced to a faulty carbon resistor in the photomultiplier socket. A 15 amp Sorenson voltage regulator was used to drive the Cary when it was found that the house

current varied over the range 112 to 122 volts, a larger variation than was recommended for the Cary by the manufacturer.

4. Data Collection

Data for this section were collected on chart paper. At maximum sensitivity, the Cary gives a full scale chart reading for absorbance ($\log_{10} I_0/I$) of 0.02. Under the experimental conditions, the vibration and irreproducibility of the baseline was about 3 percent of full scale at this setting, limiting the sensitivity to about 2×10^{-25} cm^2 for N_2O cross sections. Reproducibility from one day to the next was substantially less than this, indicating "low frequency" errors associated with the total method. At the longer wavelengths, the results sometimes indicated a negative absorption relative to the reference. These were calculated as negative cross sections and plotted with the other data to show the scatter of experimental data.

The nitrous oxide used was purified by vacuum distillation for some runs. In an effort to identify the impurity responsible for the long wavelength peak reported by Bates and Hays, we also used unpurified N_2O from the commercial cylinder (Matheson). No difference could be detected in the spectra between the purified and unpurified gas, and then most measurements (especially the long wavelength ones) were carried out with unpurified tank nitrous oxide. Most experiments were done at one atmosphere pressure and so the cell and vacuum lines were filled slightly over atmospheric pressure, then the line and cell were vented to the air and the atmospheric pressure was read off a mercury barometer in the next room. For measurements at less

than 1 atmosphere, a Wallace and Tierman dial pressure gauge was used to measure pressure, which was later calibrated against a Baracel electronic manometer. The resolution was about 1 nm and a scan speed of 0.2 and 0.05 nm sec^{-1} was used with 1 or 5 second time constant.

C. Results

1. Absorption Cross Sections, 240-330 nm

The apparent, observed N_2O cross sections ($\log_e I_o/I = \sigma NL$, cm^2 $molecule^{-1}$ were N is the number density and L is the path length in cm) are given in figure 2 for the wavelength range 245 to 328 nm at temperature 294 ± 2K. The solid curve represents the N_2O cross sections read from the first figure in the article by Bates and Hays. It can be seen that the wavelength cross sections reported by Bates and Hays are much higher than the results obtained here and are 10 times greater than the range of experimenal error of these measurements. The dashed line of figure 2 is an estimate of the Rayleigh scattering cross section for nitrous oxide; the observed values for air (Leighton,[69] Forsythe[70]) were scaled by the index of refraction function $(\eta-1)^2$ for air and N_2O. The results scatter more or less equally about the Rayleigh scattering line above 270 nm, and thus they indicate no significant absorption by nitrous oxide at room temperature in the troposphere.

Bates and Hays gave two references to the entire absorption spectrum reported, 170 to 320 nm. The references are not broken down with respect to wavelength and it is not stated whether these references were reviews of the literature or new data. One reference is to an unpublished British doctoral thesis and the other to a private communication. Because of this, the experimental basis for the long wavelength absorption is not clear. I have written to Bates and the stated addresses of the references and no further details could be obtained.

Using a 33 m stainless steel cell filled with 5 atmospheres of nitrous oxide, Sponer and Bonner[7] did report a long wavelength absorp-

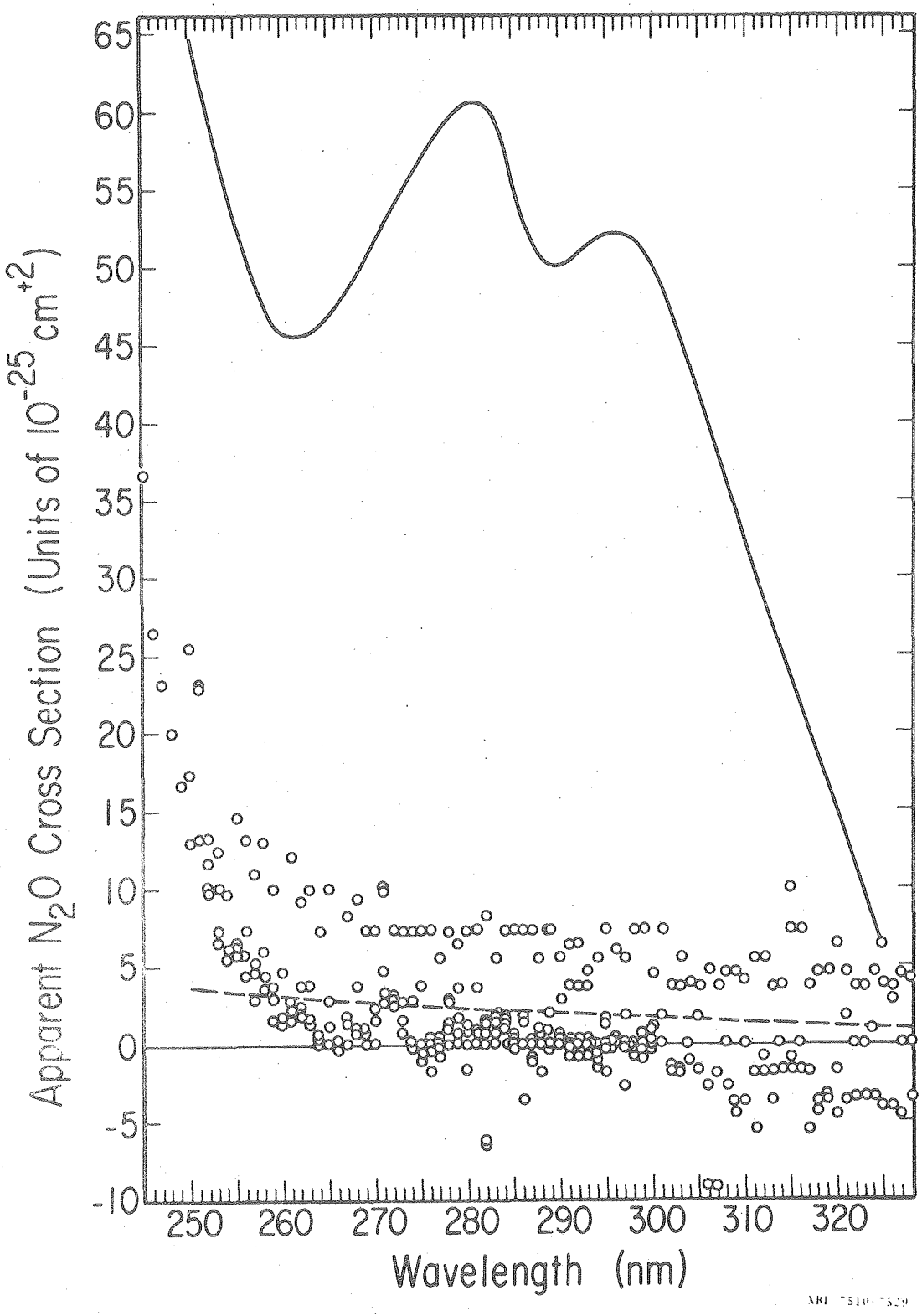
Apparent N_2O Cross Section (Units of 10^{-25} cm^{+2})
65
60
55
50
45
40
35
30
25
20
15
10
5
0
-5
-10
250
260
270
280
290
300
310
320
Wavelength (nm)

Figure 2

Table 1. Long Wavelength Absorption of N_2O

Wavelength, nm	Cross Section x 10^{24} cm^{-2}
330	0.1 ± .3
320	0.2 ± .3
310	0.2 ± .3
300	0.3 ± .3
290	0.4 ± .3
280	0.4 ± .3
270	0.5 ± .3
265	0.6 ± .3
260	0.7 ± .3
255	1.0 ± .3
250	1.9 ± .4
245	3.7 ± .4
240	9.6 ± .4

tion extending to 306 nm, but they used unpurified gas and stated that impurities could be the source of this absorption. Their findings, reproduced in figure 3, shows a microphotometer tracing of the absorption. The long wavelength absorbance of 5 atmospheres of N_2O, trace C, is clearly observed, but at 1.5 atmospheres, trace B, a proportional absorbance is not apparent relative to the vacuum trace A. The long wavelength absorption may also be due to the absorption of a dimer of nitrous oxide. This would exhibit a P^2 pressure dependence, possibly explaining the observation above. The nitrous oxide dimer produced in supersonic expansion has been observed,[71] but its ultraviolet spectrum has not been studied.

Interestingly enough, for CO_2 a similar weak absorption at wavelengths longer than its first absorption feature at 147 nm, was noted[72] only later to be proven incorrect.[73] At longer wavelengths the absorption approaches Rayleigh scattering, as was determined using a 250 m path length at one atmosphere pressure.[73]

With purified nitrous oxide and pressures less than one atmosphere, the cross sections of N_2O are in reasonably good agreement with those reported by Bates and Hays below 230 nm as shown in figure 4. These results show that there is no major discrepancy with respect to the absorption of nitrous oxide between 235-210 nm.

2. Atmospheric Implications

To estimate the atmospheric photochemical implications of these new cross sections of the near ultraviolet absorption of nitrous oxide, the program JVALVES was used. The program, developed by Whitten and Johnston, calculates the photolytic rate constant, j, using the same

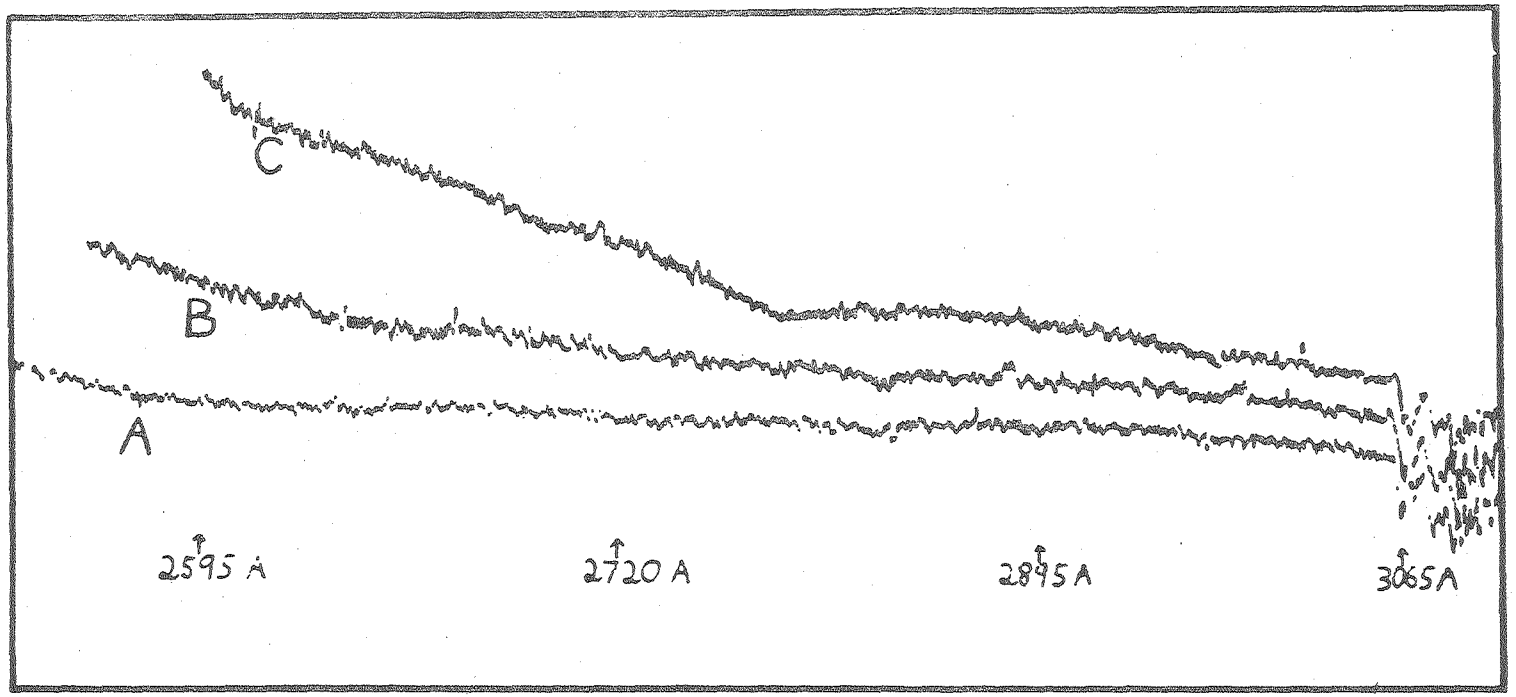

XBL 7510-7530

Figure 3

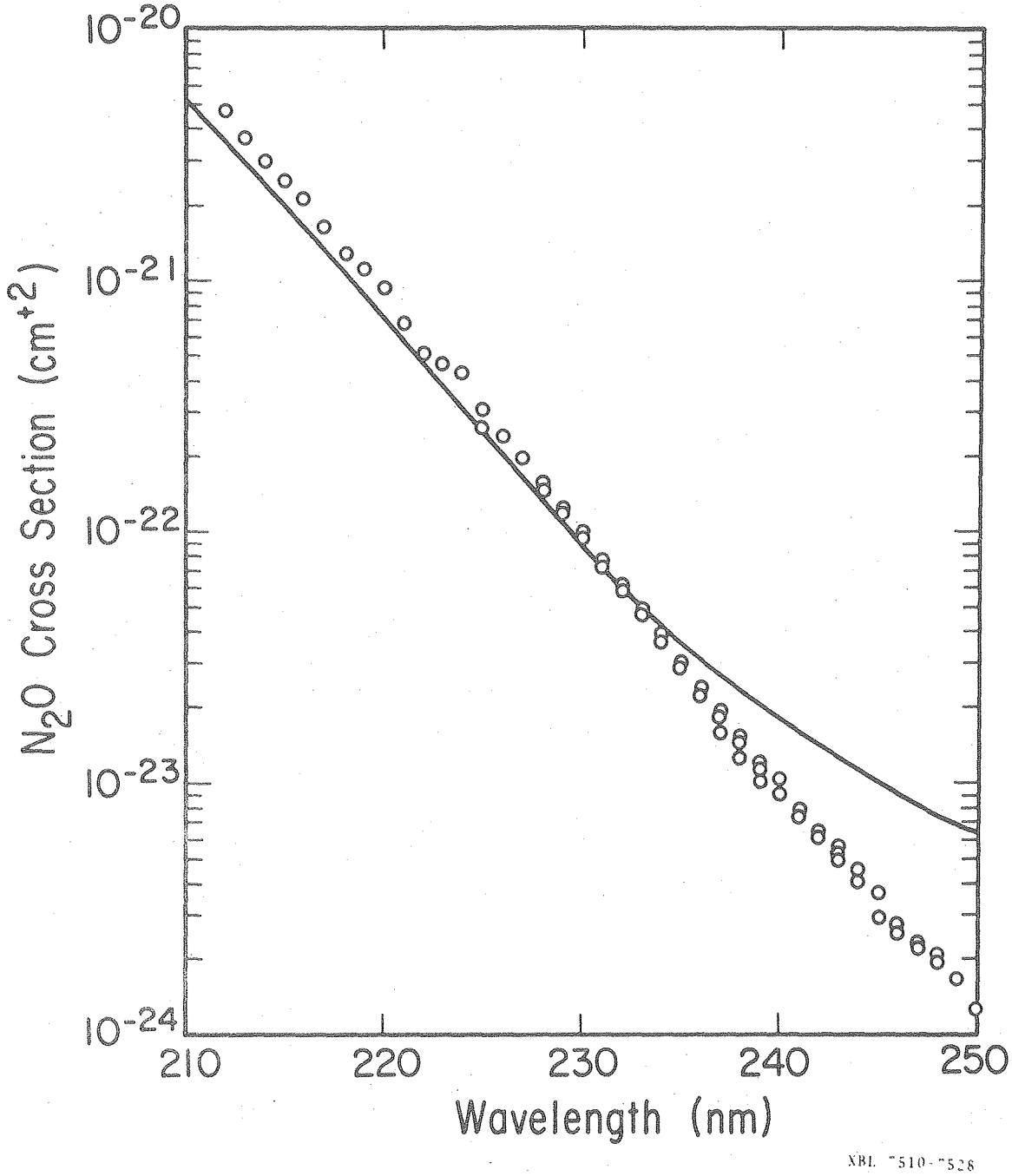
10^{-20}
10^{-21}
10^{-22}
10^{-23}
10^{-24}
N_2O Cross Section (cm^{+2})
210
220
230
240
250
Wavelength (nm)
XBL 7510-7528

Figure 4

relationship[74]

$$j = \sum_i \sigma_i(\lambda_i) I(y,z,\lambda_i) \Phi(\nu_i)$$

where the cross section σ is wavelength dependent. The attenuated light intensity, I, is input as a function of wavelength and solar zenith angle at the top of the stratosphere and is calculated below on the basis of the column density of absorbing molecules. The quantum yield of dissociation, Φ, has been taken as 1.0 over all wavelengths. J is then calculated at each altitude up to 50 km in 1 km intervals and is a function of latitude in intervals of 10 degrees.

The rate constant of photolysis will also vary with season, but it is possible to make a temporal and latitudinal average. This average result for the altitude dependent j is shown as the solid line in figure 5. The dashed line in this figure is the temporal and latitudinal average value for j given by Bates and Hays.[12] Comparable values of j are obtained above 20 km since the bulk of photolysis at these altitudes is due to the larger absorbance between 200 and 235 nm, where our cross sections values agree with Bates and Hays. In the troposphere, a difference in the two models is clearly apparent. The Bates and Hays model predicts a small but finite j of 10^{-9} sec^{-1} whereas in the absence of the long wavelength absorbance, our model indicates a negligible rate of photolysis.

Multiplying the j value by the altitude dependent concentration of nitrous oxide (Ehhalt _et al_[31]) gives the instantaneous rate of photolysis, using the 12 hour average sun,

$$\frac{-d(N_2O)}{dt} = j(N_2O) = \text{rate of destruction} = R.$$

Although the rate constant j is quite large at high altitudes,

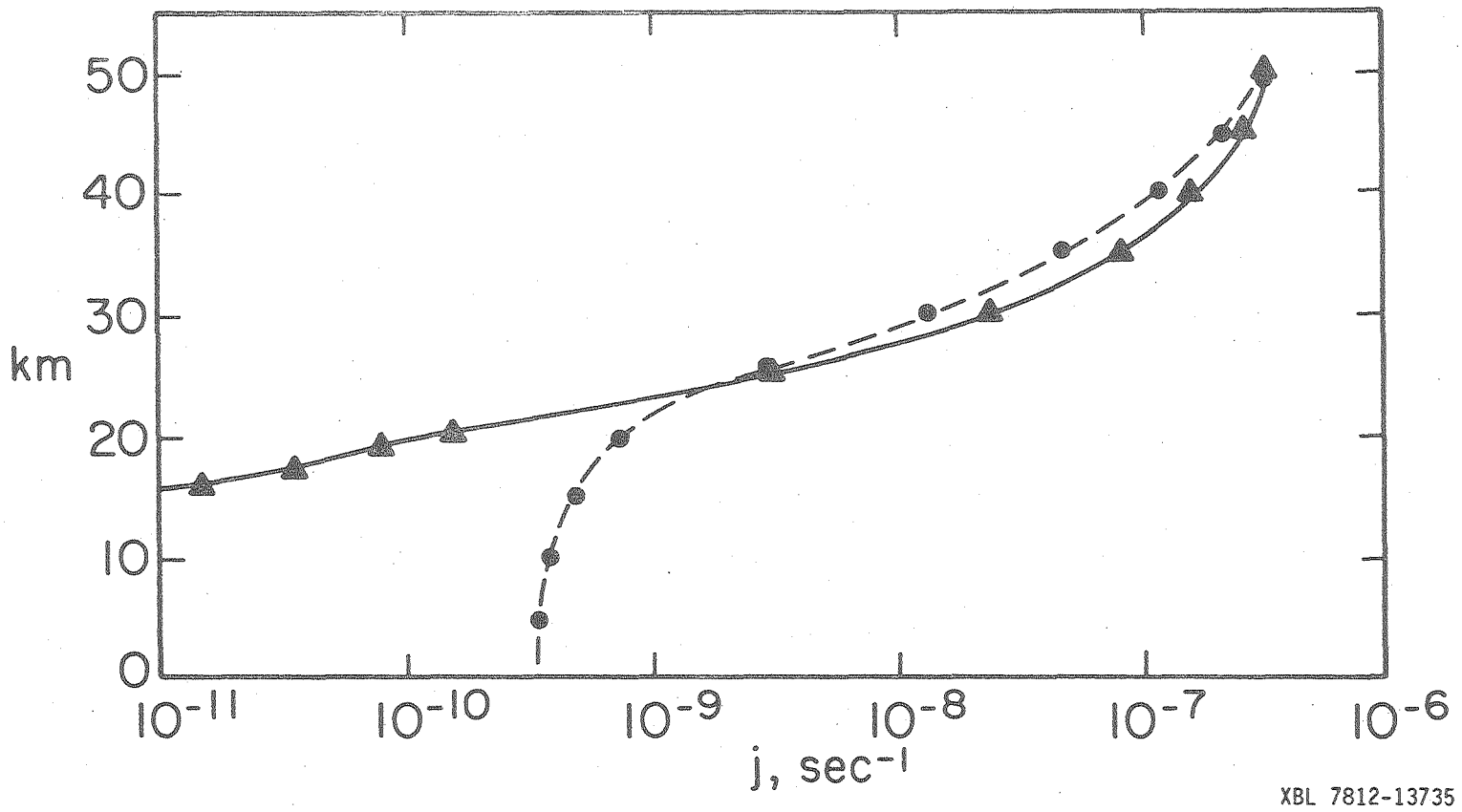
50
40
30
km
20
10
0
10^{-11}
10^{-10}
10^{-9}
10^{-8}
10^{-7}
10^{-6}
j, sec^{-1}
XBL 7812-13735

Figure 5

very little N_2O is found at these altitudes and so R is small. At altitudes below 20 km, (N_2O) is much larger and j is small, but not negligible for the Bates and Hays model. Integrating the product $j(N_2O)$ over all altitudes and over the time period of a year gives a net photolytic dissociation quantity of 12.3 MT yr^{-1} for our model. Dividing the atmospheric inventory of N_2O, obtained by integrating the concentration of N_2O as a function of altitude over all altitudes and surface of the earth, by the amount of destruction by photolysis in one year gives 191 years as the lifetime of N_2O based on photolysis. The large difference of this, from the 70 years calculated by Bates and Hays, results from the lack of photolysis in the troposphere.

The importance of the other major pathway of destruction of nitrous oxide in the stratosphere, chemical reaction with $O(^1D)$, may be accessed by a similar method using the chemical rate constant (Davidson[126]), the concentration of nitrous oxide, and the calculated $O(^1D)$ concentration primarily arising from O_3 photolysis. Adding the yearly destruction of nitrous oxide through chemical reaction, 1.6 MT yr^{-1}, to the 10.9 MT yr^{-1} calculated for photolysis alone, gives a corresponding lifetime of 160 years based upon these two known means of destruction. Clearly these results indicate a large discrepancy between the estimated atmospheric lifetime of 10 years and the known destruction pathways, too large to be accounted for by uncertainty in error.

In agreement with our prediction of a negligible rate of photolysis in the troposphere, Stedman[75] has experimentally demonstrated the lack of detectable photolysis in the troposphere, using a NO detector

sensitive enough to detect the NO produced by the Bates and Hays model and ambient sunlight.

III. Temperature Effect on The U.V. Absorption of N_2O

A. Introduction

The previous section showed that at shorter wavelengths, between 210 and 235 nm there was general agreement on the absorption cross section of nitrous oxide and so the atmospheric rate of photolysis was also agreed upon. These absorption measurements have been made at room temperature and thus do not necessarily reflect the properties of stratospheric nitrous oxide, where the temperatures range from 200 to 300 K.[78] For accurate modeling of the photolysis of nitrous oxide and temperature-dependent cross sections are required, assuming of course that a noticeable temperature dependence of absorption is noted within this temperature range.

Upon undertaking this project, there was substantial evidence of a noticeable temperature effect,[8,13] but the quantitative information was lacking. Nicolle and Vodar[8] obtained a constant ratio of absorbance at 293 and 183 K at wavelengths above 200 nm, but did not display their data or other more quantitative results. Holliday and Reuben[13] found the ultraviolet absorption to increase rapidly with increasing temperature from 293 to 953 K over the wavelength range 200 to 270 nm. The temperature effect was most pronounced at longer wavelengths; only a small temperature variation was noted at their shortest wavelength studied, 200 nm. Romand and Mayence[9] reported on the quartz ultraviolet absorption as well as the more intense absorption centered at 145 nm and 291 K. Hudson presented a plot of absorption cross sections at 183, 293, and 373 K in the wavelength range 176 to 202 nm in a review article,[79] but the experimental basis for his

plot is unclear. He cites the Holliday and Reuben paper and the Romand and Mayence paper as sources, but the former only studied two of the temperatures plotted, and in fact did not study spectra at wavelengths below 200 nm. Romand and Mayence[9] did study shorter wavelengths, but at 291 K only. Nicholle and Vodar did work at 183 K, but present no graph or tables and they worked at wavelengths greater than 200 nm. Other papers by these authors did not deal with temperature dependent measurements of nitrous oxide. Monahan and Walker[15] have studied the absorption spectrum of N_2O gas at 293 K and of the solid film at 53 K over the wavelength range 100 to 200 nm.

The purpose of this study was to record the absorption spectrum of nitrous oxide at five temperatures spanning 194 to 302 K and over the wavelength range of 173 to 240 nm. These experimental conditions cover the range of temperatures and solar radiation encountered by N_2O in the stratosphere.

Previous studies have indicated that the spectrum of nitrous oxide in the region of 180 nm may have some weak structure superimposed on the continuum absorption. Zelikoff et al [10] and Monahan and Walker[15] have found evidence of very weak diffuse bands by optical methods. Lassettre et al[80] have observed diffuse banding by electron impact spectra. Chutjian and Segal[106] take note of this diffuse banding in their theoretical study in which they note an experimental band spacing of 488 $\pm$ 30 cm^{-1}. Partly by accident, but mainly by pushing the instrumentation to its limits, we have found a pronounced, relatively strong, structured spectrum superimposed on the continuum in the wavelength range 173 to 187 nm.

B. Experimental

1. Quartz Cell Construction

Spectra were obtained with the Cary 118C spectrometer fitted with either one of two thermostated cells. A small quartz cell mounted in the nitrogen purged Cary sample compartment was used in the wavelength range 173 to 210 nm. The optical pathlength was 6.5 cm and each end was closed with a pair of suprasil windows (1/16" thick) with a vacuum between them for insulation. Because the inside diameter of the cell was smaller than the sample beam dimensions, it was necessary to block out the excess portion of the beam by placing two blackened washers with an inside diameter slightly less than the cell inside diameter, at both ends of the cell. This increases the background absorbance of the cell substantially but it was possible to subtract this background effect out and this process was necessary to insure accurate results.

The cell was enclosed in an insulating jacket constructed of 1/2" closed cell sponge rubber and was cooled by a stream of nitrogen boiled off from a liquid nitrogen dewar. An electric heater immersed in the liquid nitrogen regulated the nitrogen flow rate, thereby regulating the temperature in the cell. Temperature was measured by an iron-constant thermocouple located in the center of the cooling compartment of the cell. Voltage from the thermocouple was referenced to an ice-water bath, passed through a 1000x amplifier, and was measured with a digital voltmeter.

2. Long Pass Stainless Steel Cell Construction

A large stainless steel cell, used over the wavelength range 200 to 240 nm, had a double pass optical pathlength of 296 cm and

had a single optically flat, polished suprasil window (1/4" thick). The quartz was coated with 360 Å of MgF_2 on both sides to minimize reflective loss around 210 nm. The same optical arrangement used in Section II was employed here. In this cell, the mirror was mounted at the same location as the end mirror in Section II, and had the same focal length, but in this cell the mirror was contained internally. This was advantageous in that it resulted in a longer optical path length and it required one less window eliminating further the reflective losses.

All the mirrors, including the 3" diameter, 48" focal length concave mirror inside the cell were reconditioned by stripping down with acid, replating the front surface with aluminum and overcoating with MgF_2. To enhance reflection around 210 nm, all mirrors were applied a rapid vacuum coating of aluminum followed by a 500 Å coating of MgF_2 on all mirrors except the two 45° incident mirrors in the sample compartment which had a 475 Å coating of MgF_2 on top of aluminum. A review of the relevant literature is provided by references 81-90. Greater reflectivity could be achieved by the use of a ThO or ThF_2 overcoating, but its radioactivity made this infeasible.[91]

The stainless steel cell, 3 1/2" diameter and 1/8" thick was welded to a second 5" diameter, 1/16" thick stainless steel tube which served as a cooling jacket. Between the two tubes, 22 feet of 3/8" copper tubing was wound into a spiral, encircling the narrower tube containing the gas. The copper spiral was suspended around the inner tube by a few hundred 3/8" rubber o-rings to damp the transfer of vibration from the cooling coils to the cell. A two stage Neslab model LT-9

refrigerating bath thermostated the cell by flowing cold methanol through the copper coils. This in turn cooled by conduction an ethanol bath in the space between the two tubes and thus cooled the cell uniformly as a unit. The cell had an end-to-end temperature differential of 0.5 K at 243 K and 1.5 K at 225 K.

Temperature was measured by placing two calibrated thermometers at either end in contact with the ethanol bath. With the ethanol bath drained, bake-out was possible up to 385 K by the use of electrical heating tape encircling the outer tube. Higher temperatures would damage the sponge rubber jacket and o-ring spacers. After bake-out, the cell could be pumped down to 2×10^{-5} torr with two small glass diffusion pumps.

To avoid some of the pressure deformation effects noted in Section II and to enable the use of the cell at measures up to 170 psi, the rear mirror was mounted on a center flange with holes drilled in it to equalize pressure on both sides. Thus to adjust the rear mirror it was necessary to remove an end flange in order to have access to the adjusting screws. This was not inconvenient however, since no optical pressure effect was noted from 0 to 160 psi so the need for readjustment was infrequent. The front window flange was cut in the shape of two semicircles with an 1/8" metal strip between them to give added support to the window for use at higher pressures; this did not interfere with passage of the beam.

When the cell was cooled, a stream of dry nitrogen was passed across the window to prevent frost formation. At cooler temperatures, the flow was increased accordingly and, at temperatures below 245 K,

this was supplemented by placing a couple of trays containing P_2O_5 in the mirror housing below the path of the beam. To aid in this purging efficiency, the mirror housing was sealed and the cell was cemented to the mirror housing. Silicone cement worked best since the cell would contract about 0.5 mm when cooled to its lowest temperature. This purging procedure was efficient and the window could be kept completely free of frost for up to 48 hours. A schematic drawing of the cell is shown in figure 6.

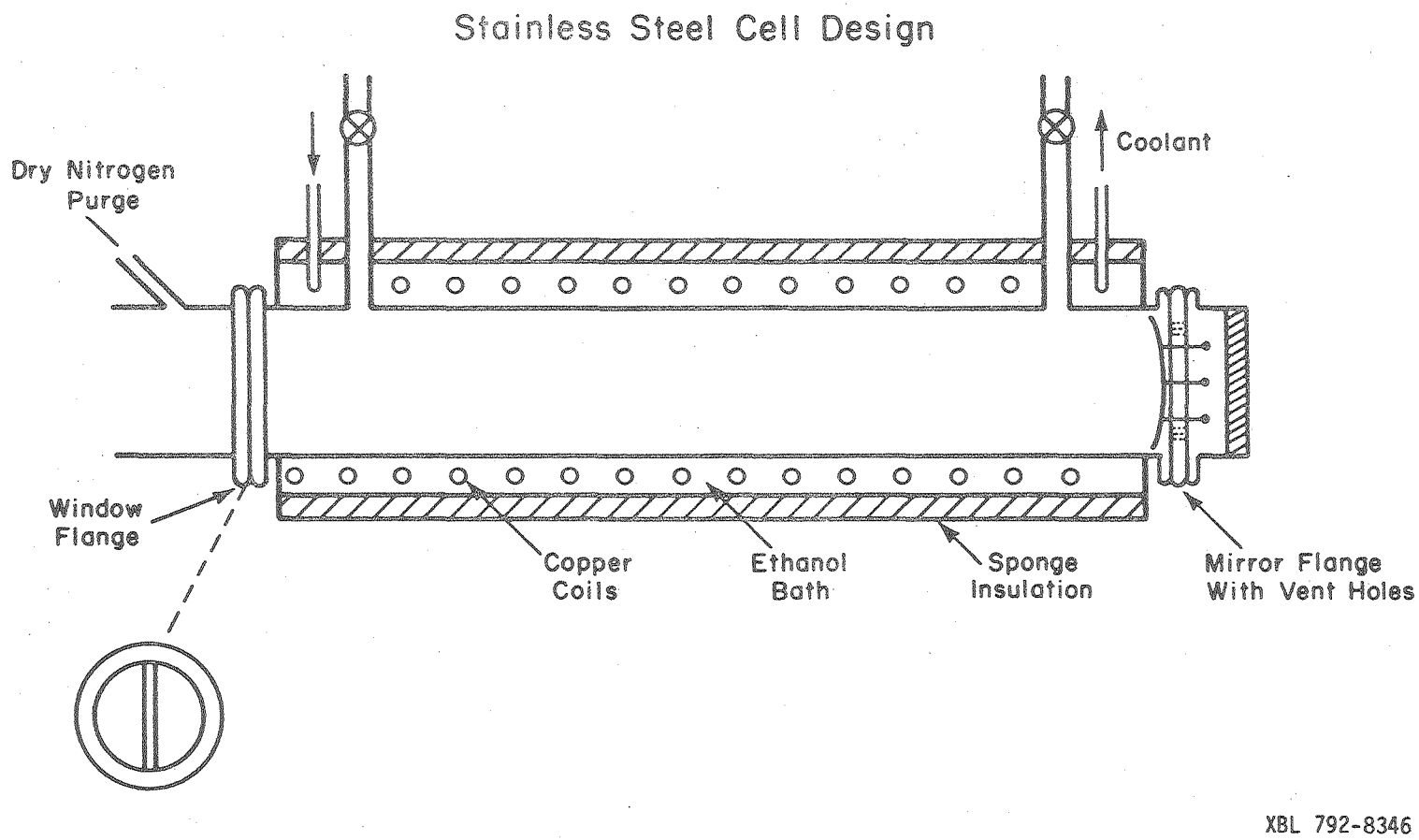
Stainless Steel Cell Design
Dry Nitrogen Purge
Coolant
Window Flange
Copper Coils
Ethanol Bath
Sponge Insulation
Mirror Flange With Vent Holes
XBL 792-8346

Figure 6

C. Experimental Procedures

1. Data Collection

The analog output of the spectrometer was collected and stored by a Fabritek 1074 data collector with a 12 bit A/D converter and 4000 words of storage. Data points were taken on a time basis, usually 1 point every 2 seconds and a scan was initiated by means of a Schmidt trigger located near the Cary. The Cary scan speed was 0.1 nm/sec so data points were recorded every 0.2 nm. Timing mismatch between the Cary and Fabritek did not prove to be a problem as evidenced by the reproducibility of spectral features and the results obtained with each run.

Data collected by the Fabritek could be arithmetically manipulated and was displayed on an oscilloscope screen. Through an interface to a PDP 8L minicomputer (DEC) further data reduction could be carried out using FOCAL programs. Control over the data collection and minicomputer was through a teletype and the final form results were stored on paper tape for further analysis. This method of data collection was superior to that used in Section II since signal averaging over several runs was possible.

All spectra were obtained in the double beam mode but were based on the ratio of I_0 through the evacuated cell and I through the same cell containing N_2O. For wavelengths greater than 187 nm, the resolution was 0.7 nm. Typically four scans of the sample and background (evacuated cell) were repeated. Each completed scan was checked for drift or error by comparison with other runs. The background scans were summed,

multiplied by 1/4 and subtracted from the result of the same procedure for the sample runs.

For all high resolution experiments in this section, the slits were set at 0.15 nm which gave an average resolution of 0.075 nm. The time constant was 25 seconds, the scan rate was 0.005 nm sec^{-1} and data points were taken every 0.05 nm in this case. For these runs, signal averaging was also carried out for four runs, both for background and sample.

Nitrous oxide from a Matheson cylinder was purified by passing through a 3A molecular sieve (Linde) to remove water and then by four successive vacuum distillations with retention of the middle portion of each. Prior usuage of a 4A molecular sieve indicated that the molecular sieve adsorbed nitrous oxide and quickly became saturated.

Gas purity was tested by a variety of techniques. By ultraviolet absorption studies, upper limits of NO and NO_2 impurity were set at < 1 ppm. By high resolution mass spectrometry, the upper limits of the following were set: $N_2 < 0.1\%$, $CO_2 < 0.01\%$, $O_2 < 0.05\%$. Mass numbers from 12 to 800 were scanned and no other impurities were detected with a sensitivity of about 0.05%. The infrared spectrum from 500 to 5000 cm^{-1} was studied on a Nicolet 7199 Fourier Transform Spectrometer at 0.06 cm^{-1} resolution and did not reveal any other noticeable impurities.

Gas pressure for these experiments was measured with a factory calibrated Baracel electronic manometer.

Wavelength calibrations were made by filling a 10 cm cell with 7.5 torr NO and observing the NO absorption doublet at 226 nm (Herzberg[92]) and by observing the rotational structuring of the Schumann-Runge

oxygen bands below 195 nm. (Knauss and Ballard[93], Ackerman et al[94]). The nominal Cary wavelengths were accurate to 0.08 nm with a reproducibility better than 0.02 nm. The wavelengths reported here are believed to be accurate to 0.04 nm.

Since several scans in this section lasted four or five hours, it was necessary to check for photolysis by the sample beam. The absence of photolysis of N_2O in these conditions was established by the absence of any detectable NO produced during a special six hour run.

2. Nitrogen Purging

The Cary spectrometer cannot be evacuated, so nitrogen purging was required for wavelengths between 173 and 200 nm to reduce the effect of the Schumann-Runge absorption of atmospheric oxygen. The "house nitrogen" supply was used for purging. It is the boil-off of the large liquid nitrogen dewar supplying the college of chemistry, and so purity of the gas is good. Typically proper purging of the spectrometer required two days for the large monochromator chamber at 50 ft^3 hr^{-1} and the lamp, photomultiplier and sample compartments were flushed clean in 1 1/2 hours at 10 ft^3 hr^{-1}. When N_2 was used to cool the cell, the cold gas was then warmed in a copper coil heat exchanger and used to purge the spectrometer.

The major problem encountered during the purging procedure was at the lamp assembly. The seal required for purging the light path was a flexible rubber gasket which would press against the flat face of the lamp. In time, the heat and UV radiation of the lamp would degrade the gasket, creating an air leak. This was further complicated

because the lamp was air cooled so the fan would below air into the leak. This part required frequent replacement.

The efficiency of purging could be estimated by monitoring the relative transmittance of an evacuated cell in the single beam mode.

Generally, these procedures resulted in an oxygen free background spectrum; at worst a very small background absorbance at 183 nm was recorded, however this would appear in both background and sample spectra so that this was subtracted off during the data reduction phase at the Fabritek.

The rapidly decreasing transmittance of the light due to oxygen at wavelengths below 177 nm was reduced further by the decreased output of the lamp in this region, and was noticeable by the increased photomultiplier gain the Cary uses to compensate for less light. This of course, resulted in more noise and so data collection rapidly became more difficult at wavelengths below 177 nm.

D. Results

1. Reliability of Data

The absorption cross sections for nitrous oxide for radiation between 173 and 240 nm and at five temperatures between 194 and 302 K are entered in table 2. Data points were collected and analyzed at every 0.2 nm over this range, but for the rate of changed noted, a data point presented for every 1 nm is sufficient. The stimated standard deviation of wavelength is ± 0.04 nm and cross section is 2%. Because only the quartz cell could be cooled to 194 K, cross sections for that temperature were only measured between 210 and 173 nm.

As stated in the introduction of this section, during the course of this study a pronounced structuring has been observed in the wavelength range 173 to 187 nm. The cross sections listed in table 2 have been averaged over this wavelength range by low resolution (0.7 nm) for the purpose of atmospheric modeling. Spectra obtained with the stainless steel cell used from 240 to 205 nm agreed with spectra obtained from the quartz cell, used from 173 to 210 nm, providing a check on systematic optical or temperature measurement errors. For the room temperature spectrum however, the stainless steel cell was at room temperature, 296 K, but inside the Cary sample compartment the "room temperature" measured was 302 K due to heat generated by the spectrometer. It proved infeasible to correct for this small temperature difference, and so two slightly different temperatures are indicated depending on the wavelength range.

Table 2. Ultraviolet absorption cross sections, $\sigma = (\ln Io/I)(CL)^{-1}$ cm^2 for nitrous oxide as a function of temperature
3.83/24 = 3.83×10^{-24}

Wave-length nm	194 K	225 K	243 K	263 K	296 K
240		3.83/24	4.80/24	5.00/24	1.01/23
239		4.40/24	5.60/24	5.95/24	1.23/23
238		5.30/24	6.70/24	7.35/24	1.52/23
237		6.60/24	8.25/24	9.50/24	1.91/23
236		7.70/24	9.90/24	1.19/23	2.40/23
235		9.65/24	1.22/23	1.49/23	3.01/23
234		1.21/23	1.54/23	1.93/23	3.60/23
233		1.51/23	1.91/23	2.46/23	4.78/23
232		1.92/23	2.43/23	3.13/23	6.05/23
231		2.50/23	3.06/23	4.05/23	7.60/23
230		3.20/23	3.91/23	5.05/23	9.55/23
229		4.05/23	5.00/23	6.45/23	1.20/22
228		5.25/23	6.40/23	8.35/23	1.51/22
227		6.81/23	8.30/23	1.06/22	1.90/22
226		9.85/23	1.07/22	1.36/22	2.39/22
225		1.16/22	1.37/22	1.75/22	3.03/22
224		1.45/22	1.81/22	2.34/22	3.75/22
223		1.87/22	2.30/22	2.95/22	4.74/22
222		2.39/22	2.93/22	3.76/22	5.88/22
221		3.08/22	3.74/22	4.73/22	7.39/22
220		3.98/22	4.82/22	6.01/22	9.22/22
219		5.19/22	6.14/22	7.58/22	1.15/21
218		6.68/22	7.85/22	9.68/22	1.42/21
217		8.75/22	1.02/21	1.22/21	1.79/21
216		1.13/21	1.29/21	1.54/21	2.23/21
215		1.44/21	1.64/21	1.95/21	2.76/21
214		1.87/21	2.08/21	2.45/21	3.42/21
213		2.36/21	2.62/21	3.05/21	4.21/21
212		3.00/21	3.31/21	3.80/21	5.18/21
211		3.80/21	4.08/21	4.72/21	6.19/21
210	4.23/21	4.70/21	5.11/21	5.79/21	7.55/21

Wave-length nm	194 K	225 K	243 K	263 K	302 K
209	5.23/21	5.95/21	6.27/21	7.15/21	9.80/21
208	6.50/21	7.35/21	7.82/21	8.75/21	1.16/20
207	7.87/21	8.95/21	9.52/21	1.07/20	1.38/20
206	9.90/21	1.09/20	1.16/20	1.30/20	1.65/20
205	1.19/20	1.33/20	1.40/20	1.57/20	1.95/20
204	1.44/20	1.62/20	1.69/20	1.85/20	2.30/20
203	1.69/20	1.90/20	2.00/20	2.20/20	2.67/20
202	2.04/20	2.26/20	2.40/20	2.60/20	3.09/20
201	2.40/20	2.67/20	2.81/20	3.01/20	3.58/20
200	2.85/20	3.08/20	3.28/20	3.52/20	4.09/20
199	3.36/20	3.64/20	3.86/20	4.06/20	4.70/20
198	3.89/20	4.24/20	4.45/20	4.73/20	5.35/20
197	4.55/20	4.88/20	5.10/20	5.42/20	6.10/20
196	5.18/20	5.53/20	5.83/20	6.14/20	6.82/20
195	5.80/20	6.20/20	6.42/20	6.85/20	7.57/20
194	6.48/20	6.90/20	7.25/20	7.51/20	8.11/20
193	7.20/20	7.64/20	7.95/20	8.32/20	8.95/20
192	7.72/20	8.40/20	8.75/20	9.20/20	9.75/20
191	8.59/20	9.02/20	9.36/20	9.81/20	1.04/19
190	9.38/20	9.85/20	1.01/19	1.06/19	1.11/19
189	9.97/20	1.05/19	1.07/19	1.12/19	1.17/19
188	1.07/19	1.11/19	1.17/19	1.19/19	1.25/19
187	1.12/19	1.17/19	1.19/19	1.23/19	1.31/19
186	1.16/19	1.22/19	1.25/19	1.29/19	1.36/19
185	1.22/19	1.27/19	1.31/19	1.35/19	1.43/19
184	1.26/19	1.30/19	1.32/19	1.36/19	1.44/19
183	1.28/19	1.33/19	1.35/19	1.39/19	1.46/19
182	1.29/19	1.33/19	1.37/19	1.40/19	1.47/19
181	1.32/19	1.34/19	1.36/19	1.39/19	1.46/19
180	1.33/19	1.35/19	1.38/19	1.39/19	1.46/19
179	1.30/19	1.32/19	1.34/19	1.37/19	1.44/19
178	1.28/19	1.28/19	1.29/19	1.31/19	1.39/19
177	1.27/19	1.28/19	1.29/19	1.31/19	1.40/19
176	1.24/19	1.23/19	1.25/19	1.27/19	1.34/19
175	1.16/19	1.15/19	1.17/19	1.18/19	1.26/19
174	1.14/19	1.14/19	1.15/19	1.17/19	1.19/19
173	1.07/19	1.08/19	1.10/19	1.11/19	1.13/19

2. Continuous Absorption

The portion of the data centered at the stratospheric "window," the region between the decreasing absorbance of the Hartley O_3 band and the increasing absorbance of the Schumann-Runge bands of O_2, is shown in figure 7. The triangles are the data points of Zelikoff, Watanabe, and Inn. Excellent agreement between the room temperature values is noted. Agreement at room temperature with the values in Section II has also been noted. The region shown here, especially from 205 to 225 nm, is important in stratospheric photolysis of N_2O as a result of larger light flux in this "window" region. It is difficult to see in this figure that the percentage change of absorbance with temperature is greatest at longer wavelengths. The ratio of the cross sections between the room temperature value and the value obtained at 225 K is about 2.9 at 240 nm, about 1.6 at 210 nm and about 1.15 at 190 nm. This is in qualitative agreement with the findings of Holliday and Reuben at elevated temperatures.

Jim Podolske was able to fit the temperature dependence at each wavelength in the empirical formula:

$$\ln\sigma(\lambda,T) = A_1 + A_2\lambda + A_3\lambda^2 + A_4\lambda^3 + A_5\lambda^4 + (T-300)\exp(B_1 + B_2\lambda + B_3\lambda^2 + B_4\lambda^3)$$

The nine parameters were fit by a nonlinear, least-squares, minimization routine to give the coefficients for λ in nm,

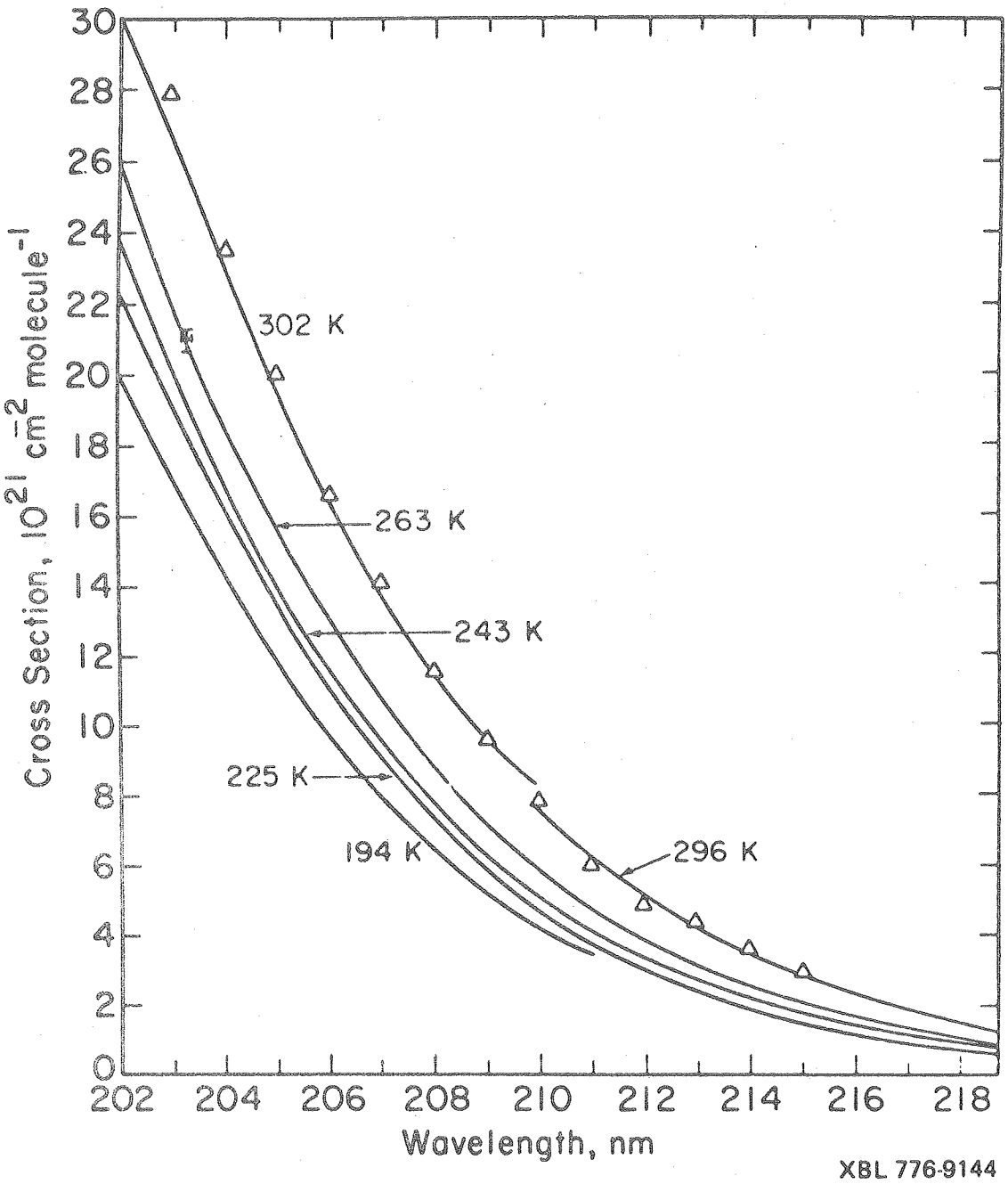
Cross Section, 10^{21} cm^{-2} molecule^{-1}
Wavelength, nm
302 K
263 K
243 K
225 K
194 K
296 K
0
2
4
6
8
10
12
14
16
18
20
22
24
26
28
30
202
204
206
208
210
212
214
216
218
XBL 776-9144

Figure 7

$A_1 = 68.21023$ $B_1 = 123.4014$

$A_2 = -4.071805$ $B_2 = -2.116255$

$A_3 = 4.301146 \times 10^{-2}$ $B_3 = 1.111522 \times 10^{-2}$

$A_4 = -1.777846 \times 10^{-4}$ $B_4 = -1.881058 \times 10^{-5}$

$A_5 = 2.520672 \times 10^{-7}$

with an estimated standard deviation of about 4 percent.

3. Structured Spectrum

While collecting low resolution data in the wavelength range 173 to 187 nm, it was noticed that small bulges in the continuum were consistently reproduced. This was not thought too unusual since a similar effect was noted by Zelikoff *et al.*[10] A spectrum taken from their paper is shown as figure 8. However upon comparing spectra taken at different temperatures in this wavelength range, it was also noticed that the extent and intensity of the "bulges" varied strongly with temperature. A spectrum taken under conditions of higher resolution was remarkably different from that expected. Under the proper experimental conditions and with signal averaging, the spectrum shown in figure 9 was obtained.

The spectrum shows a number of vibrational envelopes of varying shapes and intensities; some have bandheads and others appear as superpositions of individual features. Generally, the structuring appears to decrease in intensity towards longer wavelengths. Very weak features can be observed up to 195 nm, but above 200 nm no hint of structuring at all is detected, only a purely continuous spectrum is observed. A similar spectrum taken at 195 K shows the structuring to be reduced substantially more than the underlying continuum was reduced.

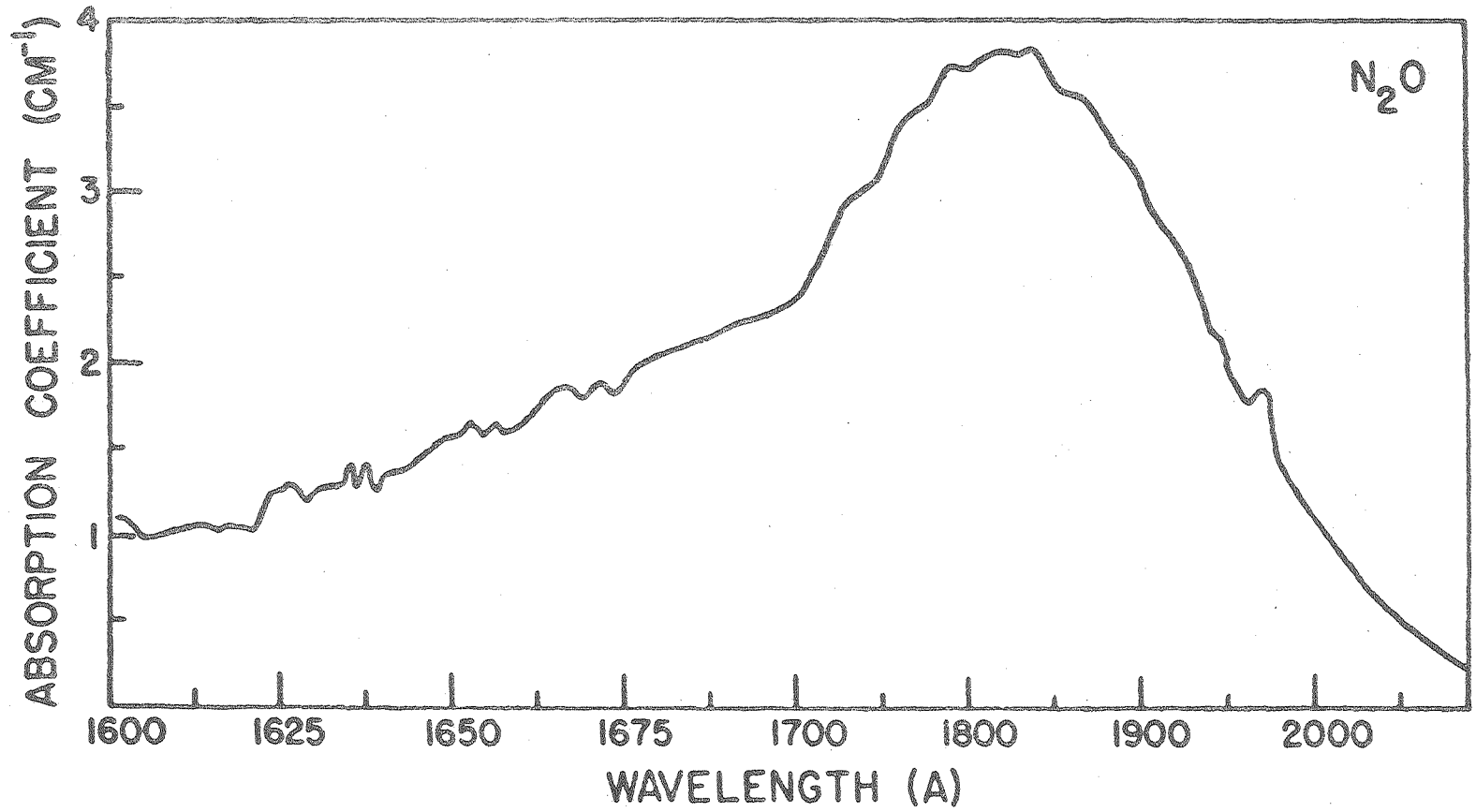

XBL 7812-14020

Figure 8

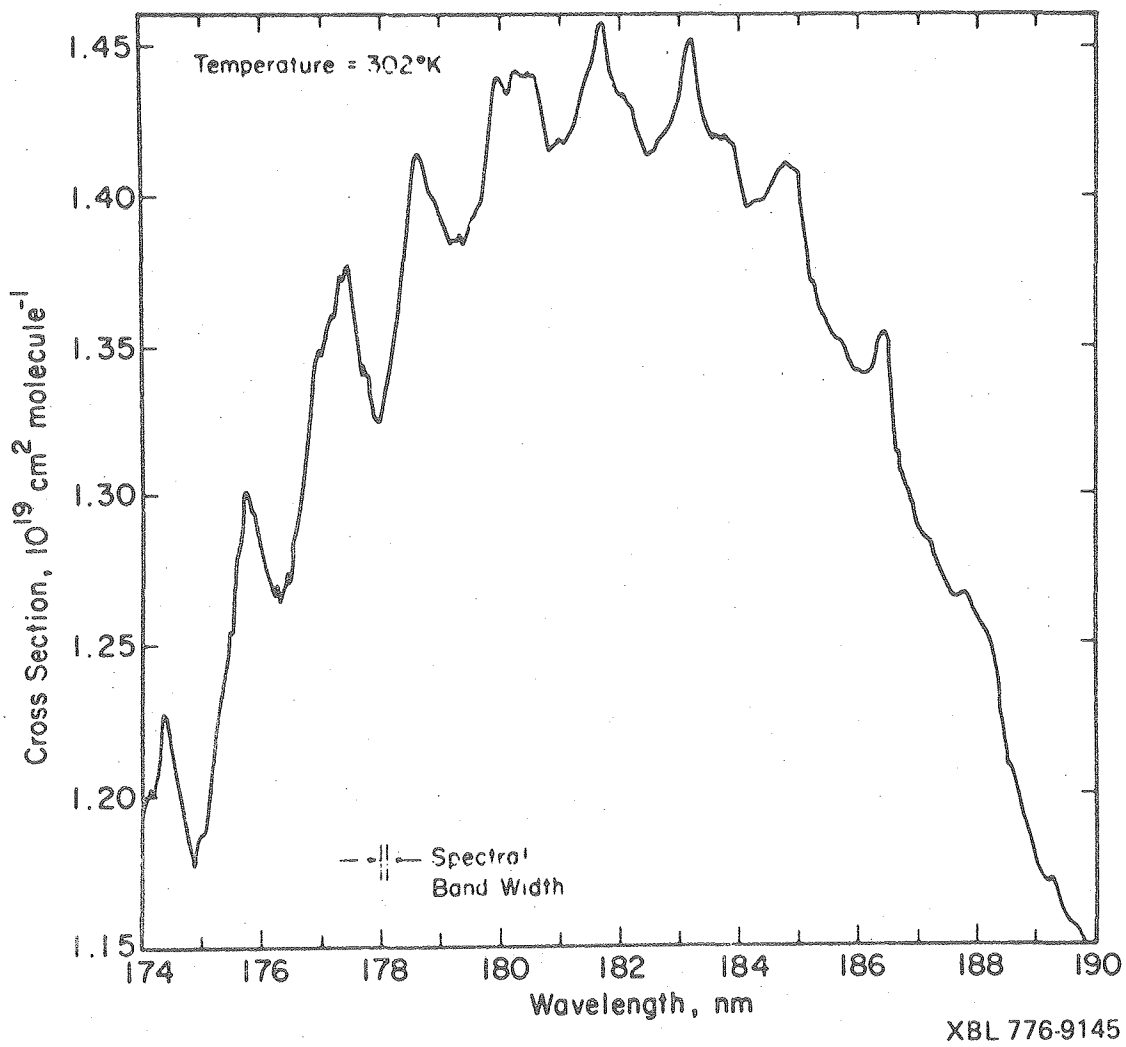
Temperature = 302°K
Cross Section, 10^{19} cm^2 molecule^{-1}
1.45
1.40
1.35
1.30
1.25
1.20
1.15
174
176
178
180
182
184
186
188
190
Wavelength, nm
Spectral
Band Width
XBL 776-9145

Figure 9

The possibility that the observed structuring was due to an impurity also received careful consideration. Confidence of the observed results was achieved only after the following considerations of purity:

1) UV spectroscopy, mass spectrometry and IR absorption did not reveal any observable impurities as mentioned previously in this section.

2) A search of the ultraviolet absorption literature did not reveal any spectra of other gases that closely fit the observed banding pattern.

3) The observed temperature effect was a function of temperature over a broad temperature range. For a condensing vapor of an impurity, one might expect a strong decrease in absorption only below a given temperature, and less effect at elevated temperatures. The temperature dependent survey is covered in Section IV.

4) The observed spectra of the four nitrogen isotopes $^{14}N^{14}NO$, $^{15}N^{14}NO$, $^{14}N^{15}NO$, and $^{15}N^{15}NO$ each show a similar spectrum but with a unique wavelength shift of the features. The remote possibility of a uniquely labeled impurity in each sample can be dismissed in conjunction with No. 1, 2 and 3 of the above for each isotope.

A more intensive survey of this structuring, its temperature dependence and theoretical basis is covered in the next section.

IV. Temperature Effect of Nitrous Oxide Vibronic Structuring at 6.8 eV

A. Introduction

1. Previous Studies

As mentioned in Section III, previous investigators have noted weak diffuse banding superimposed on the continuous absorption of N_2O. An example of this diffuse banding first observed by Zelikoff et al[10] was shown as figure 8. Monahan and Walker[15] also observed these bands, with somewhat more definition, but like previous studies were unable to analyze the banding or identify individual features.

Non-optical methods such as the high resolution electron energy loss spectra by Lassettree and coworkers[80] have also been successful in observing the diffuse banding of N_2O, although it was still too weak and diffuse for analysis by these methods.

At low resolution our spectra appeared similar to the previous studies, but at higher resolution a different spectrum resulted. Sufficient tests of purity as mentioned in Section III uphold its validity.

2. Definition of the Vibrational State Spectrum

It is the object of this study to quantify the effect of temperature on the resolved spectrum. With improved definition of the structured absorption and its temperature dependence, it should be possible to identify the active vibrations of N_2O responsible for the observed temperature effect and to analyze the energy spacing of the upper electronic state.

The initial assumption made in this study is that each vibrational mode of the lower electronic state will have a unique absorption spectrum and that the observed absorption spectrum results from the convolution of these vibrational state spectra which are individually weighted by their respective equilibrium populations at a given temperature. In other words, the observed ultraviolet spectrum, $Y(T,\lambda)$, can be expressed as the sum of individual state spactra,

$$Y(T,\lambda) = a(T)A(\lambda) + b(T)B(\lambda) + c(T)C(\lambda) + \ldots$$

where a, b, and c reflect the equilibrium macroscopic populations of the pure A, B, and C vibrational state spectra. Implicit in this expansion, is the further assumption that the vibrational state spectra, A, B and C, are independent of temperature. In a rigorous definition, the ultraviolet spectrum of a pure vibrational mode will have a temperature dependence owing to the change in the thermal distribution of its rotational members. For an ultraviolet spectrum consisting only of discrete band spectra, a change in the distribution of J" would be expected to alter the shape and intensity of the transition:

$$\nu'(K',J') \leftarrow \nu''(J'')$$

due to the quantum selection rules for J' - J". However, within the high temperature limit, the variation of the rotational distribution changes only by a small amount. This is illustrated in figure 10 which shows the normalized probability of the rotational distribution of N_2O as a function of J for three different temperatures. It is clear that between 300 and 500 K the change in the J distribution is minor and so the temperature variation of the vibrational state spectra will be small. At temperatures much below 300 K, as in the case at

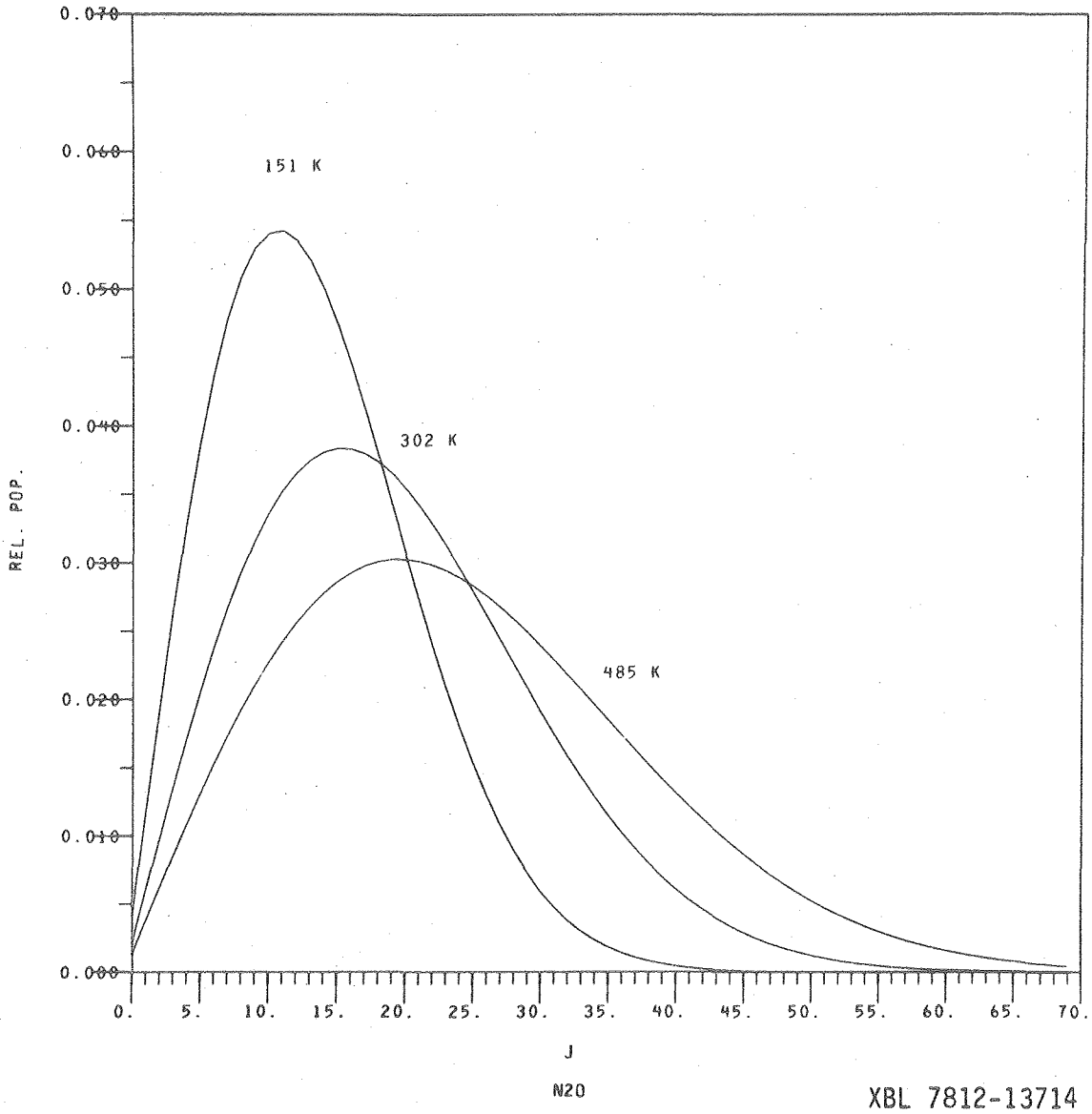

XBL 7812-13714

Figure 10

151 K, the rotational population is significantly altered. Fortunately, in the case of N_2O, at these temperatures a continuous spectrum is observed, and the discrete banding is very weak. The shape of a continuous absorption is determined by the electronic and vibrational wavefunctions of the two electronic states and the dependence on such rotational change should be minor term. For these reasons, the thermal independence of the vibrational state spectra, especially in the case of nitrous oxide, is considered valid to a first approximation.

The equilibrium populations of the vibrational modes, a,b,c ..., will be a strong function of temperature over the range 150 to 500 K, and will follow well known statistical relationships. These coefficients can be determined precisely over a wide temperature range.

3. Statistical Populations of Normal Vibrational Modes

For a one dimensional harmonic oscillator the vibrational partition function, q_v, is given by[95]

$$q_v = \sum_{n=0}^{\infty} e^{-h\nu(n+1/2)/kT} = \frac{e^{-h\nu/2kT}}{1-e^{-h\nu/kT}}$$

where ν is the energy of the vibrational mode with quantum number n at temperature T.

Neglecting anharmonicity and coupling of vibrations for a polyatomic molecule,

$$q_v = \prod_{j=1}^{\alpha} \frac{e^{-h\nu_j/2kT}}{1-e^{-h\nu_j/kT}}$$

Here, the product of all independent normal vibration energies, ν_j, has been taken up to α, where $\alpha = 3n-5$ for a linear molecule. These normal vibrational frequencies of nitrous oxide reknown from infra-

red data:[96a]

$$\nu_1 = 1284.7 \text{ cm}^{-1}$$

$$\nu_2 = 588.8 \text{ cm}^{-1} \text{ (doubly degenerate)}$$

$$\nu_3 = 2223.5 \text{ cm}^{-1}$$

The population of a given vibration irrespective of other normal vibrations is given by

$$f = \frac{\omega\, e^{-h\nu_j(n + 1/2)/kT}}{q_v}$$

where ω denotes the degeneracy of the nth level of vibration ν_j. For a triatomic of $C_{\infty}v$ symmetry, only the ν_2 vibration is degenerate and the degeneracy of the nth level is n+1:[96b]

$$\omega = (n + 1) \text{ for } \nu_2$$

To describe the population of the vibrational levels in terms of the four (two of which are degenerate) vibrations of nitrous oxide, the product of the individual populations is taken:

$$\frac{N\nu_{\ell mn}}{N_T} = \frac{e^{-h\nu_i(\ell + 1/2)/kT}(n + 1)e^{-h\nu_j(n + 1)/kT}\, e^{-h\nu_k(m + 1/2)/kT}}{q_v}$$

Here, $\nu_{\ell nm}$ will also be written as (ℓnm).

As indicated on page 49, q_v is given by

$$q_v = \left(\frac{e^{-h\nu_i/2kT}}{1-e^{-h\nu_i/kT}}\right)\left(\frac{e^{-h\nu_j/2kT}}{1-e^{-h\nu_j/kT}}\right)^2\left(\frac{e^{-h\nu_k/2kT}}{1-e^{-h\nu_k/kT}}\right)$$

The second factor is squared because it is doubly degenerate.

In this way, the populations of (000), (010), (006) or (113) may be determined as a function of temperature. In fact, over the

temperature range 150 to 485 K, only the populations of (000), (010), (020), (030), and (100) will be significant.

A plot of the populations of several vibrational modes as function of temperature is shown in figure 11. As in the case of the rotational populations, the sum of all vibrational populations at any temperature must equal 1. Also plotted in this figure, the sum of all vibrations shown, is superimposed on the top margin (1.0000), indicating this to be so.

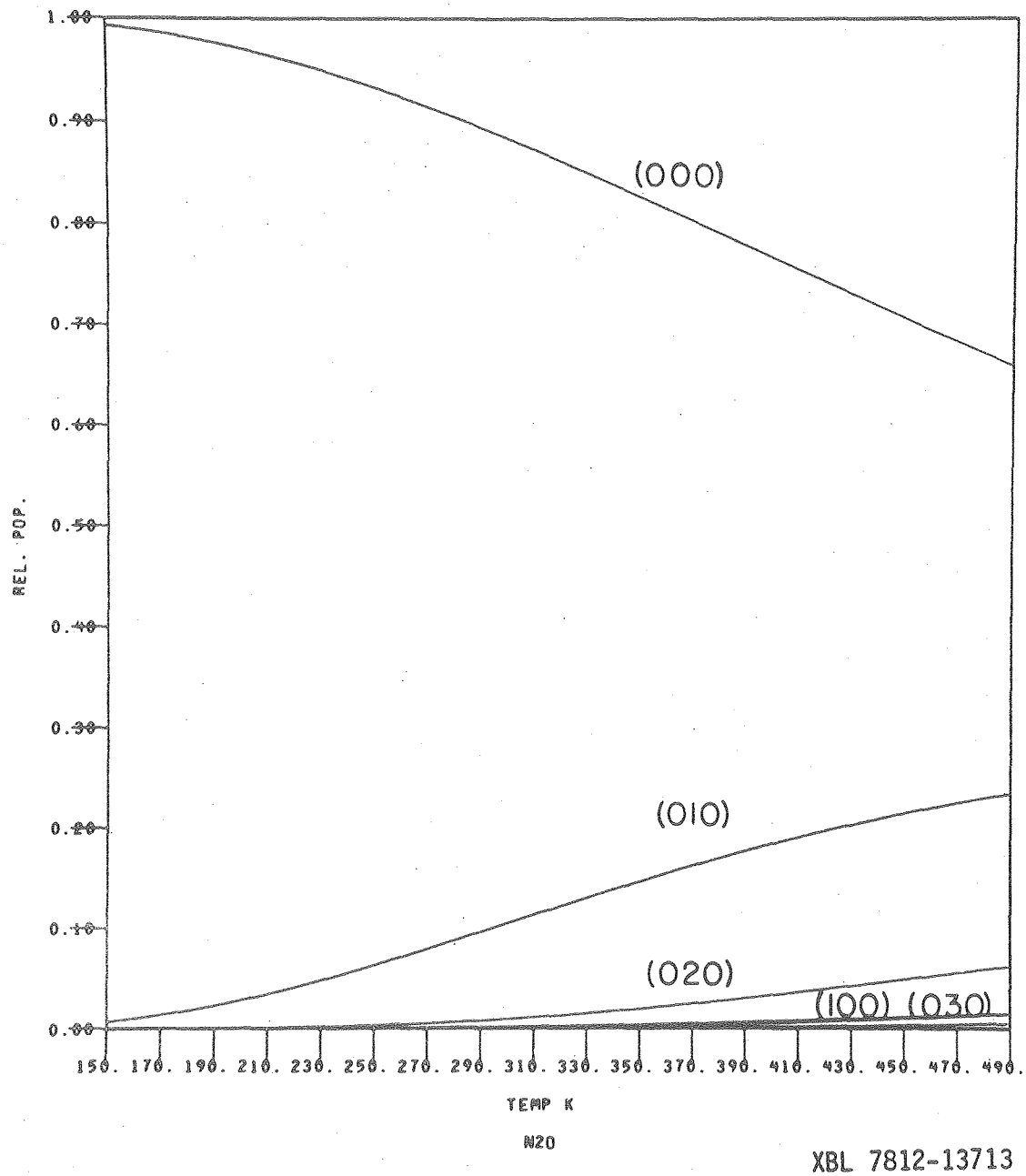

XBL 7812-13713

Figure 11

B. Theoretical Aspects of Electronic Spectrum of Polyatomic Molecules

1. Vibrational State Spectra

The observed spectrum, Y, has been described as the weighted sum of individual vibrational state spectra, A, B, C . . ., which have been assumed to be independent of temperature over the temperature range studied. If the state spectra of the different vibrational modes are not very much different, or if the populations of the excited vibrations are very small, then the observed spectrum does not vary much with temperature over this range. The magnitude of the difference in the absorption spectrum of the different vibrational modes will reflect the difference in the overlap of the differing Franck-Condon regions of the vibrational modes and the extent of vibronic interaction involved, if any.

If, for reasons of symmetry or vibrational coupling to be discussed later, the (010) state absorption is very much different than the absorption spectrum of the (000) state and the populations of other vibrations is negligible, the observed spectrum may be described simply by

$$Y(T,\lambda) = a(T)A(\lambda) + b(T)B(\lambda)$$

where, for a designating the (000) population, will decrease with temperature, and b, designating the (010) population, will increase with temperature. At lower temperature, Y will most nearly resemble A and $Y \rightarrow A$ as $a \rightarrow 1.0$. At higher temperatures, the spectrum will involve increasingly more character of B. It is not possible to occupy only B and so this state spectrum cannot be directly observed in thermal equilibrium with its surroundings. In such a case, if it is the change

in b(T) which is primarily responsible for a large temperature effect in Y(T) over a given temperature range, then it is convenient to describe B as the "active vibration" responsible for the observed temperature dependence.

The populations of all the vibrational modes will follow the statistical relations outlined previously and so it is possible to deconvolute a series of temperature dependent absorption measurements into the component state spectra. The reliability of this calculation is greatly enhanced if the vibrational energies ν_i, ν_j, and ν_k are well separated from each other and their combinations, and if there is a reasonably large temperature effect on the observed absorption spectrum.

For "allowed" electronic transitions there will often be an observable difference in the vibrational state spectra due to differing regions of Franck-Condon overlap. For "forbidden" transitions, the vibrational state spectra may be even more markedly different if the transition occurs through vibronic interaction.

2. Allowed Electronic Transitions[97a]

An electronic transition is designated as an "allowed" transition if the transition moment, R, is different from zero,

$$(1) \quad R_{e'e''} = \int \psi'^*_e \, M \, \psi''_e \, d\tau_e \neq 0$$

here $R_{e'e''}$ is the electronic transition moment of the lower electronic state, $\psi''e$, and the complex conjugate of the upper electronic state, ψ'^*e, and M is the electronic dipole operator with the components

$$\sum_i e_i x_i \quad , \qquad \sum_i e_i y_i \quad , \qquad \sum_i e_i z_i$$

where e_i are the charges or the on particles with coordinates x_i, y_i, and z_i. The integral will be unequal to zero only if the product

$$(2) \qquad \psi_e'^* M \, \psi_e''$$

has a totally symmetric character class for the symmetry of the involved species. In Group Theory notation,

$$\Gamma(\psi_e') \times \Gamma(\psi_e'') \times \Gamma(M) = \text{totally symmetric}$$

Implicit in this selection rule is the use of the Born-Oppenheimer approximation, separating the wavefunctions of nuclear and electronic motion:

$$(3) \quad \psi_{ev} = \psi_e(q,Q)\psi_v(Q)$$

A more rigorous definition of the transition moment would be

$$(4) \quad R_{e'v'e''v''} = \int \psi_{ev}'^* \, M \, \psi_{ev}'' \, d\tau_{ev} \neq 0$$

Neglecting for a moment the more rigorous definition of (4) and continuing with (1) and assuming the Born-Oppenheimer approximation holds, a similar resolution may be made for the electric dipole moment into electronic and nuclear motion:

(5) $M = M_e + M_n$

then

(6) $R_{e'v'e''v''} = \int \psi_{ev}'^{*} M \psi_{ev}'' \, d\tau_{ev}$

$= \int \psi_v'^{*} \psi_v'' \, d\tau_v \int \psi_e'^{*} M_e \psi_e'' \, d\tau_e +$

$\int \psi_v'^{*} M_n \psi_v'' \, d\tau_v \int \psi_e'^{*} \psi_e'' \, d\tau_e$

Standard analysis then assumes that for a valid Born-Oppenheimer approximation the electronic components of the wavefunctions are orthogonal, so that (6) reduces to

(7) $R_{e'v'e''v''} = \int \psi_v'^{*} \psi_v'' d\tau_v \int \psi_e'^{*} M \psi_e'' d\tau_e$

where the second integral has been defined in equation (1),

(8) $R_{e'v'e''v''} = R_{e'e''} (Q) \int \psi_v'^{*} \psi_v'' d\tau_v$

The transition moment is equal to the product of the electronic transition moment and the vibrational overlap integral.

$R_{e'e''}$ is different from zero and applies to all transitions between the two electronic states. It is the second factor which is responsible for the intensity structure (vibrational features) of the transition. The overlap integral is the quantum mechanical interpretation of the Franck-Condon principle.

Applying a similar argument for electron spin it may be shown that, as for diatomics,

$\Delta S = 0$

where S is the net electron spin of the wavefunction. Only states of the same multiplicity may combine with each other. This rule applies primarily to light molecules and tends to break down increasingly with heavier molecular weights.

3. Forbidden Transitions[97b]

Unlike diatomics, in which forbidden transitions are not usually seen optically, in polyatomics, these transitions often occur weakly. For a "forbidden" transition:

$$(1) \quad R_{e'e''} = \int \psi_{e'}^{*} M \psi_{e''} \, d\tau_e = 0$$

However, if the more rigorous form is not equal to zero,

$$(4) \quad R_{e'v'e''v''} = \int \psi_{ev'}^{*} M \psi_{ev''} \, d\tau_{ev} \neq 0$$

then the transition will occur.

Even if (4) equals zero, the transition may still occur if substitution of the magnetic dipole operator or electric quadrupole operator in (1) gives a nonvanishing result, although these transitions are much weaker than allowed electron dipole transitions, typically 10^{-5} and 10^{-8} respectively of an allowed electric dipole transition.[97g]

One way in which the transition is allowed in (4) and not in (1) is through vibronic interaction. This implies that the separability of the wavefunction as expressed in equation (6) is not valid and correspondingly, (8) is also invalid.

A first approximation to the vibronic wavefunction, is obtained from the direct product multiplication

$$(9) \quad \psi_{ev} = \psi_e \times \psi_v$$

and so it is immediately seen that if ψ_v is the totally symmetric species, (4) will give the same result as (1) and thus vibronic interaction cannot be responsible for the transition. However if ψ_v is an antisymmetric or degenerate vibration, then ψ_{ev} may have a different symmetry then

ψ_e and $R_{e'v'e''v''}$ may be unequal to zero when equation (4) is applied.

An example may be the $^1\Sigma_g^+ \leftarrow {}^1\Sigma_g^+$ transition for $D_{\infty h}$ symmetry. This transition is allowed only through the electronic quadrupole operator and thus is extremely weak. However coupling of $^1\Sigma_g^+$ with a Σ_u^+ or a π_u vibration would not result in $R_{e'v'e''v''} = 0$, and so electronic transitions due to vibronic interaction are specific for the vibration involved. The degree of intensity of a vibronically allowed transition depends on the strength of the vibronic interaction and is directly proportional to $(R_{e'v'e''v''})^2$.

Figure 12 shows a relevant possibility of vibronic interaction for the $^1\Sigma^+$ and $^1\Sigma^-$ electronic states of N_2O. (In this discussion, + and - of $'\Sigma^-$ and $'\Sigma^+$ refer to the symmetry or asymmetry of the electronic wavefunction when reflected by the vertical plane of symmetry.) The case without vibronic interaction has no transitions because of the $+ \not\rightarrow -$ selection rule of electronic transitions. With vibronic interaction, the $- \rightarrow -$ and $+ \rightarrow +$ selection rule is still maintained, as is the angular momentum selection rule, $\Delta\Lambda = 0, \pm 1$, except that with vibronic mixing a number of transitions are now possible. Note especially that the $\nu_2 = 1$, or 2 levels each have at least one transition to each ν_2 vibrational level of the upper state. In contrast, the $\nu_2 = 0$ level has a transition only to the π vibronic levels of the upper state. Since the $\nu_2 = 0$ vibronic wavefunction has the same symmetry as the totally symmetric electronic state, this transition can be attributed to the bending interaction of the upper state.

Figure 12 is useful for demonstrating the effect of vibronic interaction on observed transitions but for studies here, it is more

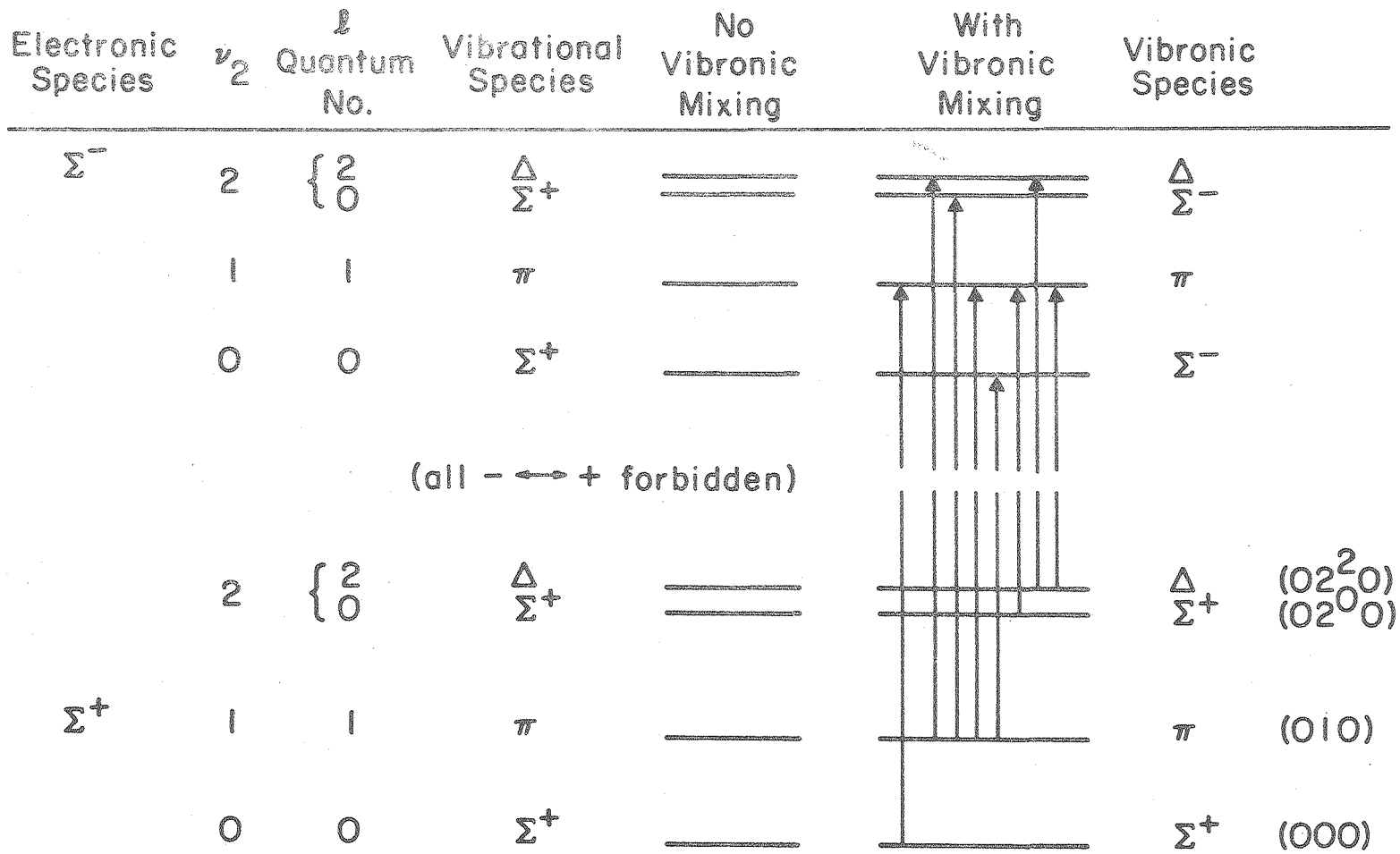

XBL 7812-13737

Figure 12

useful to compare just the differences of the $\nu_2 = 0$ and $\nu_2 = 1$ vibronic levels of the ground electronic state with higher vibrational levels of an upper $^1\Sigma^-$ electronic state. Figure 13 shows the vibronic species of the upper levels of the ν_2 vibrational mode of $^1\Sigma^-$. The quantum numbers 12, 13, 14 and 15 have been chosen arbitrarily only to demonstrate that from $\nu_2'' = 0$ the spectrum should show an energy spacing of $2\nu_2'$ whereas transitions originating from the vibrationally hot $\nu_2'' = 1$ level should show a consecutive spacing of ν_2'. This means that at low temperatures when only the $\nu_2'' = 0$ state is occupied, any observed band spectra should have a spacing which is twice as large as the spacing of hot bands originating from higher temperatures.

4. <u>Rotational Structuring</u>[97c]

The only discussion of rotational levels thus far has been the population of the different J quantum numbers as a function of temperature. For a linear triatomic of $C_{\infty v}$ symmetry, J is the only quantum number applicable to rotational structuring, and for this linear-linear transition,

$$\Delta J = 0, \pm 1 \quad (J = 0 \not\leftrightarrow J = 0)$$

with the usual selection rules for rotational symmetry,[97c]

$$+ \leftrightarrow - \qquad + \not\leftrightarrow + \qquad - \not\leftrightarrow -$$

$$s \leftrightarrow s \qquad a \leftrightarrow a \qquad s \not\leftrightarrow a$$

here the + and - refer to the symmetry of the rotational level (to be distinguished from $^+$). These selection rules lead to

$^1\Sigma - {}^1\Sigma$,	no Q, only P and R branch
$^1\Pi - {}^1\Pi$, $^1\Delta - {}^1\Delta$, ...,	weak Q, P and R branch
$^1\Sigma - {}^1\Pi$, $^1\Delta - {}^1\Pi$, ...,	strong Q, P and R branch

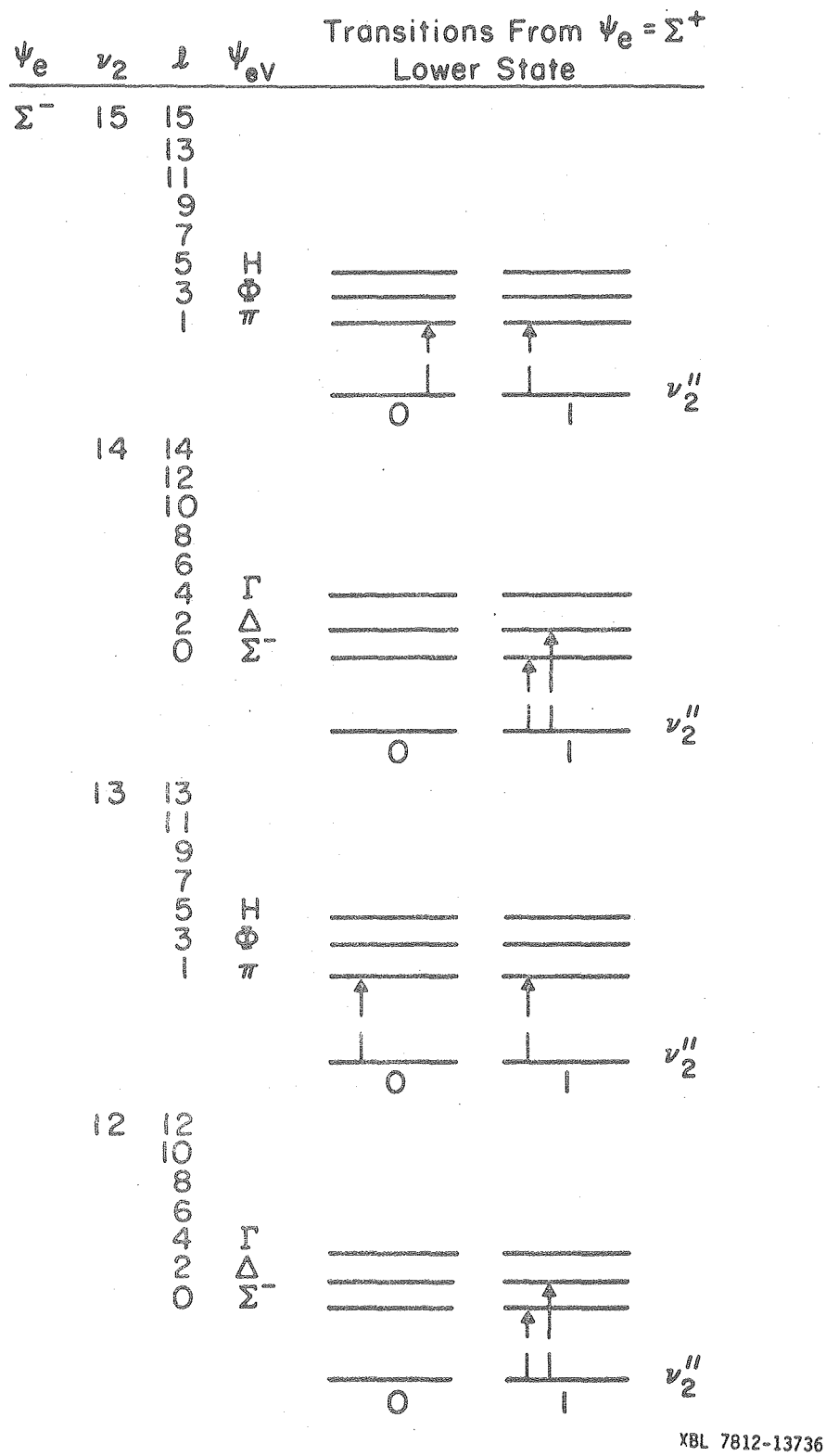
Transitions From $\psi_e = \Sigma^+$
Lower State
ψ_e
ν_2
ℓ
ψ_{ev}
Σ^-
15
15
13
11
9
7
5
3
1
H
Φ
π
0
1
ν_2''
14
14
12
10
8
6
4
2
0
Γ
Δ
Σ^-
0
1
ν_2''
13
13
11
9
7
5
3
1
H
Φ
π
0
1
ν_2''
12
12
10
8
6
4
2
0
Γ
Δ
Σ^-
0
1
ν_2''
XBL 7812-13736

Figure 13

Upon bending the molecule a second rotational quantum number arises, K, which is strictly defined only for a symmetric top. For nitrous oxide, as it is bent increasingly, the molecule less and less resembles a prolate symmetric top and becomes an asymmetric top molecule. Table 3 shows the three rotational constants, A, B, and C, for ground state N_2O for several bond angles. Kappa would be 1.0000 for a prolate symmetric top.

The rotational structure of an electronic transition between an upper electronic state which is bent in its equilibrium geometry and a lower electronic state which is linear, is determined by the selection rules for both the J and K quantum numbers. For the linear case, K represents the contribution of electronic and vibrational angular momentum,

$$K = |\Lambda + l|$$

where Λ is the electronic angular momentum and l is the vibrational angular momentum. For the ground electronic state of N_2O, $X^1 \Sigma^+$, $\Lambda = 0$ and so $K'' = |l|$. For the case of an electronic state which is slightly bent in its equilibrium geometry, K, the component of angular momentum about the top axis (i.e., the A axis for a prolate symmetric top), may also arise from the pure rotation of the molecule about its top axis. In this case, for each value of K there are a series of rotational levels with $J = K, K + 1, K + 2, \ldots$

With K defined, the additional rotational selection rules for a bent-linear electronic transition are:

$\Delta K = K' - K'' = 0$ for M_z ($\parallel$ band)

$\Delta K = K' - K'' = \pm 1$ for M_x, M_y ($\perp$ band)

plus the usual selection rules for J.

Under the instrumental conditions in this study, the resolution to reveal individual rotational features is not available. It is also likely that the structuring observed is predissociated, so that the fine structure may be smeared out and may not be observed, even with much higher resolution.

These selection rules state that from $\nu_2'' = 0$, only K = 0 for a $\parallel$ transition or K = 1 for a $\perp$ transition will be reached. That is, from the (000) level, the fine structure will appear the same as a linear-linear transition with only apparent selection from the J selection rules.

From $\nu_2'' = 1$, for a $\parallel$ transition K = 1 will be reached in the upper state with fine structure arising from the J selection rules. A $\perp$ transition of this hot band will have two sub-bands, the K = 0,2 which will be separated by 4(A' - B'). As seen in table 3 for a small bond angle, A' - B' is quite large and this separation may be substantial. By observing this "coarse" structuring of the rotational features it may be possible to determine whether the transition moment is $\parallel$ or $\perp$.

It should also be noted that for C_s symmetry a hybrid of $\parallel$ and $\perp$ transitions are possible. In this case, the rotational structuring would be the superposition of the two individual transitions with the relative intensities of each component depending on the projection of the transition moment on the principle axes. In this case, a more complicated spectrum results.

Table 3. N_2O Bond Angles and Calculated Rotational Constants, cm^{-1} for N-N 1.185 Å and N-O 1.125Å.

NNO Bond Angle, deg.	Rotational Constants, Cm^{-1} A	B	C	Kappa
180	*	0.4207	*	*
175	696.2	0.4215	0.4212	1.0000
170	174.4	0.4239	0.4229	0.9999
165	77.75	0.4280	0.4256	0.9999
160	43.93	0.4337	0.4295	0.9998
155	28.27	0.4413	0.4345	0.9995
150	19.78	0.4508	0.4407	0.9989
145	14.65	0.4624	0.4482	0.9980
140	11.33	0.4762	0.4570	0.9965
135	9.049	0.4926	0.4672	0.9941
130	7.421	0.5118	0.4788	0.9905
125	6.218	0.5342	0.4919	0.9852
120	5.304	0.5603	0.5068	0.9777
115	4.594	0.5906	0.5233	0.9669
110	4.033	0.6259	0.5418	0.9518
105	3.582	0.6670	0.5623	0.9306
100	3.214	0.7150	0.5849	0.9010
95	2.912	0.7714	0.6098	0.8596
90	2.660	0.8378	0.6372	0.8016

Kappa indicates how closely the molecule approaches a prolate symmetric top.

5. Change of Symmetry during Transition[98]

Implicit in the foregoing discussion was the assumption that in both upper and lower electronic states the symmetry class remains the same. For linear triatomics especially, this is often not the case. CO_2, HCN, CS_2, and OCS are all believed to change to bent symmetry in their excited electronic states,[97] and the evidence is quite strong for a similar change of symmetry for N_2O. For a change of bond angle, the resulting symmetry class is

$C_{\infty v} \rightarrow C_s$ or $D_{\infty h} \rightarrow C_{2v}$ (triatomics)

Evidence for such a symmetry change can be unambiguously obtained from the rotational structuring of the transition. In the absence of such rotational information, the vibrational progression pattern may also provide evidence for such a symmetry change. If the allowed electronic transition is between two different symmetry positions, the vibrational selection rules are determined by the symmetry elements common to both equilibrium positions. Thus, for an allowed $C_{\infty v}$ - C_s symmetry change the resulting vibrational selection rules are less restrictive than in the linear to linear case, and the bending vibration, asymmetric for a linear molecule, is considered now a symmetric vibration in the common symmetry class.

Consider then the vibrational selection rules for a progression in the bending mode of a triatomic[97h], ν_2: if the transition is between two linear species, the selection rule for such as asymmetri vibration predicts $\Delta\nu_2 = 0,2,4 \ldots$ with the $\Delta\nu_2 = 0$ transition the most intense. For a bent-linear transition, the selection rule for the symmetric bending vibration predicts a consecutive progression, or

$\Delta\nu_2 = 0, 1, 2, 3 \ldots$ For such a transition, the most intense peak will not necessarily be $\Delta\nu = 0$ (see below).

Note that in the case of the vibronically induced transition as in the previous example of $^1\Sigma^- \quad ^1\Sigma^+$, a consecutive progression in ν_2' originating from $\nu_2'' = 1$ or $\nu_2'' = 2$ results, but from $\nu_2'' = 0$ (or from (000)), the selection rule[97d] is $\Delta\nu_2$ ($\nu''_2 = 0$ only) = 1, 3, 5 . . . Thus, the presence of a consecutive progression of ν_2' in the hot bands ($\nu_2'' = 1, 2 \ldots$) is predicted for both the case of a bent-linear change of a symmetry, and for the case of the vibronically induced transition, and on this basis alone it is not possible to distinguish the two mechanisms unambiguously. However the progressions originating from $\nu_2'' = 0$ (or (000)) in the vibronically induced case, predict a spacing of $2\nu_2'$, whereas for the case of a change of symmetry, the symmetric ν_2 mode of the upper state would show a consecutive spacing of ν_2', as would the hot bands. Other symmetric vibrations for the bent-linear transition will also of course show a consecutive spacing in ν'.

The above discussion has dealt with the consideration of an allowed bent-linear transition and of a vibronically induced transition with no explicit mention of symmetry change. For the additional case of a bent-linear transition which is only allowed in the bent case, a slightly different situation arises. In this last case, although the product resolution of R into $R_{e'e''v'v''}$ is not strictly valid, it is useful to a first approximation provided that $R_{e'e''}$ is also considered a function of nuclear coordinates. The usual interpretation of the Franck-Condon principle in such a case would predict that the

vertical transition to the central maximum of the upper state bending potential would have the strongest intensity. For this resulting upper state configuration of 180 degrees, the $R_{e'e''}(q,Q)$ is small, and so this vertical transition is actually weak†. Instead, $R_{e'e''}(q,Q)$ will be large for a significant change in bond angle, or a non-vertical transition for which $R_{v'v''}$ (q) will be small. Clearly, the maximum of intensity of such a transition occurs at some point between the high energy limit (vertical) and low energy limit (non vertical) since for $R_{e'e''} \times R_{v'v''}$ the first product increases with bending angle whereas the second product decreases[97d]. Note however, that in a plot of potential surfaces of another vibrational mode, as in the ν_1 stretch, the usual principle of vertical transitions would still apply for that dimension.

†See figure 68 of Herzberg, Vol. III (Ref. 97)

6. Intensities of Continuous Absorptions[97e,92b]

For continuous transitions between two electronic states, the wavelength dependent intensity is given by

$$I_{abs}(\lambda) \ \alpha \ \nu\left[\int \psi_v{}'^{*}\psi_v{}''d\tau_v\right]^2$$

where ν, the energy, is derived from the energy dependence of the Einstein coefficient, B, and weights the overlap integral. For a polyatomic molecule, the vibrational eigen functions of the upper and lower electronic states, are a function of all 3n-6(5) normal coordinates. If $\psi_v{}''$ is a low energy vibration such a (000) or (010) the wavefunction of these vibrations is easily obtained. For high energy vibrations in $\psi_v{}'$ however, a much more complicated expression results and a delta function may be used to represent $\psi_v{}'$ which is different from zero only at the classical turning point. With this approximation,

$$I_{abs}(\lambda)\alpha \ \nu(\psi_v{}'')^2$$

This result predicts an intensity distribution of a continuous absorption from $\nu = 0$ which appears as an energy weighted probability distribution of the $\nu = 0$ vibrational level.

For $\psi_v{}''$ being the (000) state, this gives an energy weighted Gaussian type curve for the continuum intensity distribution.

7. Intersection of Potential Curves[97f]

For diatomics the "non-crossing rule" in which potential curves of the same electronic species cannot cross, is well known and its proof readily available[127]. In polyatomic molecules with additional degrees of freedom, however, energy surfaces can intersect even if they have the same symmetry and spin multiplicity. Herzberg and Longuet-Higgens[99] have studied this question for triatomics and have provided an example of the resulting conical intersection of HNO potential curves.

In the example of HNO, a repulsive $^1\pi$ state is formed from the $H(^2S)$ and $NO(^2\pi)$ components which may cross the bound $^1\Delta$ state formed from $H(^2S)$ and $NO(^2\Delta)$. Both these states are bent and since they are degenerate in the linear case, they will both split into $^1A'$ and $^1A''$ components in C_s symmetry. Crossing of the two states must occur because NO $(^2\Delta)$ is higher in energy than NO $(^2\pi)$, yet the HNO $^2\Delta$ state has a minimum below the $^2\pi$ state of HNO. This crossing can only take place at the point of intersection of the linear species. Once bent, the $^1A'$ components of the two species mix and the $^1A''$ components may also mix.

It is for this reason that HNO may be formed adiabatically from ground state NO $(^2\pi)$ and H in all orientations except the linear approach. In summary, for triatomics, intersection of two states of the same symmetry may occur at a point, the vertex of the resulting double conical intersection, but may not occur along a line.

A variation of this principle which is applicable to nitrous oxide will be presented in a later section.

C. Experimental

1. Instrumental Procedures

As before, spectra were obtained with the UV extended Cary 118C spectrophotometer. To overcome some of the purging problems noted in the previous section, it was necessary to design purging modifications and construct a different quartz cell. The deuterium lamp was rigidly mounted to the spectrometer and sealed with an o-ring to prevent purge leakage. This avoided the major source of leakage in Section III and was not prone to rapid deterioration. The main chamber of the monochromator was resealed by replacing the gasket material at the metal joints and by taping over the seals with 2" black photographic tape. Instead of purging the entire sample compartment, as was done in Section III, nylon tubes with sponge rubber gaskets connected the cell to the spectometer and provided a small, tight purge connection for the light path. As before, complete purging required two days prior initiation, but improvements from these modifications reduced the level of noise significantly and permitted operation down to 171 nm.

Several different instrumental parameters were tested; the best results were obtained with a scan speed of 0.01 nm sec^{-1} and with the slits set at 0.06 mm to give an average spectral band width of 0.05 nm. Data points were taken every 0.02 nm over the range 190 to 172 nm. All data in this section was collected using a time constant of 5 seconds and was stored on both chart paper and in the Fabritek. Signal averaging was carried out over four runs for both background and sample spectra for each temperature.

2. Quartz Cell Design

A single quartz cell was used for the spectra obtained in this section and it is shown schematically in figure 14. The cell consisted of a 2.2 x 10 cm quartz cylinder with fused suprasil windows (1/16" thick) which contained the gas. The cell could be used in a flow or static manner but all spectra were collected in the static mode. A quartz jacket fused to the inner cell was used for temperature control and a second quartz jacket surrounding the entire assembly also with 1/16" thick suprasil windows was evacuated to 5×10^{-6} torr, sealed in vacuum, and provided thermal insulation.

Platinum wire was spiraled about the inner cell and was fed up the quartz tubing connected to the cooling jacket, past the quartz-pyrex graded seal and was welded to two tungsten electrodes. These electrodes, fused through the pyrex section with uranium seals, provided electrical connection to the wires, which served as built-in heaters. This was convenient for vacuum bake-out and for recording spectra at elevated temperatures. Platinum was necessary to withstand the heat generated in working the quartz. A wire thickness of 0.01 inches was chosen to increase the resistivity of the heaters, smaller diameter proved impractical for glass blowing. The resistance of the built-in heater was about 10 ohms and by simply using an ac rheostat it was possible to control the temperature of the cell. The maximum possible bake-temperature without damage to the cell or heaters was about 660 K. The maximum practical temperature for recording spectra was lower, about 520 K, owing to interference from black body radiation generated by the wires.

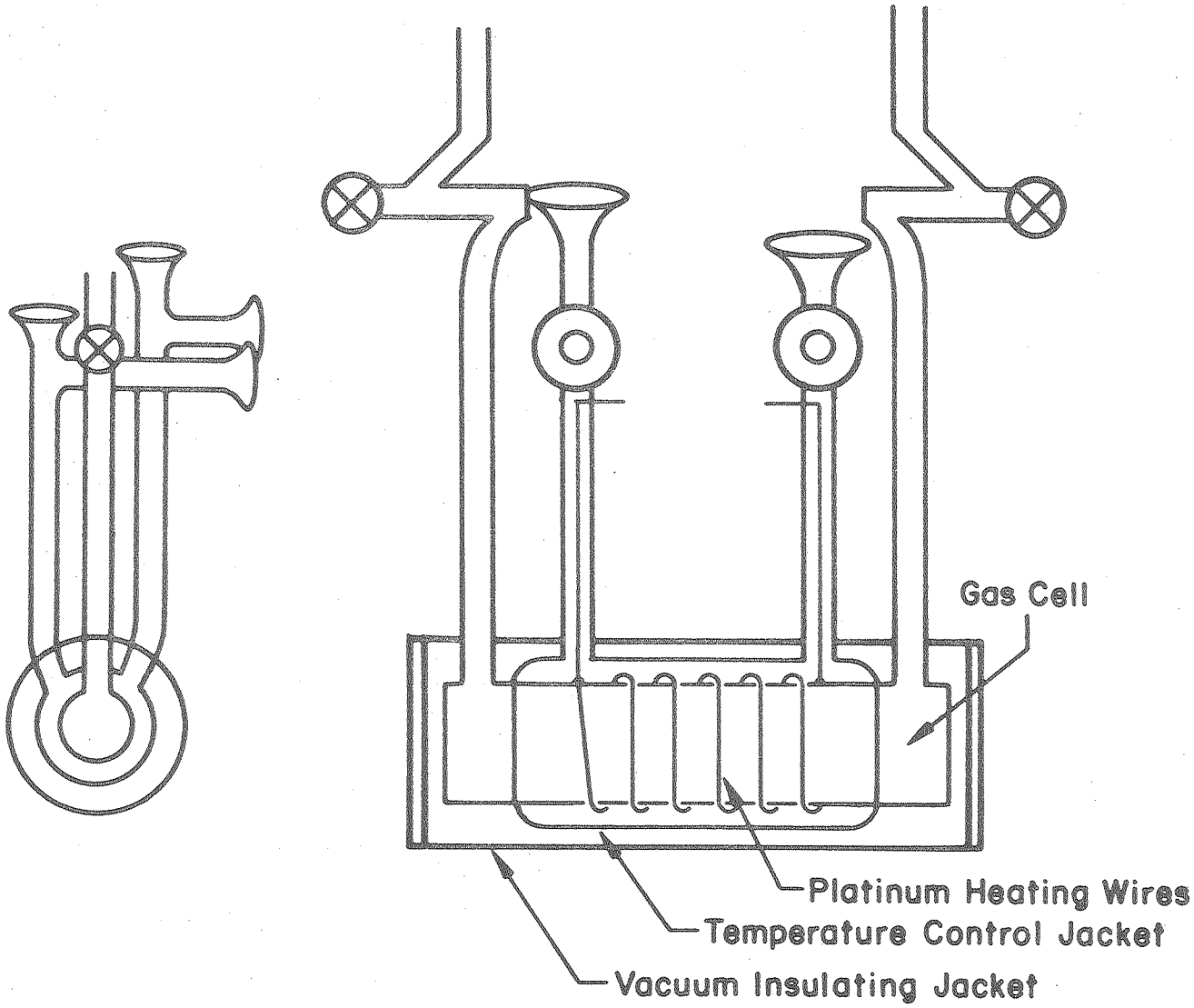

XBL 792-8344

Figure 14

Fluid was contained in the inner jacket for temperature control. For temperatures above 373 K, Dow Corning Silicone Oil was used and was heated by the Pt wires. This provided more uniform temperature control than heating an air space. For temperatures between 373 and 243 K, a Neslab model RTE - 9 thermostated circulating bath was used to flow water or methanol through the jacket. For temperatures between 243 and 200 K a Neslab double stage refrigerating bath, model LT - 9, was used to circulate methanol through the jacket. For temperatures below 200 K, a stream of cold nitrogen gas from a liquid nitrogen dewar was used to cool the cell, as in Section III. The lowest practical temperature to record spectra of nitrous oxide was determined from its equilibrium vapor pressure. To ensure enough optical density for accurate measurements, this was at about 151 K which has a vapor pressure of 28 torr.[100]

3. Temperature, Pressure and Wavelength Measurement

Pressure was measured by a 100 torr factory calibrated MKS Baraton capacitance manometer with a stated accuracy of 0.05%. Pressures used varied from 5 to 45 torr at the temperatures studied. Before recording pressure of the gas, several minutes were allowed for temperature and pressure equilibrium to be reached. The nitrous oxide was purified in the manner described in Section III and the tests of purity performed in that section did not reveal any impurity in this case as well.

Temperature was measured by two calibrated iron-constantan thermocouples in contact with the inner cell. The thermocouples were fed through the same tubing as the Pt wires and so it was necessary to

insulate the Pt wires with a length of quartz capillary tubing. A 1000x amplifier with a digital voltmeter was used to measure the thermocouple output which was referenced to an ice-water bath. No significant deviation from standard tables of thermocouple emf[101] was noted over the temperature range 78 to 490 K. Equilibrium vapor pressures of nitrous oxide at temperatures below 183 K provided a convenient check on both thermocouple and pressure measurement.

The use of two thermocouples, one at the fluid entrance and one at the fluid exit in the temperature control jacket, provided an estimate of the temperature differential in the cell. The observed temperature differential varied with the means of temperature control. When liquid nitrogen was used, an average temperature differential of 5 K resulted. The two thermostated circulating baths provided the best results with a differential of less than 0.5 K. Heating the silicone oil resulted in a higher temperature differential of about 10 K.

As in Section III, wavelength calibrations were checked by adding O_2 to the cell and observing the rotational structure of the Schumann-Runge oxygen bands.[94] Wavelength accuracy in this section is believed to be 0.05 nm.

The data stored in the PDP 8L was output in the form of paper tape and transferred to the Lawrence Berkeley Laboratory CDC-7600 computer. The most reliable means of transferring the data was by running the paper tape through a hard wired teletype located in the Vista Room. In this manner the data was converted into punch cards and further processing, graphics and corrections were possible.

4. Meter Vacuum Spectrometer

To check for the effect of lower pressuures and higher resolution, the main chamber of a 3 m MacPherson monochromator, model 241, was evacuated and filled with 50 - 250 microns of nitrous oxide.

The spectrometer was an Ebert mount type with an aluminum, 1200 lines mm^{-1} concave grating, which was used in the first order to give a dispersion of 2.7 Å mm^{-1}. The highest resolution used in these experiments was 0.03Å, or about 1 cm^{-1} at 180 nm.

An air cooled deuterium discharge lamp provided a uniform continuous light source at wavelengths above 150 nm, below this, intense line spectra from the source made data collection impossible.

Plate exposures using Kodak SWR film were taken at intervals of up to eight hours. Since this was a vacuum spectrograph, it was possible to seal in the gas; only on one occasion was leakage a problem as evidenced by the presence of the sharp Schumann-Runge lines of oxygen. Densitometer tracings of the plates also revealed N_2O banding, but did not show noticeably more detail than the room temperature results obtained with the Cary, this was probably because noise reduction was not possible on the MacPherson spectrograph and the plates are inherently less sensitive than a photomultiplier.

D. Data Processing and Graphics

1. Techniques

The data collected on a time basis by the Fabritek corresponded to a linear wavelength scale on the Cary, and was converted to a wavenumber basis by use of the formula,[102]

$$\nu = 10^7 \, (\eta\lambda)^{-1}$$

Here, the index of refraction of nitrogen, η, was taken to be 1.00035, and λ is the wavelength in nanometers.

Gas concentration was calculated by using the ideal gas equation. To avoid error in using this equation, experimental conditions near critical points were not used.

After signal averaging was completed for both the sample and background spectra, and the normalized background spectrum was subtracted from the normalized sample spectrum, a three point digital smooth of the type

$$\sum_I Y(I) + Y(I-1)/4 + Y(I)/2 + Y(I+1)/4$$

was applied to the final result. Since the three data points covered 0.06 nm and the resolution was 0.05 nm, it was not felt that information would be lost in this smoothing process. Comparison of the spectrum before and after smoothing did not reveal any noticeable differences except for reduction in the high frequency noise background.

2. Graphics

The quantitative data set at eleven different temperatures served as the experimental basis for the analysis to be discussed in the next subsection. In doing this programming analysis, it was of invaluable aid to have a graphical display of the calculation results. This

was made possible by the use of the graphics package available at LBL. The graphics routine IDDS was used for drawing the figures and slides along with on-line display units such as the Tektronics 4014 CRT display and with either calcomp or microfilm hard copy units.

The graphics program allows for variable scaling and size of output, and either plots points using two dimensional variable arrays or connects the points to give lines. Because the data points are close the plots appear smooth. For most spectra shown in this section, computer-generated 35 mm frames were photographically enlarged to give the figures, labels and plots.

All programming was done in Fortran IV with most programs run as batch jobs, although for some uses interactive programming was found to be more useful. In the appendix, two programs are listed.

3. Scale of Figures

It was found to be convenient to express the data in linear multiples of 10^{-19} cm^2 cross section. For this reason, all spectra in this section express the cross section (CSN) in units of 10^{19} cm^2 in the ordinate axis, and the abscissa axes of all figures have the same linear range of wavenumbers, cm^{-1}, corrected for vacuum. Care is necessary in the examination of these figures since the scaling of the ordinate axis varies from 0 to 5×10^{-19} cm^2 in one case to 0 to 0.3 or 0.8 to 1.2×10^{-19} cm^2 in other cases, as is needed to show the necessary detail.

The intensities of all data presented are quantitatively accurate to about 4% in absolute absorption cross sections, and the relative error of peak intensity is about 1%. For quantitative comparison

of the difference spectra only the relative intensity of peak-trough may be used.

It may be useful to compare the intensities given here with the approximate spectral intensities of other molecular absorptions:[78a]

O_2:	maximum of Schumann-Runge continuum,	1.3×10^{-17} cm^2
	Herzberg continuum at 230 nm,	2.3×10^{-24}
	SchumannRunge band structure, max.	1×10^{-19}
O_3:	maximum of Hartley band,	1.1×10^{-17}
	maximum of Chappuis band,	5×10^{-21}
H_2:	Lymann ,	$\sim 4 \times 10^{-16}$
SO_2:	maximum at 285 nm,	1.0×10^{-18}
CO_2:	maximum at 147 nm,	7×10^{-19}
CCS:	maximum at 223 nm (room temp),	3×10^{-19}
N_2:	rayleigh scattering at 300 nm,	2×10^{-25}

To convert from absorbance coefficient, cm^{-1} to cross section, cm^2, divide by 2.5×10^{19}.

E. Results

1. Temperature Effect on the Structured and Continuous Absorption

The composite profile of the absorption spectrum at eleven different temperatures from 151 to 485 K is shown as figure 15. The cross sections are believed accurate to 4%. At all temperatures a banding progression is seen superimposed on a continuous background, although at higher temperatures the banding is most pronounced. The increase in absorption in intensity and to longer wavelengths with increasing temperture has been observed by Holliday and Reuben[13].

The temperature profile shows that many of the observed broad peaks and shoulders are really composites of overlapping peaks which are resolved at lower temperatures. The effect of temperature is seen to be most pronounced on the peak structuring. The rate of temperature dependent increase varies among different members of the banding. The feature at 53200 cm^{-1} at 485 K is seen to be composed of three different peaks; at 151 K the high energy member is most intense, but at increasing temperatures, the low energy member increases rapidly and becomes predominant. The effect of temperature on the apparent underlying continuum is most noticeable at longer wavelengths.

2. Three Meter Spectrograph

The room temperature spectrum taken on the 3 m vacuum spectrograph is shown in figure 16. It is clear from this figure that the structuring continues at wavelengths below the limit of the Cary spectrometer. Since plates were used, only approximate relative intensities can be estimated.

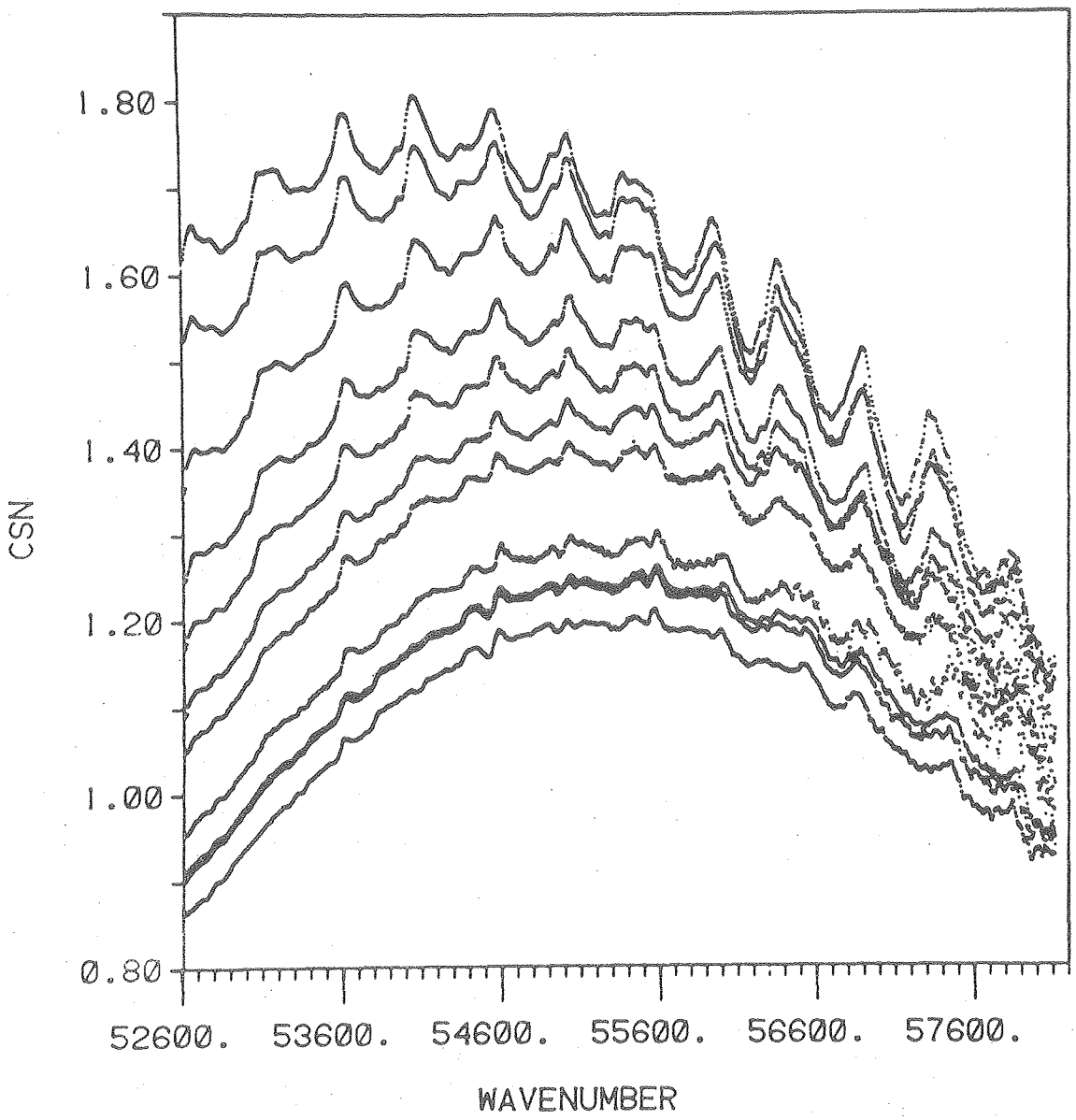

XBL 792-8250

Figure 15

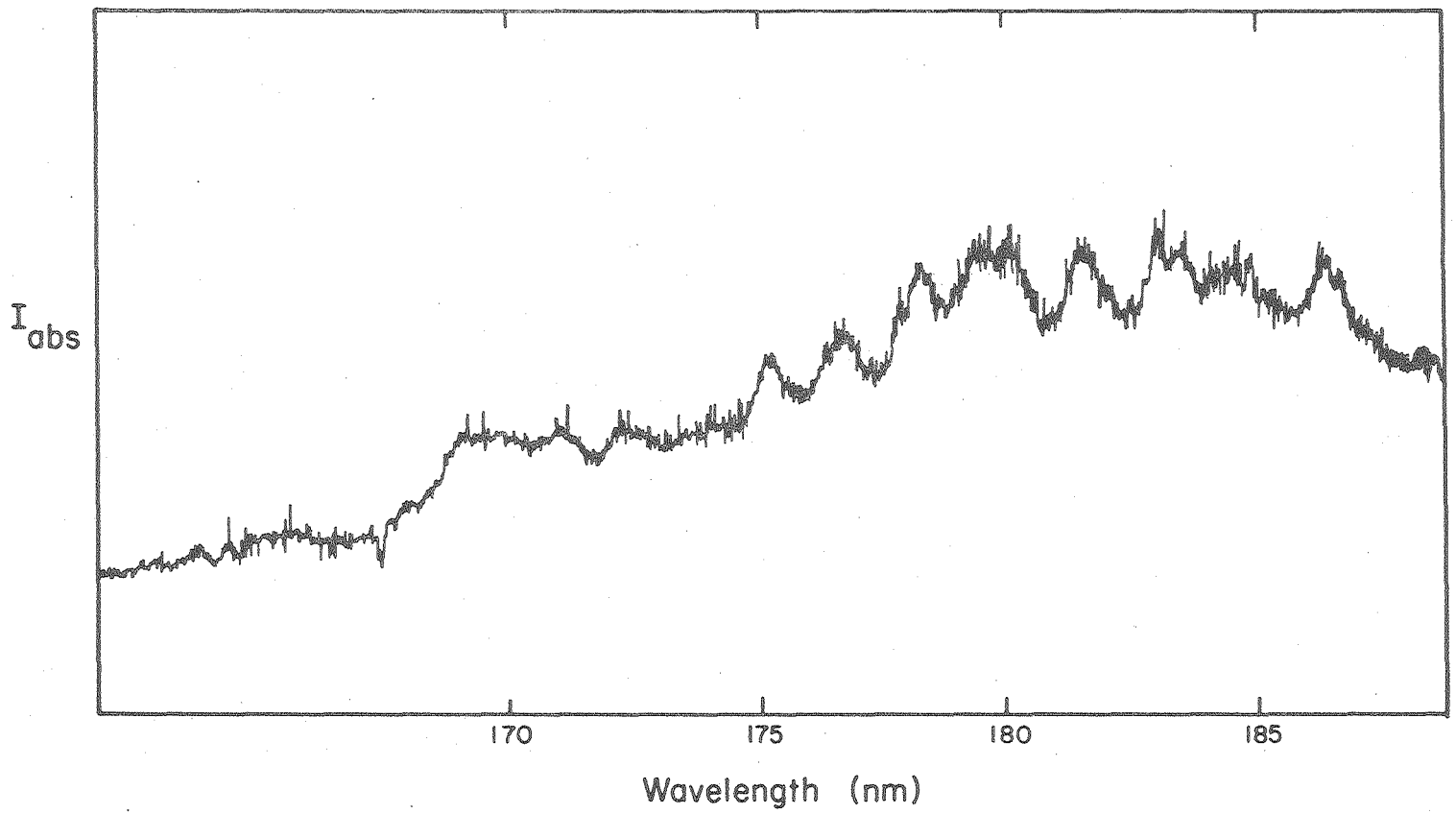

XBL 792-8574

Figure 16

F. Discussion

1. Contribution of Cold and Hot Bands of $X^1\Sigma^+$

Using the fundamental vibrational frequencies of nitrous oxide (1285, 589, 2224 cm^{-1}), it is possible to calculate the fractional population of vibrational states in the ground electronic state for any given temperature[95]. Since at the lowest temperature studied, 151 K, only 0.7% of the molecules are in the (010) state, this spectrum provides a good approximation to the spectrum of the "pure" (000) state. Weighting this spectrum by the fractional (000) population for each of the five highest temperatures studied, and subtracting the resultant spectral contribution of the (000) molecules from each of these five highest temperatures, the difference spectra obtained represent the spectral contributions of all the vibrationally "hot" molecules at these temperatures. It is possible to identify which active vibration or vibrations are responsible for these difference spectra by dividing the difference spectra by the fractional equilibrium populations of (010), (020), (100), (110), (001) and so on. Only for the (010) state with its activation energy of 589 cm^{-1} are the normalized "hot" spectra consistent and in agreement for all five highest temperatures. Applying the same procedure but using an activation energy of $2\nu_2$ or ν_1 yields widely varying normalized results for each of the five highest temperatures indicating these modes could not be primarily responsible for the observed temperature effect. Use of colder spectra for the derivation of the hot bands is less reliable due to the large error incurred by dividing a smaller temperature effect by a very small number.

The process may be summarized by use of the simple formula:

$$B(\lambda) = \frac{Y(\lambda,T) - a(T)A(\lambda)}{b(T)}$$

where A and B are the spectra of the (000) and (010) states respectively for 100% occupancy, Y is the observed spectrum at temperature T, and a and b are the fractional equilibrium populations of (000) and (010) at T. The first iteration provides an approximation to the (010) state spectrum, which is then used to correct the 151 K spectrum for the spectral contribution of the 0.7 per cent of (010) molecules present. The process is then repeated through an iterative procedure and convergence occurs quickly with the final result shown in figure 17.

The large affect of the bending vibration is very apparent in figure 17. Most of the structuring is seen to result from the excitation of the bending vibration although a small amount of structuring is seen in the pure (000) spectrum. The observed continuum is also enhanced and is red-shifted somewhat from the maximum of the (000) spectrum. The presence of a vibrational progression is noted in the (010) state spectrum, but this will be addressed later.

The reverse procedure of weighting each state spectrum by the fractional population of (000) and (010) for a given temperature and convoluting, allows a comparison of this composite spectrum with the observed spectrum over a wide temperature range. For clarity, in figure 18, the composite spectrum (solid lines) is compared with the observed spectrum (data points shown) for every other temperature studied. Figure 18 shows good agreement at some temperatures and fair agreement at other temperatures. Of the eleven temperatures studied, two were used to derive the state spectra and therefore are not independent

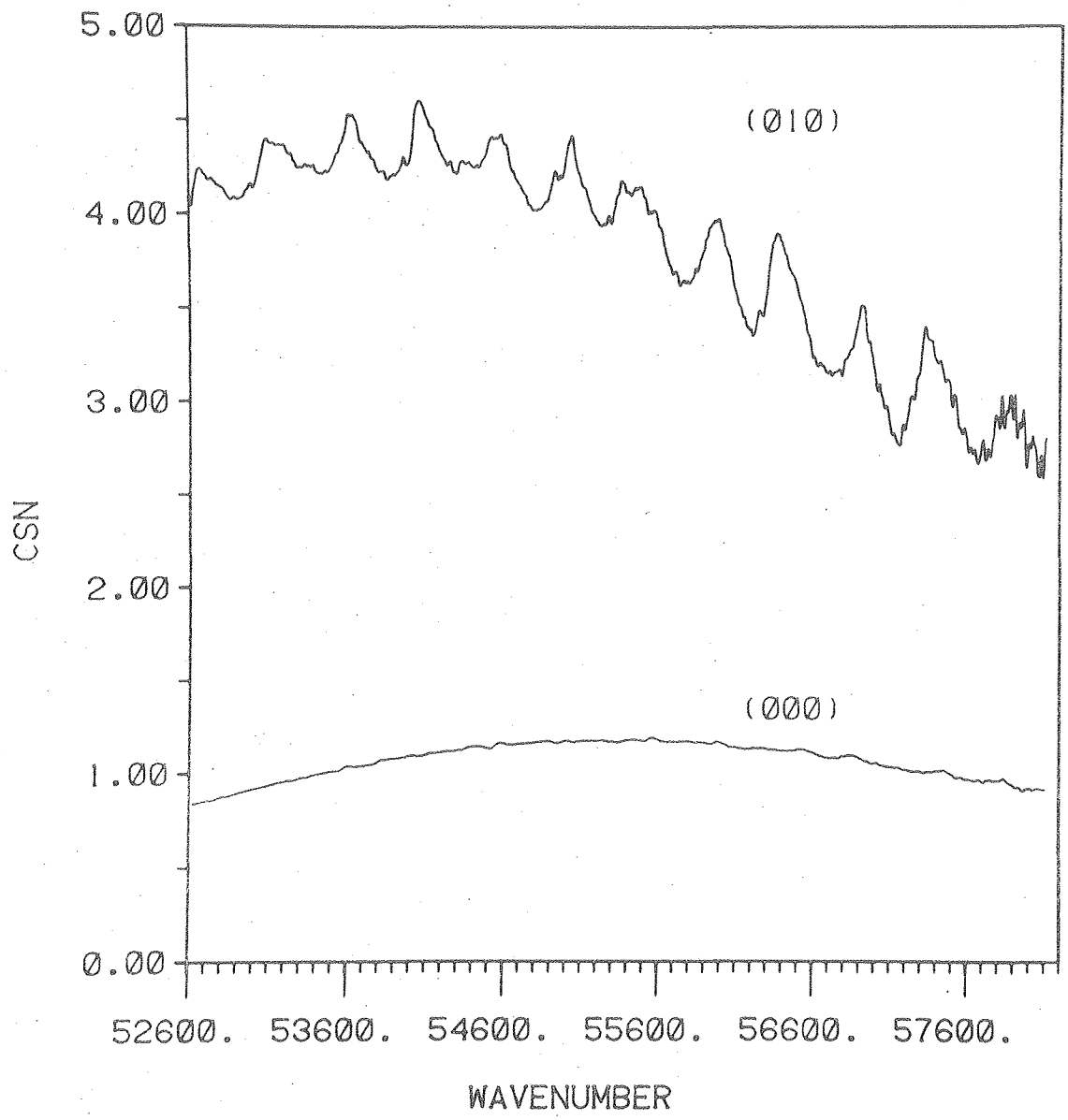

XBL 792-8249

Figure 17

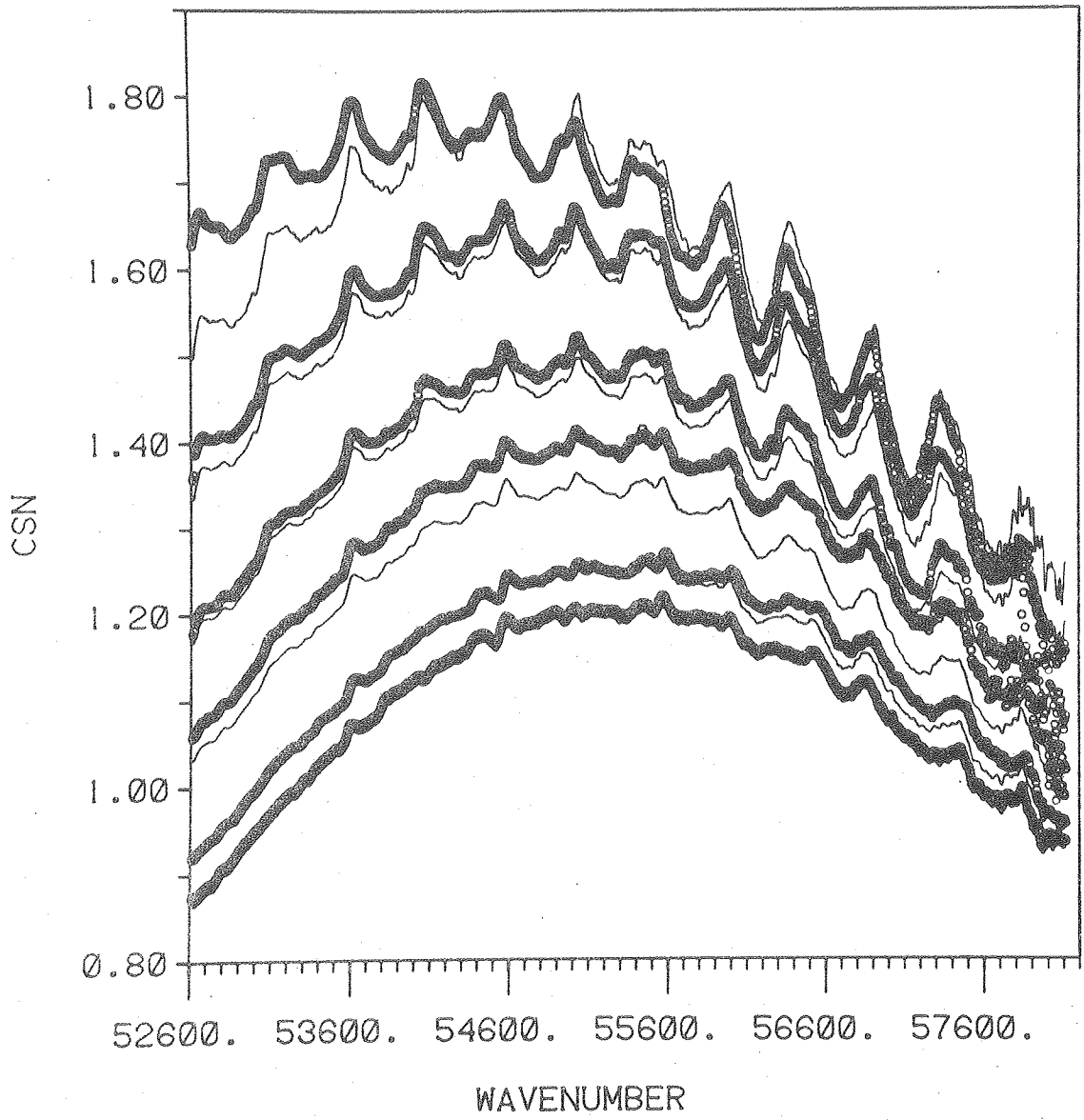

XBL 792 8246

Figure 18a

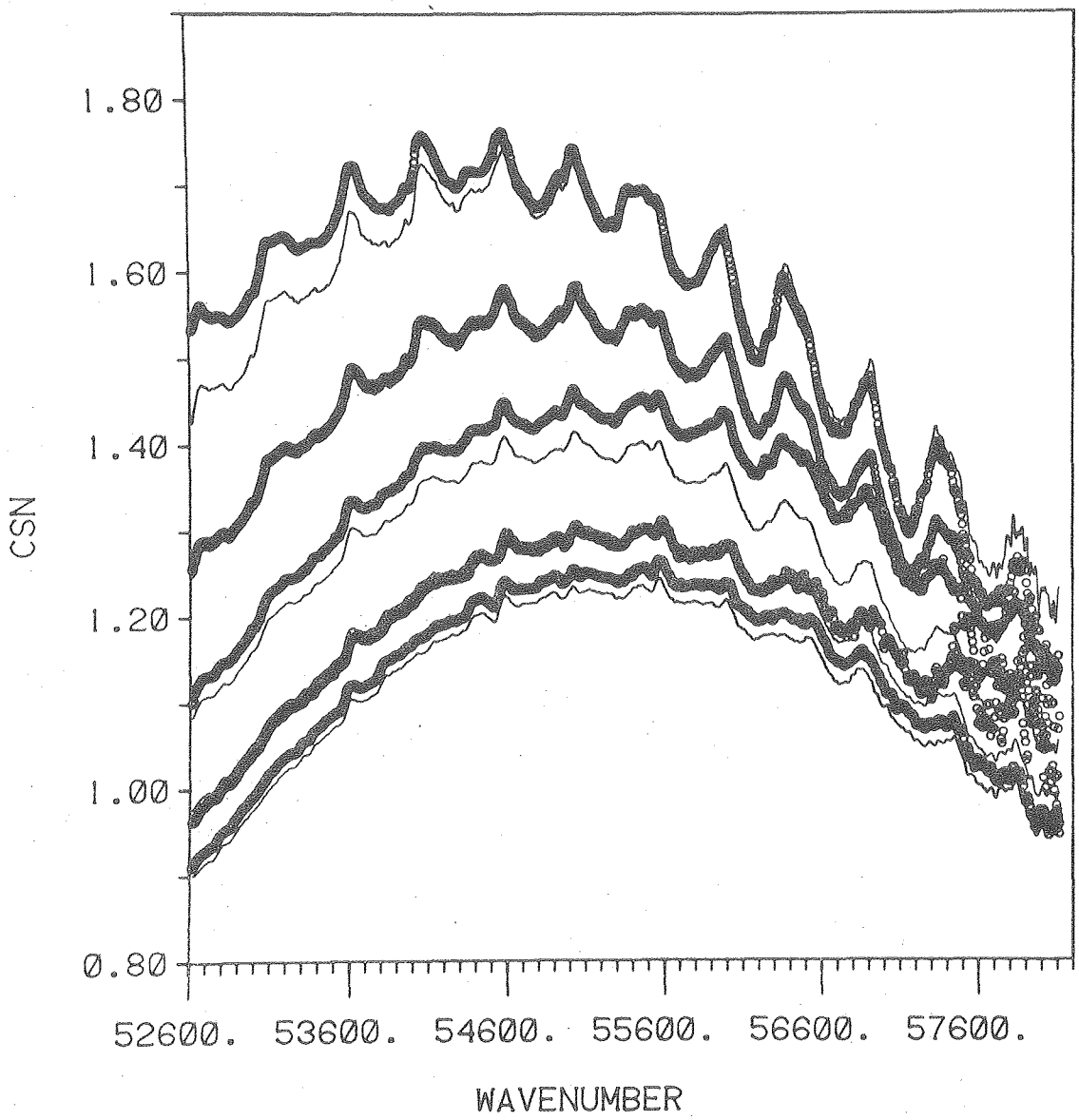

XBL 792-8247

Figure 18b

comparisons by this method. Table 4 lists for every temperature studied the correlation coefficients,[116] which measure shape similarity but are insensitive to a constant displacement. In this table, the two temperatures used in the derivation of the two state spectra will necessarily yield a correlation coefficient of 1.0000, but the correlation coefficients of the other nine temperatures demonstrate that the convoluted spectrum closely approaches the actual absorption spectrum.

From figure 18, we see that this method tends to underestimate the absorption at the highest temperature, 485 K, because at this temperature this method ignores the increasingly substantial population and spectral contribution of higher vibrational species. Similarly, in the derivation of the (010) state spectrum, this method unavoidably includes the interfering contribution of the (020) state spectrum present from the small equilibrium population of (020) at this temperature, and so at lower temperatures where there is essentially no (020) population, this convolution tends slightly to overestimate the absorption.

The overall conclusion from the agreement shown in figure 18 and table 4 is to confirm the assignment of ν_2, the bending vibration, as the "active" vibration which is responsible for the bulk of the observed temperature dependence in figure 15. Had it been the small population of another vibration, say (100) or (001) and their respective energies of activation governing the rate of temperature dependent increase of the spectrum, then this process would not converge for this noticably different activation energy of the vibrational mode. The further result that the two state spectra and their respective activation energies may be used to predict the spectra at temperatures

other than was used in their derivation, supports the assignment of these state spectra and their shape and intensities.

2. Second Order Approximation to the Hot Bands

In the derivation of the (010) state spectrum it was assumed that only two primary absorbing species were involved in the absorption spectrum: the (000) vibrational mode and a single hot band. This hot band was identified as the (010) vibrational mode because only for this respective activation energy was convergence of the normalized state spectrum achieved for several temperatures. It was also noted in the preceding discussion that the derived (010) spectrum was likely to contain some character of (020) because the iterative method used could not separate three contributing species. The (020) interference is probably not too great because the (020) population is about 1.5 percent compared to the 13.3 per cent population of (010) at 333 K. Unlike (010), the (020) state will be split into one component with two quanta of angular momentum, $(02^2 0)$, and one without net angular momentum, $(02^0 0)$. The ψ_{ev} of the $(02^0 0)$ state is $^1\Sigma^+$, and since it has not net angular momentum, it is likely that the spectrum of this state will be weak, perhaps weaker than the (000) state spectrum. This is because its probability amplitude is shaped more sharply about 180° than (000) and so for a bent-linear transition, the $R_{e'e''}(q,Q)$ factor of the transition moment will be smaller. (This is assuming that the transition is forbidden in linear case, but is allowed in a bent configuration. More evidence for this will be presented.)

The $(02^2 0)$ state with an ψ_{ev} of $^1\Delta$, has a net quantum of angular momentum. It is then likely to resemble the (010) state spectrum in intensity and may in fact be stronger due to its greater equilibrium bond angle. The population of $(02^2 0)$ at 333 K is about 1 per cent

which makes for an expected relative error of about 7 - 20% in the derived (010) spectrum depending on the extent of the (02^00) contribution and the wavelength examined.

By supplementing the previous method with an additional tier, it is possible to partially correct the (010) state spectrum for the interference of these higher order vibrations, particularly the bending vibrations. The disadvantage of this second order approach is that in solving for higher order vibrations which have very small populations and similar spectra, as in the case of (020) and (030), the final, normalized result of these spectra becomes increasingly unreliable and noisier. Specifically, in this case we are solving for 3% of the molecules at 485 K, so the degree of instrumental noise and the accuracy of data becomes extremely critical to the final result. It is unreasonable to expect then that the resulting normalized (020) and (030) state spectrum to accurately reflect the actual spectra of these higher order vibrations, but the use of this result in partially correcting the (010) state spectrum for higher order contributions is more reasonable. This is because the (010) spectrum derived previously contains only a 1% contribution of the normalized state spectra of these higher order vibrations.

Figure 19 shows the result of this second order iterative procedure. In deriving this result, three temperatures were used, 151, 333, and 485 K, to derive the (000), (010) and ((020) + (030)) state spectra. It is seen that the contribution of the higher order vibrations is most noticeable at longer wavelengths. It is not known whether the contribution of these higher order vibrations is negligible at short

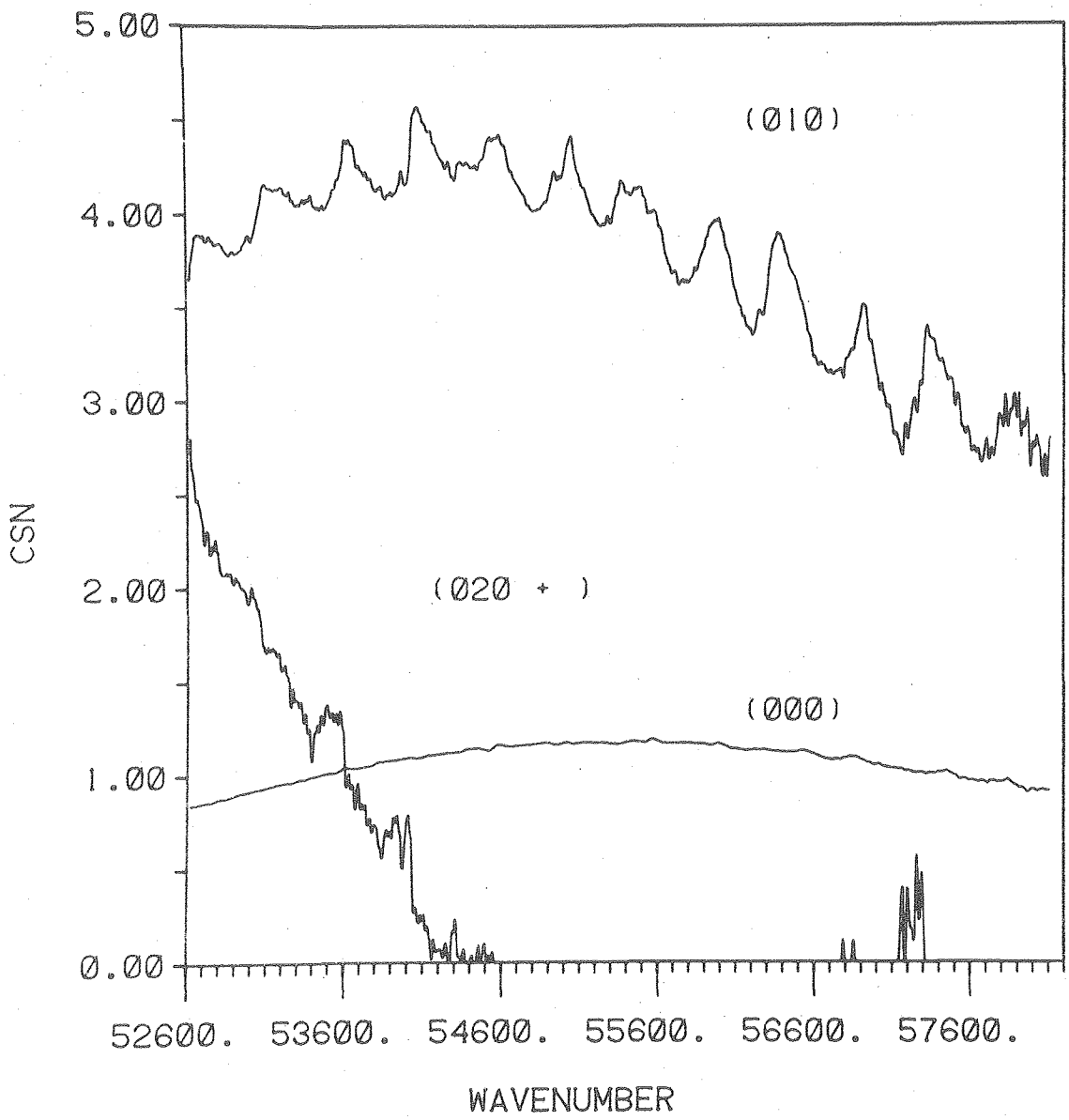

XBL 792-8251

Figure 19

wavelengths, as this result appears to show, or whether this result indicates an intrinsic failure of the method. Only a small portion of the higher vibrational spectrum is seen; this may indicate a maximum at much longer wavelengths (as demonstrated in Section II, the absorption of nitrous oxide extends to about 260 nm) although this is not possible to tell with the limited data base of this section. As expected, the (000) state spectrum is unchanged by this second order approach; the population of (020) at 151 K is about 4×10^{-3} per cent. The (010) state spectrum is unchanged at the short wavelengths, but at longer wavelengths the overall absorption is noticeably reduced, resulting in a sharper maximum than the overall appearance of the result which indicated a slightly sloping, flat maximum. Convolution of the three state spectra to give a composite spectrum gives an improved fit to the observed spectra, as indicated in figure 20 and table 4. Again, since three temperatures in this case were used to derive the state spectra, these are not independent measurements, but comparing the correlation coefficients in table 4, the improved fit of the second order approach can be seen for the other eight temperatures.

The logical process used to derive the three state spectra is outlined on the following page.

Use of higher temperatures than 485 K to derive the state spectra of higher order vibrations, was considered but rejected because the (100) state would also become occupied at nearly the same rate, as would (030) and so higher temperatures would only complicate the result increasingly. A more reasonable approach might be to cross the gas sample with a tuned, high power IR laser to selectively excite normal

Table 4. Comparison of the Correlation Coefficients of Convoluted and Observed Spectra for Each Temperature.[38a]

Temp., K	First Order Iteration	Second Order Iteration
	Correlation Coefficients	
151	1.0000	1.0000
182	0.9991	0.9992
196	0.9926	0.9935
223	0.9571	0.9619
247	0.9954	0.9963
268	0.9797	0.9812
301	0.9911	0.9908
333	1.0000	1.0000
372	0.9963	0.9968
423	0.9773	0.9935
485	0.9593	0.9902

First Order Iteration Sequence:

$$Y(T) = a(T)A + b(T)B + c(T)C$$

assumes $a = 1.000$, $b = 0$, $c = 0$ $\qquad T = 151$ K

$$A' = Y(T)$$

$$B'(\lambda) = \frac{Y(T) - a(T)A'}{b(T)} \qquad T = 333 \text{ K}$$

$$A''(\lambda) = \frac{Y(T) - b(T)B'}{a(T)} \qquad T = 151 \text{ K}$$

$$B''(\lambda) = \frac{Y(T) - a(T)A''}{b(T)} \qquad T = 333 \text{ K}$$

repeat sequence until covergence for B and A

Second Order Iteration Sequence:

$$C'(\lambda) = \frac{Y(T) - a(T)A'' - b(T)B''}{c(T)} \qquad T = 485 \text{ K}$$

$$B'''(\lambda) = \frac{Y(T) - a(T)A'' - c(T)C'}{b(T)} \qquad T = 333 \text{ K}$$

$$A'''(\lambda) = \frac{Y(T) - b(T)B''' - c(T)C'}{a(T)} \qquad T = 151 \text{ K}$$

$$C''(\lambda) = \frac{Y(T) - a(T)A''' - b(T)B'''}{c(T)} \qquad T = 485 \text{ K}$$

repeat sequences until convergence for A, B and C

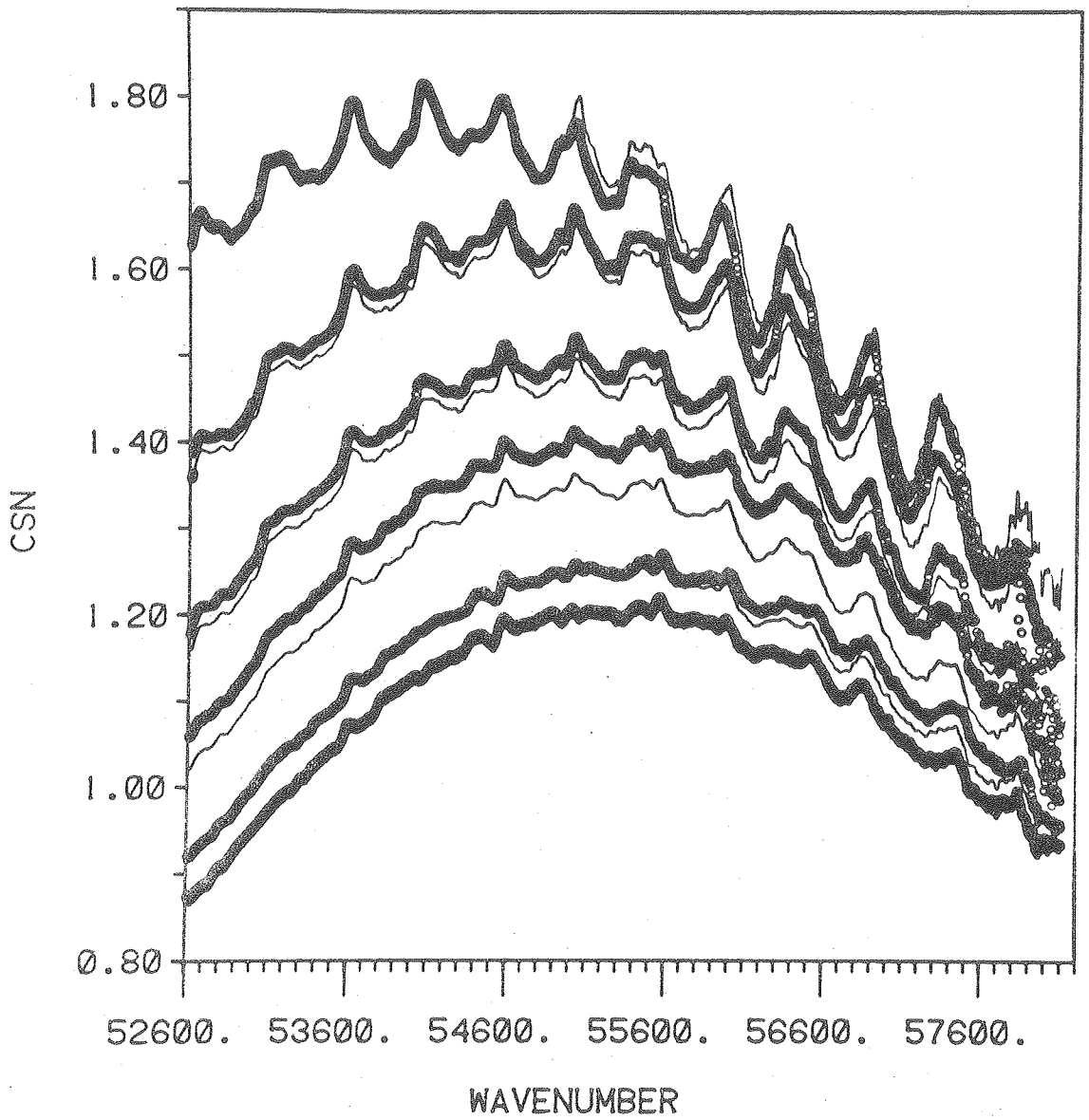

XBL 792-8245

Figure 20a

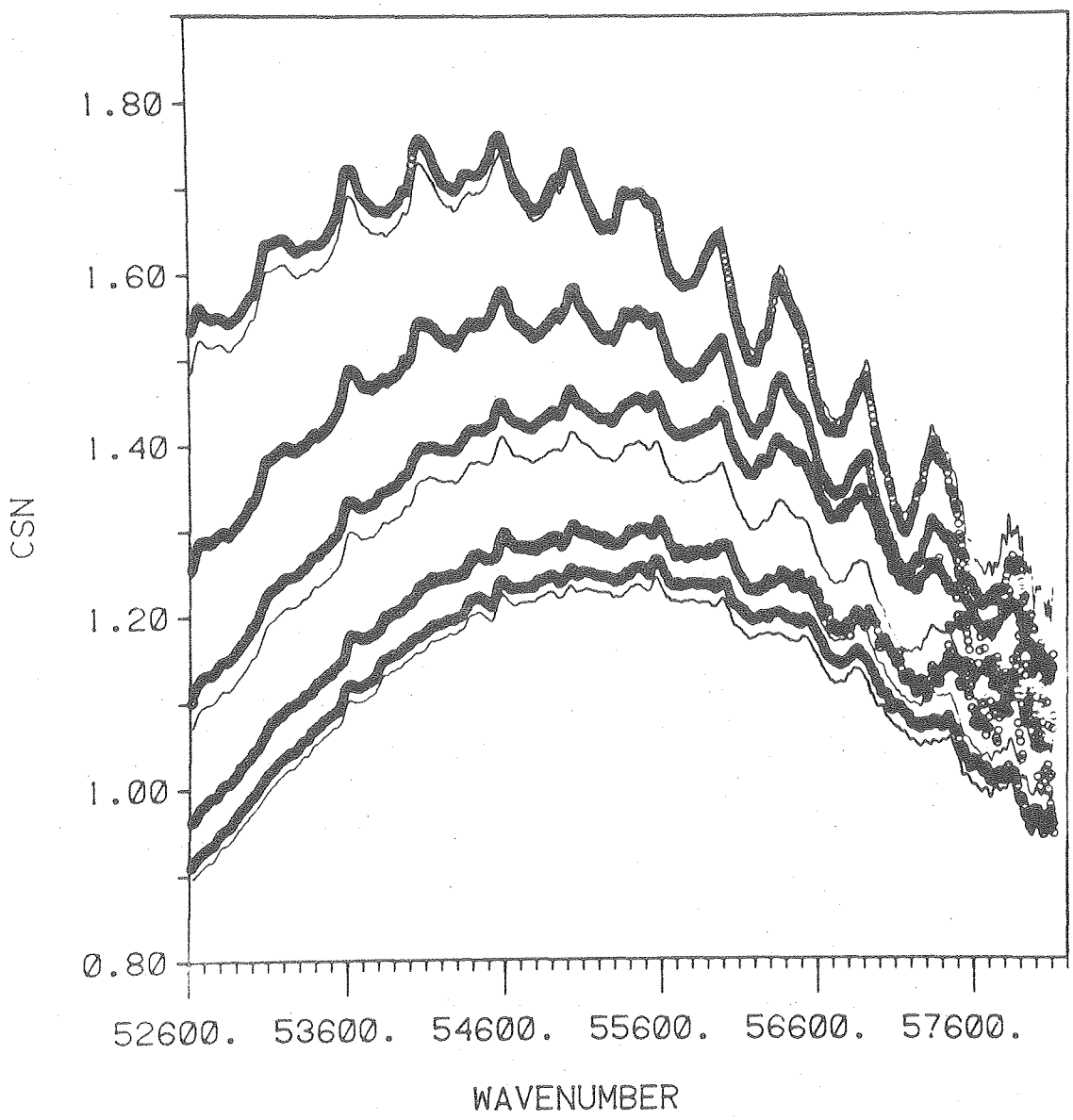

XBL 792-8253

Figure 20b

vibrations and calculate the excited species population knowing the absorbed IR power, the quenching rate, and the temperature. Most likely this would involve excitation of selective rotational quanta and then forming a Maxwell-Boltman average to simulate temperature equilibrium.

3. Energy Levels of the Upper Electronic State

In the preceding subsection, the observed spectra of N_2O were separated into the (000) and (010) state spectra. In figure 17, the (010) is seen to be strongly structured and more intense than the (000) state spectrum. Also a progression is apparent, indicating transition to discrete vibrational levels of the upper state. On the scale of figure 17, however, it is not apparent that very weak structuring can be observed in the (000) spectrum.

Figure 21 shows the (000) state spectrum on a different scale plotted as solid lines, along with the 151 K spectrum shown as individual data points. This shows that the effect of correcting the 151 K spectrum for the 0.7% of hot molecules is primarily to reduce the intensity of the 151 K spectrum by a small amount and that the observed structuring does not arise from this small fraction of hot molecules at that temperature. A weak progression is now observable at this temperature.

Figure 21 also shows an energy weighted Gaussian superimposed on the (000) state spectrum. The function shown is of the type:

$$I_{abs}(\lambda) = \nu N \exp(-D(\nu-\nu_0)^2)$$

where D, N, and ν_0 are constants. This is the equation of an energy weighted Gaussian which is seen to agree with the expected intensity distribution, as outlined in previous sections, by reaching the minima between the peak features.

It is possible the observed spectrum results from a continuous absorption, as the Gaussian curve shown in figure 21, superimposed on a separate second transition to give discrete spectra, represented by the difference between the (000) spectrum and the Gaussian curve.

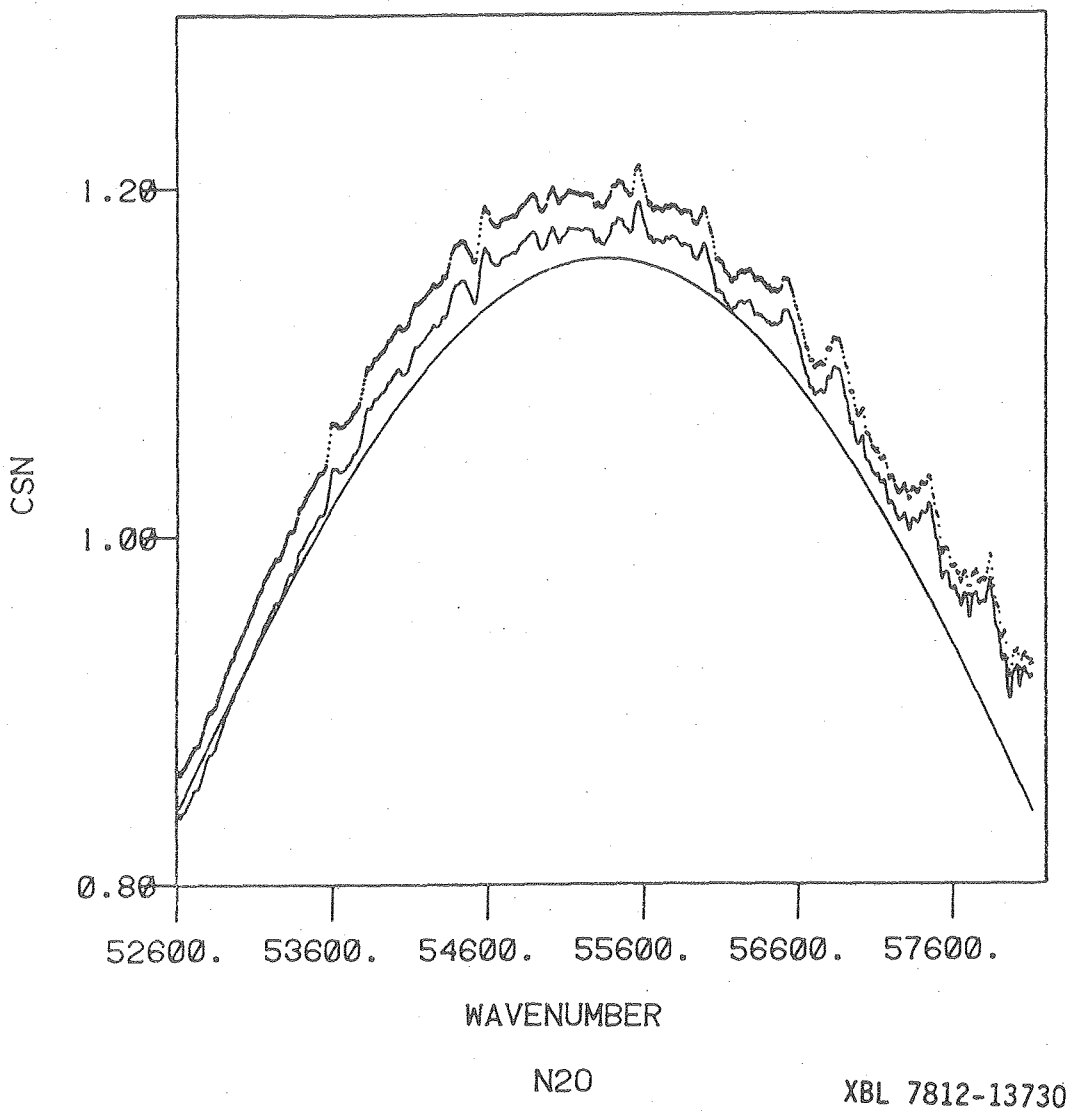
1.20
1.00
0.80
CSN
52600.
53600.
54600.
55600.
56600.
57600.
WAVENUMBER
N2O
XBL 7812-13730

Figure 21

It is also possible that the intensity of the conjugate continuum absorption results from a single, pressure dependent broadening of the banding. The measurements using the 3 m monochromator as a long path cell at pressures between 50 - 200 millitorr would appear to support the former contention. Of course, any intermediate interpretation of the two theories is also reasonable. Interestingly, in the analogous absorption of carbonyl sulfide, Price and Simpson[103] reported that at pressures less than 10 m, the continuous absorption of OCS with superimposed diffuse bands, breaks down into a series of three broad band structured features without a superimposed continuum.

In view of this unconfirmed result and the similar possibility that at lower pressures the continuum may be reduced with a subsequent increase in the apparent banding intensity, the Gaussian curve in figure 21 has been only used as a means of removing the "background" absorption of nitrous oxide.

By fitting a similar curve to the (010) state spectrum, it is possible to remove the background absorption by subtracting a temperature weighted composite of the two Gaussian curves based upon the fractional (000) and (010) populations from the observed spectra. In the resulting difference spectrum the structured spectrum may be studied without the effect of superposition on a slope which tends to change the shape and wavelength maximum of the peaks. Figure 22a shows this result at 151 K. The structuring is quite weak although the progression noted previously for this temperature is now more clearly seen with a spacing of 970 cm^{-1} and is noted by downward arrows. The peak positions of the progression and their separations are noted in table 5. At

Table 5. Vibrational Progression Members at 151 K

Peak No.	ν^{-1}, cm^{-1}	$\Delta\nu^{-1}$, cm^{-1}
1	53 595	
		983
2	54 578	
		989
3	55 567	
		96
4	56 534	
		916 (962)*
5	57 450	
	average spacing:	964

*second figure from the 182 K difference spectrum

this temperature the spectrum is least complicated by hot bands, but the weak intensity of structuring makes analysis difficult. Besides the features fit to the 970 cm^{-1} progression, there are a few other features noted which do not appear to fit another progression.

Figures 22a to 22k show the result of this correction process at each temperature between 151 K and 485 K. Wih increasing temperature, the structuring increases in intensity and the presence of a second, more intense progression with a spacing of about 480 cm^{-1} is becoming increasingly dominant with temperature. At 485 K only this dominant progression is seen as major peak features, although another minor progression is also seen as shoulders on the stronger peaks. The wavenumbers and energy separations of the major features in figure 22k are given in table 6. The slope of the difference spectra at the higher temperatures arises from the contribution of higher-order vibrations (note this is most pronounced at the longer wavelengths.)

It is useful to interpret the relative energy separations of the peak features in these figures in relation to absolute energy levels of the upper electronic state and to see if similar results are present in the less obvious progressions at lower temperatures.

To do this, a program was developed to select the major peak features using the same selection criteria for all temperatures studied. To deal with the very weak, diffuse banding as in the colder temperatures in the same objective way as the greater intensities as in figure 22k it was necessary in the peak selection process to utilize width and height criteria as well as an inflection in the first derivative of the plot. Without such width and height criteria, a simple inflection

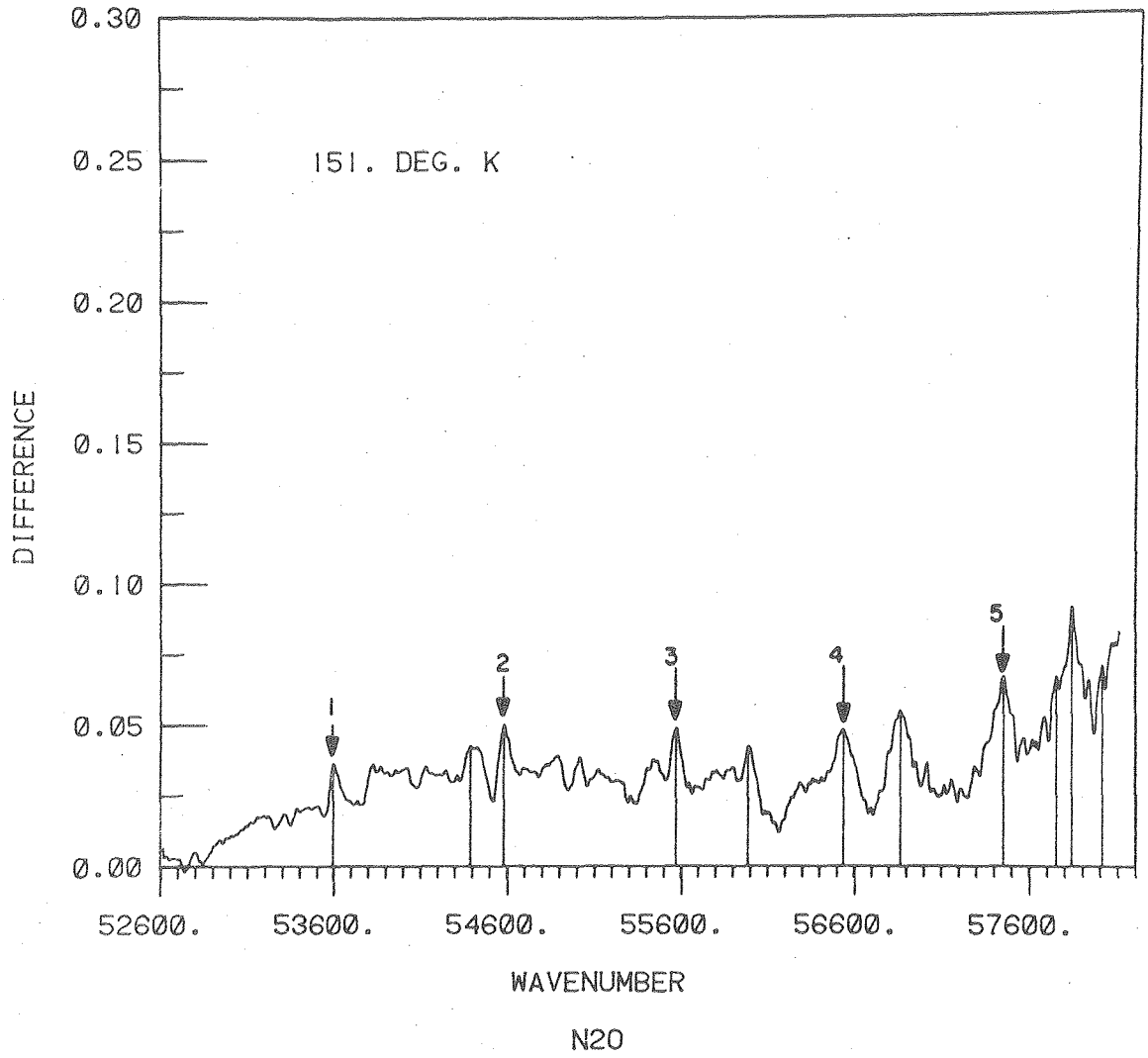

XBL 792-8397

Figure 22a

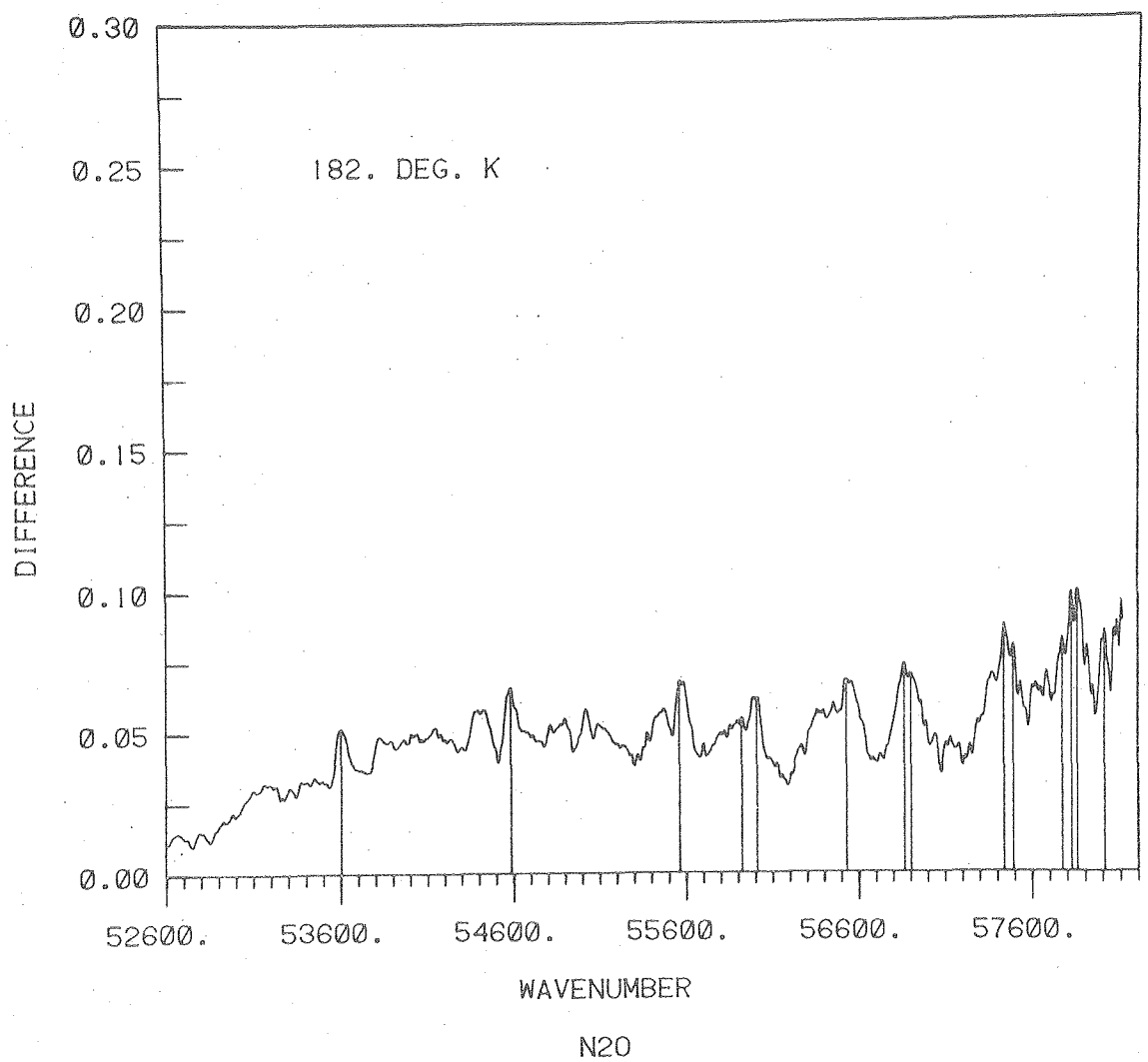

XBL 7812-13973

Figure 22b

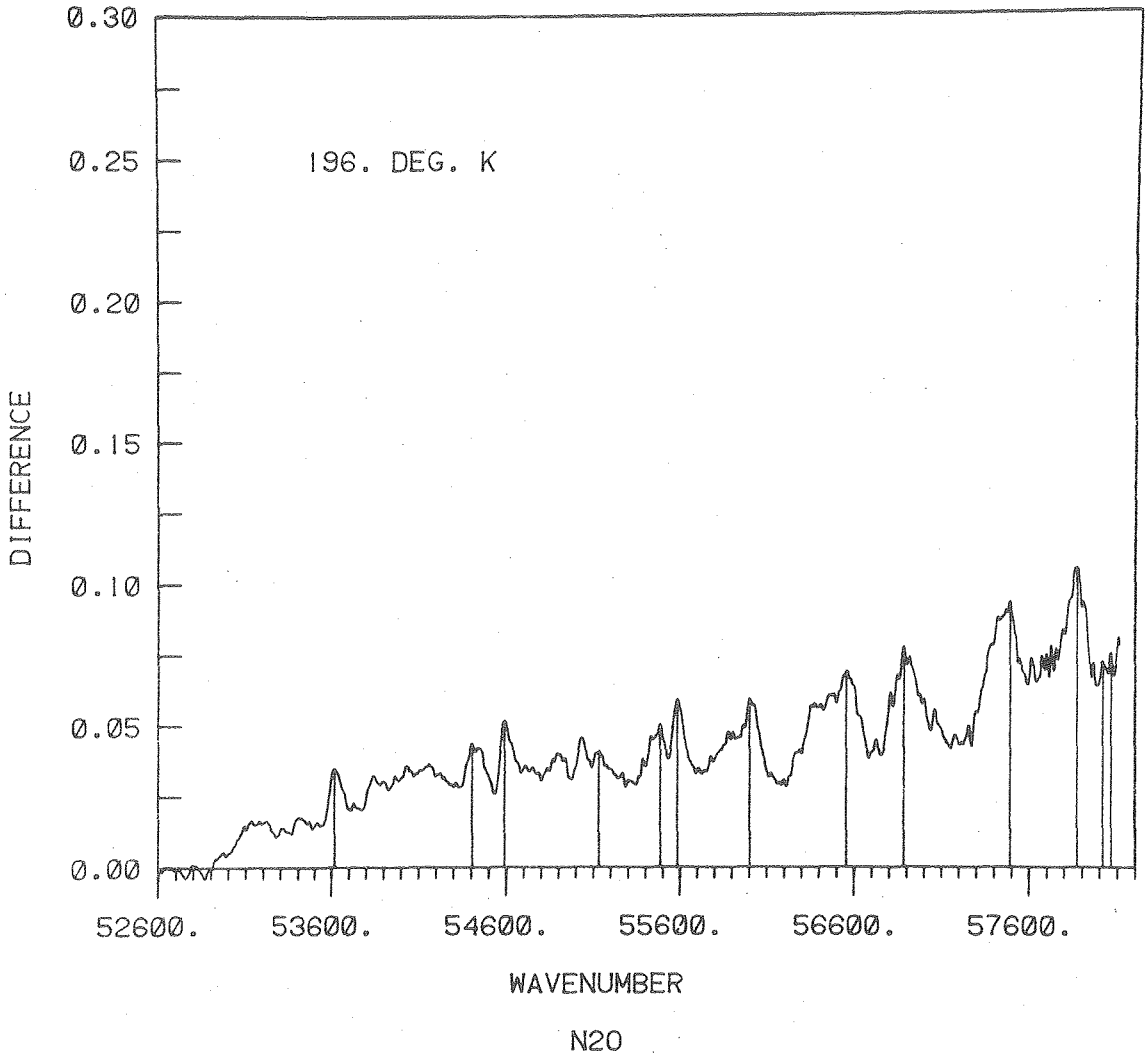

XBL 7812-13972

Figure 22c

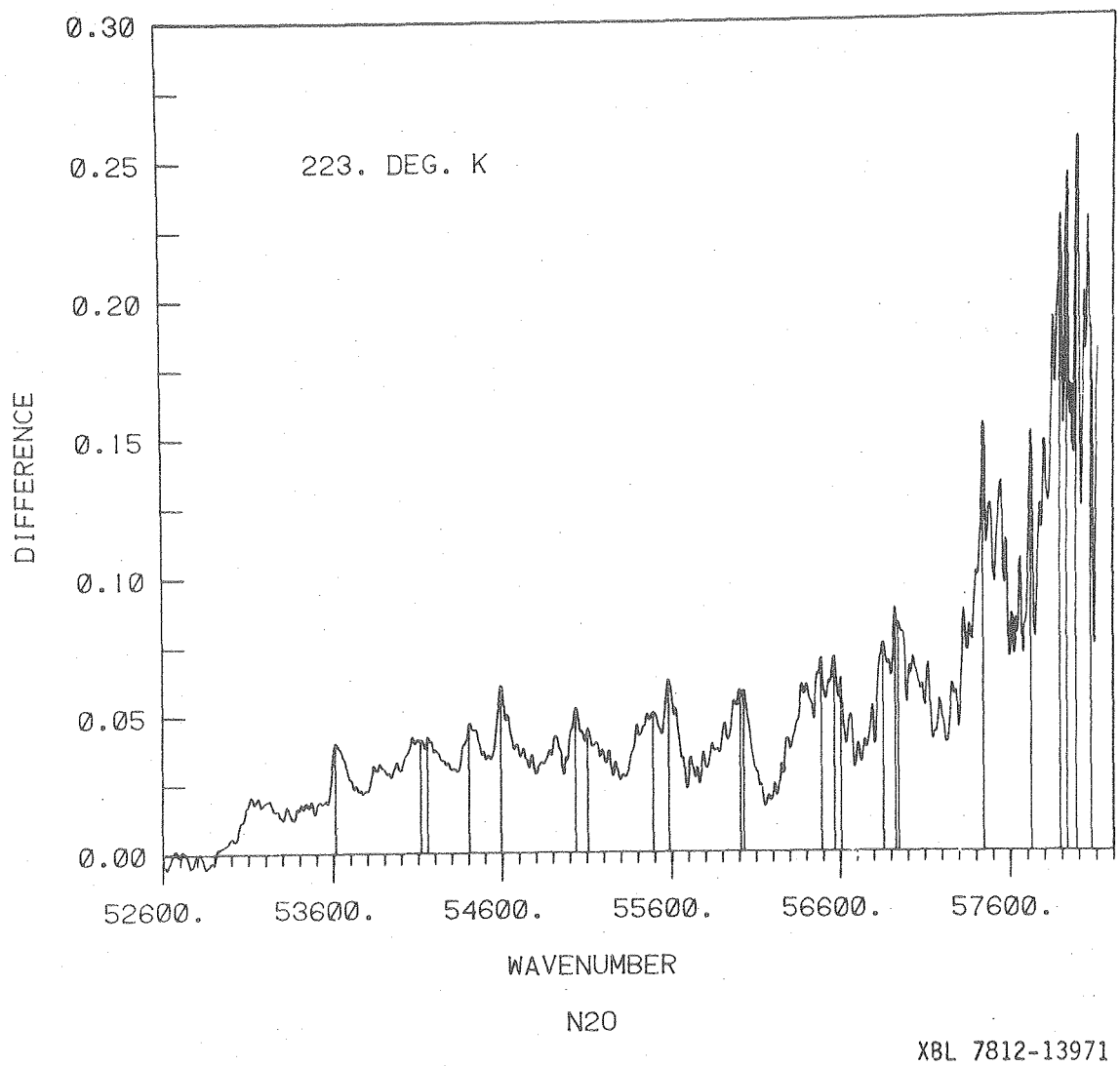

XBL 7812-13971

Figure 22d

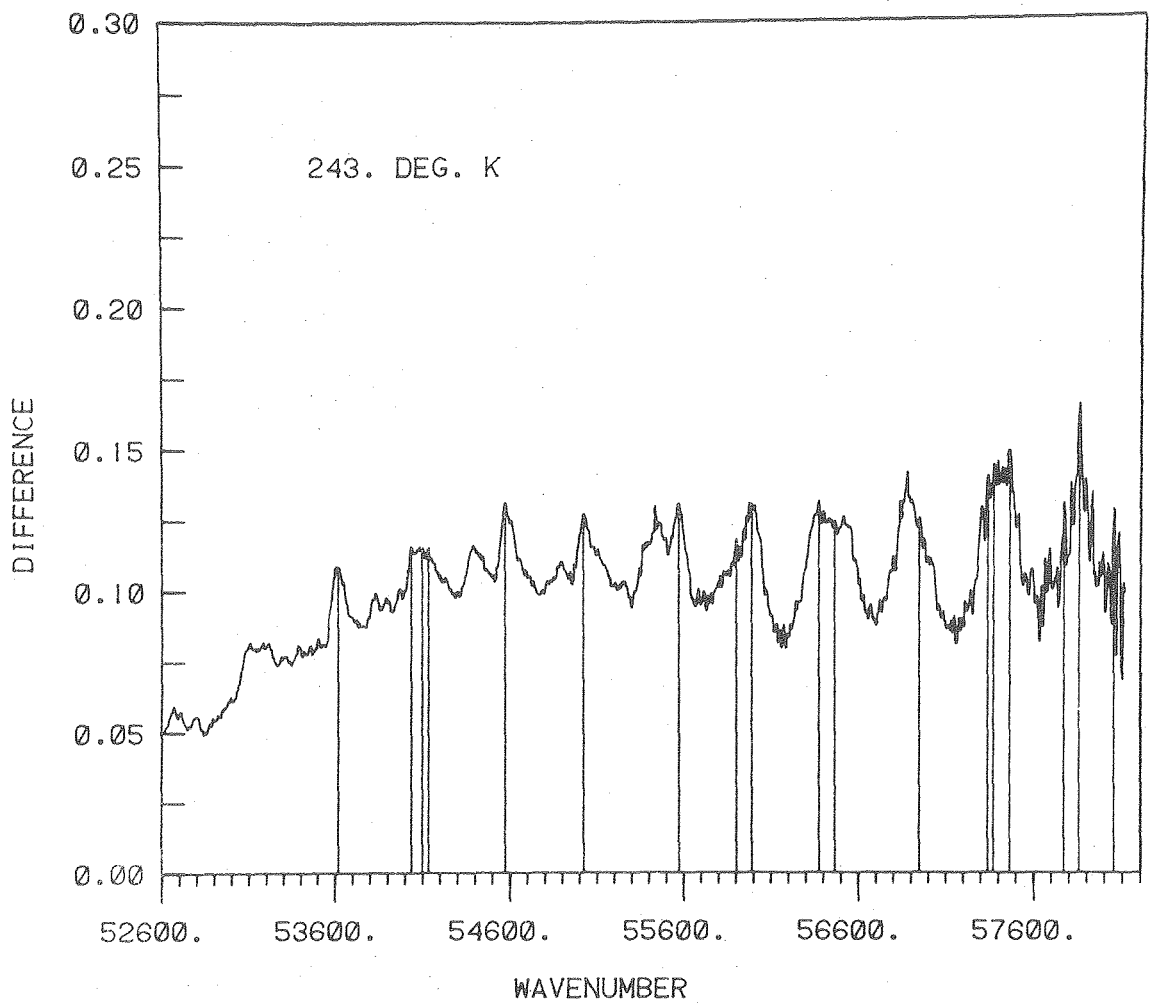

N2O

XBL 7812-13976

Figure 22e

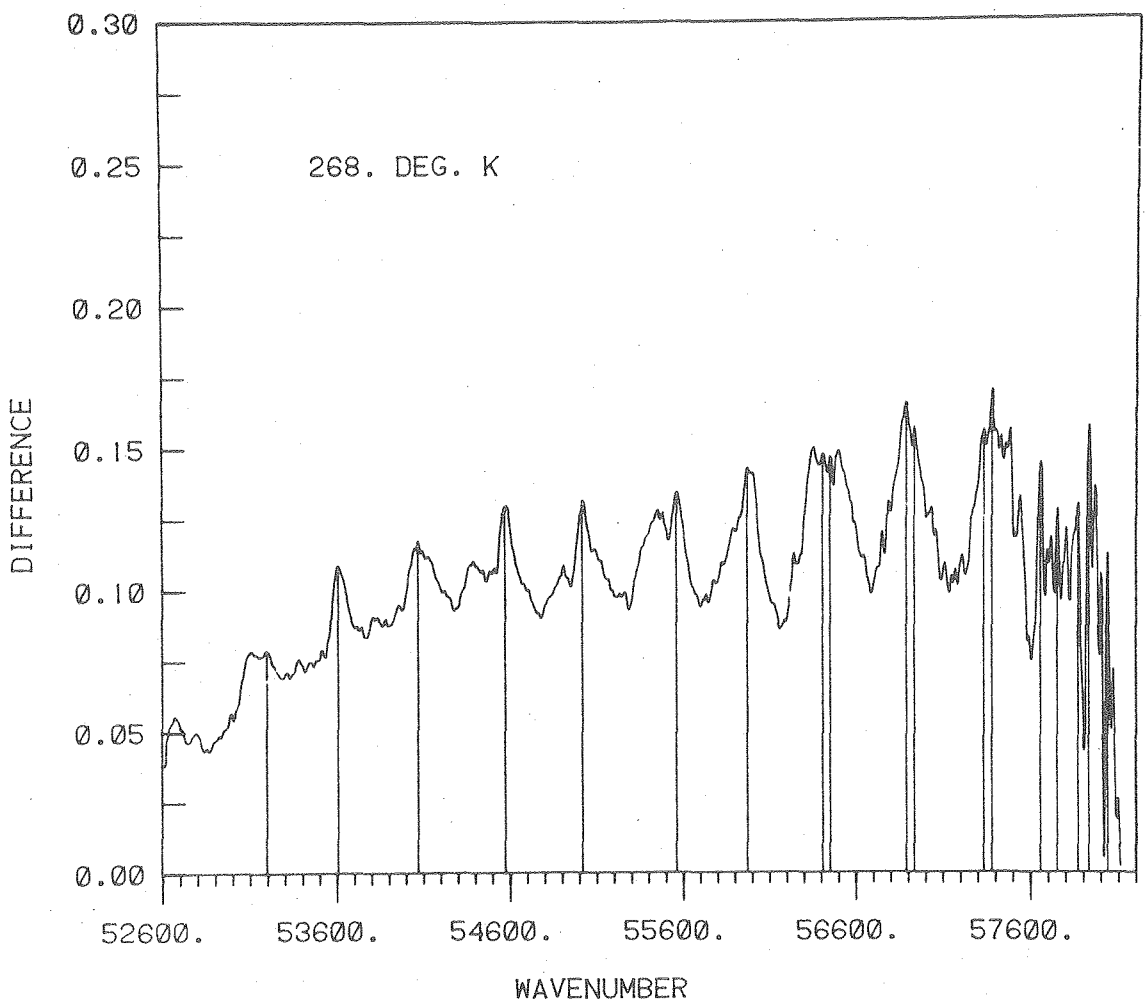

N20

XBL 7812-13977

Figure 22f

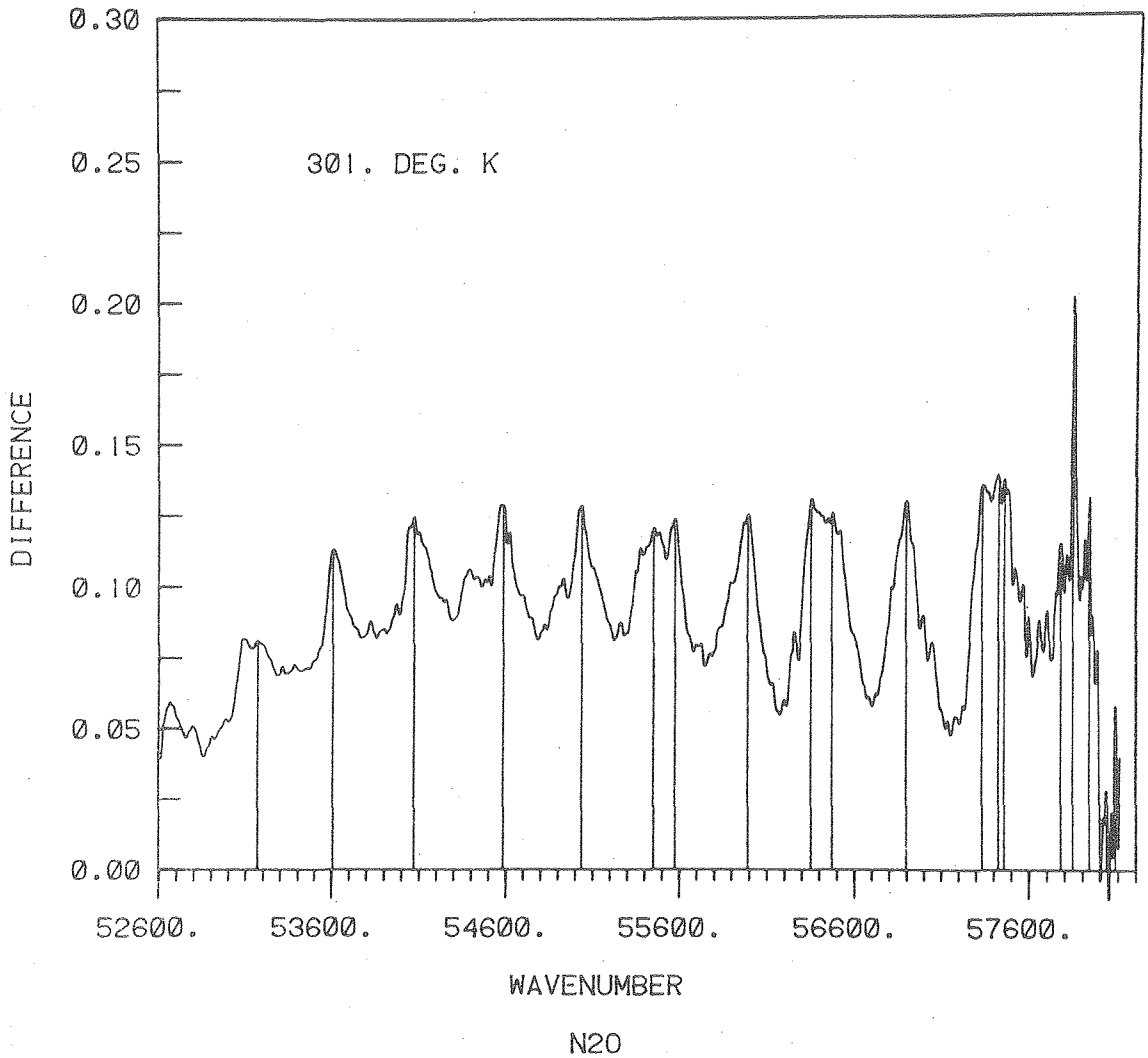

XBL 7812-13975

Figure 22g

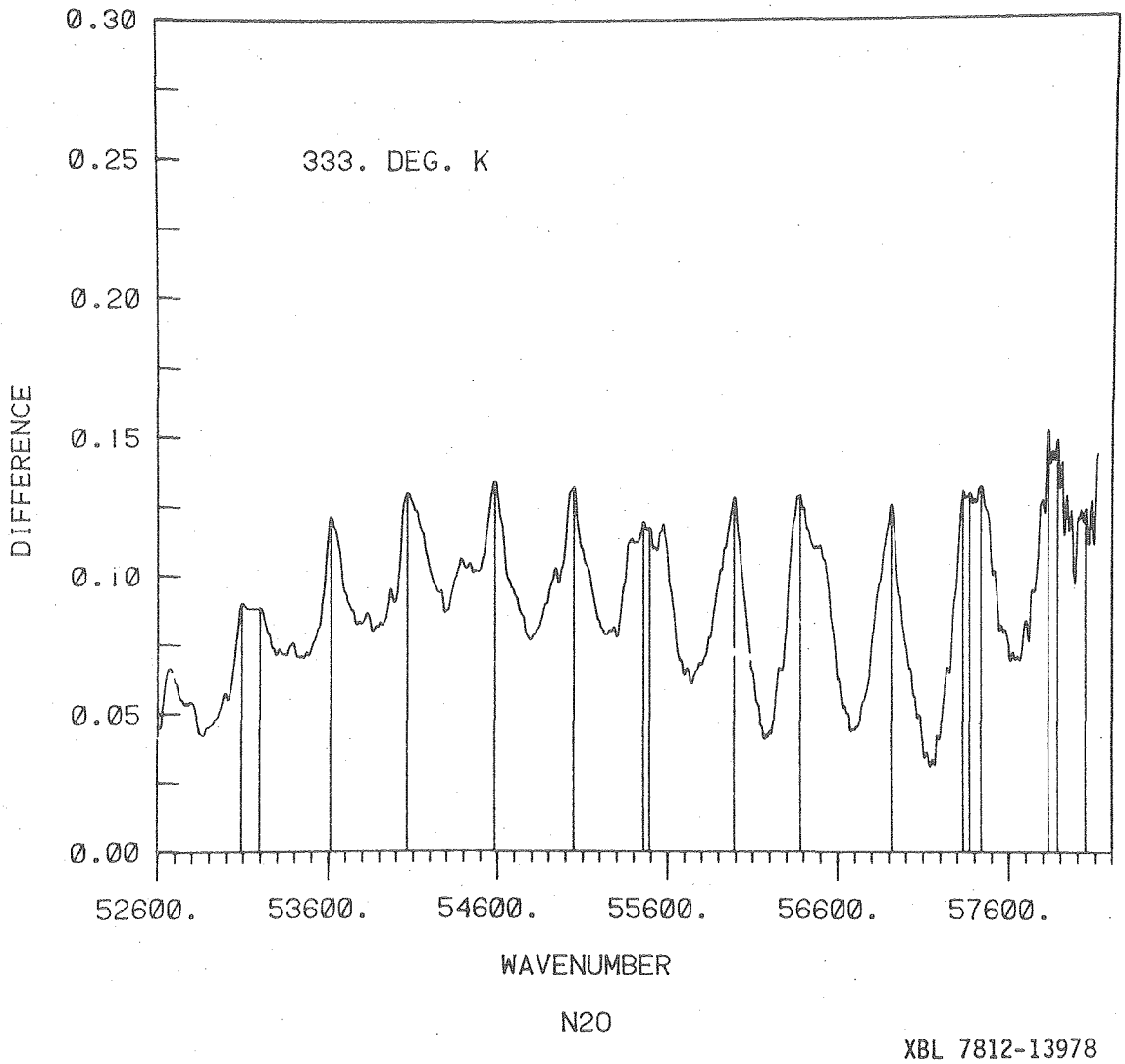
0.30
0.25
0.20
0.15
0.10
0.05
0.00
DIFFERENCE
333. DEG. K
52600.
53600.
54600.
55600.
56600.
57600.
WAVENUMBER
N2O
XBL 7812-13978

Figure 22h

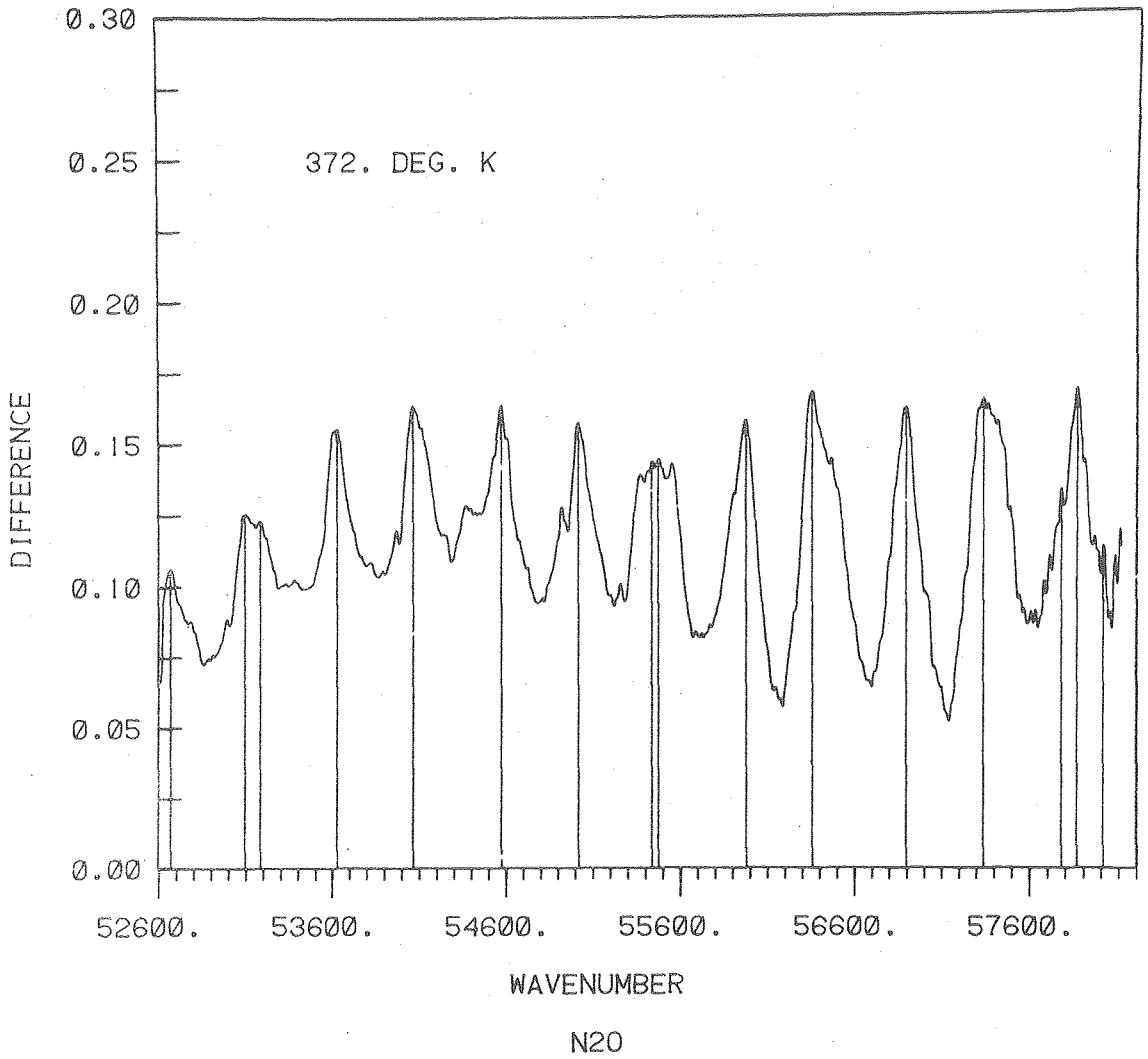

XBL 7812-13979

Figure 22i

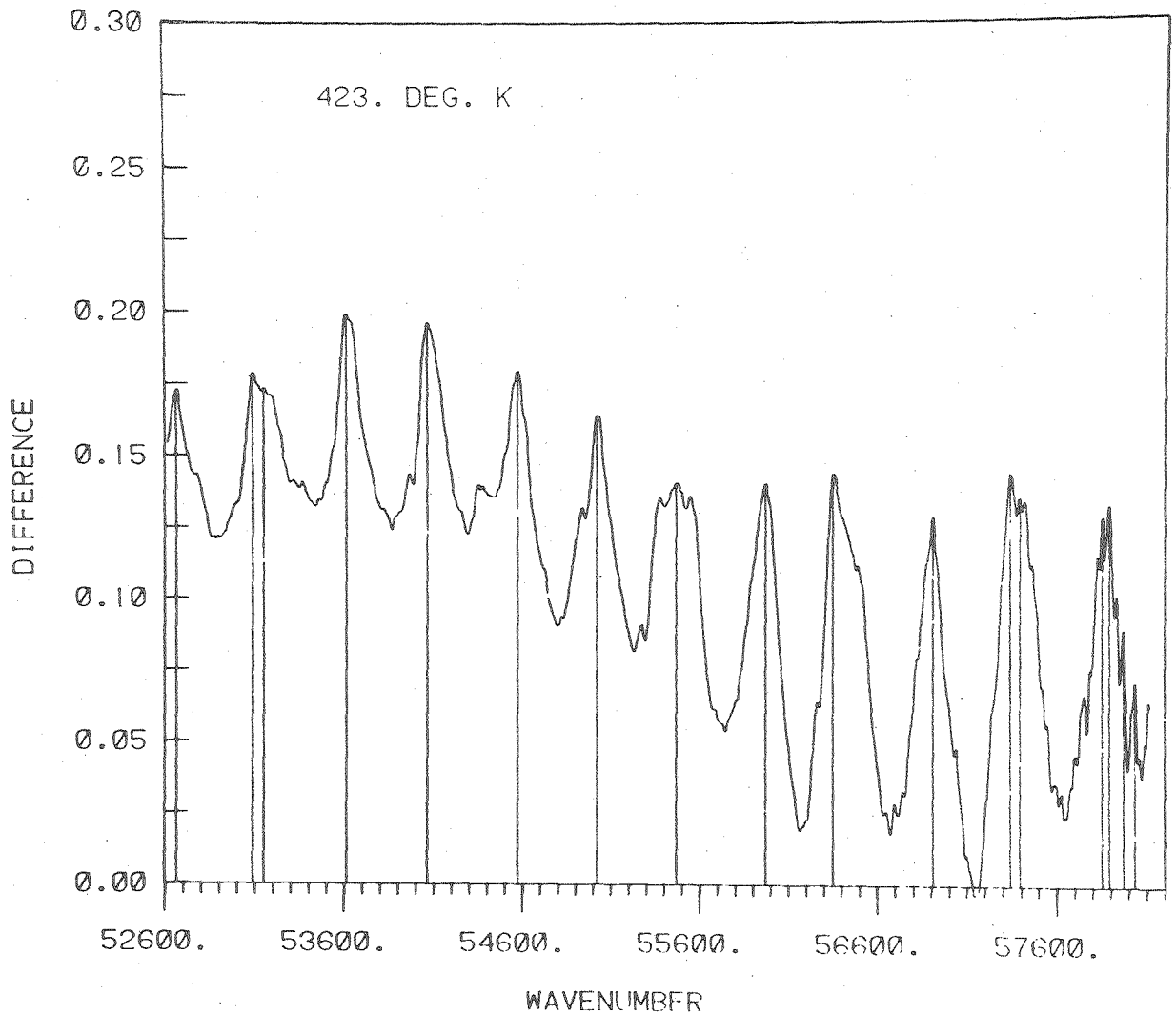

N2O

Figure 22j

XBL 7812-13980

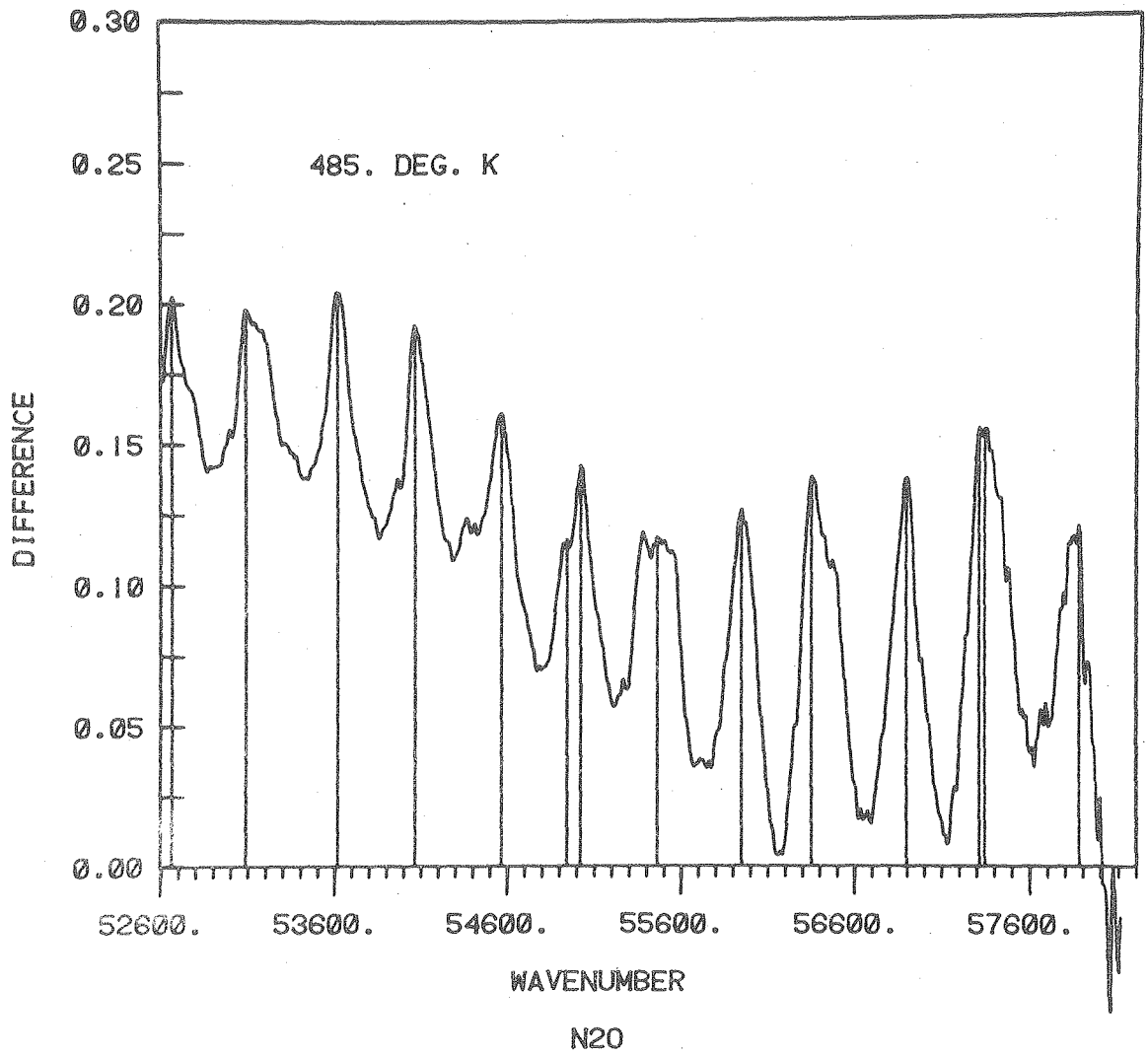

XBL 7812-13986

Figure 22k

Table 6. Selected Vibrational Progression Members at 485 K

Peak Number	Energy, cm^{-1}	Spacing, cm^{-1}
1	52 662	
		425
2	53 087	
		529
3	53 616	
		446
4	54 062	
		501
5	54 563	
		456
7	55 019	
		439
8	55 458	
		484
9	55 942	
		403
11	56 890	
		450
13	57 340	
		531
14	57 871	

in slope would have indicated hundreds of peaks at the low temperatures as in figure 22a and thereby emphasize the weak low temperature spectra much more than the stronger high temperature results. The width and height criteria were both logical decisions using the Fortran .OR. command and could be met by either large broad peaks or by smaller but sharper features. (For details see Subroutine CHECK in Program FINAL in the appendix.) Unavoidably, the program would occasionally identify two nearby peaks on a feature with a slight double maximum which a more subjective observer would place one peak, or a smaller feature appearing on the shoulder of a more intense peak might be missed. The features at each temperature which are selected as peaks by the program are indicated as solid lines in figures 22a to 22k.

The permutation of all energy separations between the selected peaks for each temperature were measured and counted in bins of 20 cm^{-1}. The grand summation of this energy separation count for all temperatures is shown in figure 23 as a histogram of frequency of occurrence in energy spacing between peaks vs. relative energy separation in cm^{-1}. The different shadings of the individual bars in the histogram represent the portion contributed by each temperature. Use of a permutation in counting all possible energy separations at a given temperature avoids overcounting the same energy separation between two peaks, although it tends to emphasize the smaller energy separations. This is seen by the decreasing intensity of the vibrational features in the histogram with increasing energy of separation.

To check the effect of the peak selection parameters on the final histogram result, the parameters were varied for ten different cases

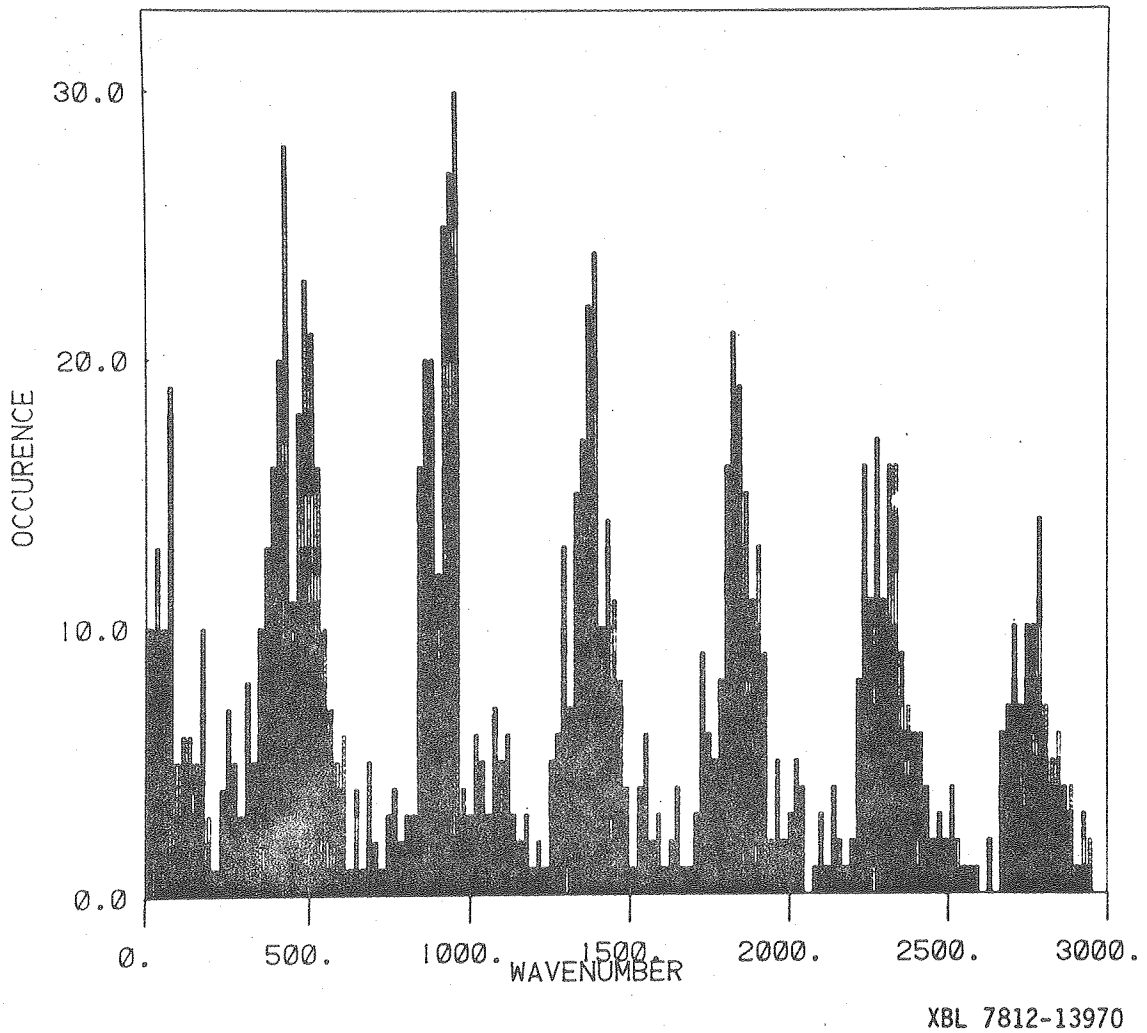
30.0
20.0
10.0
0.0
OCCURENCE
0.
500.
1000.
1500.
2000.
2500.
3000.
WAVENUMBER
XBL 7812-13970

Figure 23

varying from very restrictive criteria, yielding very few peaks, to a much less restrictive criteria, yielding many more peaks, especially at the lower temperatures. The final histogram derived from each case varied in the relative height (or signal/noise ratio) of the features seen in figure 23, but did not change the overall appearance of the histogram or the energy spacing of the features in figure 23. The sharp features of figure 23 indicate the approximate active vibrational energy levels of the upper electronic state relative to a minimum of potential energy.

The vibrational energy levels of figure 23 are listed in table 7.

Table 7. Histogram Vibrational Features and Energy Levels

Vibrational Level, n	Energy, cm^{-1}	E/n, cm^{-1}
1	500	500
2	980	490
3	1420	473
4	1880	470
5	2340	468
6	2840	473

4. Vibrational Selection Pattern

From the progressions in figures 22a to 22k, and from the energy separations indicated in the histogram, it is seen that $\nu_2' \approx 480\ cm^{-1}$. Yet in the (000) state spectrum, the spacing of the progression noted previously is 970 cm^{-1}. Since this value is very close to $2\nu_2'$, it appears that the (000) state follows the vibrational selection pattern:

$$\Delta\nu_2\ (\nu_2'' = 0) = 1,\ 3,\ 5,\ 7\ .\ .\ .$$

whereas the "hot" spectra and the spectrum of the (010) state indicate that from $\nu_2'' = 1$ or 2 consecutive values of ν_2' are selected. This pattern becomes more evident when the weak structuring of the (000) state spectrum is superimposed on the spectrum taken at 485 K. In figure 24, the two spectra have had the underlying absorbance subtracted out and they have been superimposed on the same scale. The advantage of this method of forming difference spectra to study the energy positions of the structuring is evident by allowing such a comparison. Each of the five members of the progression in the (000) state spectrum agrees well with an alternate feature of the high temperature spectrum.

As outlined in previous parts of this section, this vibrational selection pattern is symptomatic of only a vibronically allowed transition. This is to differentiated from the case of a bent-linear transition which would be rigorously forbidden in the linear-linear configuration. For such a case, as outlined previously, transitions from $\nu_2'' = 0$ (i.e. the (000) state), as well as the hot bending vibrations, would show consecutive values of ν_2'. Since the bending vibration

would show consecutive values of ν_2' since the bending vibration is a symmetric motion in Cs symmetry and the selection rules for symmetric vibrations predict[97h] a conservatiive sequence in ν_2'. Yet the alternate peaks at 53 100, 54 050 and 55 000 cm^{-1} are noticeably absent from the (000) state spectrum whereas they are strong in the 485 K spectrum (and the (010) state spectrum).

It is also noted in the 151 K spectrum that weak, vibrational peaks are observed at 55 950 and 56 850 cm^{-1}, which according to the theory outlined previously, would be expected to be absent. Two posibble explanations are offered here for the occurence of these additional features. The two unexplained peaks may be members of a different vibrational progression other than the ν_2 bending mode. The other members of this second (or third) progression may be obscured by their weak intensity in comparison with the observed ν_2 progression features. Secondly, the intensity of these two features is seen from figure 24 to be about 3×10^{-21} cm^2 (peak to trough). Accordingly, the intensities of the two features are about 10^{-5} of a fully allowed electric dipole transition. As stated previously, the intensity of an allowed magnetic dipole transition is about 10^{-5} of an allowed electric dipole transition.[97g] The $\sum^- - \sum^+$ transition is allowed by the magnetic dipole operator,[97g] so it is reasonable to believe that there may be a magnetic dipole contribution to the vibronic structure since the intensities observed are on the order of magnitude of a magnetic dipole transition. For an allowed magnetic dipole transition such as this (and for most allowed electric dipole transitions as well), the greatest intensity is expected for one or two progression

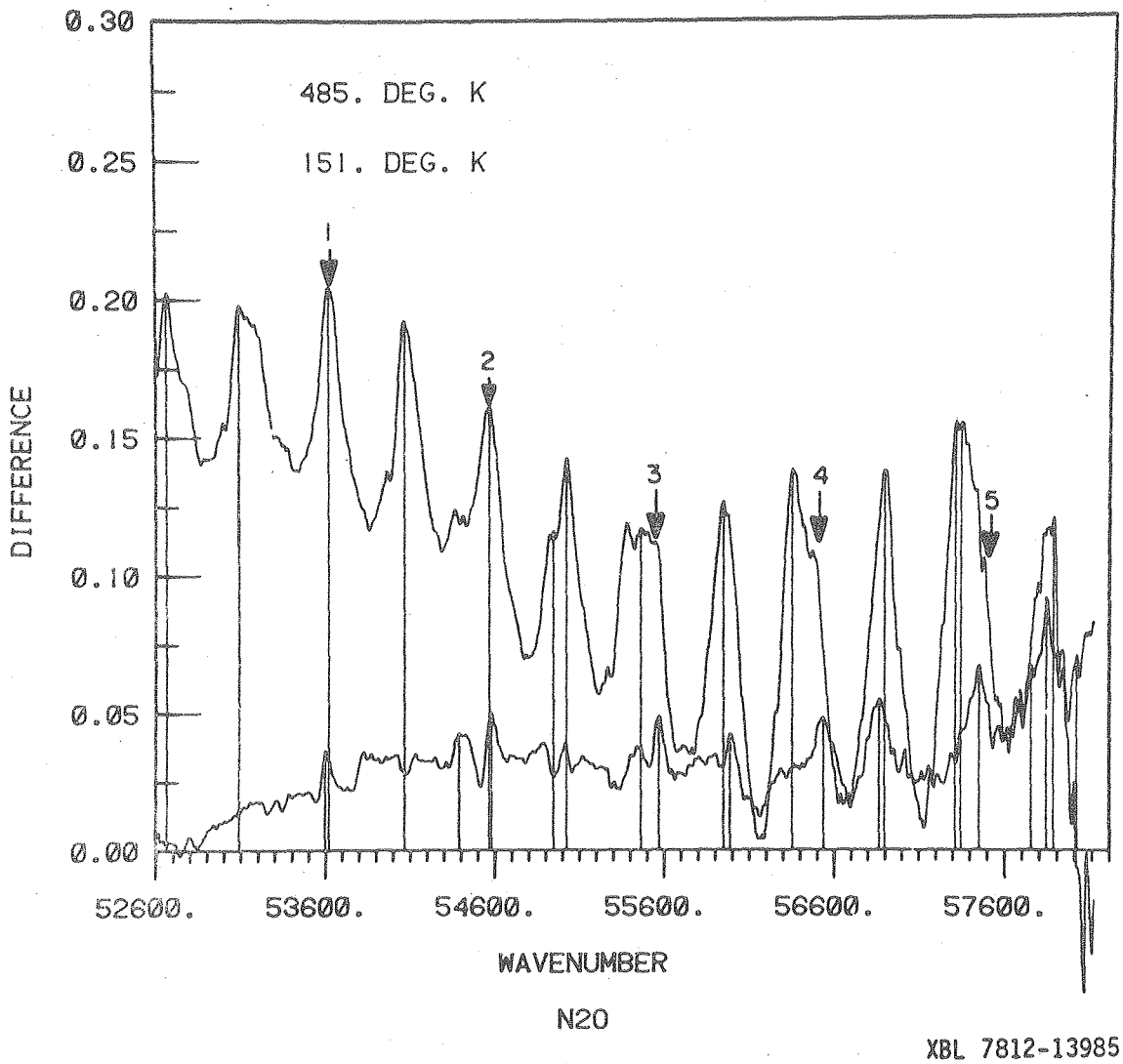

XBL 7812-13985

Figure 24

members with optimal Franck-Condon overlap (vertical transitions) and with the other members of th progression rapidly decreasing in intensity (nonvertical transitions). The two unexplained features at 151 K may then arise from the contribution of a magnetic dipole transition, which is non-negligible only in this limited short wavelength range corresponding to a vertical transition.

In view of this discussion, it is seen that the repeated absence of vibrational features at 53 100, 54 050 and 55 000 cm^{-1} is more informative than the occasional presence of an unexplained feature in one region of the spectrum since these may be complications due to additional progressions or may be bands due to magnetic dipole transitions.

Armed with this insight, it is possible to partially assign the features in the observed spectrum. Each of the five members of the progression in the (000) state represent the transitions:

$$\omega\nu_2'$$
$$\omega\nu_2' + 2$$
$$\omega\nu_2' + 4 \leftarrow \nu_2''(0)$$
$$\omega\nu_2' + 6$$
$$\omega\nu_2' + 8$$

where ω has been shown to be an odd integral quantum number.

The energy of ν_2' is approximately 480 cm^{-1}, which is 100 cm^{-1} less than the ν_2'' of 589 cm^{-1} in the ground electronic state. Thereby the transitions:

$$\begin{array}{ll} \omega\nu_2' - 1 & \\ \omega\nu_2' + 1 & \\ \omega\nu_2' + 3 & \leftarrow \nu_2''(1) \\ \omega\nu_2' + 5 & \\ \omega\nu_2' + 7 & \end{array}$$

where ω is the same odd quantum number, will be located 100 cm^{-1} below the peak positions of $\nu_2'' = 0$. Midpoint between these hot bands will be the remaining transitions of the type $\omega\nu_2' + (2, 4, 6, 8...) \leftarrow \nu_2''(1)$.

Similarly, hot band originating from ν_2'' (2) would be expected to be 95 cm^{-1} below the ν_2'' (1) levels and thus form a sequence in ν_2.

The resulting sequences in ν_2 and its peak positions is shown superimposed on the composite difference spectrum of figure 22K in the next figure.

The assigned peak positions fit the observed spectrum and this interpretation explains the different rates of activation energies of the spectra. For example, the feature at 55 500 cm^{-1} at low temperatures has a predominate feature at its short wavelength end. At higher temperatures, the absorption assigned to ν_2'' (1), located 100 cm^{-1} below the ν_2'' (0) assignment rapidly increases and becomes more intense. The lowest energy peak of this triplet structure may be the hot band from ν_2'' (2), but there is no conclusive proof for this. Similarly, the feature at 56 400 cm^{-1} at low temperatures the short wavelength absorption assigned to ν_2'' (0) is seen as predominant.

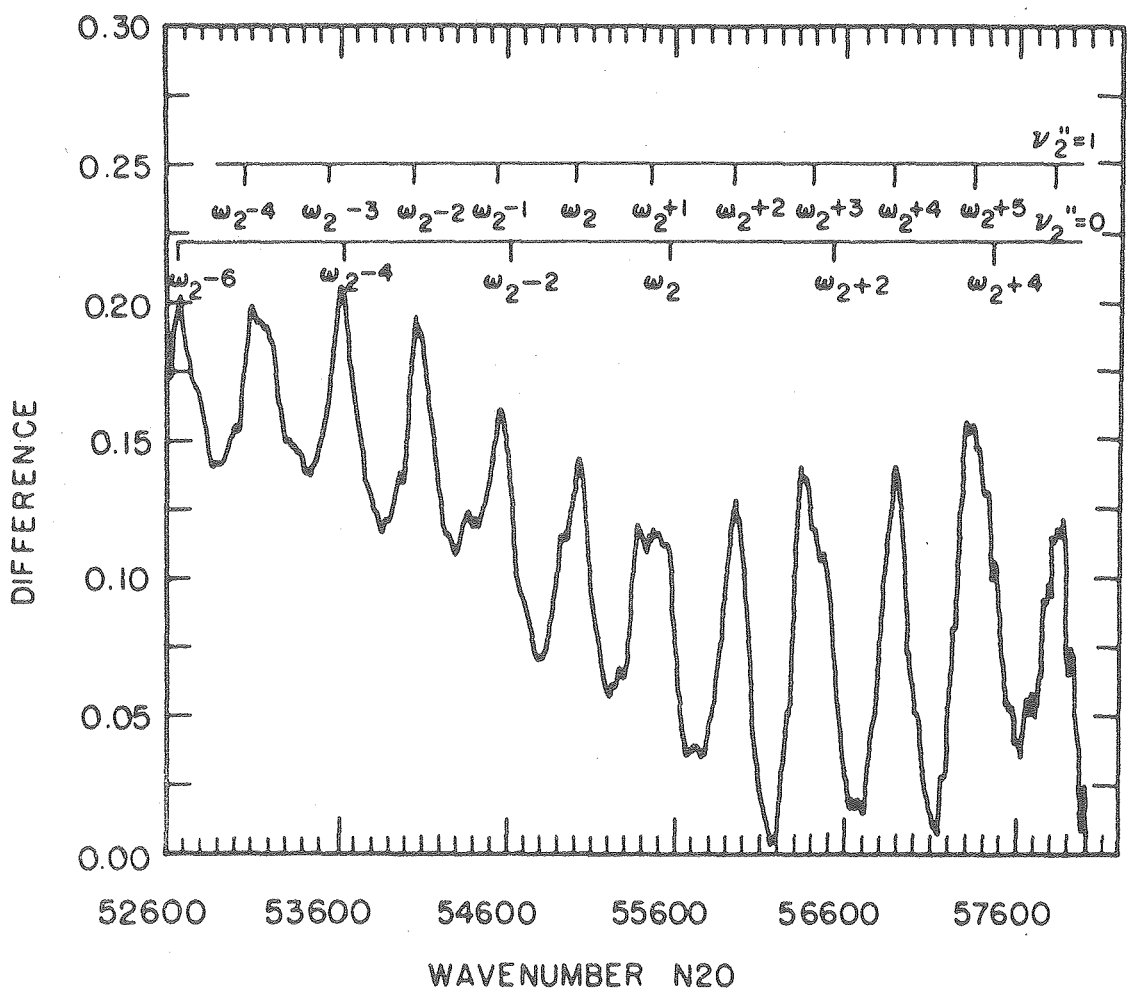

XBL 792-8573

Figure 25

At 485 K, the same feature is only seen as a sloping shoulder on top of the more intense hot bands located 100 cm^{-1} below the ν_2'' (0) assignment.

Although the vibrational pattern appears to support the contention of transition through vibronic interaction, there is evidence also for a change of symmetry between the two electronic states. For a linear-linear transition, the intensity of the observed peaks are typically most intense in one or two peaks with subsequent members of that progression rapidly decreasing in intensity due to poor Franck-Condon overlap. If there is a change of symmetry during transition, and if the transition is forbidden in the linear-linear configuration, then as previously demonstrated, there is a slow variation in the intensity of the progression members, with a maximum located somewhere between the $\Delta\nu = 0$ and the high energy limit of the bands. This is clearly the case of the observed structuring, so this may indicate that the upper state is bent, as it has been calculated to be (references 14, 124, 106) with a bond angle of 130 degrees[104].

G. Photodynamics

1. Continuous Absorption

Rabalais *et al*[14] and Fortune and coworkers[104a,b] have assigned the continuous absorption at 6.8 eV to the $^1\Delta$ state correlating with N_2 ($^1\Sigma_g^+$) and O ($^1D_2$). This could explain the weak nature of the absorbance ($f \sim 1.5 \times 10^{-2}$) since the transition $^1\Delta \leftarrow {}^1\Sigma^+$ is angular-momentum forbidden. Chutjian and Segal[106], however assign the same absorption to the $^1\pi$ state correlating to the same asymptote as the $^1\Delta$ state. A more definitive theoretical result is required here to resolve this discrepancy.

Interestingly, in a recent electron impact study of the analogous absorption of OCS, the assignment of $^1\Delta$ to the observed continuous absorption was determined by measuring the angular dependence of the electron scattering.[105] A similar experimental study of this type would be useful in confirming the calculations of Fortune and coworkers and the Rabalais study.

I shall adopt here the $^1\Delta$ assignment on the basis of these more recent calculations and since the $^1\pi$ assignment would be expected to be more intense than the absorption is actually observed to be.

2. Structured Absorption

The Chutjian and Segal study[106] has offered the most detailed explanation of the vibronic banding of nitrous oxide in this energy range. They suggest that the banding results from vibrational resonance between the strongly bound $^1\Sigma^-$ state (the only state calculated to be bound in this energy region -- agreed upon by all the theoretical studies) and the repulsive $^1\Delta$ state. Mixing of the two eigenfunctions may occur by vibronic coupling, even though the two states are separated by 2.8 eV in the Franck-Condon region. They further explain "at certain energies a band width of continuum levels (of $^1\pi$) will be in resonance with a vibrational level of the $^1\Sigma^-$ state, and electronic mixing via the A" components of the two states will take place upon bending. The resonances will occur at spacings corresponding to spacings of either the ν_2 bending vibrations of the $^1\Sigma^-$ state or to the very anharmonic ν_3 vibrations near the top of the $^1\Sigma^-$ well."

The authors state that ordinarily such vibronic coupling would be unlikely due to poor vibrational overlap, however because the minimum of the $^1\Sigma^-$ state "accidentally" (their words) is near the $^1\pi$ repulsive asymptote, therefore the "kinetic energy of translation in the $^1\pi$ state and of vibrational motion in the $^1\Sigma^-$ state will be very nearly the [same so that] the wavelengths of the vibrational wavefunctions of both states will not be very different."

In fact however, they calculate the minimum of the $^1\Sigma^-$ state as 4.23 eV and the minimum of the $^1\pi$ and $^1\Delta$ repulsive states is 3.64 eV. The Chutjian and Segal study can not explain the temperature

dependence noted by Holliday and Reuben, nor much of the new experimental evidence offered in this study.

By carrying the original hypothesis of Chutjian and Segal one step further, and discarding their theory of vibrational resonance, another interpretation of the photodynamis arises, which is compatible with the new experimental evidence of this study. In lieu of further, more definitive assignments, I have tentatively adopted the $^1\Delta$ state assignment as the repulsive curve which was designated as $^1\pi$ by Chutjian and Segal. It should be carefully noted that since both the $^1\pi$ and $^1\Delta$ states are degenerate, what I apply to one may also apply to the other; this interpretation does not critically depend on the species assignment of the degenerate, repulsive potential curve. The Chutjian and Segal interpretation of vibrational resonance does critically depend on the state assignment of the repulsive curve because a $^1\Delta$ state could not directly perturb a $^1\Sigma^-$ state since it violates the perturbation selection rules with $\Delta\Lambda = 2$.[92c]

Both the $^1\Sigma^-$ and the $^1\Delta$ states are calculated to be bent in Fortunes study, so that $^1\Sigma^-$ becomes $^1A''$ in C_s symmetry and $^1\Delta$ as well as $^1\pi$ will lose their degeneracy and will both split into $^1A'$ and $^1A''$ components in C_s symmetry. Figure 26 was taken from the Chutjian and Segal study except that the repulsive state has been tentatively relabeled $^1\Delta$. It is clear from this figure that the Franck-Condon region, indicated by the two vertical lines, does not intersect a turning point of the $^1\Sigma^-$ state near the 6.8 eV energy at which structuring is observed. Let us then assume that due to the bent geometry of both electronic states, the potential curves of figure 26 interact to yield an avoided

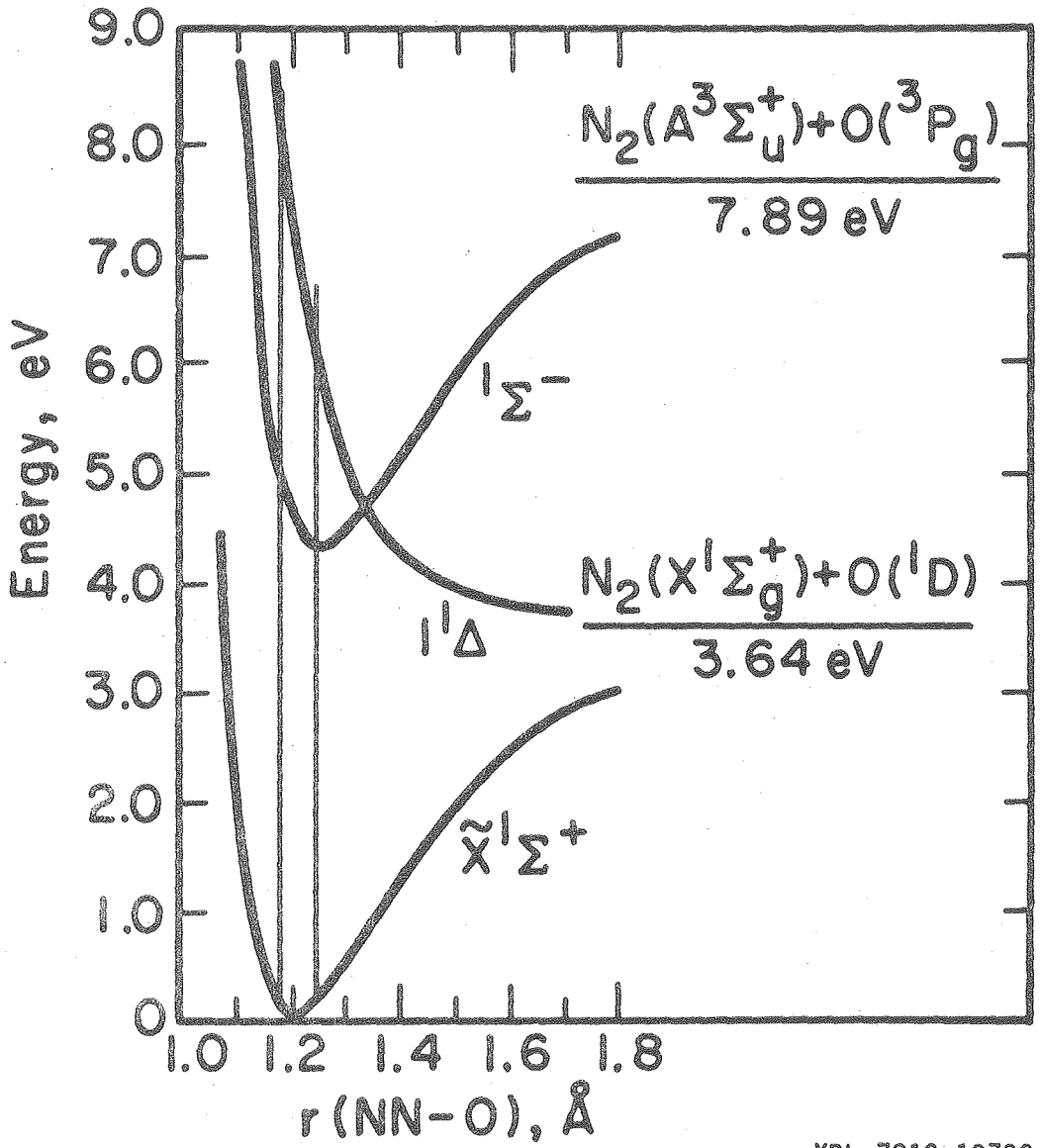

XBL 7812-13732

Figure 26

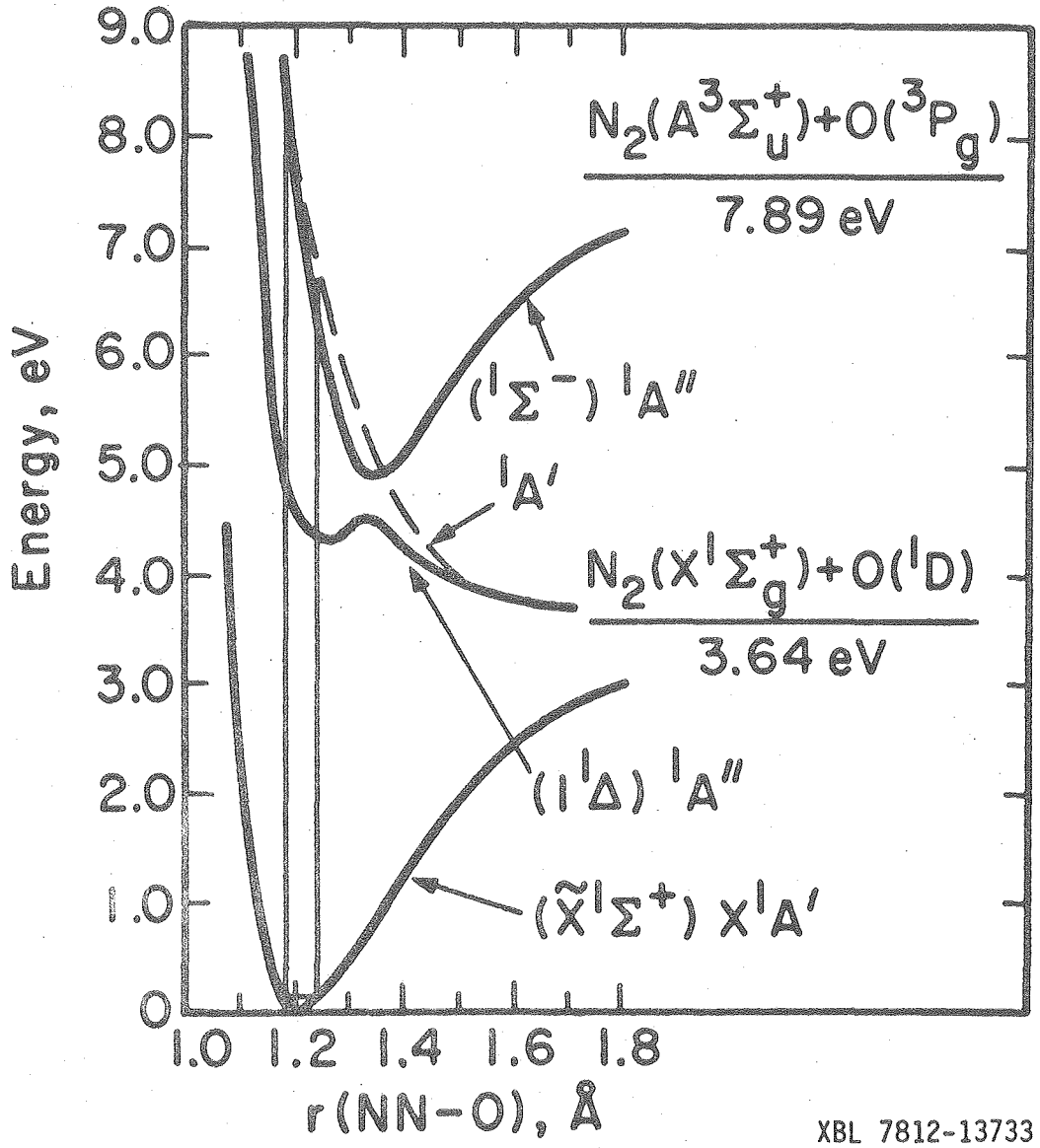
9.0
8.0
7.0
6.0
5.0
4.0
3.0
2.0
1.0
0
Energy, eV
1.0 1.2 1.4 1.6 1.8
r(NN-O), Å
$N_2(A^3\Sigma_u^+)+O(^3P_g)$
7.89 eV
$(^1\Sigma^-)\ ^1A''$
$^1A'$
$N_2(X^1\Sigma_g^+)+O(^1D)$
3.64 eV
$(1^1\Delta)\ ^1A''$
$(\tilde{X}^1\Sigma^+)\ X^1A'$
XBL 7812-13733

Figure 27

crossing as indicated in figure 27. This is the hyper conical intersection discussed by Herzberg[49] which results in an avoided crossing at all points except the point of linear intersection, which is allowed to cross. Therefore, in a strict linear geometry of the upper states no mixing can occur, and the interpretation of figure 26 is the correct one. Only the $^1A''$ components interact, and the Franck-Condon region now sees a turning point which would have vibrational overlap and thus give rise to a structured spectrum. Unlike the HNO study of Herzberg, the $^1A'$ component originating from $^1\Delta$ in this case, could only remain unperturbed and give rise to a continuous absorption. The resultant spectrum would consist of vibrational bands superimposed on a continuous background, as is observed.

3. Vibronic Enhancement of Transition

Account must also be taken of the large, fundamental differences of the derived (000) and (010) state spectra, as shown in figure 17. By thermal excitation of the ν_2 mode in the ground electronic state, the resulting ψ_{ev} is then $^1\pi$. In $C_{\infty v}$ symmetry all transitions are allowed, however it is only through the excitation of the bending mode that the molecule may be considered to some degree in Cs symmetry. Thus by excitation of the bending mode, the transition moments to the continuous state as well as to the bound state are both enhanced, as has been observed for the (010) state spectrum.

In the cold, vibrationless state, (000), there cannot be vibrational interaction in the ground electronic state and so even though mixing of the $^1\Sigma^-$ and $^1\Delta$ eigenfunctions in the upper electronic states occur through their $^1A''$ components, in no manner may the $X^1\Sigma^+$ ground state be considered in C_s symmetry. The transition moment for $^1\Sigma^- \leftarrow X^1\Sigma^+$ then remains strongly parity forbidden and $^1\Delta \leftarrow X^1\Sigma^+$ remains angular momentum forbidden and very little structuring is observed on a weaker continuum. Yet, a weak progression is noted with a spacing of 970 cm^{-1} which is very close to $2\nu_2'$ for $\nu_2' = 480$ cm^{-1}. Figure 13 demonstrates that for alternate, odd ν_2' levels in $^1\Sigma^-$, the vibronic transition $^1\pi \leftarrow X^1\Sigma^+$ is allowed. This is interpreted as due to bending interaction of the upper state and should have a spacing observed at low temperatures of $2\nu_2'$, as is observed. This proof of a vibronically-induced transition--consecutive values of ν_2' in the hot bands and alternate values of $\nu_2'' = 0$ -- confirms the same conclusion reached by Innes,[107] using conventional Herzberg-Teller theory of vibronically induced transitions.[103-112]

Lastly, the observed decrease in the fundamental frequency of ν_2 in the upper electronic state relative to the ground electronic state is reasonable since the transition involved has been interpreted as $n \rightarrow \pi^*$[14], and in this context the presence of a π^* electron would lessen the bond order, which will increase the internuclear separation and cause a reduced fundamental frequency.

A further theoretical discussion of vibronically induced transitions is provided by references 117 to 125.

H. Conclusions

1. Experimentally Deduced Conclusions

A series of measurements of the absorption spectrum of nitrous oxide at 11 different temperatures indicates a pronounced effect of temperature on the spectrum. The active vibration responsible for this temperature effect has been shown to be ν_2 and using its infrared fundamental frequency, it is possible to deconvolute the spectrum of nitrous oxide into the normalized contributions of two vibrational modes of the ground electronic state. These may be used to predict the spectrum over a wide temperature range, and their comparison points to the role of vibronic interaction of the ground electronic state and its bending vibration. In the (010) state spectrum both the continuous and the structured absorption are seen to be markedly enhanced relative to the spectrum of the (000) vibrational state.

Analysis of the observed banding incates that ν_2' levels are selected by the (000) state, this supports the theory of vibronically induced transition along with the comparison of the (010) and (000) state spectra. The peaks have been tentatively assigned; although the exact quantum numbers of the upper state bending mode are not known, from the presented theory of vibronically induced transitions, the assignment of the alternate ν_2' levels selected by the (000) state should be to an odd quantum number. On the basis of the large difference between the region of structuring and the calculated minimum of the $^1\Sigma^-$ potential well, it is expected that these are transitions to high vibrational quantum numbers of $^1\Sigma^-$.

Fortunately, on the basis of theoretical calculations, the only bound singlet state in this region is the $^1\Sigma^-$. Triplet states also exist; however, transitions to these states would require overcoming an additional degree of a forbidden nature. Chutjian and Segal have attempted to explain the transition to the $^1\Sigma^-$ through vibrational resonance since the Franck-Condon overlap with this state is well separated from a classical turning point of the potential curve and is then expected to be quite poor. However, if the state is bent in its equilibrium configuration, it has been suggested that the resulting double conical intersection of the $^1\Sigma^-$ with a repulsive, degenerate state may occur through their $^1A''$ components in C_s symmetry. This would be expected to yield an avoided crossing in all orientations except the colinear one, and the new resulting potential well would then have a classical turning point within the Franck-Condon region at 6.8 eV.

No rotational structuring can be definitely determined, even with the high resolution of a three meter vacuum spectrometer. However, from the intensity pattern of the observed vibrational features, there is evidence that the upper electronic state is bent to a large extent. This is in agreement with theoretical calculations and the model provided by Walsh diagrams.[14,113]

2. A Proposed Mechanism of Predissociation

The lack of rotational structuring, even the coarse rotational structuring arising from the K selection rules may be due to predissociation of the molecule. The short lifetime of a predissociated state would smear out fine structure due to uncertainty broadening. A mechanism of predissociation may be proposed using the theory developed in this study:

The double conical intersection of $^1\Sigma^-$ and $^1\Delta$ would break down in the linear configuration. If then, during the bending motion of the excited states, the molecule passes through the linear configuration and simultaneously the ν_1 vibration is at its left hand turning point as indicated in figure 26, then the molecule would be expected to fly apart into the fragments N_2 ($X^{1\ +}$) and O (^1D) when these two combinations are simultaneously met. This is because in the linear configuration the avoided crossing would not occur and the left hand turning point of ν_1 would be the repulsive $'\Delta$ state correlating with N_2 ($^1\Sigma\ g^+$) and O (^1D). In fact, it is interesting that the photochemical studies of Bradley et al[114] point to an excited state of N_2O with an estimated lifetime of 10^{-8} second, although this unconfirmed lifetime may also result from other physical processes such as quenching or fluorescence.

Acknowledgments

To Professor Harold S. Johnston I wish to express my unequivocal appreciation for his role in my scientific education. As an educator he has helped guide my passage through graduate school at the necessary moments while understanding my preference for self-education. As a researcher his experience and insight has been of invaluable aid to this work: many of the ideas presented here have been refined under the scrutinuous examination of Professor Johnston while his philosophy of research has allowed me the opportunity to carry on my own independent work.

I also wish to thank John Conway and George Shalimoff of the Lawrence Berkeley Laboratory who have provided an additional sounding board for my ideas as well as occasionally providing equipment and laboratory space. Special thanks are also due to Professor Andrew Yencha of SUNY Albany who has provided guidance and direction from the beginning of my undergraduate studies.

I also wish to express my appreciation to the personnel of the support facilities of the Department of Chemistry and of Lawrence Berkeley Laboratory. I especially thank Mr. Locke Yow of the Chemistry Glass Shop for the competence and patience he has shown in his work.

Support of an entirely different nature was contributed by Ms. Sharon Altman. To her I express my sincerest appreciation for her emotional aid and her understanding. In most every sense she was involved in this work.

Finally, I wish to thank the University of California and the U.S. Department of Energy for the financial aid provided during my

tenure. This work was supported by the Division of Chemical Sciences, Office of Basic Energy Sciences, U.S. Department of Energy under contract No. W-7405-ENG-48.

Appendices

A. Results of ^{15}N Substitution

1. Temperature Effect--Raw Data

To prove the reproducibility of the previous results and to demonstrate the extent of the observed isotope shift on the structured absorption, the ^{15}N isotopes of nitrous oxide, $N^{15}NO$, ^{15}NNO, $^{15}N^{15}NO$ were purchased from Prochem (British Oxygen Co.) with a stated isotopic purity of better than 99.0%.

Gas purity and isotopic labeling purity were further checked by measuring the infrared frequencies of the various isotopes with a Nicolet 7199 Fourier-Transform Spectrometer and comparing this result with literature values[128, 129]. All experimental procedures used were identical to the previous section, however a longer wavelength range was covered, 197 to 172 nm for six temperatures using 1250 data points for each spectrum.

Signal averaging was carried out for two runs on both background and sample spectra at slightly less resolution, to improve the signal/noise ratio (0.7Å). For optimal comparison with the unlabeled isotope, regular N_2O (Matheson) was also run in the same manner.

The result of the temperature dependent absorption of each isotope is shown in figures 28 a-d for six temperatures from 197 to 172 nm. As expected, isotopic substitution does not significantly alter the intensity of absorption at a given temperature. It is also clear from these figures that even at high temperatures the observed structuring is quite weak at longer wavelengths.

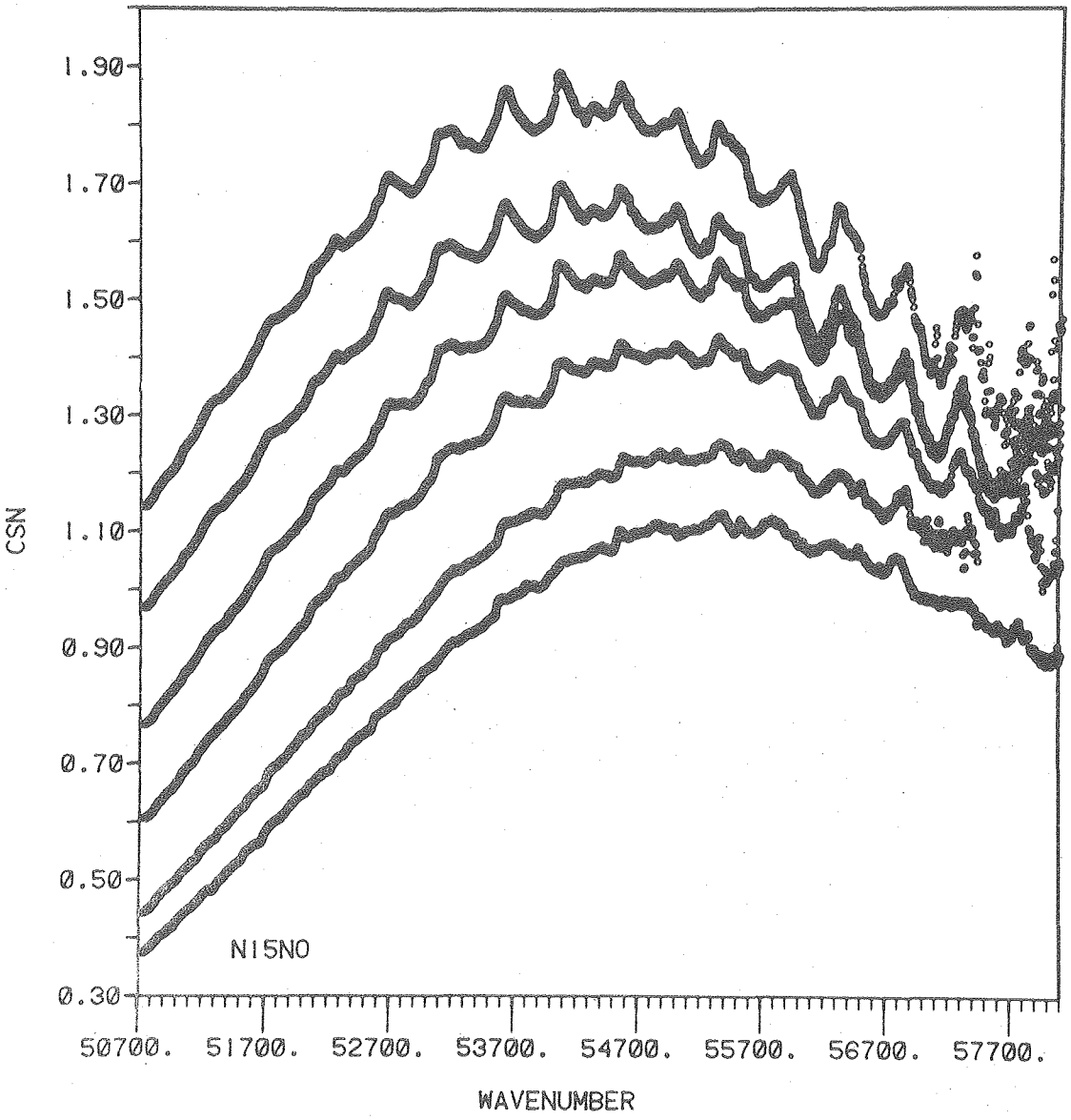

XBL 792-8602

Figure 28a

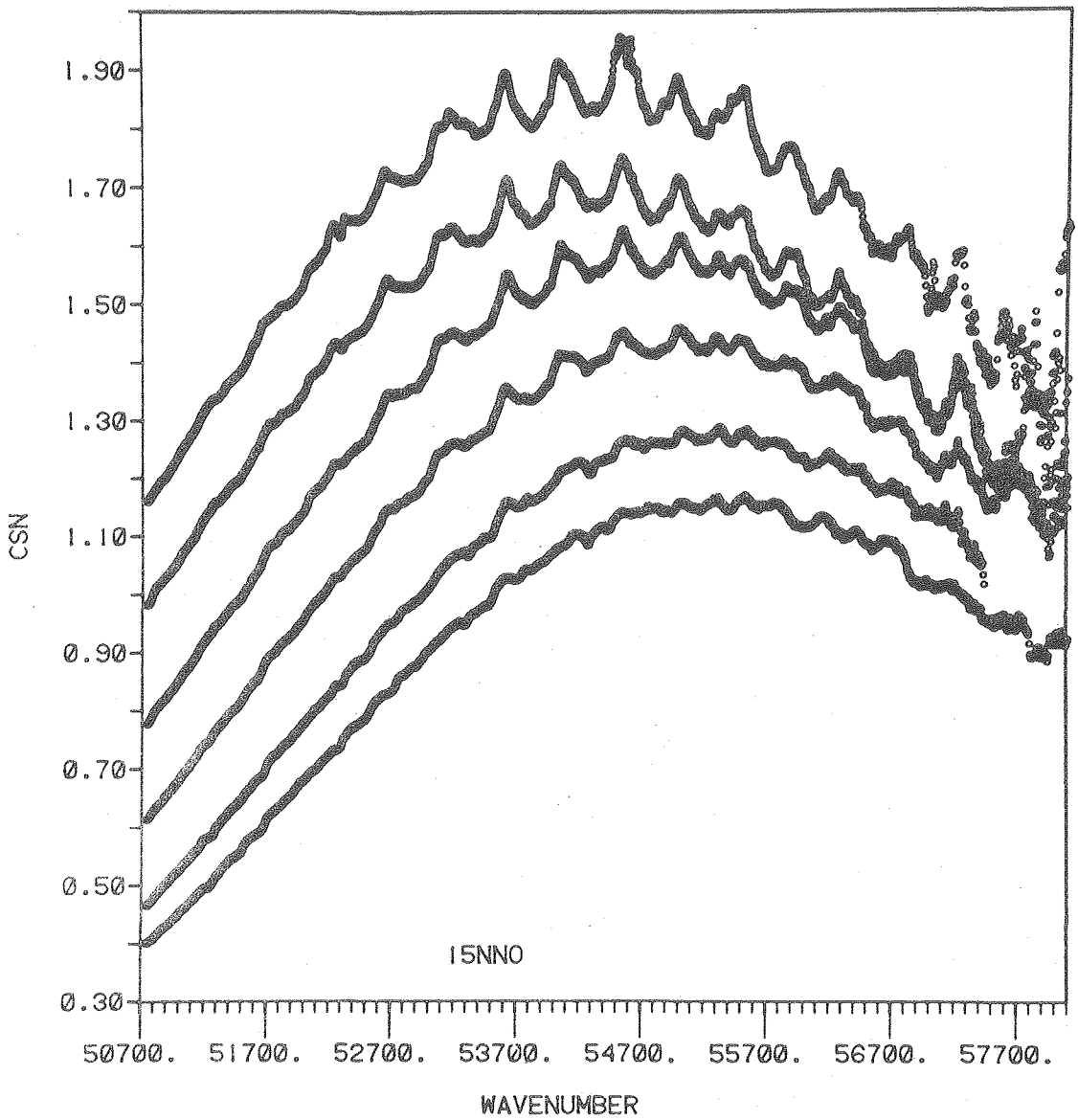

XBL 792-8600

Figure 28b

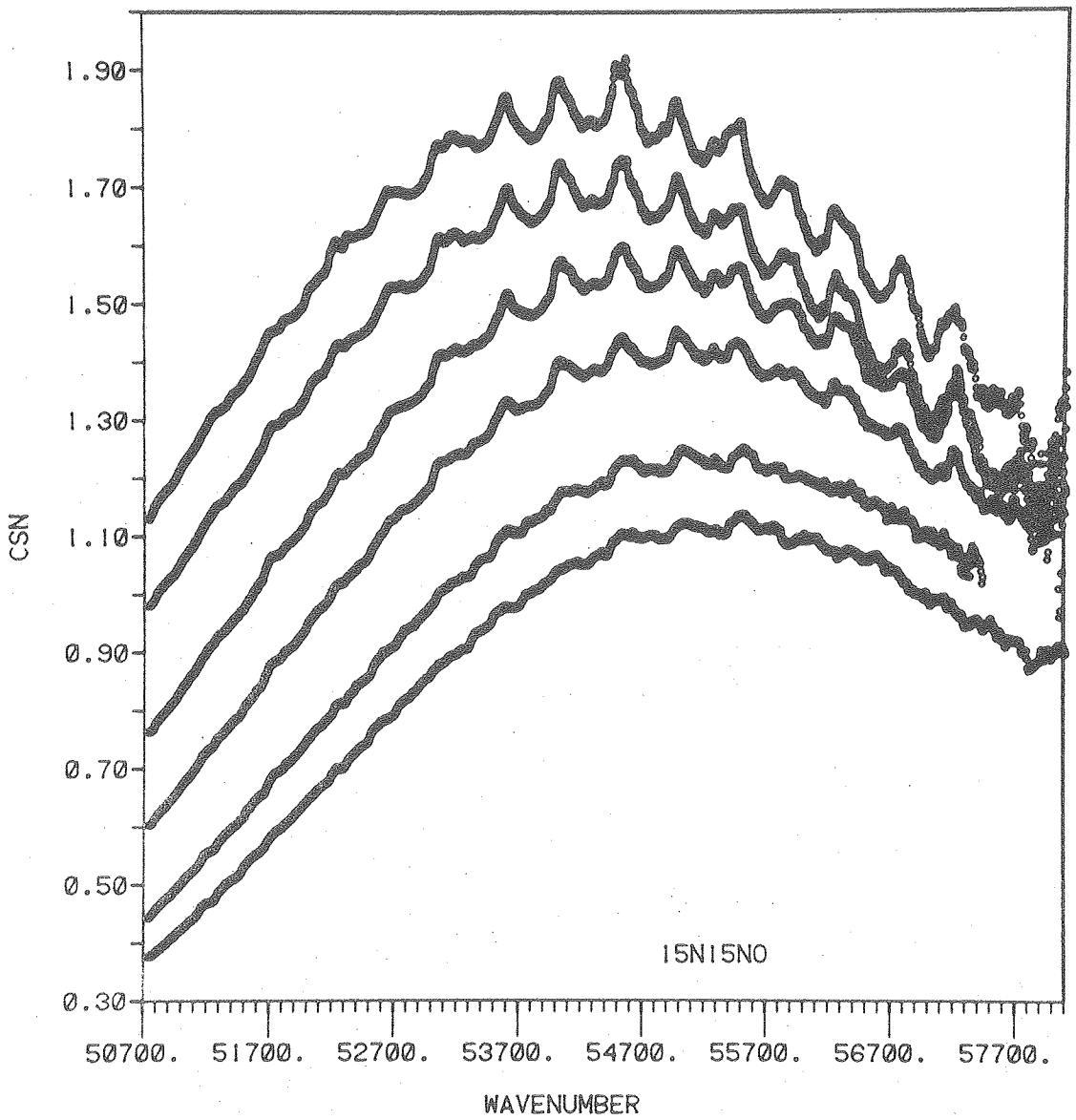

XBL 792-8588

Figure 28c

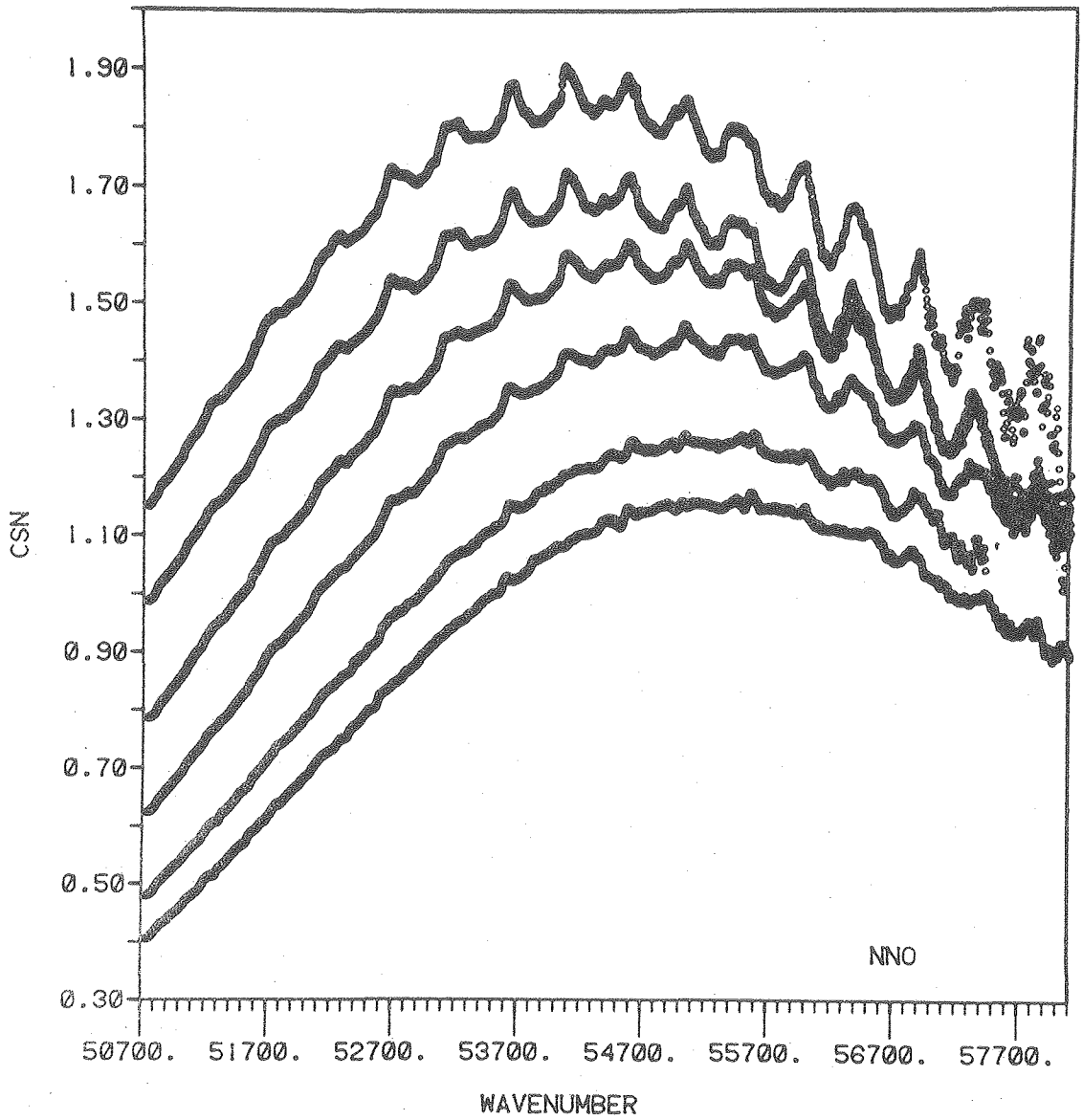

XBL 792-8580

Figure 28d

2. Deconvolution and Isotope Shift

Using the unique infrared frequencies of each nitrous oxide isotope, it is possible to deconvolute the raw data presented in figures 28 a-d using the first order or second order iterative procedures outlined in the last section. Figures 29 a-f show the result of a first order deconvolution into the (000) and (010) state spectra. To demonstrate the observed isotope shift, figures 29 a-f are shown superimposed, as a permutation of all possible isotope comparisons. In each case, the extent of the isotope shift, as indicated by the displacement of the structured spectra, is seen to increase at the shorter wavelengths. At longer wavelengths, the isotope shift is minimal and the peaks most nearly coincide. This is to be expected, since the extent of isotope shift would be greatest for high quantum vibrations, corresponding to the short wavelength transitions. It is also seen that the extent of isotope shift is greatest for the most dissimilar isotopes, such as NNO and $^{15}N^{15}NO$ whereas the isotope shift between more nearly similar species, such as $^{15}N^{15}NO$ and ^{15}NNO, show the least displacement. It is also seen that the observed isotope shift can be so large as 125 cm^{-1} at the short wavelength end of the spectrum. In comparison with the isotope shift of less than 15 cm^{-1} for $\nu_2'' = 1$ in the ground electronic state, this large isotope shift appears to indicate transition to high quantum vibrations in the upper electronic state, in agreement with the theory discussed previously.

Using the second order deconvolution procedure to solve for the (000), (010) and (020) state spectra is also revealing. With the larger wavelength range of this study, the (020) state spectrum is

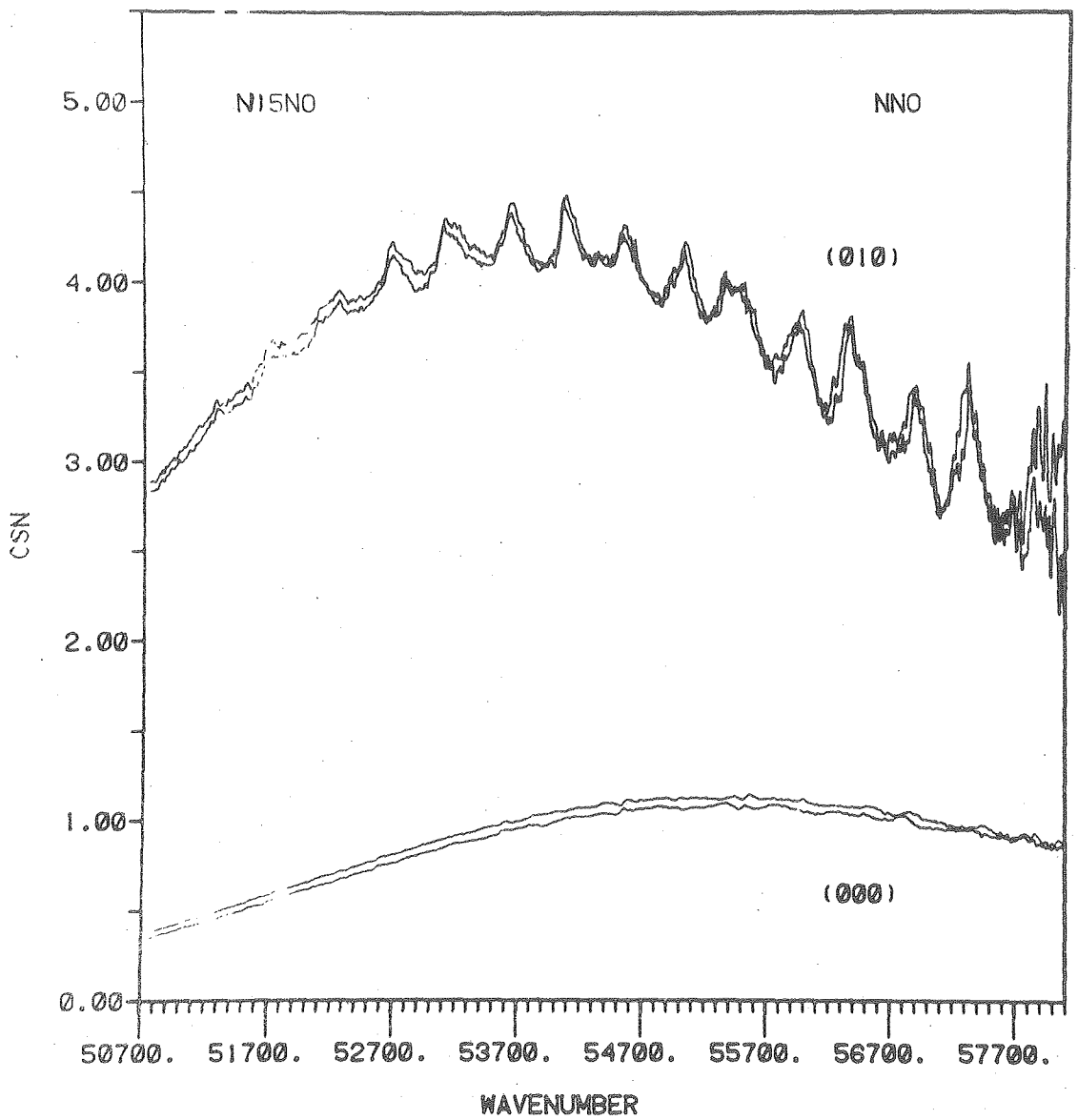

XBL 792-8607

Figure 29a

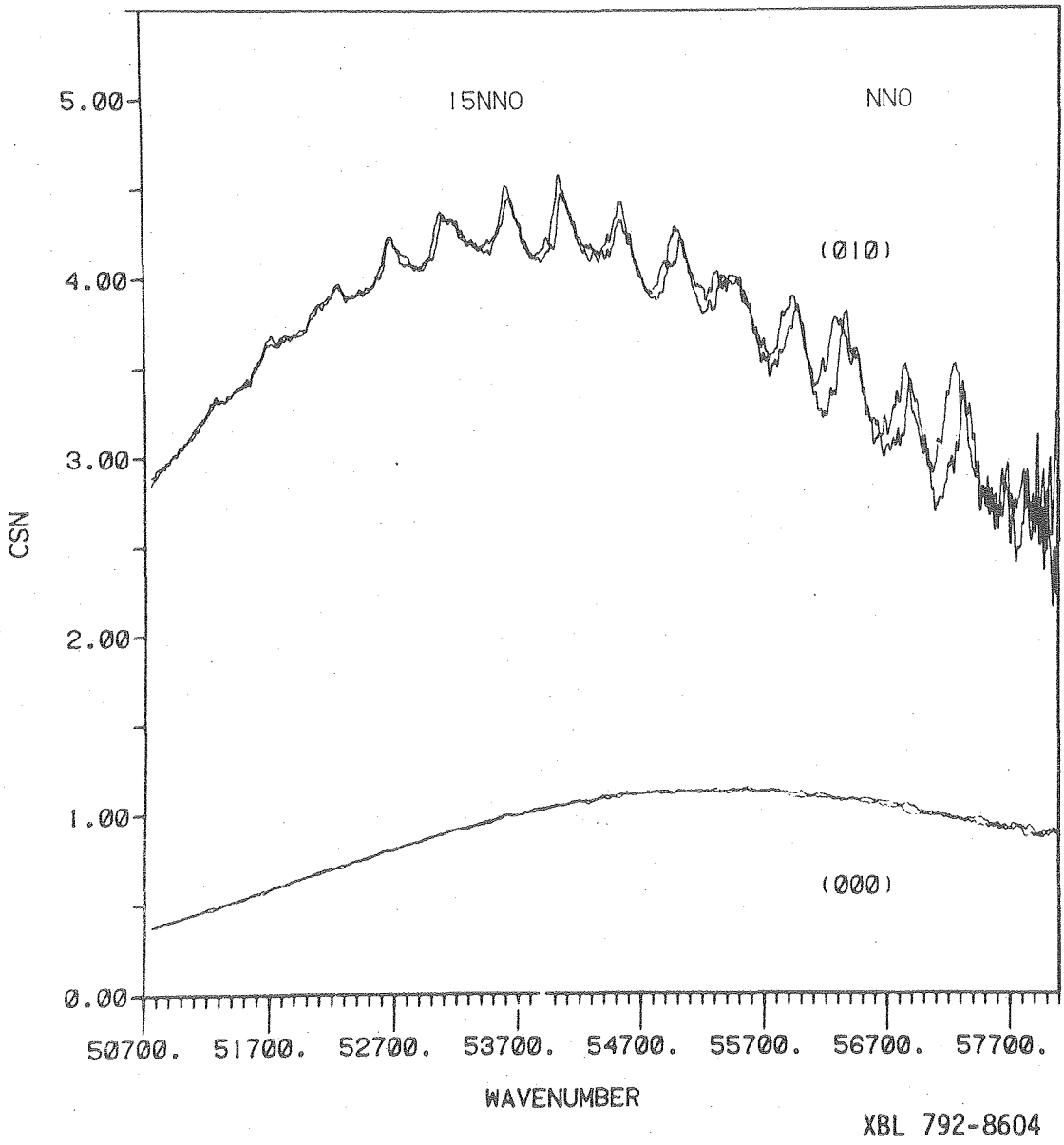
15NNO
NNO
(010)
(000)
5.00
4.00
3.00
2.00
1.00
0.00
CSN
50700.
51700.
52700.
53700.
54700.
55700.
56700.
57700.
WAVENUMBER
XBL 792-8604

Figure 29b

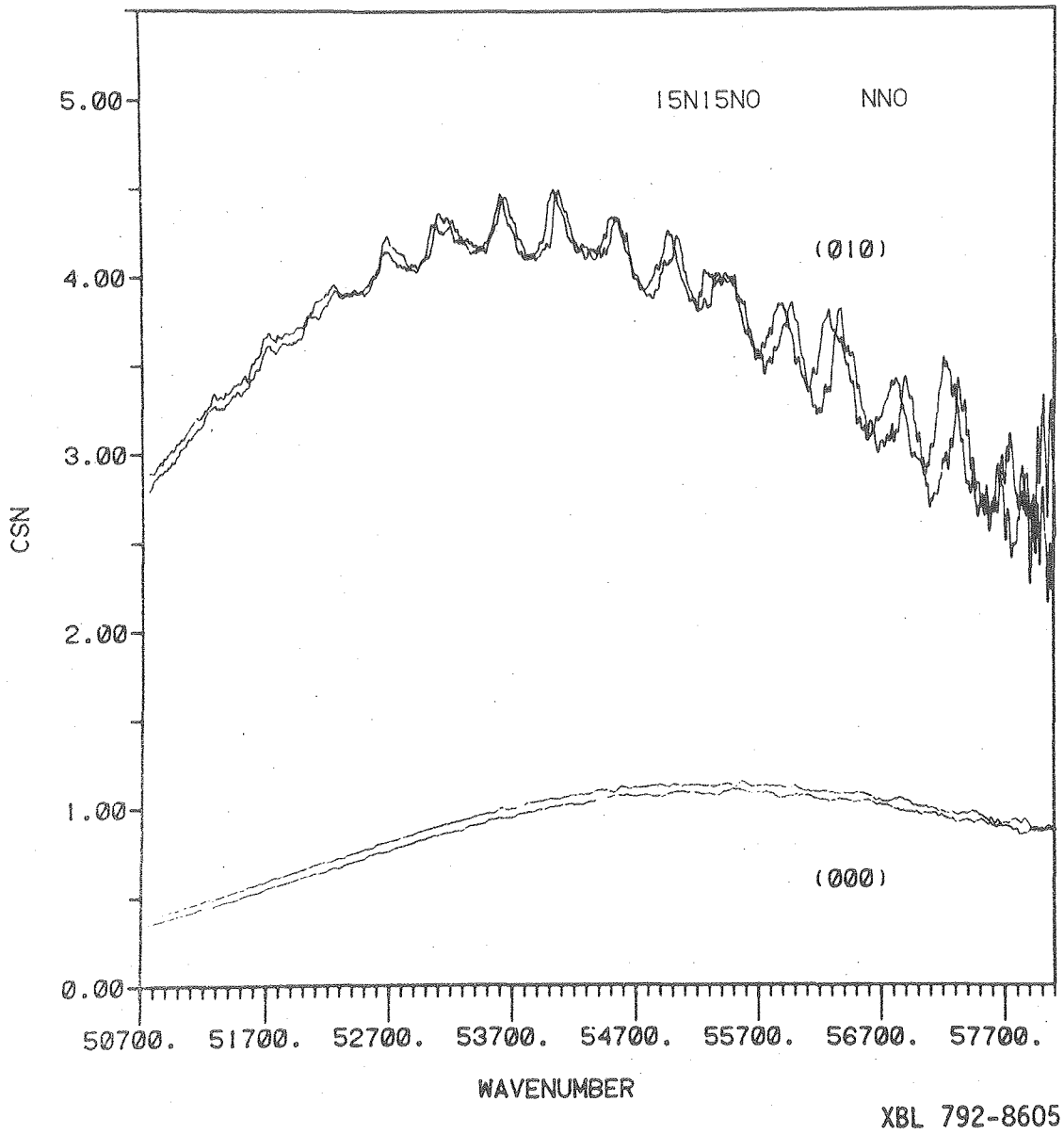
15N15NO
NNO
(010)
(000)
5.00
4.00
3.00
2.00
1.00
0.00
CSN
50700.
51700.
52700.
53700.
54700.
55700.
56700.
57700.
WAVENUMBER
XBL 792-8605

Figure 29c

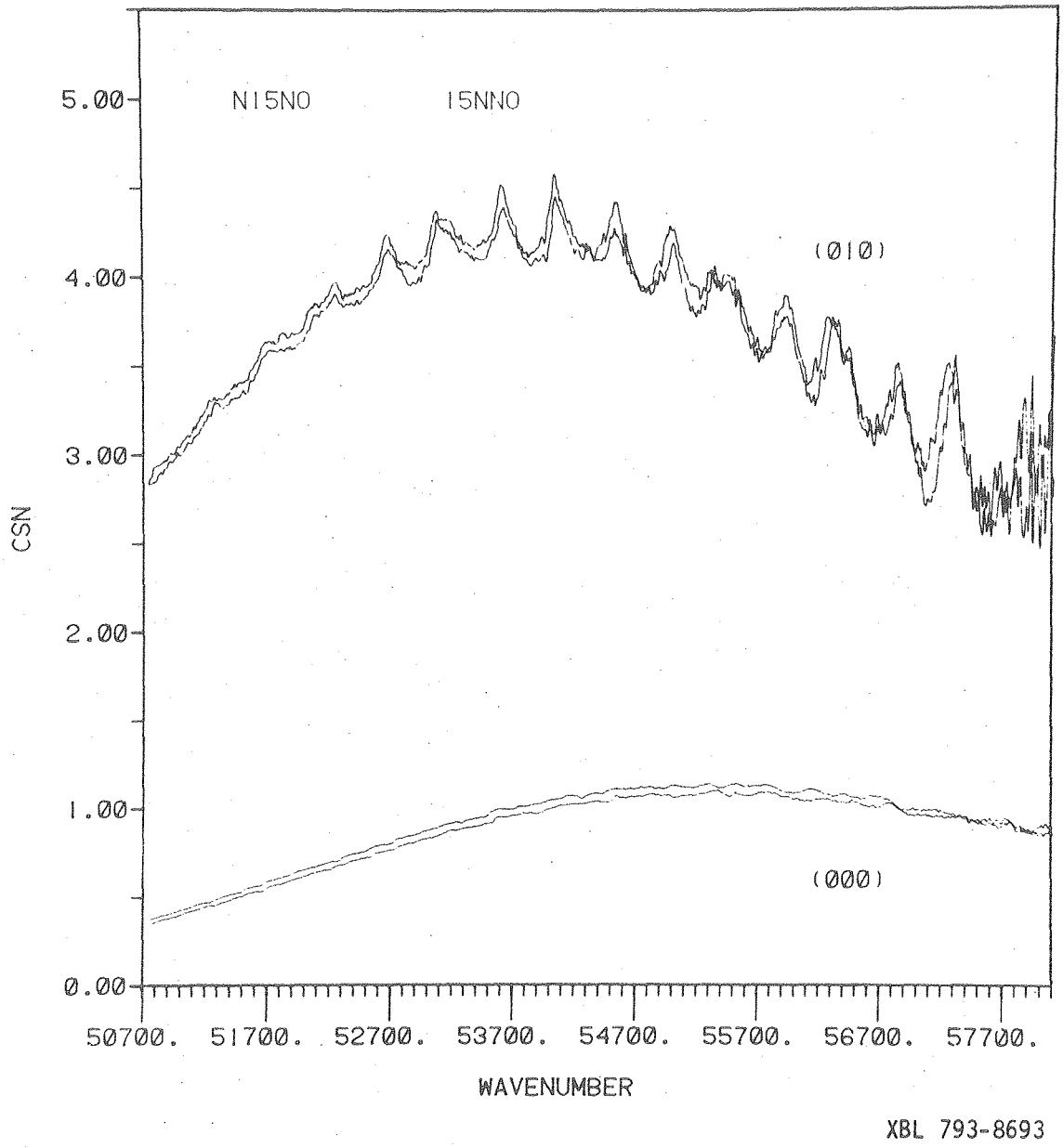

XBL 793-8693

Figure 29d

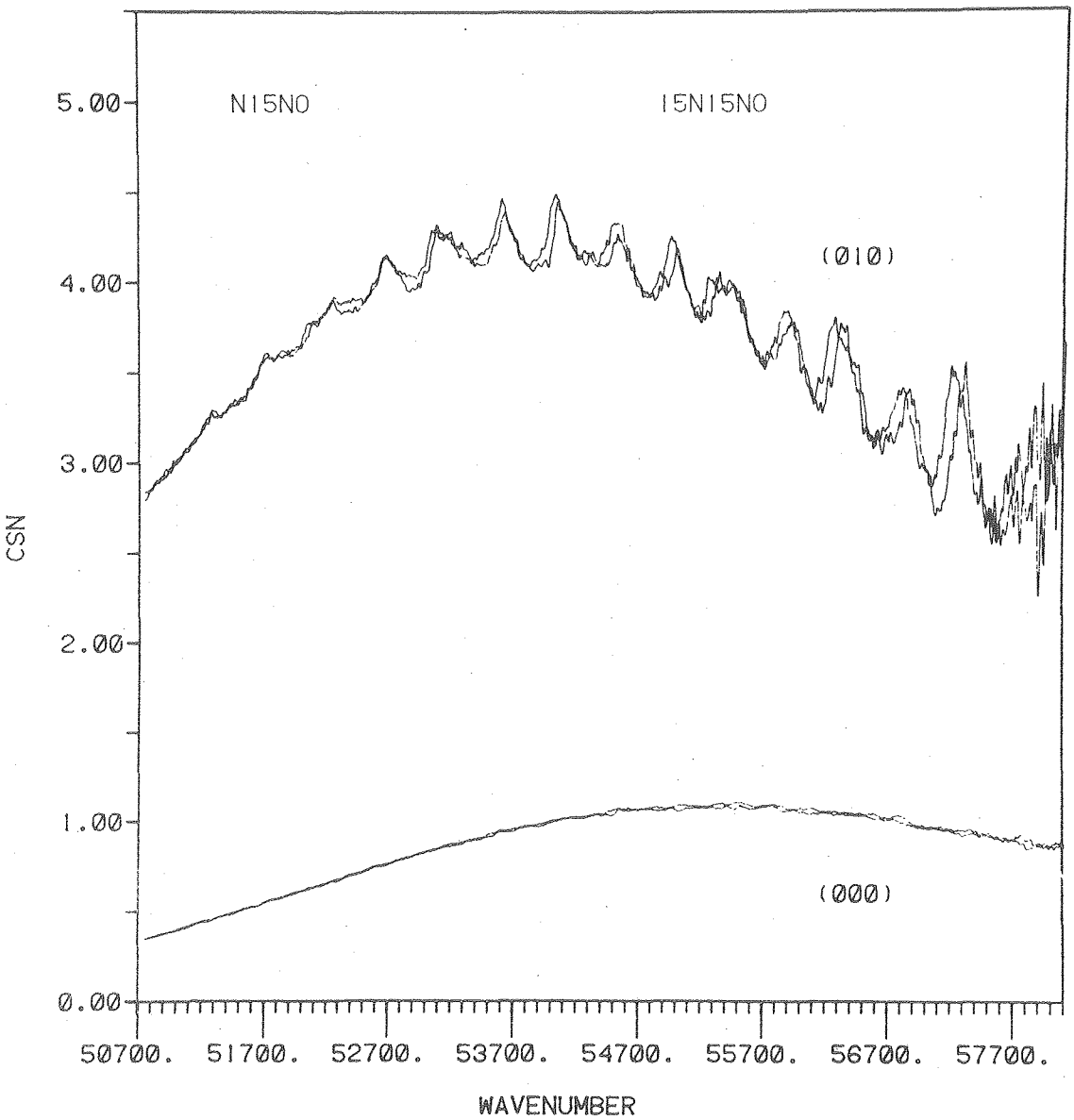

XBL 793-8694

Figure 29e

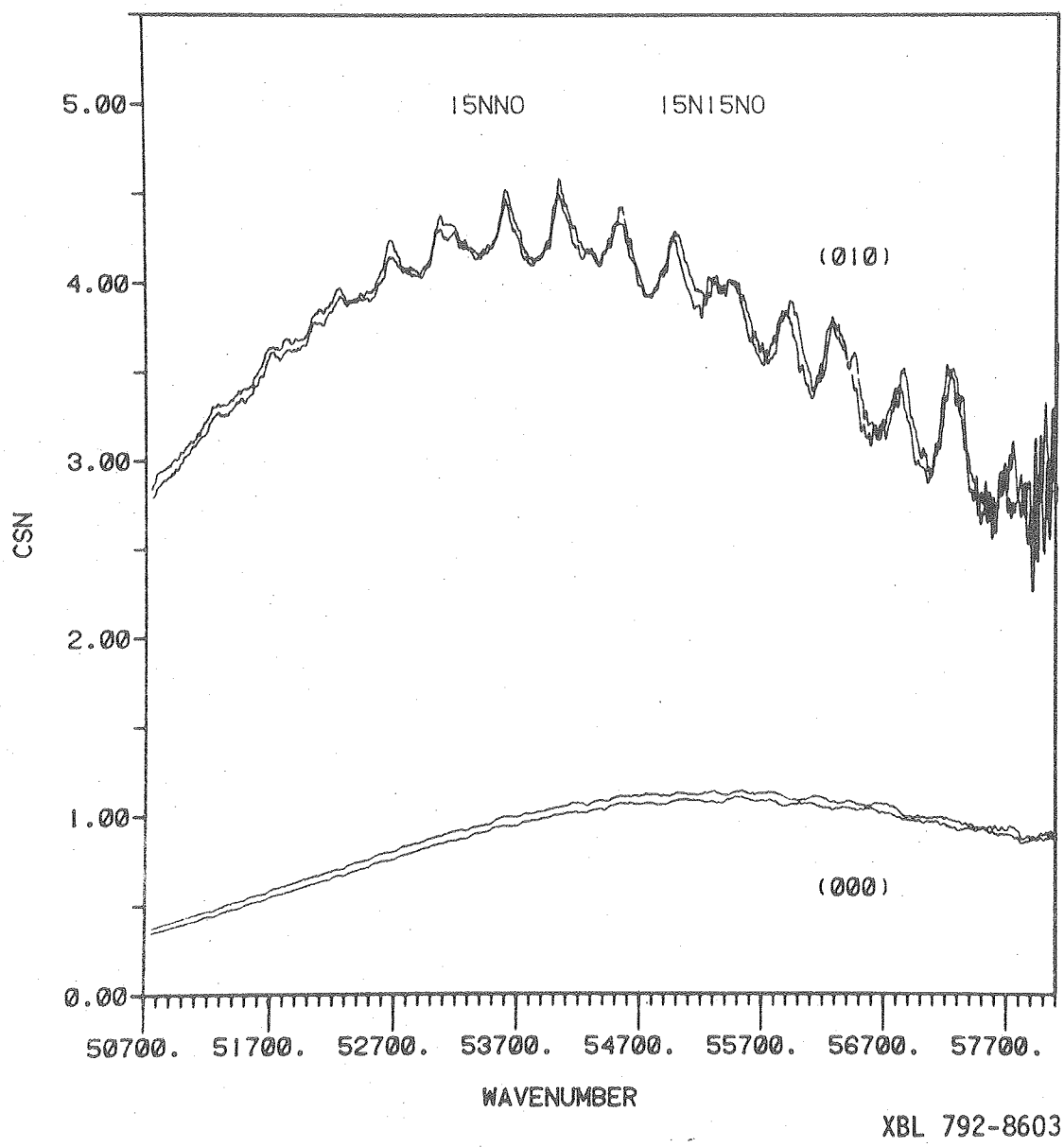

XBL 792-8603

Figure 29f

is now more clearly defined. As seen in figures 30 a-d, the (020) state spectrum is slightly more intense than the (010) state spectrum and is noticeably red-shifted. Unlike the result in the previous section, here the (020) state spectrum extends weakly to shorter wavelengths, although to avoid the very large noise resulting from small equilibrium populations of (020) and their minimal contribution at short wavelengths it was necessary here to use a seven point digital smooth and display only the portion of the (020) state spectrum above 175 nm.

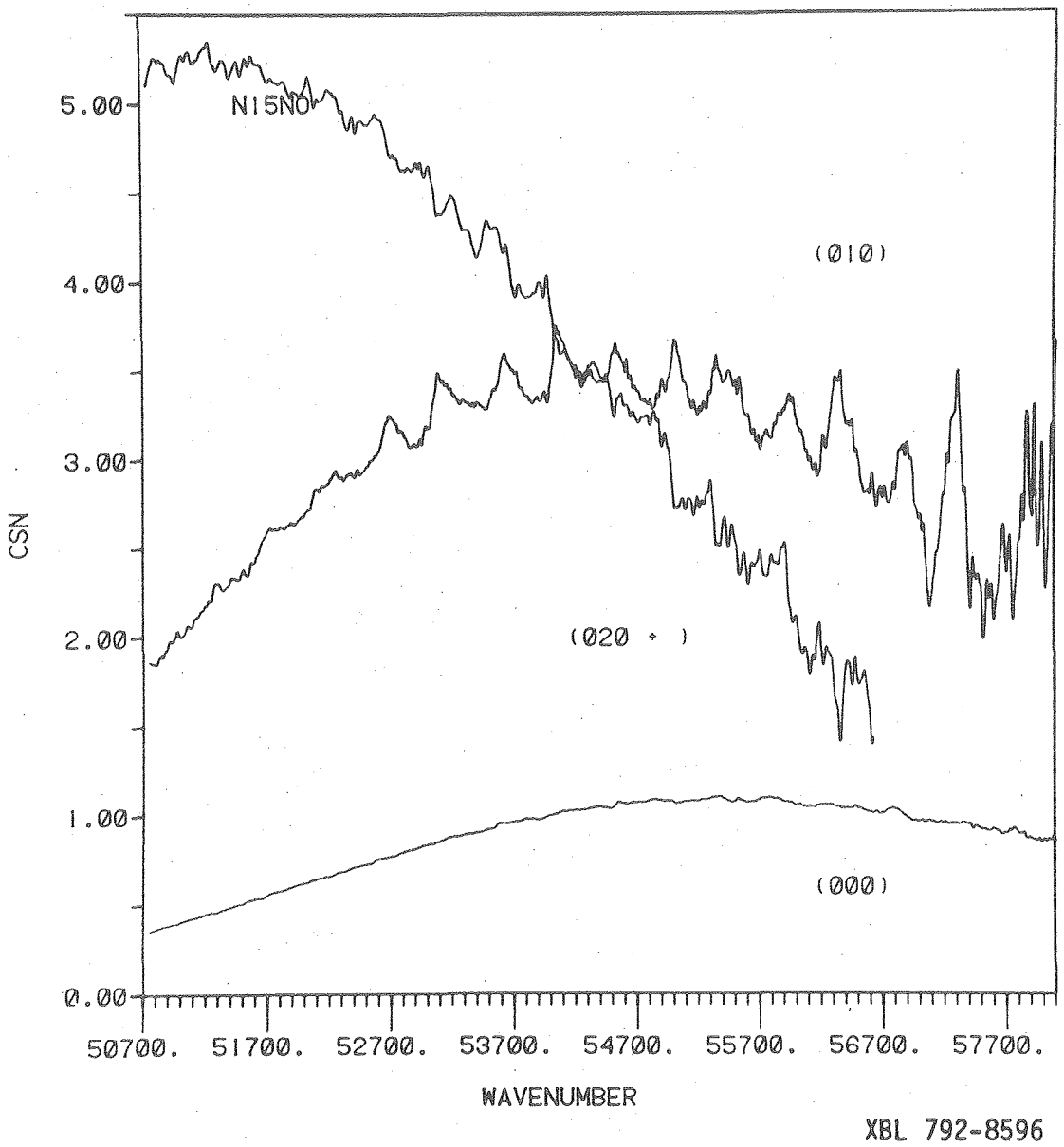
5.00
4.00
3.00
2.00
1.00
0.00
CSN
N15NO
(010)
(020 +)
(000)
50700.
51700.
52700.
53700.
54700.
55700.
56700.
57700.
WAVENUMBER
XBL 792-8596

Figure 30a

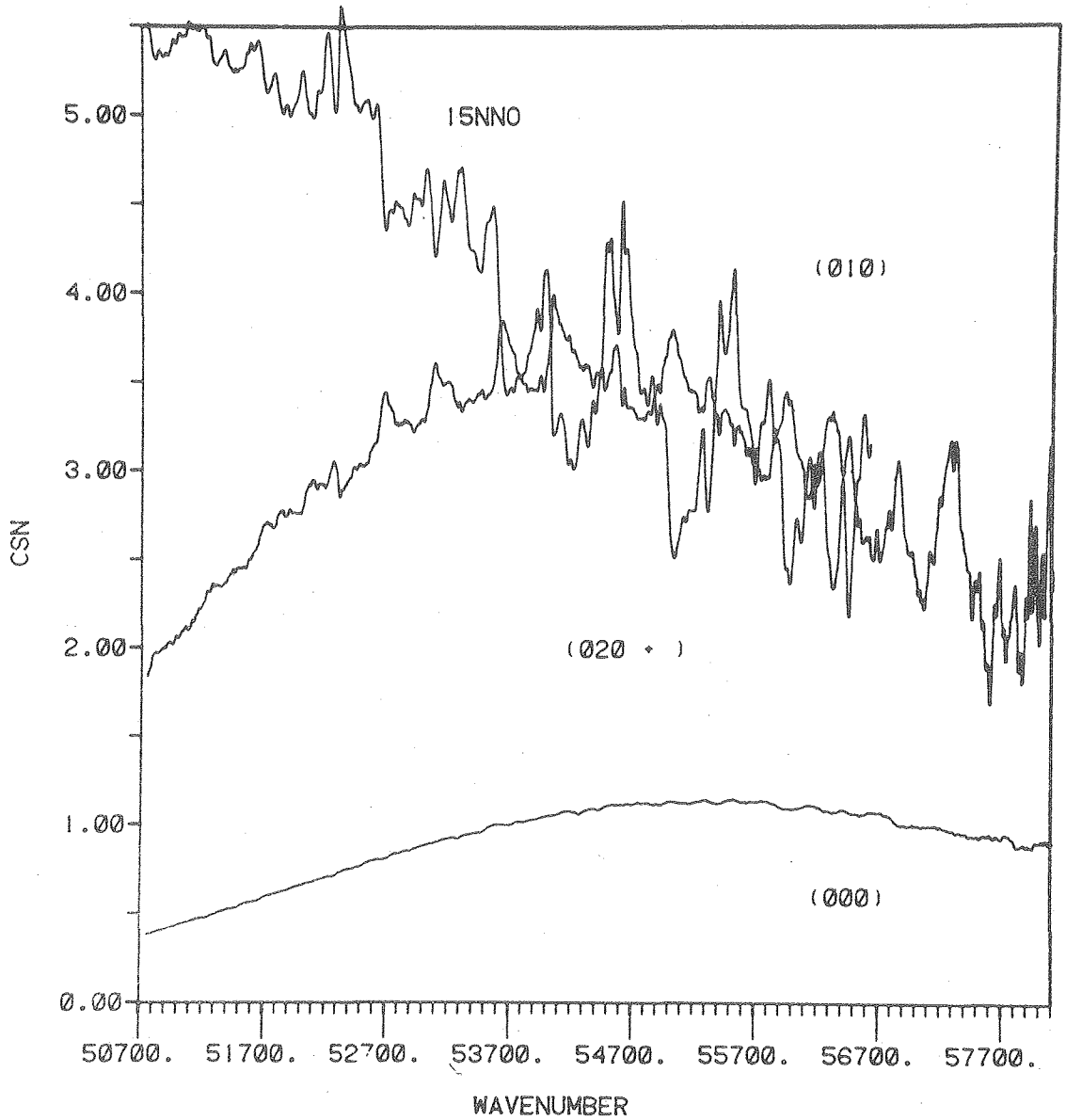

XBL 792-8589

Figure 30b

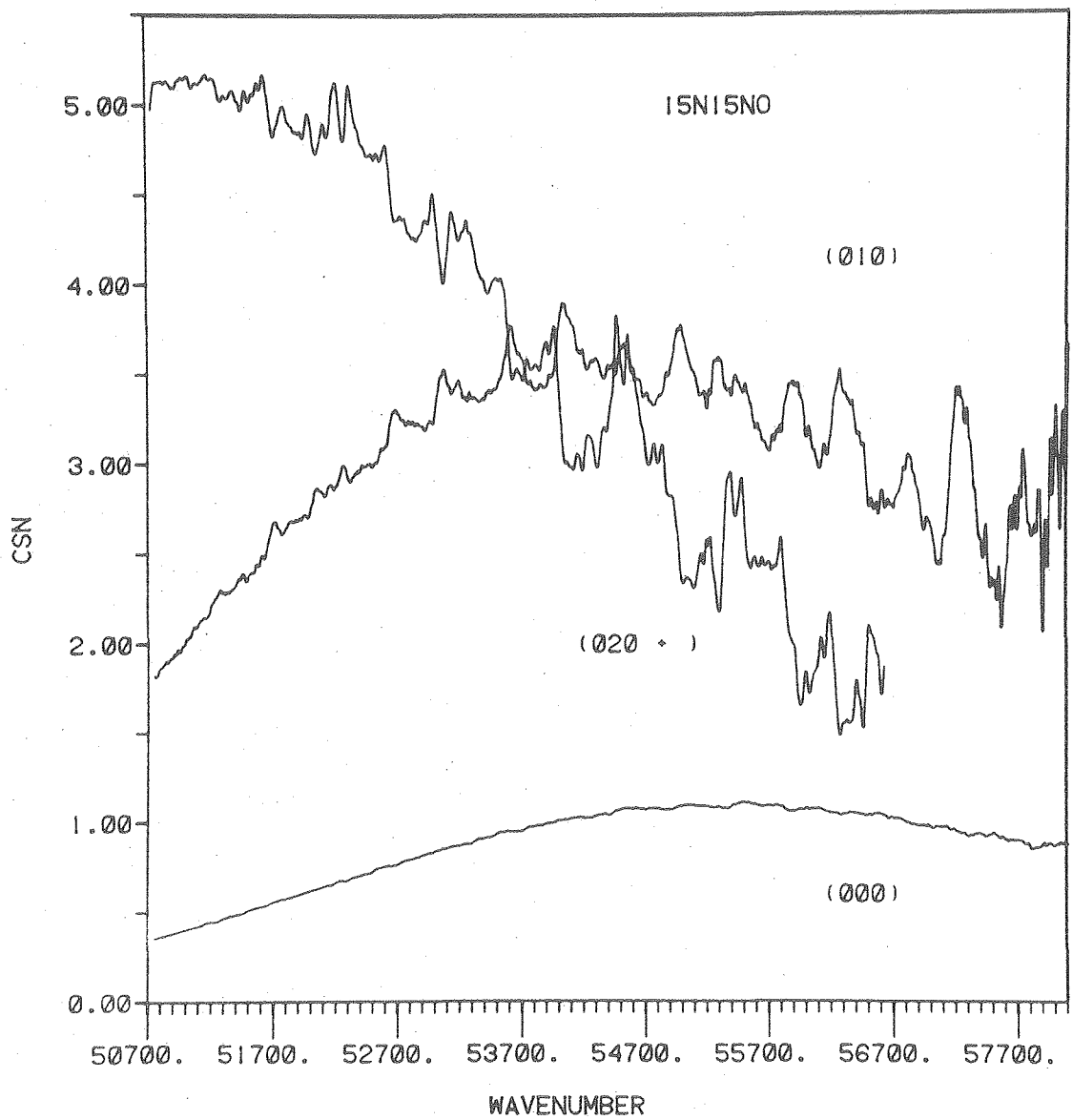

XBL 792-8584

Figure 30c

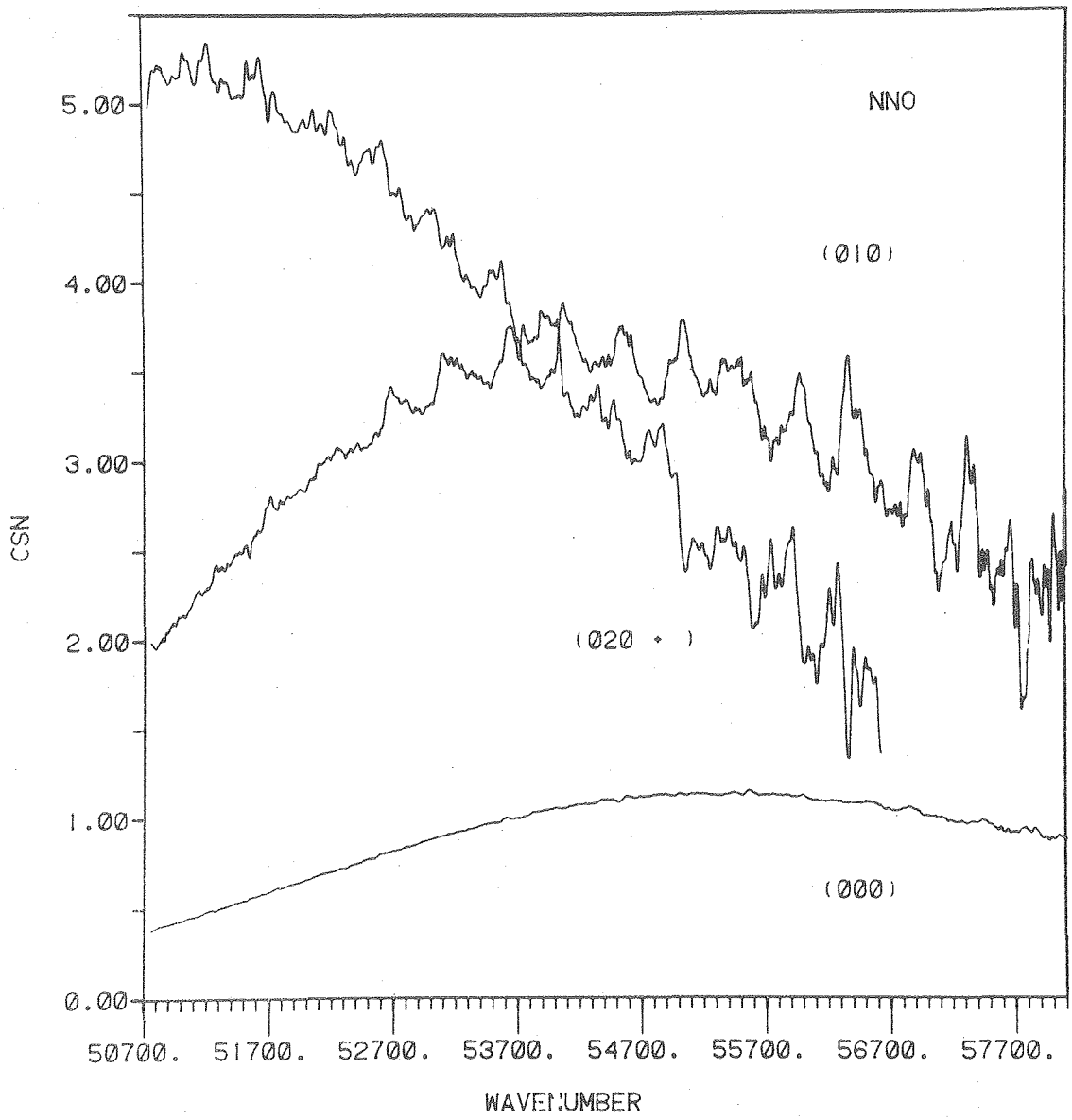

XBL 792-8576

Figure 30d

Appendix B: An Anomalous Result

In one sample of isotopic nitrous oxide, ^{15}NNO purchased from Prochem, an intensely strong and sharp absorption was noted. The sample, batch number 19X95 was found to contain a large amount of noncondensables in liquid nitrogen even though the flask was received in good condition with the seal unbroken. The noncondensables were pumped off and the remaining gas was purified by vacuum distillation. A mass spectrum of the purified gas indicated 95% atom purity of ^{15}NNO, in agreement with the manufacturers specficiations, without other noticeable impurities.

Unlike the other samples of isotopic nitrous oxide, including a sample of 99% atom purity ^{15}NNO, the sample alone indicated a series of sharp, featureless absorptions following an apparent progression. Absorption spikes were noted at 201, 197, 183 and 179 nm in the intensity pattern 3:1:3:1. By comparison with the second sample of ^{15}NNO it was concluded that these absorptions were the result of an impurity present in the 95% sample of ^{15}NNO since this other sample of the same isotope did not show these features.

Spectra of this anomalous absorption were also recorded on the 3 m vacuum spectrograph. At 0.03 Å resolution it was possible to measure the sharpness of these features: the 201 nm absorption had a full-width-half-maximum band width of 0.20 Å while the 197 nm absorption had a FWHM of 0.39 Å. Neither absorption exhibited any additional fine structure at this resolution.

Repeated exposure of the same sample to ultraviolet light weakened the intensity of these absorptions, indicating that dissociative

photolysis was resulting. This eliminated the possibility that the absorptions were atomic in nature. Additionally, the wavelengths noted did not match the absorption lines of any likely atomic species.

The temperature dependence of this unexplained absorption was also measured. From room temperature down to 200 K no significant change in absorption was noted. At temperatures below 200 K the impurity froze out. At 150 K only a very weak absorption could be noted. The 201 nm and 197 nm absorption exhibited a uniformity in their temperature dependence as described above.

In a further effort to identify the purity responsible for these sharp absorptions, the infrared spectrum of the contaminated sample of ^{15}NNO was recorded on a Nicolet 7199 Fourier Transform Spectrometer. Signal averaging was carried out for 2000 scans of sample and background at 0.06 cm^{-1} resoltuion. No impurities were identified by these techniques, although the sensitivity of results was enough to detect the "hot" (001) $\leftarrow$ (100) transition of ^{15}NNO in a 10 cm cell. At room temperature 0.2% of nitrous oxide molecules are in the (100) vibrational mode. It is possible that the impurity is not infrared active.

The impurity should not be a trace impurity because of the extremely intense absorption noted in the U.V. Knowing the total pressure of a gas sample and the absorption of these "spikes" in that sample, it is possible to estimate the concentration of the gas impurity as $>$ 0.1% since a smaller concentration would result in an absorption cross section of greater than 10^{-16} cm^2.

A mass spectrum of the contaminated sample of ^{15}NNO indicated the results shown in Table 8. Trichloroethylene was identified as

Table 8. Mass Spectrum Results for ^{15}NNO Sample

Peak No.	Mass	% Rel. Area
2	16	1.78
6	28	2.56
7	29	2.69
8	30	12.17
9	31	1.11
10	44	3.22
11	45	100.00

an impurity by this method, but this could not be responsible for the observed spectrum in the U.V.

Further spectra were obtained in the U.V. using a double beam technique in which the sample of 99% ^{15}NNO not exhibiting the spikes was placed in the reference beam of the Cary spectrometer. Using equal measures of the two samples, one in the reference beam and one in the sample beam results in subtracting out the common absorption of nitrous oxide, and leaving the spectrum of the impurities only. The result of this technique is shown in figure 31 at a SBW of 0.3 . Here, two of the spikes are noted at 201 and 197 nm and an additional weak feature is found at 193 nm. It is also seen that the spikes are not features superimposed on a weak absorption but instead the background is flat. The increasing slope below 195 nm is due to oxygen in the spectrometer (not purged for this run). The presence of some weak "negative" absorptions at longer wavelengths in the 10X curve is due to trace impurity of NO in the <u>reference</u> sample. In conclusion, this spectrum is inexplicable since the absorption spikes do not fit the absorption spectra of any likely molecular or atomic species.

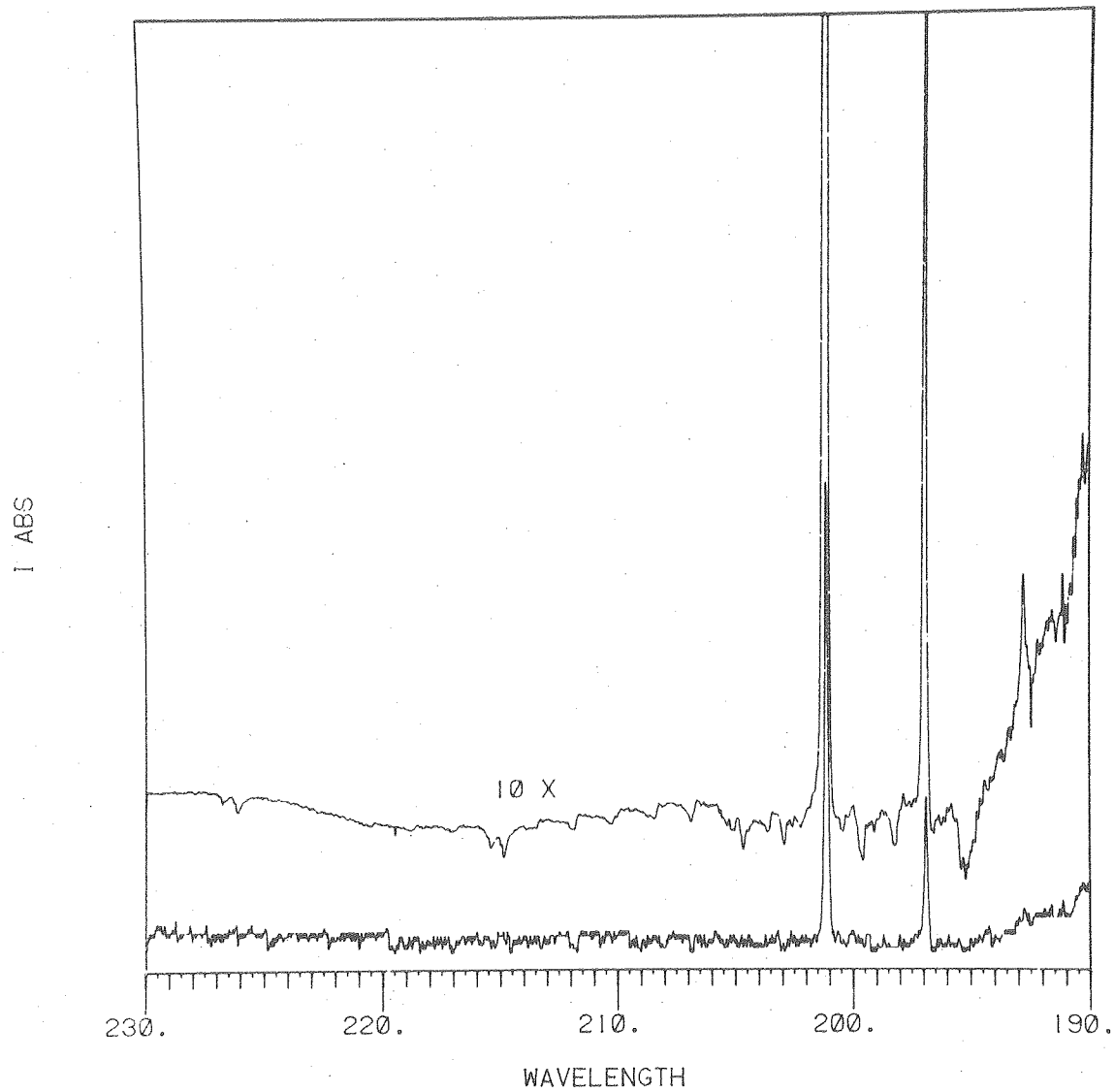

XBL 793-8696

Figure 31

C. Computer Programs

1. Deconvolution and Comparison of Observed and Predicted Spectra

```
      PROGRAM FIND(INPUT,OUTPUT,FILM,ASPEC,BSPEC,TAPE6=OUTPUT,
     A TAPE7=ASPEC,TAPE8=BSPEC)
      COMMON/RACV/TEMP(11),BTEMP(11),POPB(11),POPC(11)
      COMMON/IGSZZZ/Z(200)/NNO/SPECT(900) ,X(900)
      COMMON/FIT/Y(11,900),Y000(900),Y010(900),YGS(900),GAUSA(900)
      DIMENSION Y020(900)
      EXTERNAL FONT2
      DATA (TEMP(I),I=1,11)/151.,182.,196.,223.,247.,268.,301.,
     * 333.,372.,423.,485./
                DO 12 I=1,900
      X(I)=1/((1.00035*(190.02-I/50.))*1E-7)
       Y020(I)=0.
   12 CONTINUE

C   ******** GRAPHICS PARAMETERS ************

      CALL MODESG(Z,6,4HTEST)
      CALL VECIG(Z,FONT2,0)
      CALL SETSMG(Z,51,1.)
      CALL SETSMG(Z,93,000)
      CALL SETSMG(Z,103,-1.0)
      CALL SETSMG(Z,102,-3.)
      CALL SETSMG(Z,45,2.25)
C       ***** USED TO DRAW CIRCLES FOR DATA POINTS******
      CALL SETSMG(Z,84,3H*S2)

      CALL OBJCTG(Z,15.,15.,90.,95.)

C    *** 900 DATA POINTS ***
      III=900
      CALL SUBJEG(Z,52600.,.8,58200.,1.9)
      CALL PIKTUR(1)

                DO 15 NN=1,11
                DO 16 J=1,900,10

      IK=J+9
      READ 100, (Y(NN,K), K=J,IK)
  100 FORMAT(10F 7.4)
   16 CONTINUE

                DO 9 I=1,900

      SPECT(I)=Y(NN,I)
    9 CONTINUE

C    ***** PLOTS RAW  SPECTRAL DATA ******
C    ***** CALCULATES (000), (010), (020 + 030)
C          EQUILIBRIUM POPULATIONS FOR EACH TEMPERATURE ***


      CALL SETSMG(Z,45,.7)
         CALL POINTG(Z,III,X,SPECT)
      CALL SETSMG(Z,45,2.35)
      CALL BTEMP(NN)
```

```
   15 CONTINUE

C          INITIALIZE CALCULATION

      CALL SETSMG(Z,84,3H$SK)
      DO 7 I=1,900
      Y000(I)=Y(1,I)
      YGS(I)=Y(1,I)
    7 CONTINUE

C     ******* NJJ IS COUNTER FOR Y020 ITERATION*********

      NJJ=0
   51 CONTINUE

C  *****     JJJ IS COUNTER FOR Y010 SUB- ITERATION *********

      JJJ=0
   50 CONTINUE
      DO 5 I=1,900
      Y010(I)=0.
    5 CONTINUE
      NN=8

C     **** CALCULATES (010) STATE SPECTRUM ****
C     **** FOR FIRST-ORDER CALCULATION (020) IS SET TO 0 ****

      DO 20 I = 1,900
      Y010(I)=(Y(NN,I)-Y000(I)*QTEMP(NN)-Y020(I)*POPC(NN))/(POPB(NN))
   20 CONTINUE
      DO 23 NN = 1,11
      DO 21 I = 1,900
      SPECT(I)=Y000(I)*QTEMP(NN)+Y010(I)*POPB(NN)+Y020(I)*POPC(NN)
   21 CONTINUE

C     ******** CALCULATES CORRELATION COEFFICIENT ********

      A=0. $ C=0. $AA=0. $ CC=0. $AC=0.
      R=0.
                DO 30 I=1,900
      A=A+Y(NN,I)
      AA=AA+Y(NN,I)**2
      CC=CC+SPECT(I)**2
      C=C+SPECT(I)
      AC=AC+Y(NN,I)*SPECT(I)
   30 CONTINUE

      R=((III*AC)-A*C)/(SQRT(III*AA-A*A)*SQRT(III*CC-C*C))
      WRITE (6,200) JJJ,TEMP(NN),R
  200 FORMAT (1X,*ITER. NO. *I2,* TEMP K  *F 6.1*  COR. COEFF. *F9.6)
   23 CONTINUE

C      **** CORRECT 151 K SPECTRA FOR HOT CONTRIBUTION **

            DO 25 I = 1,900
```

```
      Y000(I)=(Y(1,I)-Y010(I)*POPB(1)-Y020(I)*POPC(1))/QTEMP(1)
   25 CONTINUE
   26 CONTINUE

      JJJ=JJJ+1
      IF (JJJ .LE. 5) GO TO 50
C     *** FIRST-ORDER RESULT OBTAINED FROM NJJ=0 ***

      IF (NJJ .EQ. 0) GO TO 14
      NN=11

C     **** USE 423 K SPECTRA TO CALCULATE (020) ****
C          NN = 10 IS THE 423 K DATA

            DO 77 I=1,900
      Y020(I)=(Y(NN,I)-Y010(I)*POPB(NN)-Y000(I)*QTEMP(NN))/(POPC(NN))
      YPOINT=Y020(I)
      IF (YPOINT .LE. 0.)  Y020(I)=0.
   77 CONTINUE

      NJJ=NJJ+1
C     ****** CONVERGENCE IS REACHED  BY 8 ITERATIONS ***
      IF (NJJ .LE. 8) GO TO 51


   14 CONTINUE
      NCONT=1
      CALL SUBJEG(Z,52600.,0.,58200.,5.0)
      CALL PIKTUR(0)

C   **** DRAW SPECTRA OF (000), (010) AND (020) ****

      CALL LINESG (Z,III,X,Y000)
      CALL LINESG (Z,III,X,Y010)
      CALL LINESG(Z,III,X,Y020)
      IF (NJJ .EQ. 0) GO TO 8


      CALL LEGNDG(Z,54200.,2.0,8,8H(020 + ))
      WRITE (8,100) Y000
      WRITE (8,105)
      WRITE (8,100) Y010
       WRITE (8,106)
      WRITE (8,100) Y020
    8 CONTINUE

      IF (NJJ .EQ. 0) WRITE (7,100) Y000
      IF (NJJ .EQ.0) WRITE (7,105)
      IF (NJJ .EQ. 0) WRITE (7,100) Y010
  105 FORMAT ( *THIS IS (010) SPECTRUM* )
  106 FORMAT ( *THIS IS (020) SPECTRUM*)
      CALL LEGNDG(Z,56200.,4.5,5,5H(010))
      CALL LEGNDG(Z,56200.,1.36,5,5H(000))

      CALL SUBJEG(Z,52600.,.8,58200.,1.3)
      CALL PIKTUR(1)
      CALL LINESG(Z,III,X,Y000)
```

```
                CALL POINTG(Z,III,X,YGS)

                CALL SUBJEG(Z,52600.,.8,58200.,1.9)
             13 CONTINUE

        C    ****** CALCULATE CONVOLUTED SPECTRUM *******

                CALL PIKTUR(1)
                DO 55 NN=NCONT,11,2
                DO 60 I=1,900


                SPECT(I)=Y000(I)*QTEMP(NN)+Y010(I)*POPB(NN)+Y020(I)*POPC(NN)
                GAUSA(I)=Y(NN,I)
             60 CONTINUE

        C       ****** PLOT CONVOLUTED AND OBSERVED SPECTRA ************

                CALL LINESG(Z,III,X,SPECT)
                CALL POINTG(Z,III,X,GAUSA)
             55 CONTINUE

                NCONT=NCONT+1
                NJJ =NJJ +1
                IF (NCONT .EQ. 2) GO TO 13
                IF (NJJ .EQ. 2) GO TO 51
                 CALL EXITG(Z)
                END
```

SYMBOLIC REFERENCE MAP (R=1)

```
ENTRY POINTS
 5257  FIND

VARIABLES      SN  TYPE            RELOCATION
 6262  A          REAL                                6264  AA        REAL
 6266  AC         REAL                                6263  C         REAL
 6265  CC         REAL                               30470  GAUSA     REAL        ARRAY    FIT
 6252  I          INTEGER                             6253  III       INTEGER
 6256  IK         INTEGER                             6255  J         INTEGER
 6261  JJJ        INTEGER                             6257  K         INTEGER
 6271  NCONT      INTEGER                             6260  NJJ       INTEGER
 6254  NN         INTEGER                               26  POPB      REAL        ARRAY    RACY
   41  POPC       REAL        ARRAY    RACY             13  QTEMP     REAL        ARRAY    RACY
 6267  R          REAL                                  0  SPECT     REAL        ARRAY    NNO
    0  TEMP       REAL        ARRAY    RACY           1604  X         REAL        ARRAY    NNO
    0  Y          REAL        ARRAY    FIT           26664  YGS       REAL        ARRAY    FIT
 6270  YPOINT     REAL                               23254  Y000      REAL        ARRAY    FIT
25060  Y010       REAL        ARRAY    FIT            6272  Y020      REAL        ARRAY
    0  Z          REAL        ARRAY    IGSZZZ
```

```
        PROGRAM FIND     7600→7600 OPT=1                          FTN 4.6+452/034    06 FEB 79 22.56.51  BKY PAGE      5

FILE NAMES          MODE
 3143  ASPEC                    4204  BSPEC                  2102  FILM                      0  INPUT      FMT
 1041  OUTPUT                    1041  TAPE6      FMT         3143  TAPE7      FMT         4204  TAPE8      FMT

EXTERNALS           TYPE    ARGS
       BTEMP                    1                            EXITG                  1
       FONT2                    0                            LEGNDG                 5
       LINESG                   4                            MODESG                 3
       OBJCTG                   5                            PIKTUR                 1
       POINTG                   4                            SETSMG                 3
       SQRT        REAL         1 LIBRARY                    SUBJEG                 5
       VECIG                    3

STATEMENT LABELS
    0  5                                    0  7                                  5621  8
    0  9                                    0  12                                 5650  13
 5571  14                                   0  15                                    0  16
    0  20                                   0  21                                    0  23
    0  25                                   0  26          INACTIVE                  0  30
 5404  50                                 5403  51                                    0  55
    0  60                                     0  77                                 6121  100      FMT
 6175  105      FMT                      6201  106      FMT                         6131  200      FMT

LOOPS  LABEL     INDEX      FROM-TO     LENGTH     PROPERTIES
 5263  12        I           11 14        10B       INSTACK
 5323  15      * NN          36 58        46B                 EXT REFS  NOT INNER
 5324  16      * J           37 42        23B                 EXT REFS  NOT INNER
 5332          * K           40 40        11B                 EXT REFS
 5353  9         I           44 47         3B       INSTACK
 5376  7         I           64 67         3B       INSTACK
 5407  5         I           78 80         2B       INSTACK
 5424  20        I           86 88         7B       INSTACK
 5435  23      * NN          89 110       66B                 EXT REFS  NOT INNER
 5444  21        I           90 92         7B       INSTACK
 5464  30        I           98 104       13B          OPT
 5526  25        I          114 116        7B       INSTACK
 5554  77        I          129 133       11B       INSTACK
 5654  55      * NN         180 192       31B                 EXT REFS  NOT INNER
 5665  60        I          181 186       10B       INSTACK

COMMON BLOCKS    LENGTH
       RACY          44
       IGSZZZ       200
       NAO         1800
       FIT        13500

STATISTICS
  PROGRAM LENGTH                 2645B    1445
  BUFFER LENGTH                  5245B    2725
  SCM LABELED COMMON LENGTH     36270B   15544
```

```
SUBROUTINE PIKTUR   7600→7600 OPT=1                    FTN 4.6+452/034    06 FEB 79 22.56.51  BKY PAGE      1

 1                SUBROUTINE PIKTUR(W)
                  COMMON/ IGSZZZ/ Z (200)
                  INTEGER W
                  CALL PAGEG(Z,0,1,1)
 5                CALL GRID G (Z,0,0,0,0)
                  FMT = 6.0
                  CALL LABEL G (Z,0,1000.,0,FMT)
                  CALL SETSMG(Z,102,-1.0)
                   CALL LABELG(Z,0,100.,1,1H )
10                CALL SETSMG(Z,102,-3.0)
                  FMT = 4.2
                  IF (W .EQ. 1) GO TO 50
                   CALL LABELG(Z,1,1.,0,FMT)
                  CALL SETSMG(Z,178,1.)
15                CALL LABELG(Z,1,0.5,1,1H )
                  CALL SETSMG(Z,178,0.)
                  GO TO 70
               50 CONTINUE
                  CALL LABELG(Z,1,.2,0,FMT)
20                CALL SETSMG(Z,178,1.)
                  CALL LABELG(Z,1,.1,1,1H )
                  CALL SETSMG(Z,178,0.)
                  CALL SETSMG(Z,103,-1.0)
               70 CONTINUE
25                CALL TITLE G (Z,10,10HWAVENUMBER,3,3HCSN,3,3HN20)
                  RETURN
                  END


      SYMBOLIC REFERENCE MAP (R=1)

ENTRY POINTS
    3  PIKTUR

VARIABLES      SN  TYPE            RELOCATION
  210  FMT        REAL                                    0  W          INTEGER              F.P.
    0  Z          REAL        ARRAY     IGSZZZ

EXTERNALS            TYPE    ARGS
       GRIDG                  5                              LABELG                5
       PAGEG                  4                              SETSMG                3
       TITLEG                 7

STATEMENT LABELS
   36  50                                   50  70

COMMON BLOCKS    LENGTH
       IGSZZZ      200

STATISTICS
  PROGRAM LENGTH                 225B      149
  SCM LABELED COMMON LENGTH      310B      200
```

```
SUBROUTINE BTEMP    7600→7600 OPT=1                    FTN 4.6+452/034    06 FEB 79 22.56.51  BKY PAGE      1

1                 SUBROUTINE BTEMP(NN)
                  COMMON/RACY/TEMP(11),QTEMP(11),POPB(11),POPC(11)
                  BB=(1-EXP(-589./(TEMP(NN)*.6952)))**2
                  BC=(1-EXP(-1284./(TEMP(NN)*.6952)))
5                 BD=(1.-EXP(-2223./(TEMP(NN)*.6952)))
                  QTEMP(NN)=BB*BC*BD
                  POPB(NN)=2*(EXP(-589./(TEMP(NN)*.6952)))*QTEMP(NN)
                  POPC(NN)=3.*(EXP(-2.*585./(TEMP(NN)*.6952)))*QTEMP(NN)
                 A  + 4.*(EXP(-3.*582./(TEMP(NN)*.6952)))*QTEMP(NN)
10                RETURN
                  END


SYMBOLIC REFERENCE MAP (R=1)

ENTRY POINTS
   3  BTEMP

VARIABLES      SN  TYPE          RELOCATION                  71  BC       REAL
   70  BB         REAL                                       0  NN       INTEGER                F.P.
   72  BD         REAL                                      41  POPC     REAL       ARRAY    RACY
   26  POPB       REAL        ARRAY    RACY                  0  TEMP     REAL       ARRAY    RACY
   13  QTEMP      REAL        ARRAY    RACY

EXTERNALS          TYPE   ARGS
      EXP         REAL      1 LIBRARY

COMMON BLOCKS    LENGTH
      RACY          44

STATISTICS
  PROGRAM LENGTH                  73B      59
  SCM LABELED COMMON LENGTH       54B      44
```

2. Computation of Difference Spectra and Energy Levels in the Upper Electronic State

```
C  ***********  MAIN PROGRAM INSIGHT ***********
      PROGRAM INSIGHT(INPUT,OUTPUT,FILM,TAPE6=OUTPUT)
      COMMON/RACY/TEMP(11)/IGSZZZ/Z(200)
      COMMON/PICKER/PEAK(200)/EASY/ISUBRT(20)
      COMMON/GRAPH/A(11,150)
      DIMENSION X(900),Y(900),GAUST(900),DIF(900)
      INTEGER W
      EXTERNAL FONT2

C     **** TEMPERATURES OF SPECTRA IN DEGREES K ****
      DATA (TEMP(I),I=1,11)/151.,182.,196.,223.,243.,260.,301.,
     * 333.,372.,423.,485./

C     ***-***  INITIALIZE ARRAY  *****

      DO 7 M=1,11
      DO 8 J=1,150
      A(M,J)=0.
    8 CONTINUE
    7 CONTINUE
C   *** CONVERT X-AXIS IN WAVELENGTH SCALE TO WAVENUMBER SCALE ***
      DO 12 I=1,900
       X(I)=1/((1.00035*(190.02-I/50.))*1E-7)
   12 CONTINUE
      III=900

C    ******* GRAPHICS PARAMETERS *********

      CALL MODESG(Z,6,4HTEST)
       CALL OBJCTG(Z,15.,22.,99.,95.)
      CALL VECIG(Z,FONT2,0)
       CALL SETSMG(Z,51,1.)
      CALL SETSMG(Z,45,2.0)
      CALL SETSMG(Z,102,-2.5)
      CALL SUBJEG(Z,52600.,0.,58200.,.3)
      CALL SETSMG(Z,93,000)
      CALL SETSMG(Z,103,4.)
      DO 03 MM=1,11
      CALL GRIDG(Z,0,0,0,0)
      FMT=6.0
      CALL LABELG(Z,0,1000.,0,FMT)
      FMT=4.2
      CALL LABELG(Z,1,0.05,0,FMT)
      CALL SETSMG(Z,102,-1.)
      CALL SETSMG(Z,178,1.)
      CALL LABELG(Z,0,100.,1,1H )
      CALL SETSMG(Z,103,2.)
      CALL LABELG(Z,1,.025,1,1H )
      CALL TITLEG(Z,10,10HWAVENUMBER,10,10HDIFFERENCE,3,3HN20)

C    **** BTEMP CALCULATES STATISTICAL POP. ****
      CALL BTEMP(MM,BTEMP,POPB)
      CALL SETSMG(Z,102,-2.5)
      CALL SETSMG(Z,178,0.)
```

```
C   ***READ RAW DATA***
      READ 100,Y
  100 FORMAT(10F7.4)
C    ******   FORM COMPOSITE GAUSSIAN CURVE FOR 000 AND 010 STATES *****
      DO 67 I=1,900
      B=1.21
      D=4.2E-8
      XC=55140.
      GAUSA     =X(I)*(B/58140.)*(EXP(-D*(X(I)-XC)*(X(I)-XC))) *QTEMP
      B=4.1
      D=2.5E-8
      XC=53100.
      GAUSB     =X(I)*(B/58140.)*(EXP(-D*(X(I)-XC)*(X(I)-XC))) *POPB
      GAUST(I)=GAUSA+GAUSB
C     ******* FORM DIFFERENCE SPECTRUM  ********
      DIF(I)=Y(I)-GAUST(I)
   67 CONTINUE
      PRINT 121,TEMP(NN),QTEMP,POPB
  121 FORMAT(1H1,10X,*TEMP IS *F5.0,* PAR FUNCT IS*F5.4,*010 IS*F5.4)
C *:*** PLOT DIFFERENCE SPECTRUM *******
      CALL LINESG(Z,III,X,DIF)
      FMT=4.0
      CALL NUMBRG(Z,53500.,.25,FMT,TEMP(NN))
      CALL LEGNDG(Z,54000.,.25,6,6HDEG. K)
C ****IDENTIFY PEAK POSITIONS*********
      CALL CHECK (X,III,DIF,W,PEAK)
C    ******  PRINTOUT OF PEAK SEPARATION PERMUTATIONS ******
      PRINT 137,W
  137 FORMAT(30X,*TOTAL NUMBER OF PEAKS IS *I4)
      WRITE (6,139)
  139 FORMAT(6X,*ENERGY SPACING BTW PEAKS IN WAVENUMBERS*)
      CALL PRINTER (W,NN)
C     *** ADVANCE PAGE ***
      CALL PAGEG(Z,0,1,1)
   83 CONTINUE
C   ******* MAKES BAR GRAPH-- HISTOGRAM  *******
C  ***NS= NUMBER SEGMENTS   NB=NUMBER OF ENERGY BINS ***
      NS=11 & NB=150
      CALL OBJCTG(Z,12.,19.,95.,95.)
      CALL SUBJEG(Z,0.,0.,3000.,5.)
      FMT=6.0
      CALL LABELG(Z,0,500.,0,FMT)
```

```
115                 CALL OBJCTG(Z,7.,14.,100.,100.)
                    CALL SETSMG(Z,117,1.0)
                    CALL KWKBRG(Z,A,NS,NB,10,10HWAVENUMBER,9,9HOCCURENCE,1,1H )
                    CALL EXITG(Z)
                    END
```

```
      SYMBOLIC REFERENCE MAP (R=1)

ENTRY POINTS
 3151  INSIGHT

VARIABLES      SN  TYPE          RELOCATION
    0  A          REAL       ARRAY    GRAPH          4010  B          REAL
 4011  D          REAL                                11233  DIF        REAL       ARRAY
 4005  FMT        REAL                                 4013  GAUSA      REAL
 4014  GAUSB      REAL                                 7427  GAUST      REAL       ARRAY
 4002  I          INTEGER                              4003  III        INTEGER
    0  ISUBRT     INTEGER    ARRAY    EASY           4001  J          INTEGER
 4000  M          INTEGER                              4016  NB         INTEGER
 4004  NN         INTEGER                              4015  NS         INTEGER
    0  PEAK       REAL       ARRAY    PICKER         4007  POPB       REAL
 4006  QTEMP      REAL                                    0  TEMP       REAL       ARRAY    RACY
 3777  W          INTEGER                              4017  X          REAL       ARRAY
 4012  XC         REAL                                 5623  Y          REAL       ARRAY
    0  Z          REAL       ARRAY    IGSZZZ

FILE NAMES        MODE
 2102  FILM                        0  INPUT     FMT          1041  OUTPUT    FMT          1041  TAPE6     FMT

EXTERNALS          TYPE    ARGS
       BTEMP                 3                                 CHECK                  5
       EXITG                 1                                 EXP        REAL        1 LIBRARY
       FONT2                 0                                 GRIDG                  5
       KWKBRG               10                                 LABELG                 5
       LEGMDG                5                                 LINESG                 4
       MODESG                3                                 NUMBRG                 5
       OBJCTG                5                                 PAGEG                  4
       PRINTER               2                                 SETSMG                 3
       SUBJEG                5                                 TITLEG                 7
       VECIG                 3

STATEMENT LABELS
    0  7                                   0  8                                       0  12
    0  67                                  0  83                                   3646  100      FMT
 3656  121      FMT                     3672  137      FMT                         3702  139      FMT
```

```
LOOPS  LABEL     INDEX      FROM-TO    LENGTH    PROPERTIES
 3153  7       * M           18 22       13B              NOT INNER
 3160  8         J           19 21        2B     INSTACK
 3170  12        I           24 26        7B     INSTACK
 3224  83      * NN          40 105     122B               EXT REFS  NOT INNER
 3261  67      * I           65 79       32B               EXT REFS

COMMON BLOCKS   LENGTH
       RACY        11
       IGSZZZ     200
       PICKER     200
       EASY        20
       GRAPH     1650

STATISTICS
  PROGRAM LENGTH                 7720B    4048
  BUFFER LENGTH                  3143B    1635
  SCM LABELED COMMON LENGTH      4041B    2081
```

```
      SUBROUTINE BTEMP (NN,QTEMP,POPB)
C     **** CALCULATES VIBRATIONAL POPULATIONS  *****
      COMMON/RACY/TEMP(11)
       T=TEMP(NN)
      BB=(1-EXP(-589./(T*.6952)))
      QTEMP=BB*BB
C ***** QTEMP IS (000)POPULATION *****
C ***** POPB IS (010) POPULATION ******
      POPB=2*(EXP(-589./(T*.6952)))*QTEMP
      RETURN
      END
```

SYMBOLIC REFERENCE MAP (R=1)

```
ENTRY POINTS
    3  BTEMP

VARIABLES      SN  TYPE          RELOCATION
   27  BB          REAL                              0  NN        INTEGER              F.P.
    0  POPB        REAL                F.P.          0  QTEMP     REAL                 F.P.
   26  T           REAL                              0  TEMP      REAL       ARRAY     RACY

EXTERNALS          TYPE    ARGS
       EXP         REAL      1 LIBRARY

COMMON BLOCKS    LENGTH
       RACY         11

STATISTICS
  PROGRAM LENGTH                  30B      24
  SCM LABELED COMMON LENGTH       13B      11
```

```
SUBROUTINE BAR      7600-7600 OPT=1                          FTN 4.6+452/034    27 JAN 79 20.40.07  BKY PAGE      1

 1
                    SUBROUTINE BAR(NN,JSUBRT)
 5          C     ***** GROUPS ENERGY SEPARATIONS INTO BINS OF 20 CM-1 ****
                    COMMON/GRAPH/A(11,150)
                    KSUBRT=JSUBRT/20
10          C      ****** FORMS BAR GRAPH ARRAYS    *******
                    A(NN,KSUBRT)=A(NN,KSUBRT)+1.
                    RETURN $END


SYMBOLIC REFERENCE MAP (R=1)

ENTRY POINTS
   3  BAR

VARIABLES      SN  TYPE            RELOCATION
   0  A           REAL        ARRAY    GRAPH            0  JSUBRT    INTEGER              F.P.
  15  KSUBRT      INTEGER                                 0  NN        INTEGER              F.P.

COMMON BLOCKS    LENGTH
       GRAPH       1650

STATISTICS
  PROGRAM LENGTH                  16B      14
  SCM LABELED COMMON LENGTH     3162B    1650
```

```
1
                SUBROUTINE CHECK(X,III,TOP,D,PEAK)
5         C  ******* SELECTS PEAKS  ********
                COMMON/IGSZZZ/Z(200)
                DIMENSION TOP(III),X(900),PEAK(200)
                LOGICAL POINT, CHECKA, CHECKB, CHECKC, CHECKD, POP
10              INTEGER D
                POP=.TRUE.
                I=5 $ D=0
          C   *** SLOPE CRITERIA ***
15           10 POINT=((TOP(I) .GT. TOP (I-1)) .AND. (TOP(I) .GE. TOP(I+1)))
                CHECKB=(TOP(I+1) .GE. TOP(I+2))
                CHECKC=((TOP(I) .GT. TOP(I-4)) .AND.(TOP(I).GT.TOP(I+4)))
                 CHECKA=((POINT .AND. CHECKB).AND.CHECKC)
                CHECKD=((TOP(I) .GT.TOP(I-10)) .OR.((TOP(I).GT.TOP(I+10))))
20              POINT=((CHECKD .AND. CHECKA) .AND. POP)
          C   *** WIDTH CRITERIA ****
                WM=TOP(I-25) $ WP=TOP(I+25)
                CHECKA=((TOP(I)-WM.GE.0.008).AND.((TOP(I)-WP).GE.0.008))
25
          C      ****** APPLICABLE TO FIRST OR LAST 25 DATA POINTS ONLY ******
                IF (I .LE. 25) CHECKA=((TOP(I)-WM).GT.0.015) .OR.
               *  ((TOP(I)-WP) .GT. 0.015)
30              IF (I.GE.(III-25)) CHECKA=((TOP(I)-WM).GT.0.024) .OR.
               *  ((TOP(I)-WP) .GT. 0.024)
                IF (POINT .AND. CHECKA) GO TO 50
                WM=TOP(I-10) $ WP=TOP(I+10)
                CHECKA=((TOP(I)-WM.GE.0.012).AND.
35             @ (TOP(I)-WP.GE.0.012))
                IF (POINT.AND.CHECKA) GO TO 50
                I=I+1
                IF (I .LE. III-4) GO TO 10
                RETURN
40
             50 CONTINUE
                 X1=X(I)
                Y1=0. $ Y2=TOP(I)
45        C    **** DRAWS VERTICAL LINES FOR PEAKS POSIITION  *****
                CALL SEGMTG(Z,1,X1,Y1,X1,Y2)
                IFMT=1
                D=D+1
50              PEAK(D)=X(I)
                I=I+2
                IF (I .LE. III-4) GO TO 10
                RETURN $ END
```

```
      SYMBOLIC REFERENCE MAP (R=1)

ENTRY POINTS
    3  CHECK

VARIABLES      SN  TYPE            RELOCATION
  134  CHECKA     LOGICAL                          135  CHECKB     LOGICAL
  136  CHECKC     LOGICAL                          137  CHECKD     LOGICAL
    0  D          INTEGER              F.P.        141  I          INTEGER
  147  IFMT       INTEGER                            0  III        INTEGER              F.P.
    0  PEAK       REAL        ARRAY    F.P.        133  POINT      LOGICAL
  140  POP        LOGICAL                            0  TOP        REAL        ARRAY    F.P.
  142  WM         REAL                             143  WP         REAL
    0  X          REAL        ARRAY    F.P.        144  X1         REAL
  145  Y1         REAL                             146  Y2         REAL
    0  Z          REAL        ARRAY   16SZZZ

EXTERNALS          TYPE    ARGS
      SEGMTG                 6

STATEMENT LABELS
   10  10                                  76  50

COMMON BLOCKS   LENGTH
      16SZZZ      200

STATISTICS
  PROGRAM LENGTH                  150B     104
  SCM LABELED COMMON LENGTH       310B     200
```

```
 1
                 SUBROUTINE PRINTER (W,NN)
           C  ****** PRINTOUT PROGRAM *******
 5               COMMON/GRAPH/A(11,150)
                 COMMON/PICKER/PEAK(200)
                 COMMON/EASY/ISUBRT(20)
                 INTEGER W
                 INTEGER R
10               DO 39 I=1,W

           C    ****** MAKES AND LABELS COLUMNS FROM START TO START+ 20 *****

                 J=I+19
15               N=0
                 DO 29 K=I,J
                 N=N+1
                  ISUBRT(N)=K
              29 CONTINUE
20               PRINT 119, ISUBRT
             119 FORMAT(10X,2016)
                 DO 40 K=I,W,20
                 KK=K+19
                 IF (KK .GT. W) KK=W
25               N=0
                 DO 45 JK =1,20
                 ISUBRT(JK)=0
              45 CONTINUE
                 DO 41 J=K,KK
                  N=N+1
           C   *** TRUNCATES REMAINDER ***
                 ISUBRT(N)=INT(ABS(PEAK(I)-PEAK(J) +.0000001))
                 JSUBRT=ISUBRT(N)
                 IF ((JSUBRT.GE.20).AND.(JSUBRT.LE.3019)) CALL BAR(NN,JSUBRT)
35            41 CONTINUE
                 PRINT 142, (ISUBRT(IN),IN=1,20)
             142 FORMAT(10X,2016)
              40 CONTINUE
                 PRINT 143
40           143 FORMAT(1X,/)
              39 CONTINUE
                 RETURN $END
```

```
      SYMBOLIC REFERENCE MAP (R=1)

ENTRY POINTS
   3  PRINTER

VARIABLES      SN  TYPE            RELOCATION
    0  A          REAL        ARRAY    GRAPH          130  I          INTEGER
  137  IN         INTEGER                                 0  ISUBRT    INTEGER    ARRAY    EASY
  131  J          INTEGER                                135  JK         INTEGER
  136  JSUBRT     INTEGER                                133  K          INTEGER
```

```
VARIABLES      SN  TYPE          RELOCATION
  134  KK         INTEGER                          132  N        INTEGER
    0  NN         INTEGER              F.P.          0  PEAK     REAL       ARRAY    PICKER
  127  R          INTEGER    *UNDEF                  0  W        INTEGER              F.P.

FILE NAMES         MODE
       OUTPUT     FMT

EXTERNALS          TYPE    ARGS
       BAR                   2

INLINE FUNCTIONS   TYPE    ARGS
       ABS        REAL       1  INTRIN                    INT       INTEGER    1  INTRIN

STATEMENT LABELS
    0  29                                    0  39                                    0  40
    0  41                                    0  45                                  111  119     FMT
  117  142     FMT                         124  143     FMT

LOOPS  LABEL     INDEX      FROM-TO     LENGTH    PROPERTIES
   17  39      * I          10 41        63B                EXT REFS  NOT INNER
   26  29        K          16 19         2B      INSTACK
   35  40      * K          22 38        41B                EXT REFS  NOT INNER
   45  45        JK         26 28         2B      INSTACK
   52  41      * J          29 35        20B                EXT REFS

COMMON BLOCKS   LENGTH
       GRAPH      1650
       PICKER      200
       EASY         20

STATISTICS
  PROGRAM LENGTH                 146B     102
  SCM LABELED COMMON LENGTH     3516B    1870
```

D. Listing of Data

1. Cross Sections from 190-172 nm for Eleven Temperatures

WAVENUMBER CM-1	WAVELENGTH NM	CROSS SECTION X E19 CM-2 , TEMPERATURE DEG. K 151.	182.	196.	223.	247.	268.	301.	333.	372.	423.	485.
52613.	190.00	.8640	.9010	.9101	.9540	1.0500	1.0925	1.1700	1.2475	1.3500	1.5253	1.6200
52619.	189.98	.8657	.9028	.9108	.9543	1.0511	1.0950	1.1750	1.2500	1.3550	1.5280	1.6263
52624.	189.96	.8634	.9047	.9112	.9545	1.0531	1.1039	1.1835	1.2561	1.3789	1.5308	1.6318
52630.	189.94	.8648	.9065	.9130	.9565	1.0546	1.1062	1.1859	1.2598	1.3829	1.5348	1.6373
52635.	189.92	.8659	.9082	.9144	.9585	1.0561	1.1090	1.1889	1.2641	1.3861	1.5382	1.6425
52641.	189.90	.8673	.9095	.9157	.9600	1.0592	1.1118	1.1918	1.2682	1.3896	1.5419	1.6472
52646.	189.88	.8677	.9109	.9169	.9620	1.0612	1.1138	1.1942	1.2718	1.3926	1.5455	1.6510
52652.	189.86	.8679	.9121	.9182	.9643	1.0632	1.1153	1.1956	1.2750	1.3950	1.5487	1.6540
52658.	189.84	.8691	.9135	.9191	.9663	1.0652	1.1168	1.1975	1.2769	1.3974	1.5513	1.6567
52663.	189.82	.8707	.9149	.9198	.9682	1.0663	1.1191	1.1994	1.2786	1.3987	1.5534	1.6587
52669.	189.80	.8716	.9158	.9209	.9700	1.0693	1.1209	1.1999	1.2798	1.4001	1.5542	1.6589
52674.	189.78	.8727	.9165	.9223	.9712	1.0688	1.1214	1.2004	1.2803	1.4009	1.5532	1.6584
52680.	189.76	.8738	.9177	.9232	.9717	1.0688	1.1219	1.2012	1.2805	1.4009	1.5508	1.6567
52685.	189.74	.8748	.9184	.9238	.9721	1.0688	1.1226	1.2018	1.2805	1.4001	1.5487	1.6543
52691.	189.72	.8759	.9191	.9245	.9721	1.0688	1.1232	1.2015	1.2803	1.3993	1.5469	1.6521
52696.	189.70	.8768	.9197	.9261	.9731	1.0718	1.1229	1.2010	1.2800	1.3979	1.5461	1.6496
52702.	189.68	.8775	.9207	.9277	.9753	1.0728	1.1226	1.2010	1.2808	1.3966	1.5448	1.6472
52707.	189.66	.8786	.9211	.9281	.9769	1.0749	1.1237	1.2015	1.2812	1.3958	1.5434	1.6455
52713.	189.64	.8800	.9223	.9295	.9785	1.0738	1.1247	1.2021	1.2803	1.3961	1.5424	1.6450
52719.	189.62	.8802	.9235	.9304	.9790	1.0743	1.1247	1.2021	1.2795	1.3966	1.5419	1.6444
52724.	189.60	.8800	.9244	.9308	.9793	1.0738	1.1242	1.2018	1.2793	1.3966	1.5416	1.6444
52730.	189.58	.8802	.9246	.9315	.9807	1.0743	1.1239	1.2021	1.2795	1.3966	1.5416	1.6441
52735.	189.56	.8804	.9248	.9320	.9815	1.0749	1.1242	1.2026	1.2803	1.3966	1.5406	1.6428
52741.	189.54	.8804	.9253	.9322	.9815	1.0754	1.1249	1.2026	1.2812	1.3966	1.5395	1.6417
52746.	189.52	.8816	.9260	.9331	.9815	1.0754	1.1262	1.2029	1.2815	1.3963	1.5392	1.6411
52752.	189.50	.8834	.9267	.9338	.9814	1.0779	1.1270	1.2031	1.2817	1.3966	1.5398	1.6417
52758.	189.48	.8852	.9281	.9342	.9813	1.0789	1.1282	1.2042	1.2824	1.3977	1.5400	1.6420
52763.	189.46	.8873	.9304	.9356	.9815	1.0794	1.1297	1.2058	1.2844	1.3977	1.5408	1.6425
52769.	189.44	.8888	.9327	.9374	.9826	1.0814	1.1318	1.2080	1.2849	1.3985	1.5419	1.6430
52774.	189.42	.8911	.9348	.9389	.9841	1.0835	1.1335	1.2096	1.2853	1.3998	1.5432	1.6436
52780.	189.40	.8932	.9364	.9407	.9858	1.0855	1.1348	1.2109	1.2870	1.4014	1.5432	1.6436
52785.	189.38	.8950	.9383	.9430	.9882	1.0870	1.1363	1.2126	1.2887	1.4022	1.5429	1.6433
52791.	189.36	.8968	.9394	.9453	.9905	1.0880	1.1376	1.2142	1.2894	1.4020	1.5424	1.6430
52797.	189.34	.8979	.9404	.9464	.9922	1.0895	1.1386	1.2152	1.2902	1.4014	1.5421	1.6417
52802.	189.32	.8991	.9411	.9473	.9937	1.0905	1.1391	1.2158	1.2911	1.4014	1.5421	1.6403
52808.	189.30	.9000	.9425	.9482	.9949	1.0911	1.1396	1.2163	1.2916	1.4022	1.5411	1.6392
52813.	189.28	.9002	.9434	.9493	.9960	1.0911	1.1401	1.2163	1.2911	1.4020	1.5400	1.6381
52819.	189.26	.8997	.9436	.9502	.9967	1.0900	1.1396	1.2161	1.2899	1.4009	1.5392	1.6359
52824.	189.24	.9000	.9441	.9504	.9970	1.0900	1.1389	1.2155	1.2894	1.4009	1.5387	1.6346
52830.	189.22	.9013	.9448	.9511	.9976	1.0911	1.1389	1.2152	1.2892	1.4006	1.5382	1.6332
52836.	189.20	.9022	.9452	.9518	.9977	1.0916	1.1394	1.2155	1.2885	1.3998	1.5366	1.6313
52841.	189.18	.9022	.9462	.9525	.9971	1.0911	1.1401	1.2150	1.2877	1.3985	1.5350	1.6299
52847.	189.16	.9034	.9464	.9527	.9973	1.0931	1.1417	1.2142	1.2877	1.3985	1.5340	1.6294
52852.	189.14	.9050	.9471	.9534	.9977	1.0936	1.1432	1.2147	1.2887	1.3987	1.5340	1.6291
52858.	189.12	.9068	.9487	.9540	.9987	1.0946	1.1439	1.2155	1.2892	1.3990	1.5345	1.6288
52864.	189.10	.9082	.9506	.9540	1.0007	1.0971	1.1442	1.2169	1.2899	1.4006	1.5356	1.6285
52869.	189.08	.9097	.9524	.9549	1.0017	1.0991	1.1450	1.2193	1.2911	1.4022	1.5371	1.6299
52875.	189.06	.9111	.9545	.9570	1.0030	1.1012	1.1467	1.2214	1.2933	1.4036	1.5377	1.6318
52880.	189.04	.9131	.9566	.9592	1.0050	1.1012	1.1485	1.2228	1.2957	1.4049	1.5377	1.6335
52886.	189.02	.9143	.9575	.9608	1.0063	1.1022	1.1505	1.2241	1.2972	1.4063	1.5390	1.6343
52892.	189.00	.9156	.9587	.9622	1.0068	1.1062	1.1526	1.2260	1.2981	1.4065	1.5406	1.6346

WAVENUMBER CM-1	WAVELENGTH NM	CROSS SECTION X E19 CM-2 , TEMPERATURE DEG. K 151.	182.	196.	223.	247.	268.	301.	333.	372.	423.	485.
52892.	189.00	.9156	.9587	.9622	1.0068	1.1062	1.1526	1.2260	1.2981	1.4065	1.5406	1.6346
52897.	188.98	.9177	.9605	.9635	1.0076	1.1062	1.1538	1.2290	1.2991	1.4073	1.5413	1.6354
52903.	188.96	.9200	.9624	.9649	1.0091	1.1078	1.1548	1.2306	1.3003	1.4092	1.5416	1.6367
52908.	188.94	.9213	.9638	.9658	1.0119	1.1083	1.1561	1.2311	1.3017	1.4114	1.5429	1.6376
52914.	188.92	.9225	.9649	.9682	1.0152	1.1093	1.1574	1.2317	1.3029	1.4119	1.5442	1.6381
52920.	188.90	.9236	.9668	.9707	1.0170	1.1123	1.1591	1.2325	1.3039	1.4122	1.5455	1.6392
52925.	188.88	.9252	.9684	.9721	1.0176	1.1128	1.1607	1.2338	1.3056	1.4138	1.5471	1.6403
52931.	188.86	.9266	.9693	.9732	1.0187	1.1138	1.1614	1.2354	1.3073	1.4154	1.5482	1.6414
52936.	188.84	.9284	.9696	.9741	1.0203	1.1143	1.1619	1.2373	1.3087	1.4165	1.5492	1.6420
52942.	188.82	.9293	.9707	.9757	1.0214	1.1179	1.1640	1.2389	1.3099	1.4181	1.5519	1.6430
52948.	188.80	.9302	.9719	.9770	1.0225	1.1184	1.1662	1.2406	1.3114	1.4202	1.5540	1.6452
52953.	188.78	.9302	.9733	.9786	1.0237	1.1209	1.1678	1.2422	1.3136	1.4224	1.5555	1.6488
52959.	188.76	.9311	.9744	.9797	1.0251	1.1214	1.1688	1.2430	1.3157	1.4237	1.5574	1.6515
52964.	188.74	.9331	.9761	.9813	1.0263	1.1229	1.1700	1.2449	1.3177	1.4256	1.5595	1.6532
52970.	188.72	.9350	.9781	.9827	1.0273	1.1245	1.1718	1.2467	1.3198	1.4288	1.5613	1.6545
52976.	188.70	.9363	.9800	.9836	1.0285	1.1270	1.1741	1.2486	1.3220	1.4310	1.5631	1.6565
52981.	188.68	.9372	.9812	.9838	1.0299	1.1280	1.1771	1.2500	1.3244	1.4339	1.5647	1.6589
52987.	188.66	.9381	.9814	.9843	1.0318	1.1290	1.1794	1.2511	1.3263	1.4366	1.5671	1.6611
52992.	188.64	.9390	.9819	.9854	1.0334	1.1315	1.1802	1.2516	1.3273	1.4377	1.5679	1.6633
52998.	188.62	.9406	.9826	.9872	1.0347	1.1310	1.1799	1.2519	1.3268	1.4371	1.5673	1.6630
53004.	188.60	.9422	.9844	.9885	1.0360	1.1320	1.1797	1.2532	1.3266	1.4371	1.5676	1.6625
53009.	188.58	.9431	.9858	.9894	1.0366	1.1331	1.1817	1.2546	1.3278	1.4382	1.5684	1.6628
53015.	188.56	.9436	.9870	.9908	1.0370	1.1351	1.1850	1.2564	1.3302	1.4401	1.5705	1.6652
53021.	188.54	.9450	.9881	.9926	1.0378	1.1361	1.1870	1.2583	1.3326	1.4433	1.5750	1.6682
53026.	188.52	.9463	.9902	.9944	1.0390	1.1396	1.1883	1.2615	1.3358	1.4473	1.5802	1.6726
53032.	188.50	.9477	.9921	.9960	1.0408	1.1412	1.1903	1.2648	1.3396	1.4508	1.5841	1.6773
53037.	188.48	.9486	.9939	.9971	1.0428	1.1442	1.1934	1.2685	1.3432	1.4546	1.5876	1.6819
53043.	188.46	.9495	.9953	.9989	1.0451	1.1452	1.1972	1.2720	1.3466	1.4597	1.5923	1.6866
53049.	188.44	.9513	.9972	1.0012	1.0480	1.1477	1.2007	1.2753	1.3507	1.4648	1.5973	1.6926
53054.	188.42	.9529	.9983	1.0023	1.0503	1.1513	1.2030	1.2790	1.3551	1.4691	1.6025	1.6978
53060.	188.40	.9543	.9997	1.0036	1.0516	1.1533	1.2050	1.2834	1.3592	1.4731	1.6073	1.7025
53066.	188.38	.9552	1.0011	1.0057	1.0525	1.1563	1.2083	1.2869	1.3625	1.4763	1.6112	1.7060
53071.	188.36	.9561	1.0025	1.0070	1.0540	1.1604	1.2114	1.2909	1.3669	1.4806	1.6159	1.7101
53077.	188.34	.9575	1.0041	1.0084	1.0560	1.1624	1.2139	1.2939	1.3710	1.4852	1.6212	1.7148
53083.	188.32	.9595	1.0055	1.0104	1.0587	1.1639	1.2159	1.2955	1.3739	1.4881	1.6251	1.7184
53088.	188.30	.9606	1.0074	1.0127	1.0617	1.1649	1.2174	1.2963	1.3756	1.4892	1.6275	1.7192
53094.	188.28	.9615	1.0092	1.0140	1.0631	1.1670	1.2185	1.2974	1.3763	1.4906	1.6283	1.7194
53099.	188.26	.9622	1.0104	1.0138	1.0642	1.1690	1.2202	1.2982	1.3768	1.4914	1.6280	1.7194
53105.	188.24	.9643	1.0108	1.0142	1.0666	1.1705	1.2215	1.2990	1.3772	1.4919	1.6272	1.7194
53111.	188.22	.9659	1.0115	1.0158	1.0691	1.1695	1.2225	1.2995	1.3777	1.4924	1.6272	1.7194
53116.	188.20	.9670	1.0122	1.0181	1.0705	1.1700	1.2228	1.2990	1.3782	1.4932	1.6277	1.7189
53122.	188.18	.9679	1.0134	1.0196	1.0712	1.1710	1.2233	1.2990	1.3789	1.4930	1.6280	1.7186
53128.	188.16	.9686	1.0145	1.0208	1.0713	1.1720	1.2238	1.3000	1.3797	1.4932	1.6277	1.7197
53133.	188.14	.9695	1.0155	1.0226	1.0708	1.1730	1.2251	1.3003	1.3806	1.4935	1.6280	1.7211
53139.	188.12	.9709	1.0169	1.0235	1.0718	1.1725	1.2258	1.3014	1.3814	1.4946	1.6290	1.7216
53145.	188.10	.9731	1.0185	1.0233	1.0736	1.1751	1.2261	1.3025	1.3826	1.4951	1.6304	1.7216
53150.	188.08	.9747	1.0206	1.0239	1.0752	1.1751	1.2268	1.3041	1.3835	1.4949	1.6314	1.7211
53156.	188.06	.9756	1.0222	1.0248	1.0769	1.1761	1.2278	1.3060	1.3840	1.4951	1.6319	1.7216
53162.	188.04	.9763	1.0231	1.0260	1.0776	1.1776	1.2291	1.3073	1.3850	1.4965	1.6319	1.7216
53167.	188.02	.9770	1.0240	1.0271	1.0770	1.1796	1.2299	1.3087	1.3859	1.4983	1.6319	1.7222
53173.	188.00	.9781	1.0245	1.0284	1.0764	1.1806	1.2309	1.3095	1.3869	1.4994	1.6322	1.7233

WAVENUMBER CM-1	WAVELENGTH NM	CROSS SECTION X E19 CM-2 , TEMPERATURE DEG. K 151.	182.	196.	223.	247.	268.	301.	333.	372.	423.	485.
53173.	188.00	.9781	1.0245	1.0284	1.0764	1.1806	1.2309	1.3095	1.3869	1.4994	1.6322	1.7233
53179.	187.98	.9793	1.0252	1.0302	1.0774	1.1827	1.2324	1.3095	1.3876	1.5005	1.6330	1.7244
53184.	187.96	.9806	1.0268	1.0309	1.0789	1.1816	1.2344	1.3103	1.3886	1.5018	1.6340	1.7241
53190.	187.94	.9818	1.0277	1.0311	1.0804	1.1822	1.2357	1.3114	1.3898	1.5021	1.6346	1.7230
53196.	187.92	.9827	1.0284	1.0318	1.0817	1.1837	1.2367	1.3116	1.3908	1.5013	1.6348	1.7227
53201.	187.90	.9833	1.0294	1.0332	1.0828	1.1852	1.2370	1.3122	1.3912	1.5000	1.6346	1.7230
53207.	187.88	.9838	1.0298	1.0343	1.0841	1.1867	1.2375	1.3124	1.3915	1.4997	1.6343	1.7233
53213.	187.86	.9854	1.0301	1.0357	1.0850	1.1882	1.2377	1.3127	1.3915	1.5002	1.6335	1.7222
53218.	187.84	.9865	1.0315	1.0368	1.0862	1.1877	1.2375	1.3124	1.3903	1.5008	1.6325	1.7200
53224.	187.82	.9872	1.0331	1.0377	1.0875	1.1877	1.2367	1.3124	1.3898	1.5005	1.6309	1.7173
53230.	187.80	.9877	1.0340	1.0379	1.0875	1.1887	1.2370	1.3124	1.3893	1.4989	1.6293	1.7148
53235.	187.78	.9877	1.0342	1.0386	1.0875	1.1867	1.2377	1.3130	1.3886	1.4978	1.6290	1.7131
53241.	187.76	.9874	1.0340	1.0393	1.0877	1.1877	1.2377	1.3135	1.3881	1.4975	1.6288	1.7115
53247.	187.74	.9874	1.0331	1.0384	1.0875	1.1872	1.2380	1.3135	1.3891	1.4973	1.6267	1.7093
53252.	187.72	.9877	1.0328	1.0388	1.0881	1.1877	1.2380	1.3130	1.3888	1.4959	1.6241	1.7060
53258.	187.70	.9888	1.0342	1.0397	1.0891	1.1877	1.2387	1.3130	1.3874	1.4951	1.6220	1.7044
53264.	187.68	.9904	1.0359	1.0397	1.0898	1.1882	1.2390	1.3132	1.3864	1.4957	1.6212	1.7041
53269.	187.66	.9918	1.0361	1.0397	1.0911	1.1897	1.2392	1.3132	1.3874	1.4954	1.6212	1.7036
53275.	187.64	.9931	1.0368	1.0406	1.0919	1.1908	1.2398	1.3132	1.3879	1.4935	1.6204	1.7011
53281.	187.62	.9949	1.0384	1.0417	1.0917	1.1933	1.2403	1.3143	1.3871	1.4922	1.6191	1.6986
53286.	187.60	.9963	1.0403	1.0431	1.0914	1.1953	1.2413	1.3149	1.3871	1.4927	1.6178	1.6973
53292.	187.58	.9981	1.0421	1.0442	1.0921	1.1948	1.2425	1.3159	1.3881	1.4938	1.6178	1.6975
53298.	187.56	.9999	1.0437	1.0462	1.0929	1.1968	1.2443	1.3175	1.3898	1.4951	1.6188	1.6989
53303.	187.54	1.0015	1.0456	1.0483	1.0930	1.1978	1.2458	1.3200	1.3917	1.4962	1.6201	1.7000
53309.	187.52	1.0024	1.0465	1.0494	1.0942	1.1989	1.2471	1.3216	1.3927	1.4970	1.6212	1.7003
53315.	187.50	1.0033	1.0470	1.0501	1.0969	1.1999	1.2479	1.3216	1.3927	1.4978	1.6217	1.7008
53320.	187.48	1.0036	1.0474	1.0512	1.1001	1.1994	1.2471	1.3210	1.3929	1.4986	1.6217	1.7011
53326.	187.46	1.0033	1.0479	1.0517	1.1016	1.1994	1.2474	1.3213	1.3934	1.5000	1.6222	1.7011
53332.	187.44	1.0031	1.0484	1.0519	1.1017	1.2009	1.2491	1.3224	1.3941	1.5008	1.6222	1.7008
53337.	187.42	1.0033	1.0481	1.0526	1.1016	1.2014	1.2507	1.3235	1.3951	1.5010	1.6225	1.7003
53343.	187.40	1.0038	1.0488	1.0537	1.1019	1.2009	1.2517	1.3240	1.3958	1.5016	1.6235	1.7011
53349.	187.38	1.0056	1.0505	1.0544	1.1018	1.2029	1.2529	1.3254	1.3961	1.5021	1.6241	1.7022
53355.	187.36	1.0077	1.0530	1.0550	1.1015	1.2044	1.2542	1.3264	1.3970	1.5032	1.6254	1.7022
53360.	187.34	1.0095	1.0553	1.0555	1.1024	1.2059	1.2567	1.3275	1.3994	1.5045	1.6269	1.7014
53366.	187.32	1.0113	1.0576	1.0564	1.1033	1.2075	1.2593	1.3291	1.4014	1.5056	1.6277	1.7022
53372.	187.30	1.0138	1.0588	1.0582	1.1037	1.2095	1.2608	1.3307	1.4028	1.5069	1.6275	1.7036
53377.	187.28	1.0158	1.0593	1.0609	1.1061	1.2105	1.2621	1.3324	1.4038	1.5083	1.6272	1.7036
53383.	187.26	1.0165	1.0600	1.0632	1.1095	1.2145	1.2626	1.3326	1.4050	1.5091	1.6269	1.7022
53389.	187.24	1.0170	1.0609	1.0650	1.1109	1.2145	1.2623	1.3329	1.4064	1.5091	1.6272	1.7008
53394.	187.22	1.0172	1.0620	1.0663	1.1107	1.2156	1.2628	1.3334	1.4067	1.5096	1.6269	1.6997
53400.	187.20	1.0179	1.0632	1.0674	1.1122	1.2156	1.2631	1.3337	1.4055	1.5102	1.6264	1.6992
53406.	187.18	1.0195	1.0641	1.0688	1.1144	1.2140	1.2626	1.3342	1.4045	1.5102	1.6264	1.6995
53412.	187.16	1.0206	1.0646	1.0692	1.1160	1.2145	1.2626	1.3348	1.4045	1.5102	1.6269	1.6997
53417.	187.14	1.0215	1.0648	1.0699	1.1159	1.2176	1.2638	1.3356	1.4052	1.5104	1.6272	1.7006
53423.	187.12	1.0229	1.0655	1.0713	1.1157	1.2181	1.2659	1.3367	1.4062	1.5110	1.6275	1.7014
53429.	187.10	1.0240	1.0671	1.0717	1.1172	1.2181	1.2674	1.3377	1.4062	1.5120	1.6277	1.7019
53434.	187.08	1.0249	1.0688	1.0722	1.1196	1.2191	1.2692	1.3385	1.4076	1.5126	1.6277	1.7022
53440.	187.06	1.0261	1.0704	1.0731	1.1208	1.2196	1.2702	1.3399	1.4086	1.5134	1.6283	1.7025
53446.	187.04	1.0272	1.0720	1.0735	1.1209	1.2221	1.2712	1.3404	1.4091	1.5142	1.6298	1.7044
53452.	187.02	1.0277	1.0725	1.0735	1.1208	1.2242	1.2719	1.3412	1.4093	1.5150	1.6319	1.7066
53457.	187.00	1.0281	1.0727	1.0744	1.1214	1.2257	1.2722	1.3426	1.4108	1.5161	1.6332	1.7082

WAVENUMBER CM-1	WAVELENGTH NM	CROSS SECTION X E19 CM-2 , TEMPERATURE DEG. K 151.	182.	196.	223.	247.	268.	301.	333.	372.	423.	485.
53457.	187.00	1.0281	1.0727	1.0744	1.1214	1.2257	1.2722	1.3426	1.4108	1.5161	1.6332	1.7082
53463.	186.98	1.0290	1.0732	1.0758	1.1234	1.2257	1.2719	1.3431	1.4125	1.5169	1.6335	1.7093
53469.	186.96	1.0299	1.0741	1.0771	1.1258	1.2237	1.2737	1.3437	1.4139	1.5174	1.6338	1.7104
53474.	186.94	1.0313	1.0743	1.0774	1.1261	1.2257	1.2757	1.3445	1.4139	1.5188	1.6348	1.7115
53480.	186.92	1.0322	1.0753	1.0774	1.1253	1.2267	1.2768	1.3466	1.4139	1.5198	1.6364	1.7126
53486.	186.90	1.0333	1.0769	1.0771	1.1244	1.2287	1.2775	1.3485	1.4154	1.5209	1.6398	1.7148
53492.	186.88	1.0345	1.0778	1.0776	1.1242	1.2292	1.2783	1.3496	1.4171	1.5228	1.6424	1.7173
53497.	186.86	1.0354	1.0780	1.0792	1.1260	1.2328	1.2793	1.3509	1.4192	1.5252	1.6437	1.7189
53503.	186.84	1.0363	1.0785	1.0805	1.1290	1.2348	1.2813	1.3517	1.4209	1.5276	1.6440	1.7203
53509.	186.82	1.0372	1.0797	1.0819	1.1308	1.2343	1.2844	1.3525	1.4228	1.5290	1.6461	1.7219
53514.	186.80	1.0367	1.0806	1.0834	1.1321	1.2333	1.2854	1.3544	1.4238	1.5314	1.6487	1.7249
53520.	186.78	1.0367	1.0810	1.0846	1.1332	1.2338	1.2851	1.3568	1.4255	1.5341	1.6519	1.7285
53526.	186.76	1.0372	1.0810	1.0850	1.1336	1.2358	1.2849	1.3585	1.4274	1.5359	1.6553	1.7315
53532.	186.74	1.0374	1.0815	1.0850	1.1339	1.2368	1.2849	1.3601	1.4301	1.5375	1.6579	1.7340
53537.	186.72	1.0381	1.0827	1.0857	1.1350	1.2373	1.2877	1.3612	1.4315	1.5400	1.6598	1.7359
53543.	186.70	1.0390	1.0845	1.0870	1.1360	1.2373	1.2917	1.3625	1.4327	1.5421	1.6616	1.7383
53549.	186.68	1.0406	1.0871	1.0877	1.1371	1.2393	1.2942	1.3649	1.4349	1.5448	1.6650	1.7419
53555.	186.66	1.0420	1.0894	1.0886	1.1386	1.2414	1.2960	1.3690	1.4390	1.5488	1.6695	1.7463
53560.	186.64	1.0445	1.0922	1.0907	1.1392	1.2459	1.2993	1.3733	1.4434	1.5545	1.6745	1.7509
53566.	186.62	1.0476	1.0961	1.0925	1.1390	1.2510	1.3049	1.3773	1.4467	1.5598	1.6797	1.7556
53572.	186.60	1.0515	1.1007	1.0952	1.1407	1.2550	1.3107	1.3816	1.4503	1.5655	1.6842	1.7608
53578.	186.58	1.0551	1.1056	1.0985	1.1443	1.2576	1.3153	1.3870	1.4554	1.5708	1.6900	1.7663
53583.	186.56	1.0592	1.1084	1.1022	1.1486	1.2626	1.3188	1.3924	1.4619	1.5759	1.6963	1.7715
53589.	186.54	1.0629	1.1098	1.1055	1.1534	1.2682	1.3216	1.3967	1.4668	1.5805	1.7023	1.7761
53595.	186.52	1.0654	1.1114	1.1096	1.1583	1.2697	1.3244	1.4002	1.4709	1.5848	1.7073	1.7805
53601.	186.50	1.0658	1.1126	1.1127	1.1626	1.2733	1.3269	1.4029	1.4757	1.5878	1.7112	1.7838
53606.	186.48	1.0654	1.1130	1.1152	1.1657	1.2748	1.3277	1.4042	1.4798	1.5894	1.7139	1.7860
53612.	186.46	1.0649	1.1130	1.1168	1.1678	1.2748	1.3277	1.4048	1.4815	1.5896	1.7146	1.7868
53618.	186.44	1.0651	1.1133	1.1177	1.1685	1.2763	1.3277	1.4053	1.4817	1.5904	1.7152	1.7876
53624.	186.42	1.0656	1.1135	1.1179	1.1683	1.2768	1.3272	1.4045	1.4810	1.5921	1.7146	1.7879
53629.	186.40	1.0649	1.1133	1.1182	1.1687	1.2753	1.3272	1.4040	1.4800	1.5929	1.7146	1.7874
53635.	186.38	1.0635	1.1123	1.1184	1.1689	1.2743	1.3269	1.4042	1.4800	1.5923	1.7149	1.7860
53641.	186.36	1.0631	1.1107	1.1184	1.1693	1.2733	1.3259	1.4034	1.4800	1.5910	1.7149	1.7852
53647.	186.34	1.0631	1.1100	1.1179	1.1694	1.2753	1.3249	1.4021	1.4786	1.5891	1.7136	1.7838
53652.	186.32	1.0635	1.1098	1.1173	1.1689	1.2728	1.3237	1.4013	1.4774	1.5861	1.7115	1.7813
53658.	186.30	1.0635	1.1096	1.1166	1.1687	1.2712	1.3219	1.3999	1.4762	1.5835	1.7083	1.7778
53664.	186.28	1.0635	1.1091	1.1166	1.1690	1.2697	1.3206	1.3986	1.4752	1.5816	1.7044	1.7728
53670.	186.26	1.0635	1.1091	1.1170	1.1689	1.2702	1.3198	1.3975	1.4730	1.5789	1.7005	1.7674
53675.	186.24	1.0640	1.1093	1.1170	1.1679	1.2672	1.3193	1.3964	1.4696	1.5767	1.6970	1.7630
53681.	186.22	1.0645	1.1098	1.1161	1.1666	1.2677	1.3186	1.3943	1.4665	1.5751	1.6928	1.7597
53687.	186.20	1.0658	1.1105	1.1150	1.1658	1.2682	1.3183	1.3932	1.4643	1.5738	1.6892	1.7561
53693.	186.18	1.0663	1.1112	1.1143	1.1656	1.2687	1.3183	1.3935	1.4636	1.5725	1.6863	1.7523
53698.	186.16	1.0663	1.1119	1.1148	1.1661	1.2697	1.3181	1.3932	1.4641	1.5708	1.6844	1.7498
53704.	186.14	1.0667	1.1126	1.1159	1.1669	1.2692	1.3186	1.3929	1.4634	1.5698	1.6831	1.7474
53710.	186.12	1.0674	1.1135	1.1159	1.1665	1.2697	1.3201	1.3935	1.4622	1.5684	1.6813	1.7460
53716.	186.10	1.0685	1.1144	1.1168	1.1653	1.2697	1.3209	1.3927	1.4622	1.5668	1.6800	1.7446
53722.	186.08	1.0692	1.1147	1.1191	1.1657	1.2717	1.3204	1.3921	1.4622	1.5671	1.6792	1.7433
53727.	186.06	1.0708	1.1154	1.1211	1.1677	1.2722	1.3204	1.3921	1.4619	1.5668	1.6784	1.7414
53733.	186.04	1.0722	1.1163	1.1211	1.1689	1.2702	1.3216	1.3927	1.4617	1.5652	1.6771	1.7408
53739.	186.02	1.0722	1.1165	1.1211	1.1687	1.2728	1.3234	1.3929	1.4624	1.5636	1.6758	1.7403
53745.	186.00	1.0722	1.1172	1.1215	1.1683	1.2728	1.3242	1.3935	1.4629	1.5631	1.6753	1.7381

WAVENUMBER CM-1	WAVELENGTH NM	CROSS SECTION X E19 CM-2 , TEMPERATURE DEG. K 151.	182.	196.	223.	247.	268.	301.	333.	372.	423.	485.
53745.	186.00	1.0722	1.1172	1.1215	1.1683	1.2728	1.3242	1.3935	1.4629	1.5631	1.6753	1.7381
53750.	185.98	1.0729	1.1181	1.1222	1.1687	1.2728	1.3229	1.3937	1.4617	1.5625	1.6745	1.7351
53756.	185.96	1.0740	1.1188	1.1231	1.1703	1.2738	1.3221	1.3929	1.4602	1.5620	1.6734	1.7323
53762.	185.94	1.0749	1.1195	1.1236	1.1710	1.2748	1.3226	1.3927	1.4598	1.5622	1.6713	1.7318
53768.	185.92	1.0754	1.1207	1.1240	1.1704	1.2748	1.3231	1.3929	1.4605	1.5631	1.6695	1.7312
53774.	185.90	1.0772	1.1225	1.1247	1.1708	1.2758	1.3239	1.3937	1.4619	1.5625	1.6684	1.7301
53779.	185.88	1.0799	1.1246	1.1254	1.1721	1.2763	1.3254	1.3945	1.4629	1.5622	1.6674	1.7296
53785.	185.86	1.0826	1.1269	1.1267	1.1735	1.2793	1.3277	1.3953	1.4629	1.5620	1.6669	1.7288
53791.	185.84	1.0851	1.1297	1.1283	1.1744	1.2814	1.3297	1.3964	1.4631	1.5620	1.6666	1.7274
53797.	185.82	1.0881	1.1323	1.1306	1.1749	1.2814	1.3325	1.3972	1.4641	1.5622	1.6661	1.7263
53802.	185.80	1.0906	1.1350	1.1337	1.1755	1.2849	1.3348	1.3986	1.4651	1.5633	1.6658	1.7257
53808.	185.78	1.0931	1.1371	1.1364	1.1768	1.2884	1.3353	1.4005	1.4663	1.5644	1.6658	1.7252
53814.	185.76	1.0949	1.1390	1.1382	1.1795	1.2905	1.3351	1.4032	1.4680	1.5652	1 6663	1.7244
53820.	185.74	1.0965	1.1401	1.1396	1.1824	1.2910	1.3358	1.4048	1.4701	1.5657	1.6674	1.7249
53826.	185.72	1.0976	1.1406	1.1414	1.1844	1.2920	1.3371	1.4053	1.4709	1.5663	1.6674	1.7252
53831.	185.70	1.0976	1.1411	1.1434	1.1871	1.2950	1.3381	1.4045	1.4709	1.5663	1.6671	1.7244
53837.	185.68	1.0969	1.1415	1.1450	1.1896	1.2945	1.3381	1.4032	1.4709	1.5652	1.6669	1.7230
53843.	185.66	1.0969	1.1418	1.1459	1.1898	1.2935	1.3381	1.4029	1.4699	1.5644	1.6666	1.7214
53849.	185.64	1.0978	1.1420	1.1463	1.1891	1.2935	1.3384	1.4032	1.4684	1.5644	1.6663	1.7203
53855.	185.62	1.0990	1.1425	1.1461	1.1895	1.2915	1.3384	1.4026	1.4672	1.5644	1.6650	1.7194
53860.	185.60	1.1003	1.1432	1.1461	1.1905	1.2935	1.3384	1.4034	1.4677	1.5647	1.6637	1.7203
53866.	185.58	1.1022	1.1436	1.1461	1.1924	1.2930	1.3389	1.4053	1.4689	1.5652	1.6637	1.7219
53872.	185.56	1.1028	1.1446	1.1466	1.1946	1.2945	1.3406	1.4069	1.4704	1.5660	1.6661	1.7238
53878.	185.54	1.1024	1.1457	1.1470	1.1949	1.2965	1.3429	1.4077	1.4716	1.5671	1.6687	1.7249
53884.	185.52	1.1022	1.1469	1.1479	1.1946	1.2976	1.3432	1.4085	1.4718	1.5684	1.6700	1.7257
53889.	185.50	1.1028	1.1476	1.1495	1.1949	1.3001	1.3422	1.4091	1.4721	1.5695	1.6708	1.7266
53895.	185.48	1.1038	1.1480	1.1504	1.1954	1.3006	1.3422	1.4102	1.4737	1.5698	1.6713	1.7274
53901.	185.46	1.1044	1.1478	1.1513	1.1958	1.2996	1.3432	1.4110	1.4752	1.5695	1.6724	1.7290
53907.	185.44	1.1056	1.1471	1.1515	1.1956	1.3011	1.3442	1.4107	1.4754	1.5700	1.6737	1.7312
53913.	185.42	1.1060	1.1476	1.1517	1.1955	1.3006	1.3444	1.4104	1.4752	1.5716	1.6739	1.7329
53919.	185.40	1.1058	1.1483	1.1515	1.1962	1.2986	1.3447	1.4118	1.4759	1.5733	1.6747	1.7340
53924.	185.38	1.1060	1.1494	1.1511	1.1973	1.2996	1.3475	1.4128	1.4774	1.5751	1.6758	1.7356
53930.	185.36	1.1072	1.1503	1.1515	1.1980	1.2996	1.3495	1.4137	1.4786	1.5770	1.6774	1.7381
53936.	185.34	1.1076	1.1517	1.1529	1.1976	1.3011	1.3513	1.4155	1.4798	1.5786	1.6792	1.7403
53942.	185.32	1.1088	1.1529	1.1542	1.1977	1.3031	1.3528	1.4180	1.4822	1.5802	1.6821	1.7419
53948.	185.30	1.1103	1.1543	1.1554	1.1998	1.3051	1.3546	1.4196	1.4848	1.5829	1.6855	1.7433
53953.	185.28	1.1122	1.1554	1.1569	1.2019	1.3062	1.3561	1.4209	1.4877	1.5856	1.6886	1.7457
53959.	185.26	1.1126	1.1566	1.1592	1.2030	1.3097	1.3566	1.4231	1.4909	1.5883	1.6907	1.7482
53965.	185.24	1.1124	1.1575	1.1610	1.2041	1.3117	1.3566	1.4260	1.4935	1.5904	1.6913	1.7482
53971.	185.22	1.1131	1.1575	1.1608	1.2061	1.3127	1.3563	1.4268	1.4933	1.5902	1.6907	1.7468
53977.	185.20	1.1140	1.1575	1.1608	1.2075	1.3122	1.3566	1.4258	1.4914	1.5883	1.6894	1.7457
53983.	185.18	1.1151	1.1580	1.1614	1.2067	1.3102	1.3579	1.4242	1.4902	1.5872	1.6886	1.7463
53988.	185.16	1.1163	1.1589	1.1617	1.2058	1.3112	1.3604	1.4247	1.4904	1.5888	1.6892	1.7482
53994.	185.14	1.1167	1.1596	1.1630	1.2062	1.3148	1.3632	1.4268	1.4914	1.5923	1.6931	1.7515
54000.	185.12	1.1176	1.1622	1.1644	1.2069	1.3148	1.3652	1.4303	1.4935	1.5972	1.6984	1.7556
54006.	185.10	1.1188	1.1643	1.1653	1.2085	1.3168	1.3680	1.4333	1.4962	1.6031	1.7028	1.7602
54012.	185.08	1.1197	1.1645	1.1657	1.2104	1.3213	1.3723	1.4344	1.5010	1.6092	1.7060	1.7652
54018.	185.06	1.1203	1.1645	1.1682	1.2126	1.3244	1.3754	1.4384	1.5061	1.6146	1.7112	1.7720
54023.	185.04	1.1212	1.1656	1.1709	1.2145	1.3249	1.3766	1.4478	1.5116	1.6205	1.7202	1.7800
54029.	185.02	1.1210	1.1666	1.1720	1.2156	1.3310	1.3784	1.4570	1.5191	1.6267	1.7291	1.7871
54035.	185.00	1.1199	1.1675	1.1725	1.2165	1.3345	1.3812	1.4600	1.5263	1.6294	1.7362	1.7931

WAVENUMBER CM-1	WAVELENGTH NM	CROSS SECTION X E19 CM-2 , TEMPERATURE DEG. K 151.	182.	196.	223.	247.	268.	301.	333.	372.	423.	485.
54035.	185.00	1.1199	1.1675	1.1725	1.2165	1.3345	1.3812	1.4600	1.5263	1.6294	1.7362	1.7931
54041.	184.98	1.1185	1.1684	1.1727	1.2176	1.3340	1.3837	1.4605	1.5307	1.6315	1.7412	1.7986
54047.	184.96	1.1183	1.1680	1.1720	1.2192	1.3335	1.3855	1.4613	1.5326	1.6353	1.7440	1.8032
54053.	184.94	1.1188	1.1670	1.1723	1.2208	1.3340	1.3865	1.4618	1.5343	1.6393	1.7461	1.8063
54059.	184.92	1.1192	1.1675	1.1732	1.2231	1.3345	1.3865	1.4637	1.5360	1.6417	1.7485	1.8082
54064.	184.90	1.1192	1.1691	1.1732	1.2260	1.3355	1.3885	1.4661	1.5370	1.6425	1.7506	1.8087
54070.	184.88	1.1199	1.1696	1.1725	1.2268	1.3370	1.3908	1.4670	1.5374	1.6423	1.7506	1.8071
54076.	184.86	1.1203	1.1693	1.1734	1.2257	1.3375	1.3893	1.4645	1.5372	1.6415	1.7496	1.8063
54082.	184.84	1.1210	1.1705	1.1750	1.2254	1.3391	1.3875	1.4624	1.5365	1.6415	1.7490	1.8063
54088.	184.82	1.1222	1.1719	1.1756	1.2265	1.3385	1.3885	1.4624	1.5362	1.6412	1.7485	1.8049
54094.	184.80	1.1235	1.1726	1.1759	1.2283	1.3391	1.3896	1.4635	1.5360	1.6398	1.7464	1.8019
54099.	184.78	1.1256	1.1731	1.1774	1.2288	1.3406	1.3896	1.4643	1.5353	1.6382	1.7451	1.7997
54105.	184.76	1.1278	1.1742	1.1788	1.2289	1.3401	1.3885	1.4632	1.5345	1.6374	1.7435	1.7972
54111.	184.74	1.1294	1.1754	1.1795	1.2299	1.3385	1.3883	1.4616	1.5345	1.6382	1.7417	1.7942
54117.	184.72	1.1308	1.1763	1.1797	1.2308	1.3385	1.3890	1.4616	1.5350	1.6382	1.7396	1.7917
54123.	184.70	1.1324	1.1775	1.1804	1.2310	1.3396	1.3903	1.4613	1.5348	1.6361	1.7377	1.7898
54129.	184.68	1.1337	1.1789	1.1815	1.2311	1.3426	1.3908	1.4616	1.5331	1.6339	1.7356	1.7868
54135.	184.66	1.1340	1.1802	1.1829	1.2305	1.3441	1.3908	1.4616	1.5319	1.6329	1.7341	1.7838
54140.	184.64	1.1333	1.1812	1.1835	1.2299	1.3411	1.3906	1.4610	1.5309	1.6318	1.7314	1.7808
54146.	184.62	1.1333	1.1821	1.1842	1.2304	1.3411	1.3906	1.4600	1.5302	1.6299	1.7283	1.7786
54152.	184.60	1.1337	1.1823	1.1851	1.2331	1.3421	1.3903	1.4591	1.5302	1.6286	1.7246	1.7759
54158.	184.58	1.1344	1.1812	1.1865	1.2359	1.3411	1.3893	1.4575	1.5297	1.6267	1.7209	1.7720
54164.	184.56	1.1351	1.1805	1.1865	1.2357	1.3416	1.3880	1.4565	1.5273	1.6237	1.7186	1.7696
54170.	184.54	1.1356	1.1814	1.1865	1.2350	1.3421	1.3870	1.4554	1.5246	1.6213	1.7167	1.7668
54176.	184.52	1.1358	1.1830	1.1871	1.2360	1.3401	1.3868	1.4540	1.5237	1.6194	1.7144	1.7635
54182.	184.50	1.1365	1.1830	1.1874	1.2366	1.3396	1.3868	1.4530	1.5230	1.6178	1.7112	1.7602
54187.	184.48	1.1367	1.1823	1.1865	1.2353	1.3406	1.3868	1.4519	1.5215	1.6157	1.7091	1.7570
54193.	184.46	1.1376	1.1821	1.1856	1.2337	1.3391	1.3860	1.4513	1.5201	1.6130	1.7078	1.7542
54199.	184.44	1.1383	1.1835	1.1862	1.2343	1.3406	1.3852	1.4511	1.5191	1.6103	1.7057	1.7520
54205.	184.42	1.1390	1.1837	1.1874	1.2359	1.3385	1.3850	1.4508	1.5184	1.6090	1.7028	1.7501
54211.	184.40	1.1397	1.1833	1.1880	1.2358	1.3401	1.3852	1.4508	1.5174	1.6084	1.6999	1.7479
54217.	184.38	1.1399	1.1840	1.1887	1.2358	1.3406	1.3863	1.4508	1.5167	1.6082	1.6989	1.7460
54223.	184.36	1.1406	1.1853	1.1898	1.2363	1.3401	1.3870	1.4513	1.5160	1.6076	1.6984	1.7438
54229.	184.34	1.1412	1.1863	1.1898	1.2358	1.3426	1.3865	1.4519	1.5160	1.6079	1.6973	1.7419
54234.	184.32	1.1426	1.1872	1.1889	1.2350	1.3421	1.3860	1.4513	1.5157	1.6084	1.6963	1.7405
54240.	184.30	1.1440	1.1874	1.1894	1.2351	1.3421	1.3863	1.4511	1.5150	1.6084	1.6957	1.7403
54246.	184.28	1.1449	1.1877	1.1907	1.2356	1.3411	1.3865	1.4516	1.5148	1.6090	1.6957	1.7403
54252.	184.26	1.1444	1.1874	1.1903	1.2362	1.3401	1.3870	1.4530	1.5150	1.6092	1.6957	1.7403
54258.	184.24	1.1435	1.1874	1.1901	1.2366	1.3411	1.3868	1.4532	1.5155	1.6087	1.6955	1.7397
54264.	184.22	1.1431	1.1870	1.1905	1.2359	1.3406	1.3850	1.4519	1.5167	1.6074	1.6942	1.7389
54270.	184.20	1.1431	1.1863	1.1910	1.2360	1.3401	1.3840	1.4497	1.5162	1.6049	1.6923	1.7372
54276.	184.18	1.1435	1.1863	1.1907	1.2376	1.3411	1.3842	1.4486	1.5136	1.6023	1.6905	1.7351
54282.	184.16	1.1440	1.1872	1.1912	1.2381	1.3406	1.3850	1.4484	1.5104	1.6015	1.6894	1.7342
54288.	184.14	1.1446	1.1886	1.1919	1.2378	1.3401	1.3860	1.4481	1.5099	1.6020	1.6892	1.7345
54293.	184.12	1.1453	1.1895	1.1923	1.2370	1.3426	1.3870	1.4484	1.5111	1.6028	1.6892	1.7356
54299.	184.10	1.1462	1.1902	1.1919	1.2368	1.3436	1.3870	1.4492	1.5116	1.6044	1.6907	1.7364
54305.	184.08	1.1483	1.1904	1.1928	1.2378	1.3436	1.3888	1.4500	1.5119	1.6071	1.6926	1.7378
54311.	184.06	1.1494	1.1904	1.1948	1.2385	1.3426	1.3916	1.4508	1.5136	1.6095	1.6944	1.7386
54317.	184.04	1.1490	1.1907	1.1948	1.2386	1.3436	1.3936	1.4516	1.5164	1.6111	1.6955	1.7397
54323.	184.02	1.1483	1.1911	1.1941	1.2393	1.3472	1.3946	1.4532	1.5189	1.6125	1.6965	1.7416
54329.	184.00	1.1487	1.1930	1.1946	1.2392	1.3477	1.3959	1.4559	1.5205	1.6138	1.6989	1.7438

WAVENUMBER CM-1	WAVELENGTH NM	CROSS SECTION X E19 CM-2 , TEMPERATURE DEG. K 151.	182.	196.	223.	247.	268.	301.	333.	372.	423.	485.
54329.	184.00	1.1487	1.1930	1.1946	1.2392	1.3477	1.3959	1.4559	1.5205	1.6138	1.6989	1.7438
54335.	183.98	1.1499	1.1948	1.1950	1.2391	1.3492	1.3967	1.4586	1.5222	1.6157	1.7028	1.7457
54341.	183.96	1.1519	1.1965	1.1955	1.2400	1.3517	1.3982	1.4613	1.5244	1.6181	1.7060	1.7477
54347.	183.94	1.1542	1.1986	1.1964	1.2413	1.3532	1.4007	1.4635	1.5261	1.6202	1.7083	1.7482
54352.	183.92	1.1565	1.2016	1.1980	1.2428	1.3552	1.4035	1.4661	1.5271	1.6219	1.7094	1.7496
54358.	183.90	1.1594	1.2041	1.2002	1.2461	1.3568	1.4055	1.4678	1.5288	1.6240	1.7086	1.7515
54364.	183.88	1.1619	1.2067	1.2038	1.2504	1.3603	1.4065	1.4688	1.5304	1.6253	1.7078	1.7518
54370.	183.86	1.1631	1.2087	1.2063	1.2522	1.3623	1.4073	1.4696	1.5319	1.6259	1.7089	1.7512
54376.	183.84	1.1640	1.2099	1.2077	1.2523	1.3639	1.4078	1.4710	1.5333	1.6259	1.7097	1.7498
54382.	183.82	1.1656	1.2101	1.2090	1.2538	1.3649	1.4091	1.4723	1.5353	1.6253	1.7091	1.7479
54388.	183.80	1.1669	1.2108	1.2110	1.2550	1.3669	1.4103	1.4729	1.5353	1.6248	1.7083	1.7468
54394.	183.78	1.1669	1.2118	1.2131	1.2561	1.3669	1.4103	1.4729	1.5348	1.6259	1.7083	1.7474
54400.	183.76	1.1669	1.2115	1.2153	1.2592	1.3664	1.4093	1.4723	1.5338	1.6264	1.7081	1.7485
54406.	183.74	1.1674	1.2113	1.2167	1.2626	1.3654	1.4093	1.4713	1.5333	1.6253	1.7073	1.7504
54412.	183.72	1.1678	1.2120	1.2164	1.2629	1.3664	1.4101	1.4707	1.5333	1.6245	1.7076	1.7509
54418.	183.70	1.1685	1.2134	1.2149	1.2618	1.3659	1.4098	1.4713	1.5338	1.6253	1.7078	1.7490
54423.	183.68	1.1694	1.2143	1.2149	1.2614	1.3654	1.4096	1.4723	1.5345	1.6259	1.7078	1.7471
54429.	183.66	1.1696	1.2148	1.2160	1.2617	1.3669	1.4093	1.4726	1.5360	1.6253	1.7073	1.7471
54435.	183.64	1.1692	1.2150	1.2176	1.2621	1.3649	1.4093	1.4729	1.5365	1.6251	1.7076	1.7479
54441.	183.62	1.1694	1.2145	1.2178	1.2628	1.3659	1.4106	1.4729	1.5357	1.6262	1.7078	1.7493
54447.	183.60	1.1694	1.2134	1.2180	1.2632	1.3674	1.4108	1.4721	1.5343	1.6267	1.7081	1.7518
54453.	183.58	1.1683	1.2122	1.2187	1.2622	1.3633	1.4093	1.4707	1.5338	1.6264	1.7089	1.7537
54459.	183.56	1.1665	1.2115	1.2185	1.2607	1.3628	1.4078	1.4707	1.5343	1.6264	1.7104	1.7542
54465.	183.54	1.1656	1.2113	1.2164	1.2599	1.3639	1.4078	1.4721	1.5353	1.6272	1.7115	1.7548
54471.	183.52	1.1646	1.2104	1.2140	1.2593	1.3644	1.4091	1.4731	1.5353	1.6283	1.7123	1.7561
54477.	183.50	1.1635	1.2087	1.2133	1.2578	1.3633	1.4111	1.4745	1.5355	1.6299	1.7141	1.7581
54483.	183.48	1.1628	1.2069	1.2128	1.2566	1.3633	1.4129	1.4740	1.5357	1.6323	1.7165	1.7602
54489.	183.46	1.1619	1.2062	1.2126	1.2577	1.3639	1.4131	1.4740	1.5360	1.6339	1.7194	1.7633
54495.	183.44	1.1606	1.2064	1.2124	1.2589	1.3628	1.4126	1.4756	1.5367	1.6347	1.7223	1.7660
54501.	183.42	1.1587	1.2053	1.2117	1.2576	1.3639	1.4131	1.4769	1.5382	1.6364	1.7241	1.7679
54507.	183.40	1.1578	1.2034	1.2113	1.2565	1.3644	1.4149	1.4753	1.5403	1.6396	1.7251	1.7704
54512.	183.38	1.1574	1.2023	1.2108	1.2577	1.3623	1.4157	1.4737	1.5420	1.6431	1.7257	1.7739
54518.	183.36	1.1578	1.2041	1.2092	1.2590	1.3639	1.4146	1.4756	1.5437	1.6466	1.7288	1.7780
54524.	183.34	1.1594	1.2074	1.2081	1.2593	1.3684	1.4144	1.4812	1.5461	1.6490	1.7338	1.7808
54530.	183.32	1.1628	1.2097	1.2081	1.2589	1.3684	1.4172	1.4861	1.5500	1.6492	1.7388	1.7830
54536.	183.30	1.1676	1.2120	1.2088	1.2586	1.3709	1.4233	1.4888	1.5534	1.6500	1.7430	1.7860
54542.	183.28	1.1724	1.2157	1.2106	1.2596	1.3765	1.4286	1.4920	1.5563	1.6538	1.7469	1.7890
54548.	183.26	1.1762	1.2210	1.2135	1.2617	1.3806	1.4319	1.4963	1.5594	1.6584	1.7493	1.7904
54554.	183.24	1.1794	1.2261	1.2173	1.2634	1.3851	1.4342	1.5006	1.5632	1.6611	1.7501	1.7909
54560.	183.22	1.1828	1.2294	1.2221	1.2665	1.3871	1.4375	1.5036	1.5661	1.6643	1.7511	1.7915
54566.	183.20	1.1855	1.2305	1.2270	1.2716	1.3912	1.4400	1.5049	1.5678	1.6672	1.7532	1.7917
54572.	183.18	1.1878	1.2317	1.2311	1.2761	1.3942	1.4410	1.5049	1.5700	1.6686	1.7543	1.7909
54578.	183.16	1.1894	1.2335	1.2349	1.2793	1.3937	1.4413	1.5052	1.5719	1.6670	1.7540	1.7887
54584.	183.14	1.1885	1.2340	1.2374	1.2827	1.3917	1.4410	1.5055	1.5727	1.6637	1.7522	1.7854
54590.	183.12	1.1867	1.2322	1.2383	1.2868	1.3897	1.4402	1.5038	1.5722	1.6603	1.7493	1.7813
54596.	183.10	1.1862	1.2301	1.2381	1.2894	1.3881	1.4380	1.4982	1.5698	1.6578	1.7448	1.7780
54602.	183.08	1.1852	1.2287	1.2367	1.2889	1.3897	1.4349	1.4928	1.5669	1.6573	1.7412	1.7767
54608.	183.06	1.1849	1.2284	1.2354	1.2863	1.3897	1.4309	1.4928	1.5637	1.6578	1.7391	1.7750
54614.	183.04	1.1821	1.2287	1.2340	1.2820	1.3876	1.4286	1.4968	1.5608	1.6557	1.7383	1.7696
54620.	183.02	1.1805	1.2278	1.2324	1.2781	1.3861	1.4278	1.4974	1.5596	1.6495	1.7359	1.7630
54626.	183.00	1.1801	1.2252	1.2327	1.2783	1.3836	1.4261	1.4928	1.5584	1.6425	1.7314	1.7594

WAVENUMBER CM-1	WAVELENGTH NM	CROSS SECTION X E19 CM-2 , TEMPERATURE DEG. K 151.	182.	196.	223.	247.	268.	301.	333.	372.	423.	485.
54626.	183.00	1.1801	1.2252	1.2327	1.2783	1.3836	1.4261	1.4928	1.5584	1.6425	1.7314	1.7594
54632.	182.98	1.1794	1.2233	1.2327	1.2809	1.3821	1.4238	1.4874	1.5555	1.6369	1.7254	1.7561
54638.	182.96	1.1790	1.2229	1.2311	1.2807	1.3795	1.4225	1.4853	1.5509	1.6342	1.7186	1.7498
54644.	182.94	1.1778	1.2227	1.2288	1.2777	1.3775	1.4215	1.4842	1.5459	1.6315	1.7133	1.7430
54650.	182.92	1.1776	1.2227	1.2277	1.2754	1.3780	1.4205	1.4820	1.5423	1.6294	1.7097	1.7389
54656.	182.90	1.1780	1.2236	1.2275	1.2742	1.3790	1.4200	1.4801	1.5403	1.6270	1.7068	1.7351
54662.	182.88	1.1780	1.2238	1.2279	1.2727	1.3785	1.4187	1.4793	1.5391	1.6245	1.7044	1.7318
54668.	182.86	1.1774	1.2238	1.2275	1.2709	1.3775	1.4177	1.4788	1.5394	1.6229	1.7015	1.7301
54673.	182.84	1.1778	1.2238	1.2266	1.2704	1.3760	1.4182	1.4777	1.5382	1.6232	1.6991	1.7282
54679.	182.82	1.1799	1.2245	1.2250	1.2718	1.3740	1.4184	1.4775	1.5367	1.6229	1.6968	1.7260
54685.	182.80	1.1812	1.2247	1.2257	1.2730	1.3765	1.4177	1.4775	1.5367	1.6211	1.6949	1.7247
54691.	182.78	1.1815	1.2240	1.2270	1.2731	1.3765	1.4167	1.4777	1.5365	1.6192	1.6931	1.7233
54697.	182.76	1.1817	1.2236	1.2277	1.2720	1.3740	1.4164	1.4780	1.5350	1.6176	1.6913	1.7219
54703.	182.74	1.1819	1.2240	1.2291	1.2701	1.3750	1.4172	1.4777	1.5343	1.6162	1.6894	1.7208
54709.	182.72	1.1824	1.2252	1.2293	1.2694	1.3750	1.4172	1.4756	1.5341	1.6143	1.6879	1.7189
54715.	182.70	1.1824	1.2254	1.2291	1.2707	1.3755	1.4152	1.4740	1.5331	1.6135	1.6865	1.7162
54721.	182.68	1.1821	1.2243	1.2284	1.2722	1.3730	1.4141	1.4731	1.5312	1.6141	1.6868	1.7145
54727.	182.66	1.1824	1.2240	1.2282	1.2736	1.3725	1.4136	1.4721	1.5300	1.6141	1.6858	1.7131
54733.	182.64	1.1824	1.2240	1.2286	1.2729	1.3745	1.4129	1.4710	1.5290	1.6117	1.6831	1.7115
54739.	182.62	1.1830	1.2245	1.2295	1.2705	1.3725	1.4119	1.4713	1.5283	1.6084	1.6797	1.7093
54745.	182.60	1.1833	1.2250	1.2304	1.2703	1.3725	1.4114	1.4718	1.5280	1.6068	1.6760	1.7074
54751.	182.58	1.1835	1.2250	1.2311	1.2705	1.3709	1.4108	1.4715	1.5278	1.6063	1.6742	1.7055
54757.	182.56	1.1840	1.2252	1.2304	1.2687	1.3709	1.4108	1.4699	1.5254	1.6052	1.6732	1.7025
54763.	182.54	1.1844	1.2257	1.2297	1.2679	1.3709	1.4111	1.4680	1.5222	1.6036	1.6716	1.6997
54769.	182.52	1.1835	1.2250	1.2295	1.2703	1.3709	1.4106	1.4664	1.5215	1.6023	1.6703	1.6984
54775.	182.50	1.1830	1.2243	1.2297	1.2733	1.3714	1.4096	1.4659	1.5213	1.6023	1.6695	1.6992
54781.	182.48	1.1835	1.2245	1.2306	1.2736	1.3730	1.4103	1.4648	1.5203	1.6020	1.6679	1.7003
54787.	182.46	1.1849	1.2261	1.2309	1.2707	1.3735	1.4116	1.4648	1.5198	1.6020	1.6663	1.6997
54793.	182.44	1.1860	1.2282	1.2293	1.2677	1.3720	1.4136	1.4661	1.5201	1.6023	1.6661	1.6984
54799.	182.42	1.1876	1.2301	1.2284	1.2669	1.3735	1.4149	1.4678	1.5208	1.6025	1.6661	1.6986
54805.	182.40	1.1883	1.2322	1.2297	1.2677	1.3765	1.4154	1.4680	1.5218	1.6033	1.6661	1.6992
54811.	182.38	1.1885	1.2340	1.2311	1.2694	1.3775	1.4169	1.4688	1.5222	1.6039	1.6676	1.6989
54817.	182.36	1.1896	1.2338	1.2318	1.2708	1.3770	1.4179	1.4707	1.5225	1.6031	1.6690	1.6989
54823.	182.34	1.1903	1.2329	1.2327	1.2713	1.3765	1.4182	1.4710	1.5234	1.6025	1.6692	1.7000
54829.	182.32	1.1903	1.2319	1.2343	1.2724	1.3785	1.4190	1.4696	1.5246	1.6047	1.6684	1.7006
54835.	182.30	1.1899	1.2319	1.2347	1.2730	1.3780	1.4192	1.4691	1.5244	1.6076	1.6692	1.7006
54841.	182.28	1.1912	1.2329	1.2345	1.2729	1.3780	1.4200	1.4702	1.5249	1.6087	1.6713	1.7022
54847.	182.26	1.1921	1.2340	1.2338	1.2726	1.3801	1.4207	1.4726	1.5261	1.6092	1.6729	1.7047
54853.	182.24	1.1926	1.2347	1.2352	1.2730	1.3795	1.4220	1.4758	1.5275	1.6103	1.6739	1.7060
54860.	182.22	1.1928	1.2349	1.2379	1.2743	1.3795	1.4230	1.4766	1.5288	1.6119	1.6763	1.7077
54866.	182.20	1.1942	1.2359	1.2390	1.2752	1.3816	1.4235	1.4780	1.5307	1.6130	1.6795	1.7110
54872.	182.18	1.1949	1.2368	1.2381	1.2765	1.3846	1.4245	1.4801	1.5324	1.6143	1.6826	1.7153
54878.	182.16	1.1953	1.2363	1.2388	1.2784	1.3841	1.4255	1.4818	1.5338	1.6162	1.6847	1.7189
54884.	182.14	1.1960	1.2368	1.2410	1.2789	1.3846	1.4271	1.4820	1.5338	1.6186	1.6873	1.7227
54890.	182.12	1.1962	1.2384	1.2421	1.2775	1.3866	1.4273	1.4826	1.5341	1.6219	1.6892	1.7257
54896.	182.10	1.1955	1.2398	1.2417	1.2772	1.3871	1.4278	1.4839	1.5360	1.6237	1.6915	1.7277
54902.	182.08	1.1949	1.2398	1.2419	1.2802	1.3866	1.4301	1.4855	1.5389	1.6243	1.6942	1.7301
54908.	182.06	1.1942	1.2382	1.2424	1.2840	1.3851	1.4319	1.4855	1.5403	1.6275	1.6960	1.7334
54914.	182.04	1.1924	1.2373	1.2419	1.2850	1.3846	1.4304	1.4853	1.5415	1.6326	1.6984	1.7375
54920.	182.02	1.1901	1.2370	1.2403	1.2850	1.3836	1.4281	1.4866	1.5425	1.6355	1.7002	1.7400
54926.	182.00	1.1880	1.2366	1.2403	1.2849	1.3831	1.4276	1.4885	1.5437	1.6353	1.7026	1.7386

WAVENUMBER CM-1	WAVELENGTH NM	CROSS SECTION X E19 CM-2 , TEMPERATURE DEG. K 151.	182.	196.	223.	247.	268.	301.	333.	372.	423.	485.
54926.	182.00	1.1880	1.2366	1.2403	1.2849	1.3831	1.4276	1.4885	1.5437	1.6353	1.7026	1.7386
54932.	181.98	1.1869	1.2347	1.2415	1.2831	1.3816	1.4278	1.4885	1.5461	1.6323	1.7044	1.7381
54938.	181.96	1.1867	1.2315	1.2419	1.2812	1.3826	1.4268	1.4858	1.5471	1.6302	1.7054	1.7397
54944.	181.94	1.1862	1.2294	1.2406	1.2810	1.3846	1.4253	1.4834	1.5459	1.6294	1.7041	1.7405
54950.	181.92	1.1862	1.2301	1.2374	1.2802	1.3806	1.4248	1.4818	1.5432	1.6275	1.7018	1.7383
54956.	181.90	1.1874	1.2310	1.2356	1.2761	1.3801	1.4266	1.4818	1.5413	1.6264	1.7007	1.7372
54962.	181.88	1.1883	1.2317	1.2358	1.2723	1.3816	1.4291	1.4828	1.5423	1.6280	1.7026	1.7383
54968.	181.86	1.1887	1.2326	1.2356	1.2732	1.3876	1.4311	1.4847	1.5456	1.6323	1.7041	1.7394
54974.	181.84	1.1903	1.2345	1.2354	1.2772	1.3866	1.4347	1.4874	1.5471	1.6369	1.7062	1.7411
54980.	181.82	1.1933	1.2363	1.2356	1.2791	1.3866	1.4382	1.4909	1.5473	1.6417	1.7097	1.7438
54986.	181.80	1.1953	1.2368	1.2381	1.2777	1.3927	1.4415	1.4944	1.5497	1.6468	1.7139	1.7471
54992.	181.78	1.1964	1.2375	1.2397	1.2794	1.3952	1.4451	1.4966	1.5531	1.6517	1.7178	1.7518
54998.	181.76	1.1969	1.2398	1.2403	1.2847	1.3988	1.4479	1.4995	1.5567	1.6565	1.7230	1.7553
55004.	181.74	1.1985	1.2428	1.2424	1.2884	1.3993	1.4509	1.5052	1.5623	1.6608	1.7286	1.7578
55010.	181.72	1.2003	1.2454	1.2453	1.2897	1.4023	1.4539	1.5108	1.5678	1.6637	1.7325	1.7600
55017.	181.70	1.2001	1.2470	1.2480	1.2905	1.4054	1.4565	1.5133	1.5717	1.6640	1.7346	1.7622
55023.	181.68	1.1987	1.2470	1.2500	1.2927	1.4064	1.4562	1.5133	1.5739	1.6627	1.7351	1.7638
55029.	181.66	1.1967	1.2458	1.2514	1.2964	1.4054	1.4542	1.5143	1.5741	1.4613	1.7349	1.7630
55035.	181.64	1.1951	1.2442	1.2518	1.2981	1.4043	1.4517	1.5146	1.5746	1.6592	1.7341	1.7589
55041.	181.62	1.1939	1.2426	1.2514	1.2979	1.4018	1.4494	1.5116	1.5751	1.6570	1.7322	1.7545
55047.	181.60	1.1924	1.2407	1.2505	1.2964	1.4008	1.4471	1.5079	1.5756	1.6543	1.7275	1.7515
55053.	181.58	1.1908	1.2393	1.2489	1.2937	1.4008	1.4453	1.5057	1.5741	1.6514	1.7207	1.7468
55059.	181.56	1.1910	1.2377	1.2462	1.2907	1.3968	1.4430	1.5046	1.5688	1.6471	1.7162	1.7403
55065.	181.54	1.1926	1.2373	1.2446	1.2899	1.3947	1.4400	1.5020	1.5637	1.6425	1.7136	1.7351
55071.	181.52	1.1939	1.2386	1.2446	1.2902	1.3952	1.4385	1.4985	1.5608	1.6396	1.7104	1.7315
55077.	181.50	1.1942	1.2410	1.2446	1.2895	1.3952	1.4387	1.4958	1.5577	1.6380	1.7070	1.7279
55083.	181.48	1.1942	1.2430	1.2430	1.2877	1.3952	1.4395	1.4944	1.5543	1.6355	1.7028	1.7238
55089.	181.46	1.1946	1.2435	1.2421	1.2867	1.3937	1.4397	1.4928	1.5529	1.6339	1.6989	1.7194
55095.	181.44	1.1955	1.2433	1.2435	1.2881	1.3922	1.4390	1.4923	1.5526	1.6318	1.6965	1.7156
55101.	181.42	1.1962	1.2428	1.2455	1.2907	1.3932	1.4377	1.4925	1.5507	1.6286	1.6939	1.7121
55108.	181.40	1.1971	1.2428	1.2473	1.2917	1.3947	1.4364	1.4917	1.5483	1.6259	1.6910	1.7096
55114.	181.38	1.1983	1.2424	1.2478	1.2905	1.3927	1.4354	1.4901	1.5468	1.6237	1.6876	1.7069
55120.	181.36	1.1987	1.2419	1.2478	1.2893	1.3912	1.4354	1.4890	1.5461	1.6213	1.6842	1.7052
55126.	181.34	1.1978	1.2424	1.2482	1.2873	1.3907	1.4354	1.4877	1.5454	1.6197	1.6805	1.7030
55132.	181.32	1.1971	1.2426	1.2489	1.2854	1.3897	1.4339	1.4863	1.5444	1.6184	1.6779	1.6995
55138.	181.30	1.1971	1.2419	1.2478	1.2853	1.3892	1.4316	1.4847	1.5432	1.6162	1.6760	1.6962
55144.	181.28	1.1974	1.2414	1.2471	1.2860	1.3892	1.4299	1.4834	1.5406	1.6146	1.6734	1.6945
55150.	181.26	1.1971	1.2414	1.2473	1.2866	1.3887	1.4288	1.4818	1.5374	1.6130	1.6708	1.6918
55156.	181.24	1.1967	1.2405	1.2457	1.2871	1.3876	1.4286	1.4804	1.5357	1.6108	1.6690	1.6880
55162.	181.22	1.1962	1.2403	1.2437	1.2869	1.3861	1.4288	1.4788	1.5336	1.6087	1.6669	1.6847
55168.	181.20	1.1964	1.2393	1.2442	1.2859	1.3846	1.4286	1.4766	1.5309	1.6063	1.6640	1.6814
55174.	181.18	1.1969	1.2384	1.2444	1.2834	1.3846	1.4258	1.4753	1.5292	1.6033	1.6606	1.6792
55181.	181.16	1.1967	1.2380	1.2433	1.2817	1.3816	1.4245	1.4734	1.5273	1.6004	1.6579	1.6773
55187.	181.14	1.1958	1.2382	1.2430	1.2827	1.3821	1.4248	1.4723	1.5249	1.5985	1.6553	1.6745
55193.	181.12	1.1951	1.2375	1.2433	1.2844	1.3816	1.4240	1.4718	1.5244	1.5977	1.6537	1.6718
55199.	181.10	1.1955	1.2377	1.2430	1.2838	1.3821	1.4223	1.4707	1.5234	1.5977	1.6524	1.6702
55205.	181.08	1.1955	1.2382	1.2428	1.2817	1.3831	1.4220	1.4691	1.5215	1.5977	1.6498	1.6688
55211.	181.06	1.1955	1.2373	1.2424	1.2798	1.3811	1.4220	1.4678	1.5208	1.5961	1.6482	1.6677
55217.	181.04	1.1962	1.2363	1.2410	1.2793	1.3801	1.4217	1.4656	1.5203	1.5931	1.6458	1.6677
55223.	181.02	1.1964	1.2368	1.2415	1.2810	1.3816	1.4220	1.4648	1.5189	1.5929	1.6443	1.6682
55229.	181.00	1.1960	1.2375	1.2412	1.2840	1.3821	1.4230	1.4656	1.5184	1.5945	1.6435	1.6693

WAVENUMBER CM-1	WAVELENGTH NM	CROSS SECTION X E19 CM-2 , TEMPERATURE DEG. K 151.	182.	196.	223.	247.	268.	301.	333.	372.	423.	485.
55229.	181.00	1.1960	1.2375	1.2412	1.2840	1.3821	1.4230	1.4656	1.5184	1.5945	1.6435	1.6693
55235.	180.98	1.1964	1.2377	1.2399	1.2838	1.3806	1.4225	1.4656	1.5181	1.5950	1.6437	1.6704
55241.	180.96	1.1962	1.2373	1.2399	1.2799	1.3831	1.4215	1.4667	1.5177	1.5950	1.6453	1.6702
55248.	180.94	1.1958	1.2373	1.2403	1.2763	1.3821	1.4217	1.4686	1.5186	1.5963	1.6466	1.669[illegible]
55254.	180.92	1.1953	1.2366	1.2403	1.2745	1.3831	1.4225	1.4702	1.5191	1.5988	1.6477	1.6710
55260.	180.90	1.1960	1.2361	1.2415	1.2759	1.3831	1.4230	1.4705	1.5184	1.5993	1.6490	1.6740
55266.	180.88	1.1958	1.2352	1.2421	1.2791	1.3811	1.4225	1.4702	1.5181	1.5972	1.6500	1.6743
55272.	180.86	1.1937	1.2340	1.2412	1.2798	1.3811	1.4200	1.4675	1.5184	1.5945	1.6508	1.6715
55278.	180.84	1.1908	1.2338	1.2385	1.2779	1.3790	1.4172	1.4653	1.5193	1.5926	1.6495	1.6699
55284.	180.82	1.1890	1.2345	1.2370	1.2761	1.3770	1.4162	1.4651	1.5189	1.5918	1.6461	1.6691
55290.	180.80	1.1887	1.2333	1.2381	1.2739	1.3775	1.4174	1.4656	1.5169	1.5921	1.6437	1.6688
55296.	180.78	1.1899	1.2308	1.2394	1.2727	1.3740	1.4184	1.4659	1.5150	1.5942	1.6437	1.6699
55303.	180.76	1.1912	1.2301	1.2392	1.2736	1.3730	1.4197	1.4653	1.5148	1.5980	1.6458	1.6734
55309.	180.74	1.1914	1.2315	1.2390	1.2746	1.3765	1.4230	1.4670	1.5167	1.6033	1.6495	1.6784
55315.	180.72	1.1896	1.2331	1.2390	1.2749	1.3790	1.4261	1.4707	1.5201	1.6071	1.6545	1.6825
55321.	180.70	1.1885	1.2345	1.2388	1.2744	1.3785	1.4271	1.4731	1.5230	1.6108	1.6613	1.6874
55327.	180.68	1.1890	1.2338	1.2381	1.2736	1.3790	1.4283	1.4742	1.5256	1.6154	1.6671	1.6934
55333.	180.66	1.1890	1.2322	1.2383	1.2739	1.3811	1.4299	1.4775	1.5297	1.6192	1.6716	1.6989
55339.	180.64	1.1883	1.2319	1.2376	1.2751	1.3841	1.4311	1.4828	1.5319	1.6213	1.6750	1.7038
55345.	180.62	1.1892	1.2347	1.2374	1.2759	1.3866	1.4329	1.4861	1.5326	1.6237	1.6792	1.7074
55352.	180.60	1.1903	1.2368	1.2385	1.2771	1.3836	1.4352	1.4850	1.5350	1.6272	1.6837	1.7090
55358.	180.58	1.1919	1.2363	1.2406	1.2795	1.3866	1.4367	1.4855	1.5401	1.6304	1.6863	1.7123
55364.	180.56	1.1928	1.2368	1.2401	1.2816	1.3942	1.4367	1.4904	1.5456	1.6321	1.6873	1.7153
55370.	180.54	1.1935	1.2403	1.2401	1.2825	1.3922	1.4370	1.4933	1.5464	1.6323	1.6884	1.7170
55376.	180.52	1.1946	1.2419	1.2437	1.2829	1.3942	1.4382	1.4928	1.5459	1.6315	1.6892	1.7184
55382.	180.50	1.1955	1.2405	1.2466	1.2845	1.3947	1.4395	1.4912	1.5468	1.6304	1.6879	1.7173
55388.	180.48	1.1976	1.2386	1.2451	1.2886	1.3927	1.4397	1.4898	1.5468	1.6291	1.6863	1.7156
55395.	180.46	1.2001	1.2384	1.2435	1.2918	1.3947	1.4400	1.4901	1.5452	1.6280	1.6850	1.7131
55401.	180.44	1.2010	1.2403	1.2435	1.2901	1.3937	1.4402	1.4917	1.5444	1.6294	1.6842	1.7112
55407.	180.42	1.2005	1.2430	1.2451	1.2876	1.3937	1.4415	1.4923	1.5447	1.6307	1.6837	1.7101
55413.	180.40	1.2001	1.2451	1.2471	1.2875	1.3942	1.4430	1.4920	1.5444	1.6310	1.6842	1.7082
55419.	180.38	1.2003	1.2465	1.2489	1.2878	1.3973	1.4438	1.4923	1.5439	1.6307	1.6847	1.7055
55425.	180.36	1.2019	1.2470	1.2512	1.2890	1.3973	1.4438	1.4928	1.5437	1.6299	1.6844	1.7047
55431.	180.34	1.2037	1.2465	1.2536	1.2904	1.3973	1.4438	1.4933	1.5444	1.6310	1.6850	1.7069
55438.	180.32	1.2037	1.2468	1.2534	1.2900	1.4064	1.4448	1.4947	1.5456	1.6329	1.6865	1.7088
55444.	180.30	1.2030	1.2479	1.2525	1.2907	1.3978	1.4466	1.4963	1.5468	1.6323	1.6871	1.7079
55450.	180.28	1.2026	1.2481	1.2523	1.2935	1.4003	1.4473	1.4971	1.5478	1.6299	1.6868	1.7079
55456.	180.26	1.2028	1.2475	1.2527	1.2946	1.3993	1.4463	1.4958	1.5497	1.6299	1.6871	1.7096
55462.	180.24	1.2030	1.2481	1.2532	1.2932	1.3998	1.4440	1.4939	1.5490	1.6304	1.6876	1.7093
55468.	180.22	1.2014	1.2491	1.2536	1.2918	1.3993	1.4430	1.4933	1.5466	1.6310	1.6873	1.7082
55474.	180.20	1.1992	1.2488	1.2548	1.2923	1.3947	1.4443	1.4936	1.5456	1.6315	1.6868	1.7074
55481.	180.18	1.1983	1.2477	1.2561	1.2935	1.3942	1.4453	1.4941	1.5459	1.6307	1.6858	1.7055
55487.	180.16	1.1980	1.2465	1.2568	1.2939	1.3927	1.4435	1.4928	1.5456	1.6286	1.6839	1.7044
55493.	180.14	1.1976	1.2447	1.2552	1.2941	1.3927	1.4405	1.4906	1.5454	1.6272	1.6826	1.7047
55499.	180.12	1.1964	1.2426	1.2521	1.2938	1.3932	1.4392	1.4890	1.5442	1.6262	1.6818	1.7047
55505.	180.10	1.1951	1.2414	1.2505	1.2927	1.3897	1.4375	1.4877	1.5398	1.6237	1.6787	1.7033
55511.	180.08	1.1949	1.2405	1.2498	1.2918	1.3866	1.4342	1.4853	1.5365	1.6219	1.6753	1.7011
55518.	180.06	1.1953	1.2384	1.2471	1.2897	1.3887	1.4339	1.4831	1.5365	1.6213	1.6745	1.6992
55524.	180.04	1.1964	1.2382	1.2442	1.2877	1.3897	1.4352	1.4823	1.5365	1.6213	1.6737	1.6986
55530.	180.02	1.1989	1.2410	1.2433	1.2870	1.3927	1.4377	1.4839	1.5353	1.6205	1.6739	1.6975
55536.	180.00	1.2030	1.2461	1.2437	1.2859	1.3917	1.4413	1.4871	1.5343	1.6211	1.6758	1.6964

WAVENUMBER CM-1	WAVELENGTH NM	CROSS SECTION X E19 CM-2 , TEMPERATURE DEG. K 151.	182.	196.	223.	247.	268.	301.	333.	372.	423.	485.
55536.	180.00	1.2030	1.2461	1.2437	1.2859	1.3917	1.4413	1.4871	1.5343	1.6211	1.6758	1.6964
55542.	179.98	1.2071	1.2500	1.2453	1.2845	1.3962	1.4448	1.4906	1.5350	1.6229	1.6766	1.6970
55548.	179.96	1.2096	1.2521	1.2482	1.2850	1.3973	1.4468	1.4920	1.5382	1.6245	1.6763	1.6962
55555.	179.94	1.2108	1.2542	1.2518	1.2892	1.3988	1.4486	1.4920	1.5401	1.6240	1.6745	1.6945
55561.	179.92	1.2117	1.2570	1.2561	1.2935	1.3988	1.4491	1.4925	1.5396	1.6219	1.6711	1.6934
55567.	179.90	1.2126	1.2563	1.2593	1.2958	1.4028	1.4484	1.4941	1.5406	1.6197	1.6690	1.6910
55573.	179.88	1.2119	1.2549	1.2609	1.2991	1.4028	1.4458	1.4941	1.5418	1.6165	1.6669	1.6855
55579.	179.86	1.2094	1.2551	1.2624	1.3027	1.4008	1.4433	1.4920	1.5398	1.6117	1.6632	1.6773
55586.	179.84	1.2067	1.2560	1.2631	1.3028	1.3988	1.4410	1.4882	1.5365	1.6063	1.6571	1.6685
55592.	179.82	1.2039	1.2542	1.2615	1.3011	1.3947	1.4387	1.4831	1.5338	1.6001	1.6503	1.6608
55598.	179.80	1.2014	1.2509	1.2595	1.2993	1.3912	1.4362	1.4791	1.5295	1.5963	1.6427	1.6554
55604.	179.78	1.1996	1.2481	1.2581	1.2957	1.3881	1.4329	1.4742	1.5234	1.5923	1.6356	1.6491
55610.	179.76	1.1974	1.2456	1.2563	1.2903	1.3846	1.4281	1.4694	1.5181	1.5872	1.6296	1.6420
55616.	179.74	1.1946	1.2421	1.2532	1.2886	1.3836	1.4243	1.4664	1.5155	1.5819	1.6246	1.6354
55623.	179.72	1.1924	1.2398	1.2494	1.2911	1.3816	1.4223	1.4640	1.5133	1.5767	1.6193	1.6302
55629.	179.70	1.1901	1.2391	1.2473	1.2898	1.3765	1.4200	1.4594	1.5090	1.5733	1.6133	1.6274
55635.	179.68	1.1896	1.2373	1.2451	1.2847	1.3750	1.4164	1.4546	1.5056	1.5700	1.6080	1.6247
55641.	179.66	1.1912	1.2333	1.2428	1.2816	1.3679	1.4134	1.4513	1.5025	1.5660	1.6054	1.6214
55647.	179.64	1.1908	1.2305	1.2401	1.2789	1.3659	1.4114	1.4492	1.4969	1.5625	1.6015	1.6179
55654.	179.62	1.1883	1.2289	1.2390	1.2750	1.3654	1.4108	1.4484	1.4916	1.5606	1.5970	1.6135
55660.	179.60	1.1865	1.2282	1.2385	1.2713	1.3633	1.4096	1.4473	1.4887	1.5580	1.5933	1.6099
55666.	179.58	1.1867	1.2275	1.2370	1.2711	1.3623	1.4076	1.4443	1.4863	1.5545	1.5912	1.6083
55672.	179.56	1.1883	1.2266	1.2365	1.2711	1.3618	1.4073	1.4419	1.4851	1.5531	1.5902	1.6069
55678.	179.54	1.1890	1.2259	1.2358	1.2672	1.3649	1.4065	1.4406	1.4851	1.5537	1.5899	1.6066
55685.	179.52	1.1883	1.2257	1.2338	1.2619	1.3674	1.4048	1.4416	1.4829	1.5545	1.5891	1.6069
55691.	179.50	1.1880	1.2273	1.2329	1.2587	1.3633	1.4025	1.4425	1.4795	1.5537	1.5876	1.6058
55697.	179.48	1.1880	1.2298	1.2340	1.2594	1.3608	1.4012	1.4419	1.4781	1.5520	1.5852	1.6055
55703.	179.46	1.1878	1.2301	1.2345	1.2639	1.3613	1.4010	1.4411	1.4788	1.5507	1.5831	1.6064
55709.	179.44	1.1871	1.2271	1.2340	1.2686	1.3628	1.4022	1.4406	1.4795	1.5499	1.5823	1.6055
55716.	179.42	1.1865	1.2247	1.2324	1.2692	1.3649	1.4027	1.4406	1.4791	1.5499	1.5813	1.6044
55722.	179.40	1.1858	1.2250	1.2315	1.2665	1.3633	1.4020	1.4408	1.4774	1.5507	1.5805	1.6039
55728.	179.38	1.1862	1.2250	1.2313	1.2647	1.3583	1.4035	1.4390	1.4752	1.5488	1.5797	1.6022
55734.	179.36	1.1880	1.2254	1.2322	1.2624	1.3568	1.4035	1.4344	1.4725	1.5475	1.5781	1.6011
55740.	179.34	1.1892	1.2257	1.2320	1.2603	1.3618	1.4007	1.4314	1.4713	1.5483	1.5757	1.5995
55747.	179.32	1.1890	1.2266	1.2313	1.2622	1.3588	1.3994	1.4309	1.4723	1.5483	1.5750	1.5979
55753.	179.30	1.1885	1.2273	1.2309	1.2635	1.3598	1.4005	1.4314	1.4733	1.5475	1.5765	1.5984
55759.	179.28	1.1880	1.2268	1.2318	1.2598	1.3618	1.4017	1.4325	1.4737	1.5483	1.5776	1.5992
55765.	179.26	1.1876	1.2268	1.2329	1.2567	1.3573	1.4032	1.4336	1.4742	1.5496	1.5776	1.5970
55772.	179.24	1.1887	1.2278	1.2347	1.2580	1.3608	1.4055	1.4336	1.4737	1.5488	1.5778	1.5949
55778.	179.22	1.1901	1.2287	1.2354	1.2609	1.3613	1.4058	1.4328	1.4737	1.5472	1.5781	1.5949
55784.	179.20	1.1896	1.2291	1.2336	1.2650	1.3618	1.4043	1.4314	1.4754	1.5472	1.5786	1.5973
55790.	179.18	1.1890	1.2291	1.2324	1.2671	1.3618	1.4035	1.4320	1.4747	1.5486	1.5786	1.6003
55797.	179.16	1.1894	1.2296	1.2331	1.2643	1.3633	1.4035	1.4325	1.4733	1.5494	1.5799	1.6028
55803.	179.14	1.1896	1.2287	1.2338	1.2611	1.3613	1.4043	1.4328	1.4733	1.5496	1.5802	1.6039
55809.	179.12	1.1887	1.2280	1.2340	1.2599	1.3649	1.4050	1.4344	1.4740	1.5510	1.5789	1.6039
55815.	179.10	1.1876	1.2287	1.2345	1.2597	1.3603	1.4068	1.4371	1.4747	1.5520	1.5799	1.6033
55821.	179.08	1.1871	1.2291	1.2343	1.2609	1.3603	1.4086	1.4381	1.4745	1.5518	1.5834	1.6039
55828.	179.06	1.1865	1.2278	1.2347	1.2627	1.3654	1.4086	1.4379	1.4752	1.5529	1.5860	1.6064
55834.	179.04	1.1858	1.2259	1.2347	1.2657	1.3639	1.4070	1.4379	1.4771	1.5553	1.5873	1.6102
55840.	179.02	1.1846	1.2257	1.2340	1.2673	1.3639	1.4070	1.4373	1.4795	1.5580	1.5894	1.6154
55846.	179.00	1.1846	1.2280	1.2345	1.2658	1.3623	1.4078	1.4371	1.4793	1.5588	1.5925	1.6209

WAVENUMBER CM-1	WAVELENGTH NM	CROSS SECTION X E19 CM-2 , TEMPERATURE DEG. K 151.	182.	196.	223.	247.	268.	301.	333.	372.	423.	485.
55846.	179.00	1.1846	1.2280	1.2345	1.2658	1.3623	1.4078	1.4371	1.4793	1.5588	1.5925	1.6209
55853.	178.98	1.1862	1.2294	1.2352	1.2637	1.3639	1.4083	1.4387	1.4783	1.5614	1.5960	1.6231
55859.	178.96	1.1867	1.2284	1.2349	1.2634	1.3633	1.4098	1.4406	1.4807	1.5647	1.5975	1.6233
55865.	178.94	1.1865	1.2271	1.2347	1.2634	1.3608	1.4111	1.4419	1.4836	1.5676	1.5994	1.6258
55871.	178.92	1.1860	1.2278	1.2367	1.2633	1.3633	1.4124	1.4430	1.4861	1.5698	1.6029	1.6291
55878.	178.90	1.1858	1.2282	1.2383	1.2628	1.3649	1.4139	1.4438	1.4877	1.5727	1.6075	1.6324
55884.	178.88	1.1858	1.2280	1.2381	1.2611	1.3633	1.4152	1.4465	1.4894	1.5754	1.6101	1.6357
55890.	178.86	1.1860	1.2280	1.2356	1.2608	1.3649	1.4157	1.4489	1.4918	1.5773	1.6120	1.6403
55896.	178.84	1.1860	1.2287	1.2345	1.2639	1.3679	1.4152	1.4481	1.4930	1.5792	1.6141	1.6455
55903.	178.82	1.1855	1.2280	1.2363	1.2673	1.3714	1.4136	1.4473	1.4945	1.5813	1.6162	1.6491
55909.	178.80	1.1835	1.2261	1.2365	1.2693	1.3664	1.4131	1.4470	1.4974	1.5813	1.6170	1.6510
55915.	178.78	1.1810	1.2266	1.2340	1.2698	1.3628	1.4144	1.4473	1.4971	1.5802	1.6196	1.6535
55921.	178.76	1.1796	1.2282	1.2331	1.2677	1.3674	1.4159	1.4481	1.4959	1.5824	1.6235	1.6584
55928.	178.74	1.1794	1.2275	1.2331	1.2639	1.3659	1.4167	1.4492	1.4998	1.5859	1.6264	1.6625
55934.	178.72	1.1796	1.2245	1.2324	1.2620	1.3628	1.4162	1.4511	1.5029	1.5880	1.6288	1.6636
55940.	178.70	1.1787	1.2227	1.2327	1.2624	1.3709	1.4184	1.4538	1.5020	1.5910	1.6306	1.6647
55946.	178.68	1.1787	1.2217	1.2322	1.2633	1.3720	1.4220	1.4570	1.5032	1.5947	1.6325	1.6650
55953.	178.66	1.1805	1.2224	1.2315	1.2656	1.3674	1.4248	1.4589	1.5061	1.5963	1.6335	1.6614
55959.	178.64	1.1821	1.2243	1.2338	1.2695	1.3755	1.4263	1.4613	1.5073	1.5963	1.6346	1.6581
55965.	178.62	1.1830	1.2245	1.2352	1.2726	1.3725	1.4291	1.4632	1.5092	1.5985	1.6361	1.6576
55971.	178.60	1.1844	1.2261	1.2338	1.2738	1.3735	1.4306	1.4621	1.5116	1.6001	1.6359	1.6570
55978.	178.58	1.1867	1.2303	1.2333	1.2728	1.3785	1.4286	1.4618	1.5123	1.5996	1.6335	1.6537
55984.	178.56	1.1883	1.2312	1.2358	1.2709	1.3775	1.4276	1.4635	1.5140	1.5969	1.6304	1.6485
55990.	178.54	1.1878	1.2308	1.2390	1.2706	1.3770	1.4273	1.4637	1.5155	1.5934	1.6272	1.6436
55997.	178.52	1.1865	1.2298	1.2412	1.2728	1.3750	1.4261	1.4624	1.5145	1.5894	1.6248	1.6398
56003.	178.50	1.1851	1.2289	1.2419	1.2751	1.3740	1.4261	1.4594	1.5111	1.5840	1.6196	1.6337
56009.	178.48	1.1826	1.2296	1.2403	1.2749	1.3750	1.4243	1.4551	1.5046	1.5776	1.6125	1.6260
56015.	178.46	1.1792	1.2291	1.2390	1.2721	1.3704	1.4195	1.4505	1.4998	1.5722	1.6052	1.6242
56022.	178.44	1.1769	1.2261	1.2381	1.2716	1.3649	1.4154	1.4457	1.4964	1.5655	1.5981	1.6195
56028.	178.42	1.1751	1.2217	1.2379	1.2732	1.3633	1.4096	1.4408	1.4911	1.5593	1.5920	1.6124
56034.	178.40	1.1735	1.2176	1.2363	1.2721	1.3618	1.4030	1.4357	1.4851	1.5537	1.5847	1.6033
56040.	178.38	1.1710	1.2136	1.2329	1.2676	1.3598	1.3984	1.4306	1.4807	1.5478	1.5768	1.5946
56047.	178.36	1.1680	1.2097	1.2295	1.2634	1.3568	1.3944	1.4260	1.4762	1.5416	1.5705	1.5872
56053.	178.34	1.1651	1.2074	1.2273	1.2607	1.3477	1.3918	1.4223	1.4718	1.5362	1.5645	1.5806
56059.	178.32	1.1612	1.2057	1.2252	1.2579	1.3426	1.3903	1.4190	1.4680	1.5316	1.5587	1.5760
56066.	178.30	1.1585	1.2041	1.2223	1.2543	1.3385	1.3878	1.4150	1.4631	1.5265	1.5526	1.5718
56072.	178.28	1.1581	1.2030	1.2189	1.2500	1.3401	1.3840	1.4099	1.4585	1.5209	1.5469	1.5666
56078.	178.26	1.1590	1.2032	1.2162	1.2464	1.3380	1.3809	1.4061	1.4542	1.5163	1.5411	1.5601
56084.	178.24	1.1585	1.2025	1.2146	1.2439	1.3330	1.3784	1.4048	1.4487	1.5115	1.5361	1.5540
56091.	178.22	1.1569	1.2016	1.2119	1.2416	1.3315	1.3764	1.4032	1.4431	1.5077	1.5319	1.5486
56097.	178.20	1.1567	1.2009	1.2097	1.2390	1.3284	1.3743	1.3988	1.4409	1.5053	1.5282	1.5450
56103.	178.18	1.1569	1.1992	1.2083	1.2374	1.3284	1.3721	1.3948	1.4395	1.5026	1.5235	1.5404
56110.	178.16	1.1558	1.1974	1.2061	1.2370	1.3274	1.3698	1.3929	1.4354	1.4981	1.5190	1.5346
56116.	178.14	1.1540	1.1969	1.2061	1.2336	1.3208	1.3690	1.3910	1.4301	1.4924	1.5146	1.5300
56122.	178.12	1.1517	1.1979	1.2067	1.2304	1.3218	1.3685	1.3900	1.4265	1.4881	1.5109	1.5269
56129.	178.10	1.1508	1.1972	1.2054	1.2309	1.3229	1.3672	1.3902	1.4250	1.4855	1.5077	1.5245
56135.	178.08	1.1508	1.1930	1.2038	1.2297	1.3218	1.3650	1.3889	1.4241	1.4847	1.5043	1.5204
56141.	178.06	1.1501	1.1909	1.2034	1.2262	1.3148	1.3632	1.3848	1.4202	1.4852	1.5007	1.5163
56148.	178.04	1.1487	1.1918	1.2022	1.2230	1.3163	1.3612	1.3805	1.4156	1.4841	1.4962	1.5138
56154.	178.02	1.1467	1.1914	1.2007	1.2204	1.3183	1.3576	1.3776	1.4146	1.4809	1.4920	1.5124
56160.	178.00	1.1453	1.1893	1.1995	1.2203	1.3112	1.3556	1.3765	1.4127	1.4785	1.4894	1.5113

WAVENUMBER CM-1	WAVELENGTH NM	CROSS SECTION X E19 CM-2 , TEMPERATURE DEG. K 151.	182.	196.	223.	247.	268.	301.	333.	372.	423.	485.
56160.	178.00	1.1453	1.1893	1.1995	1.2203	1.3112	1.3556	1.3765	1.4127	1.4785	1.4894	1.5113
56166.	177.98	1.1451	1.1884	1.1998	1.2217	1.3132	1.3558	1.3757	1.4081	1.4774	1.4883	1.5108
56173.	177.96	1.1465	1.1877	1.1991	1.2228	1.3183	1.3553	1.3738	1.4069	1.4769	1.4886	1.5111
56179.	177.94	1.1478	1.1860	1.1975	1.2221	1.3117	1.3556	1.3741	1.4084	1.4742	1.4883	1.5089
56185.	177.92	1.1476	1.1844	1.1971	1.2196	1.3087	1.3563	1.3754	1.4072	1.4723	1.4870	1.5075
56192.	177.90	1.1469	1.1846	1.1980	1.2190	1.3132	1.3551	1.3762	1.4052	1.4747	1.4873	1.5089
56198.	177.88	1.1476	1.1853	1.1980	1.2193	1.3122	1.3546	1.3765	1.4067	1.4774	1.4875	1.5097
56204.	177.86	1.1499	1.1872	1.1962	1.2211	1.3107	1.3566	1.3746	1.4064	1.4779	1.4867	1.5130
56211.	177.84	1.1506	1.1872	1.1941	1.2237	1.3148	1.3584	1.3725	1.4043	1.4809	1.4865	1.5184
56217.	177.82	1.1506	1.1856	1.1948	1.2215	1.3122	1.3622	1.3738	1.4057	1.4844	1.4901	1.5228
56223.	177.80	1.1512	1.1872	1.1966	1.2177	1.3132	1.3645	1.3792	1.4074	1.4868	1.4951	1.5253
56230.	177.78	1.1519	1.1900	1.1962	1.2189	1.3137	1.3665	1.3857	1.4110	1.4892	1.5007	1.5291
56236.	177.76	1.1517	1.1907	1.1957	1.2206	1.3148	1.3721	1.3883	1.4151	1.4914	1.5056	1.5327
56242.	177.74	1.1508	1.1911	1.1975	1.2215	1.3198	1.3738	1.3881	1.4178	1.4946	1.5096	1.5379
56249.	177.72	1.1503	1.1918	1.2002	1.2252	1.3158	1.3708	1.3908	1.4212	1.4973	1.5138	1.5428
56255.	177.70	1.1512	1.1916	1.2013	1.2265	1.3183	1.3683	1.3937	1.4226	1.4965	1.5177	1.5431
56261.	177.68	1.1517	1.1916	1.2016	1.2222	1.3173	1.3678	1.3927	1.4212	1.4962	1.5193	1.5417
56268.	177.66	1.1515	1.1918	1.2011	1.2219	1.3168	1.3670	1.3881	1.4204	1.4989	1.5169	1.5428
56274.	177.64	1.1517	1.1900	1.2002	1.2288	1.3168	1.3680	1.3827	1.4190	1.5034	1.5156	1.5469
56280.	177.62	1.1528	1.1877	1.2000	1.2329	1.3224	1.3693	1.3803	1.4199	1.5077	1.5172	1.5543
56287.	177.60	1.1524	1.1860	1.2004	1.2324	1.3249	1.3683	1.3843	1.4245	1.5139	1.5211	1.5639
56293.	177.58	1.1510	1.1870	1.1986	1.2317	1.3254	1.3713	1.3913	1.4286	1.5217	1.5280	1.5724
56299.	177.56	1.1499	1.1907	1.1975	1.2289	1.3249	1.3779	1.3975	1.4318	1.5276	1.5350	1.5798
56306.	177.54	1.1492	1.1930	1.1986	1.2263	1.3274	1.3819	1.4034	1.4376	1.5333	1.5403	1.5872
56312.	177.52	1.1474	1.1930	1.2000	1.2268	1.3289	1.3852	1.4102	1.4448	1.5381	1.5476	1.5938
56318.	177.50	1.1458	1.1925	1.2009	1.2282	1.3330	1.3896	1.4153	1.4496	1.5437	1.5576	1.5987
56325.	177.48	1.1462	1.1932	1.2018	1.2292	1.3350	1.3921	1.4182	1.4537	1.5507	1.5666	1.6036
56331.	177.46	1.1474	1.1937	1.2034	1.2299	1.3355	1.3939	1.4201	1.4590	1.5561	1.5718	1.6080
56337.	177.44	1.1476	1.1944	1.2052	1.2317	1.3365	1.3964	1.4233	1.4626	1.5588	1.5778	1.6124
56344.	177.42	1.1462	1.1941	1.2072	1.2326	1.3385	1.3982	1.4268	1.4641	1.5598	1.5839	1.6151
56350.	177.40	1.1465	1.1948	1.2095	1.2319	1.3385	1.3982	1.4287	1.4646	1.5596	1.5855	1.6154
56356.	177.38	1.1474	1.1958	1.2086	1.2334	1.3380	1.3982	1.4277	1.4675	1.5596	1.5844	1.6135
56363.	177.36	1.1465	1.1941	1.2077	1.2379	1.3370	1.3956	1.4244	1.4701	1.5582	1.5823	1.6116
56369.	177.34	1.1449	1.1930	1.2083	1.2423	1.3380	1.3928	1.4225	1.4694	1.5550	1.5784	1.6105
56375.	177.32	1.1446	1.1930	1.2077	1.2427	1.3406	1.3908	1.4215	1.4677	1.5515	1.5744	1.6080
56382.	177.30	1.1444	1.1916	1.2058	1.2395	1.3355	1.3888	1.4196	1.4680	1.5475	1.5705	1.6017
56388.	177.28	1.1428	1.1914	1.2047	1.2374	1.3310	1.3880	1.4185	1.4648	1.5435	1.5666	1.5962
56395.	177.26	1.1417	1.1918	1.2043	1.2385	1.3320	1.3875	1.4180	1.4610	1.5418	1.5639	1.5935
56401.	177.24	1.1419	1.1897	1.2038	1.2398	1.3340	1.3883	1.4163	1.4610	1.5397	1.5621	1.5905
56407.	177.22	1.1428	1.1874	1.2040	1.2380	1.3289	1.3896	1.4145	1.4590	1.5367	1.5603	1.5864
56414.	177.20	1.1417	1.1865	1.2025	1.2345	1.3284	1.3885	1.4142	1.4537	1.5338	1.5576	1.5833
56420.	177.18	1.1399	1.1863	1.2004	1.2320	1.3274	1.3850	1.4126	1.4503	1.5306	1.5553	1.5828
56426.	177.16	1.1394	1.1865	1.1998	1.2308	1.3284	1.3825	1.4099	1.4496	1.5287	1.5529	1.5806
56433.	177.14	1.1401	1.1867	1.2004	1.2287	1.3274	1.3797	1.4088	1.4472	1.5265	1.5505	1.5762
56439.	177.12	1.1410	1.1863	1.2009	1.2242	1.3254	1.3787	1.4085	1.4441	1.5236	1.5484	1.5713
56446.	177.10	1.1410	1.1874	1.2016	1.2218	1.3254	1.3809	1.4091	1.4419	1.5214	1.5461	1.5688
56452.	177.08	1.1399	1.1884	1.2022	1.2272	1.3218	1.3830	1.4077	1.4397	1.5193	1.5427	1.5669
56458.	177.06	1.1392	1.1863	1.2018	1.2345	1.3218	1.3812	1.4053	1.4380	1.5179	1.5403	1.5642
56465.	177.04	1.1394	1.1840	1.2007	1.2366	1.3229	1.3741	1.4061	1.4366	1.5196	1.5382	1.5645
56471.	177.02	1.1406	1.1826	1.2000	1.2352	1.3198	1.3700	1.4075	1.4368	1.5182	1.5335	1.5650
56477.	177.00	1.1406	1.1814	1.2000	1.2350	1.3163	1.3749	1.4058	1.4359	1.5131	1.5308	1.5628

WAVENUMBER CM-1	WAVELENGTH NM	CROSS SECTION X E19 CM-2 , TEMPERATURE DEG. K 151.	182.	196.	223	247.	268.	301.	333.	372.	423.	485.
56477.	177.00	1.1406	1.1814	1.2000	1.2350	1.3163	1.3749	1.4058	1.4359	1.5131	1.5308	1.5628
56484.	176.98	1.1408	1.1819	1.1993	1.2392	1.3168	1.3789	1.4023	1.4339	1.5091	1.5316	1.5598
56490.	176.96	1.1428	1.1812	1.1968	1.2391	1.3173	1.3789	1.3988	1.4339	1.5067	1.5303	1.5573
56497.	176.94	1.1460	1.1802	1.1944	1.2307	1.3163	1.3794	1.3962	1.4335	1.5040	1.5266	1.5543
56503.	176.92	1.1474	1.1819	1.1953	1.2256	1.3168	1.3779	1.3953	1.4313	1.5026	1.5227	1.5494
56509.	176.90	1.1469	1.1860	1.1971	1.2241	1.3188	1.3751	1.3951	1.4279	1.5005	1.5209	1.5412
56516.	176.88	1.1469	1.1886	1.1966	1.2210	1.3183	1.3718	1.3951	1.4255	1.4975	1.5190	1.5335
56522.	176.86	1.1469	1.1888	1.1964	1.2206	1.3143	1.3690	1.3927	1.4245	1.4932	1.5140	1.5280
56529.	176.84	1.1469	1.1881	1.1984	1.2237	1.3132	1.3675	1.3862	1.4224	1.4871	1.5059	1.5220
56535.	176.82	1.1462	1.1870	1.1998	1.2255	1.3127	1.3652	1.3800	1.4183	1.4804	1.4978	1.5157
56541.	176.80	1.1444	1.1849	1.1991	1.2238	1.3107	1.3614	1.3762	1.4142	1.4747	1.4917	1.5100
56548.	176.78	1.1426	1.1844	1.1989	1.2239	1.3107	1.3591	1.3722	1.4101	1.4699	1.4859	1.5050
56554.	176.76	1.1408	1.1844	1.1993	1.2281	1.3092	1.3574	1.3679	1.4038	1.4669	1.4778	1.4985
56560.	176.74	1.1390	1.1830	1.1982	1.2308	1.3067	1.3538	1.3638	1.3975	1.4637	1.4710	1.4913
56567.	176.72	1.1369	1.1807	1.1955	1.2302	1.2981	1.3515	1.3590	1.3941	1.4583	1.4644	1.4853
56573.	176.70	1.1340	1.1782	1.1941	1.2256	1.2950	1.3503	1.3539	1.3905	1.4522	1.4584	1.4793
56580.	176.68	1.1315	1.1761	1.1932	1.2193	1.2950	1.3455	1.3507	1.3862	1.4481	1.4542	1.4738
56586.	176.66	1.1312	1.1733	1.1905	1.2142	1.2935	1.3416	1.3488	1.3814	1.4455	1.4495	1.4686
56593.	176.64	1.1294	1.1719	1.1894	1.2119	1.2905	1.3411	1.3474	1.3744	1.4420	1.4447	1.4642
56599.	176.62	1.1265	1.1691	1.1885	1.2155	1.2834	1.3391	1.3458	1.3690	1.4401	1.4408	1.4626
56605.	176.60	1.1249	1.1652	1.1849	1.2177	1.2844	1.3356	1.3437	1.3686	1.4377	1.4366	1.4590
56612.	176.58	1.1235	1.1636	1.1799	1.2104	1.2803	1.3313	1.3404	1.3662	1.4334	1.4319	1.4538
56618.	176.56	1.1206	1.1626	1.1761	1.2006	1.2753	1.3272	1.3377	1.3616	1.4288	1.4269	1.4483
56625.	176.54	1.1174	1.1608	1.1750	1.1965	1.2738	1.3252	1.3350	1.3565	1.4248	1.4221	1.4448
56631.	176.52	1.1149	1.1585	1.1741	1.1936	1.2753	1.3231	1.3313	1.3534	1.4213	1.4187	1.4456
56637.	176.50	1.1128	1.1554	1.1727	1.1893	1.2692	1.3221	1.3275	1.3534	1.4197	1.4179	1.4462
56644.	176.48	1.1099	1.1510	1.1700	1.1905	1.2672	1.3221	1.3237	1.3522	1.4181	1.4174	1.4426
56650.	176.46	1.1078	1.1471	1.1666	1.1954	1.2667	1.3204	1.3208	1.3490	1.4159	1.4166	1.4396
56657.	176.44	1.1074	1.1459	1.1637	1.1969	1.2631	1.3166	1.3192	1.3473	1.4124	1.4132	1.4390
56663.	176.42	1.1058	1.1443	1.1614	1.1969	1.2662	1.3117	1.3157	1.3466	1.4092	1.4085	1.4385
56670.	176.40	1.1026	1.1422	1.1578	1.1945	1.2667	1.3095	1.3130	1.3430	1.4073	1.4048	1.4382
56676.	176.38	1.0999	1.1420	1.1538	1.1873	1.2636	1.3067	1.3127	1.3384	1.4060	1.4043	1.4382
56682.	176.36	1.0999	1.1420	1.1526	1.1788	1.2596	1.3029	1.3116	1.3370	1.4052	1.4064	1.4349
56689.	176.34	1.1006	1.1401	1.1535	1.1740	1.2591	1.3019	1.3095	1.3370	1.4033	1.4093	1.4316
56695.	176.32	1.0999	1.1388	1.1533	1.1750	1.2555	1.3031	1.3068	1.3355	1.4003	1.4111	1.4297
56702.	176.30	1.0965	1.1376	1.1524	1.1786	1.2550	1.3041	1.3052	1.3343	1.4012	1.4082	1.4303
56708.	176.28	1.0956	1.1369	1.1522	1.1804	1.2581	1.3051	1.3060	1.3345	1.4033	1.4046	1.4333
56715.	176.26	1.0969	1.1378	1.1531	1.1775	1.2576	1.3062	1.3065	1.3336	1.4025	1.4030	1.4363
56721.	176.24	1.0978	1.1383	1.1538	1.1731	1.2611	1.3064	1.3068	1.3324	1.4014	1.4027	1.4377
56727.	176.22	1.0974	1.1371	1.1535	1.1704	1.2591	1.3054	1.3052	1.3331	1.4017	1.4038	1.4390
56734.	176.20	1.0978	1.1355	1.1506	1.1708	1.2545	1.3044	1.3041	1.3345	1.4036	1.4061	1.4404
56740.	176.18	1.0990	1.1339	1.1475	1.1736	1.2576	1.3062	1.3060	1.3362	1.4065	1.4069	1.4420
56747.	176.16	1.0994	1.1327	1.1454	1.1762	1.2581	1.3120	1.3079	1.3367	1.4076	1.4040	1.4459
56753.	176.14	1.0985	1.1341	1.1443	1.1746	1.2571	1.3143	1.3081	1.3360	1.4073	1.4027	1.4483
56760.	176.12	1.0974	1.1357	1.1441	1.1714	1.2550	1.3084	1.3089	1.3355	1.4076	1.4040	1.4486
56766.	176.10	1.0972	1.1350	1.1441	1.1721	1.2586	1.3041	1.3108	1.3365	1.4103	1.4088	1.4486
56772.	176.08	1.0976	1.1350	1.1466	1.1741	1.2621	1.3074	1.3130	1.3367	1.4135	1.4148	1.4514
56779.	176.06	1.1008	1.1364	1.1493	1.1759	1.2631	1.3148	1.3149	1.3379	1.4159	1.4187	1.4552
56785.	176.04	1.1063	1.1376	1.1506	1.1800	1.2616	1.3201	1.3167	1.3394	1.4213	1.4198	1.4593
56792.	176.02	1.1074	1.1383	1.1533	1.1823	1.2611	1.3181	1.3178	1.3432	1.4264	1.4211	1.4634
56798.	176.00	1.1063	1.1392	1.1578	1.1762	1.2652	1.3140	1.3197	1.3478	1.4275	1.4242	1.4675

WAVENUMBER CM-1	WAVELENGTH NM	CROSS SECTION X E19 CM-2 , TEMPERATURE DEG. K 151.	182.	196.	223.	247.	268.	301.	333.	372.	423.	485.
56798.	176.00	1.1063	1.1392	1.1578	1.1762	1.2652	1.3140	1.3197	1.3478	1.4275	1.4242	1.4675
56805.	175.98	1.1056	1.1404	1.1596	1.1662	1.2591	1.3158	1.3254	1.3505	1.4272	1.4300	1.4716
56811.	175.96	1.1069	1.1418	1.1567	1.1662	1.2581	1.3206	1.3297	1.3517	1.4307	1.4363	1.4744
56818.	175.94	1.1103	1.1429	1.1526	1.1757	1.2631	1.3216	1.3280	1.3548	1.4379	1.4382	1.4771
56824.	175.92	1.1126	1.1457	1.1522	1.1846	1.2707	1.3221	1.3270	1.3582	1.4436	1.4366	1.4809
56831.	175.90	1.1135	1.1476	1.1556	1.1908	1.2717	1.3231	1.3310	1.3608	1.4457	1.4382	1.4856
56837.	175.88	1.1128	1.1478	1.1592	1.1931	1.2788	1.3239	1.3345	1.3623	1.4463	1.4434	1.4891
56844.	175.86	1.1122	1.1487	1.1605	1.1937	1.2717	1.3254	1.3361	1.3630	1.4497	1.4476	1.4919
56850.	175.84	1.1122	1.1503	1.1578	1.1960	1.2768	1.3285	1.3380	1.3630	1.4538	1.4495	1.4957
56856.	175.82	1.1126	1.1517	1.1572	1.1957	1.2753	1.3330	1.3388	1.3645	1.4551	1.4526	1.4987
56863.	175.80	1.1126	1.1515	1.1590	1.1928	1.2778	1.3358	1.3383	1.3681	1.4554	1.4589	1.5012
56869.	175.78	1.1110	1.1492	1.1603	1.1893	1.2788	1.3356	1.3396	1.3703	1.4586	1.4615	1.5045
56876.	175.76	1.1090	1.1455	1.1635	1.1857	1.2834	1.3368	1.3418	1.3712	1.4629	1.4607	1.5086
56882.	175.74	1.1072	1.1432	1.1648	1.1840	1.2733	1.3394	1.3445	1.3729	1.4642	1.4621	1.5127
56889.	175.72	1.1049	1.1429	1.1612	1.1844	1.2728	1.3386	1.3463	1.3744	1.4637	1.4628	1.5135
56895.	175.70	1.1019	1.1434	1.1572	1.1820	1.2692	1.3338	1.3458	1.3748	1.4629	1.4644	1.5122
56902.	175.68	1.0985	1.1425	1.1554	1.1768	1.2692	1.3285	1.3439	1.3760	1.4605	1.4694	1.5108
56908.	175.66	1.0965	1.1404	1.1560	1.1770	1.2672	1.3262	1.3388	1.3789	1.4567	1.4699	1.5083
56915.	175.64	1.0958	1.1385	1.1567	1.1832	1.2647	1.3229	1.3329	1.3789	1.4527	1.4626	1.5028
56921.	175.62	1.0929	1.1369	1.1542	1.1920	1.2596	1.3178	1.3272	1.3753	1.4465	1.4552	1.4957
56928.	175.60	1.0872	1.1344	1.1506	1.1975	1.2566	1.3188	1.3251	1.3705	1.4385	1.4510	1.4886
56934.	175.58	1.0824	1.1320	1.1484	1.1938	1.2545	1.3226	1.3240	1.3647	1.4310	1.4460	1.4793
56941.	175.56	1.0815	1.1297	1.1461	1.1890	1.2560	1.3196	1.3205	1.3563	1.4248	1.4395	1.4675
56947.	175.54	1.0824	1.1258	1.1441	1.1892	1.2560	1.3140	1.3140	1.3488	1.4194	1.4316	1.4568
56954.	175.52	1.0817	1.1242	1.1409	1.1875	1.2520	1.3100	1.3065	1.3425	1.4143	1.4235	1.4508
56960.	175.50	1.0781	1.1242	1.1375	1.1846	1.2474	1.3057	1.3014	1.3382	1.4089	1.4135	1.4453
56967.	175.48	1.0740	1.1204	1.1348	1.1826	1.2419	1.3024	1.2949	1.3360	1.4036	1.4059	1.4366
56973.	175.46	1.0715	1.1144	1.1348	1.1820	1.2444	1.2981	1.2877	1.3304	1.3990	1.4019	1.4308
56980.	175.44	1.0692	1.1119	1.1328	1.1806	1.2419	1.2955	1.2863	1.3237	1.3958	1.3980	1.4303
56986.	175.42	1.0683	1.1130	1.1292	1.1714	1.2338	1.2932	1.2879	1.3198	1.3896	1.3920	1.4292
56993.	175.40	1.0690	1.1121	1.1288	1.1575	1.2343	1.2877	1.2887	1.3155	1.3810	1.3880	1.4234
56999.	175.38	1.0697	1.1065	1.1294	1.1522	1.2338	1.2811	1.2874	1.3124	1.3775	1.3843	1.4166
57006.	175.36	1.0708	1.1021	1.1265	1.1592	1.2297	1.2783	1.2815	1.3090	1.3767	1.3788	1.4103
57012.	175.34	1.0724	1.1003	1.1215	1.1637	1.2312	1.2788	1.2731	1.3039	1.3743	1.3725	1.4045
57019.	175.32	1.0722	1.1001	1.1186	1.1593	1.2282	1.2783	1.2680	1.3001	1.3727	1.3670	1.4002
57025.	175.30	1.0674	1.0996	1.1166	1.1602	1.2272	1.2770	1.2685	1.2993	1.3705	1.3628	1.3977
57032.	175.28	1.0617	1.1003	1.1136	1.1639	1.2226	1.2780	1.2699	1.2964	1.3638	1.3623	1.3936
57038.	175.26	1.0588	1.1005	1.1118	1.1617	1.2166	1.2757	1.2707	1.2892	1.3536	1.3628	1.3862
57045.	175.24	1.0579	1.0998	1.1127	1.1577	1.2109	1.2681	1.2702	1.2853	1.3445	1.3570	1.3791
57051.	175.22	1.0581	1.0980	1.1155	1.1558	1.2064	1.2643	1.2677	1.2841	1.3410	1.3471	1.3733
57058.	175.20	1.0572	1.0938	1.1166	1.1532	1.2075	1.2656	1.2632	1.2791	1.3402	1.3421	1.3684
57064.	175.18	1.0551	1.0880	1.1150	1.1498	1.2054	1.2636	1.2572	1.2740	1.3381	1.3384	1.3654
57071.	175.16	1.0535	1.0827	1.1107	1.1477	1.2004	1.2567	1.2524	1.2728	1.3354	1.3334	1.3615
57077.	175.14	1.0513	1.0808	1.1080	1.1445	1.2004	1.2486	1.2481	1.2728	1.3321	1.3276	1.3569
57084.	175.12	1.0501	1.0836	1.1069	1.1448	1.2009	1.2433	1.2422	1.2706	1.3281	1.3192	1.3536
57090.	175.10	1.0501	1.0861	1.1053	1.1442	1.1968	1.2418	1.2381	1.2660	1.3262	1.3142	1.3511
57097.	175.08	1.0490	1.0873	1.1037	1.1373	1.1928	1.2430	1.2371	1.2605	1.3249	1.3137	1.3489
57103.	175.06	1.0479	1.0878	1.1017	1.1341	1.1913	1.2441	1.2344	1.2547	1.3211	1.3108	1.3448
57110.	175.04	1.0488	1.0861	1.0990	1.1350	1.1913	1.2448	1.2311	1.2506	1.3163	1.3066	1.3399
57116.	175.02	1.0497	1.0841	1.0970	1.1460	1.1903	1.2418	1.2279	1.2508	1.3128	1.3037	1.3388
57123.	175.00	1.0472	1.0852	1.0956	1.1466	1.1872	1.2362	1.2252	1.2504	1.3107	1.3006	1.3369

WAVENUMBER CM-1	WAVELENGTH NM	CROSS SECTION X E19 CM-2 , TEMPERATURE DEG. K 151.	182.	196.	223.	247.	268.	301.	333.	372.	423.	485.
57123.	175.00	1.0472	1.0852	1.0956	1.1466	1.1872	1.2362	1.2252	1.2504	1.3107	1.3006	1.3369
57129.	174.98	1.0442	1.0857	1.0934	1.1370	1.1897	1.2319	1.2252	1.2475	1.3088	1.2966	1.3325
57136.	174.96	1.0438	1.0834	1.0922	1.1272	1.1842	1.2294	1.2257	1.2436	1.3061	1.2922	1.3311
57142.	174.94	1.0436	1.0808	1.0904	1.1199	1.1852	1.2319	1.2222	1.2412	1.3034	1.2898	1.3320
57149.	174.92	1.0442	1.0790	1.0882	1.1145	1.1882	1.2334	1.2182	1.2414	1.3048	1.2885	1.3361
57156.	174.90	1.0456	1.0771	1.0879	1.1157	1.1771	1.2294	1.2169	1.2414	1.3072	1.2869	1.3405
57162.	174.88	1.0440	1.0760	1.0884	1.1152	1.1761	1.2296	1.2174	1.2388	1.3069	1.2861	1.3429
57169.	174.86	1.0408	1.0755	1.0891	1.1139	1.1811	1.2321	1.2196	1.2368	1.3091	1.2882	1.3440
57175.	174.84	1.0386	1.0757	1.0891	1.1161	1.1827	1.2281	1.2198	1.2412	1.3136	1.2911	1.3426
57182.	174.82	1.0342	1.0748	1.0875	1.1201	1.1771	1.2240	1.2182	1.2453	1.3171	1.2935	1.3396
57188.	174.80	1.0322	1.0711	1.0859	1.1227	1.1806	1.2268	1.2171	1.2436	1.3182	1.2964	1.3413
57195.	174.78	1.0338	1.0660	1.0830	1.1189	1.1781	1.2289	1.2147	1.2407	1.3203	1.3019	1.3492
57201.	174.76	1.0345	1.0637	1.0810	1.1139	1.1751	1.2294	1.2120	1.2419	1.3244	1.3069	1.3583
57208.	174.74	1.0342	1.0655	1.0803	1.1115	1.1832	1.2301	1.2115	1.2463	1.3249	1.3095	1.3632
57214.	174.72	1.0331	1.0653	1.0801	1.1078	1.1806	1.2268	1.2134	1.2494	1.3257	1.3137	1.3651
57221.	174.70	1.0311	1.0627	1.0780	1.1030	1.1771	1.2212	1.2150	1.2516	1.3297	1.3184	1.3689
57228.	174.68	1.0283	1.0625	1.0769	1.1001	1.1776	1.2192	1.2131	1.2549	1.3346	1.3253	1.3771
57234.	174.66	1.0270	1.0639	1.0776	1.0994	1.1781	1.2200	1.2109	1.2574	1.3364	1.3323	1.3826
57241.	174.64	1.0261	1.0653	1.0774	1.1011	1.1811	1.2197	1.2134	1.2578	1.3356	1.3339	1.3813
57247.	174.62	1.0245	1.0627	1.0774	1.1057	1.1746	1.2210	1.2193	1.2561	1.3364	1.3342	1.3810
57254.	174.60	1.0238	1.0590	1.0794	1.1118	1.1700	1.2271	1.2241	1.2532	1.3426	1.3355	1.3887
57260.	174.58	1.0249	1.0588	1.0778	1.1161	1.1786	1.2337	1.2287	1.2545	1.3504	1.3373	1.3971
57267.	174.56	1.0258	1.0618	1.0715	1.1143	1.1801	1.2352	1.2371	1.2612	1.3560	1.3400	1.4021
57273.	174.54	1.0265	1.0641	1.0686	1.1096	1.1791	1.2344	1.2449	1.2687	1.3620	1.3452	1.4056
57280.	174.52	1.0281	1.0658	1.0724	1.1088	1.1811	1.2357	1.2473	1.2730	1.3649	1.3547	1.4122
57287.	174.50	1.0295	1.0662	1.0767	1.1088	1.1892	1.2372	1.2494	1.2742	1.3665	1.3628	1.4210
57293.	174.48	1.0279	1.0639	1.0776	1.1016	1.1953	1.2377	1.2546	1.2757	1.3711	1.3681	1.4284
57300.	174.46	1.0256	1.0627	1.0762	1.0932	1.1989	1.2390	1.2554	1.2805	1.3770	1.3709	1.4338
57306.	174.44	1.0247	1.0639	1.0749	1.0961	1.1989	1.2433	1.2575	1.2870	1.3791	1.3741	1.4382
57313.	174.42	1.0222	1.0632	1.0756	1.1052	1.1953	1.2491	1.2637	1.2926	1.3781	1.3791	1.4388
57319.	174.40	1.0204	1.0618	1.0785	1.1147	1.1842	1.2507	1.2688	1.2976	1.3765	1.3846	1.4363
57326.	174.38	1.0217	1.0627	1.0798	1.1262	1.1897	1.2504	1.2710	1.3013	1.3767	1.3885	1.4325
57333.	174.36	1.0254	1.0653	1.0792	1.1303	1.2019	1.2512	1.2707	1.3029	1.3767	1.3917	1.4311
57339.	174.34	1.0274	1.0683	1.0807	1.1225	1.2039	1.2484	1.2691	1.3005	1.3762	1.3935	1.4316
57346.	174.32	1.0272	1.0697	1.0814	1.1132	1.1973	1.2430	1.2677	1.2974	1.3732	1.3912	1.4308
57352.	174.30	1.0267	1.0690	1.0810	1.1118	1.1933	1.2441	1.2648	1.2964	1.3695	1.3859	1.4292
57359.	174.28	1.0261	1.0690	1.0832	1.1172	1.1973	1.2456	1.2626	1.2955	1.3679	1.3822	1.4270
57365.	174.26	1.0249	1.0692	1.0855	1.1190	1.1948	1.2441	1.2618	1.2943	1.3687	1.3772	1.4215
57372.	174.24	1.0242	1.0683	1.0859	1.1139	1.2019	1.2517	1.2589	1.2940	1.3660	1.3715	1.4163
57379.	174.22	1.0249	1.0662	1.0861	1.1107	1.1984	1.2565	1.2556	1.2921	1.3617	1.3715	1.4152
57385.	174.20	1.0267	1.0637	1.0855	1.1153	1.1918	1.2453	1.2551	1.2875	1.3601	1.3746	1.4136
57392.	174.18	1.0292	1.0614	1.0837	1.1236	1.1994	1.2392	1.2554	1.2863	1.3582	1.3733	1.4075
57398.	174.16	1.0306	1.0609	1.0834	1.1288	1.1897	1.2385	1.2567	1.2865	1.3560	1.3686	1.4010
57405.	174.14	1.0297	1.0625	1.0855	1.1310	1.1892	1.2367	1.2578	1.2836	1.3531	1.3657	1.3958
57412.	174.12	1.0292	1.0639	1.0884	1.1284	1.1903	1.2337	1.2572	1.2824	1.3507	1.3662	1.3930
57418.	174.10	1.0292	1.0646	1.0893	1.1279	1.1923	1.2278	1.2572	1.2836	1.3512	1.3662	1.3900
57425.	174.08	1.0290	1.0669	1.0877	1.1378	1.1852	1.2299	1.2562	1.2846	1.3491	1.3633	1.3873
57431.	174.06	1.0304	1.0720	1.0855	1.1431	1.1892	1.2304	1.2492	1.2836	1.3437	1.3562	1.3862
57438.	174.04	1.0333	1.0743	1.0850	1.1547	1.1867	1.2223	1.2427	1.2827	1.3391	1.3463	1.3848
57445.	174.02	1.0342	1.0715	1.0848	1.1771	1.1806	1.2190	1.2438	1.2810	1.3367	1.3379	1.3777
57451.	174.00	1.0338	1.0681	1.0834	1.1736	1.1903	1.2212	1.2484	1.2764	1.3348	1.3350	1.3673

WAVENUMBER CM-1	WAVELENGTH NM	CROSS SECTION X E19 CM-2 , TEMPERATURE DEG. K 151.	182.	196.	223.	247.	268.	301.	333.	372.	423.	485.
57451.	174.00	1.0338	1.0681	1.0834	1.1736	1.1903	1.2212	1.2484	1.2764	1.3348	1.3350	1.3673
57458.	173.98	1.0317	1.0648	1.0832	1.1460	1.1908	1.2223	1.2478	1.2716	1.3316	1.3352	1.3563
57464.	173.96	1.0267	1.0602	1.0837	1.1300	1.1897	1.2190	1.2422	1.2692	1.3254	1.3318	1.3487
57471.	173.94	1.0233	1.0565	1.0819	1.1338	1.1822	1.2182	1.2397	1.2670	1.3163	1.3242	1.3492
57478.	173.92	1.0213	1.0558	1.0803	1.1395	1.1720	1.2220	1.2400	1.2646	1.3074	1.3184	1.3509
57484.	173.90	1.0177	1.0572	1.0828	1.1405	1.1710	1.2223	1.2371	1.2607	1.3050	1.3137	1.3476
57491.	173.88	1.0136	1.0579	1.0819	1.1390	1.1634	1.2101	1.2290	1.2532	1.3048	1.3077	1.3402
57497.	173.86	1.0122	1.0546	1.0769	1.1265	1.1558	1.1896	1.2139	1.2431	1.3002	1.2966	1.3295
57504.	173.84	1.0106	1.0465	1.0733	1.1120	1.1584	1.1799	1.2010	1.2366	1.2935	1.2846	1.3229
57511.	173.82	1.0052	1.0375	1.0697	1.1074	1.1584	1.1804	1.2012	1.2366	1.2868	1.2798	1.3188
57517.	173.80	.9986	1.0345	1.0656	1.1130	1.1472	1.1774	1.2045	1.2354	1.2782	1.2783	1.3092
57524.	173.78	.9927	1.0363	1.0632	1.1231	1.1361	1.1777	1.2015	1.2294	1.2701	1.2720	1.3005
57531.	173.76	.9895	1.0375	1.0566	1.1281	1.1310	1.1860	1.1980	1.2233	1.2640	1.2641	1.2966
57537.	173.74	.9911	1.0335	1.0517	1.1312	1.1280	1.1883	1.1934	1.2159	1.2621	1.2599	1.2898
57544.	173.72	.9929	1.0284	1.0523	1.1364	1.1310	1.1827	1.1875	1.2079	1.2621	1.2596	1.2832
57550.	173.70	.9924	1.0245	1.0501	1.1362	1.1290	1.1766	1.1854	1.2072	1.2575	1.2557	1.2829
57557.	173.68	.9927	1.0231	1.0456	1.1229	1.1260	1.1685	1.1872	1.2072	1.2527	1.2441	1.2819
57564.	173.66	.9922	1.0217	1.0435	1.1012	1.1204	1.1597	1.1891	1.2038	1.2529	1.2336	1.2769
57570.	173.64	.9911	1.0178	1.0420	1.0958	1.1179	1.1495	1.1872	1.2014	1.2508	1.2305	1.2750
57577.	173.62	.9868	1.0129	1.0393	1.1103	1.1245	1.1348	1.1741	1.2014	1.2457	1.2307	1.2747
57584.	173.60	.9827	1.0141	1.0359	1.1079	1.1250	1.1277	1.1595	1.1992	1.2427	1.2300	1.2684
57590.	173.58	.9820	1.0206	1.0343	1.0816	1.1234	1.1282	1.1630	1.1958	1.2417	1.2284	1.2602
57597.	173.56	.9818	1.0240	1.0359	1.0643	1.1169	1.1224	1.1708	1.1917	1.2417	1.2255	1.2567
57603.	173.54	.9815	1.0217	1.0390	1.0671	1.1088	1.1168	1.1633	1.1850	1.2430	1.2194	1.2567
57610.	173.52	.9831	1.0210	1.0404	1.0775	1.1098	1.1191	1.1520	1.1826	1.2401	1.2158	1.2556
57617.	173.50	.9824	1.0215	1.0381	1.0749	1.1088	1.1219	1.1455	1.1840	1.2355	1.2176	1.2498
57623.	173.48	.9790	1.0199	1.0341	1.0602	1.1022	1.1237	1.1455	1.1830	1.2355	1.2173	1.2452
57630.	173.46	.9774	1.0162	1.0291	1.0625	1.0900	1.1333	1.1471	1.1799	1.2374	1.2118	1.2482
57637.	173.44	.9781	1.0143	1.0266	1.0707	1.1012	1.1483	1.1477	1.1773	1.2331	1.2053	1.2515
57643.	173.42	.9747	1.0150	1.0266	1.0640	1.1072	1.1642	1.1506	1.1765	1.2277	1.2034	1.2506
57650.	173.40	.9724	1.0136	1.0257	1.0670	1.0916	1.1736	1.1552	1.1758	1.2282	1.2029	1.2526
57657.	173.38	.9745	1.0094	1.0246	1.0857	1.0951	1.1761	1.1571	1.1734	1.2288	1.2008	1.2564
57663.	173.36	.9768	1.0076	1.0273	1.0873	1.1128	1.1723	1.1520	1.1712	1.2277	1.2021	1.2561
57670.	173.34	.9784	1.0111	1.0300	1.0620	1.0997	1.1508	1.1444	1.1707	1.2307	1.2066	1.2528
57677.	173.32	.9793	1.0148	1.0264	1.0503	1.0986	1.1265	1.1415	1.1727	1.2368	1.2071	1.2471
57683.	173.30	.9784	1.0131	1.0221	1.0591	1.1078	1.1232	1.1434	1.1756	1.2355	1.2050	1.2476
57690.	173.28	.9754	1.0085	1.0244	1.0586	1.1113	1.1348	1.1469	1.1780	1.2290	1.2084	1.2520
57697.	173.26	.9706	1.0053	1.0255	1.0593	1.0971	1.1371	1.1506	1.1782	1.2290	1.2126	1.2468
57703.	173.24	.9659	.9999	1.0187	1.0718	1.0941	1.1310	1.1504	1.1768	1.2360	1.2113	1.2400
57710.	173.22	.9656	.9972	1.0147	1.0888	1.0941	1.1338	1.1407	1.1712	1.2384	1.2068	1.2400
57717.	173.20	.9706	.9988	1.0196	1.1087	1.0951	1.1376	1.1304	1.1662	1.2331	1.2053	1.2389
57723.	173.18	.9763	.9972	1.0237	1.1211	1.0941	1.1280	1.1286	1.1715	1.2296	1.2113	1.2386
57730.	173.16	.9781	.9960	1.0190	1.1078	1.0966	1.1161	1.1280	1.1802	1.2339	1.2184	1.2413
57737.	173.14	.9777	1.0002	1.0118	1.0750	1.0809	1.1133	1.1307	1.1806	1.2390	1.2200	1.2435
57743.	173.12	.9788	1.0046	1.0120	1.0470	1.0830	1.1259	1.1409	1.1780	1.2401	1.2200	1.2490
57750.	173.10	.9804	1.0062	1.0174	1.0420	1.0956	1.1406	1.1469	1.1768	1.2398	1.2210	1.2547
57757.	173.08	.9781	1.0057	1.0156	1.0557	1.1002	1.1346	1.1444	1.1787	1.2384	1.2160	1.2567
57763.	173.06	.9734	1.0080	1.0106	1.0703	1.1017	1.1166	1.1501	1.1816	1.2384	1.2045	1.2610
57770.	173.04	.9724	1.0090	1.0111	1.0814	1.1113	1.1041	1.1590	1.1845	1.2441	1.2042	1.2654
57777.	173.02	.9745	1.0046	1.0140	1.0846	1.1002	1.1072	1.1582	1.1937	1.2462	1.2171	1.2635
57783.	173.00	.9747	1.0004	1.0160	1.0742	1.0865	1.1138	1.1523	1.2009	1.2414	1.2213	1.2630

WAVENUMBER CM-1	WAVELENGTH NM	CROSS SECTION X E19 CM-2 , TEMPERATURE DEG. K 151.	182.	196.	223.	247.	268.	301.	333.	372.	423.	485.
57783.	173.00	.9747	1.0004	1.0160	1.0742	1.0865	1.1138	1.1523	1.2009	1.2414	1.2213	1.2630
57790.	172.98	.9749	.9985	1.0165	1.0787	1.0880	1.1133	1.1426	1.1999	1.2371	1.2184	1.2662
57797.	172.96	.9754	1.0013	1.0140	1.1035	1.0875	1.1178	1.1364	1.1995	1.2355	1.2210	1.2630
57803.	172.94	.9738	1.0034	1.0118	1.1020	1.0860	1.1226	1.1423	1.1956	1.2360	1.2278	1.2589
57810.	172.92	.9752	1.0062	1.0140	1.0853	1.1103	1.1143	1.1471	1.1917	1.2401	1.2357	1.2665
57817.	172.90	.9764	1.0134	1.0187	1.0797	1.0941	1.0945	1.1436	1.2033	1.2470	1.2457	1.2769
57823.	172.88	.9806	1.0150	1.0201	1.0756	1.0926	1.0925	1.1350	1.2188	1.2527	1.2515	1.2758
57830.	172.86	.9843	1.0080	1.0192	1.0779	1.1052	1.1054	1.1415	1.2173	1.2548	1.2468	1.2731
57837.	172.84	.9888	1.0013	1.0185	1.0955	1.1067	1.1097	1.1881	1.2064	1.2554	1.2441	1.2742
57843.	172.82	.9872	1.0011	1.0205	1.1211	1.1062	1.1115	1.2306	1.2021	1.2567	1.2520	1.2723
57850.	172.80	.9799	1.0064	1.0239	1.1371	1.1250	1.1110	1.2136	1.2043	1.2583	1.2588	1.2714
57857.	172.78	.9747	1.0092	1.0248	1.1224	1.1285	1.1112	1.1735	1.2036	1.2621	1.2515	1.2695
57864.	172.76	.9702	1.0078	1.0235	1.1105	1.1159	1.1171	1.1512	1.1987	1.2613	1.2405	1.2649
57870.	172.74	.9638	1.0029	1.0226	1.1307	1.1007	1.1171	1.1385	1.1975	1.2562	1.2428	1.2668
57877.	172.72	.9606	.9983	1.0208	1.1385	1.0951	1.0955	1.1210	1.2021	1.2505	1.2491	1.2684
57884.	172.70	.9595	.9921	1.0151	1.1458	1.0845	1.0649	1.1148	1.2016	1.2411	1.2531	1.2635
57890.	172.68	.9581	.9802	1.0061	1.1652	1.0951	1.0527	1.1218	1.1903	1.2307	1.2531	1.2526
57897.	172.66	.9552	.9742	1.0032	1.1507	1.0911	1.0436	1.1159	1.1809	1.2269	1.2431	1.2320
57904.	172.64	.9490	.9779	1.0041	1.1124	1.0789	1.0228	1.1173	1.1867	1.2266	1.2281	1.2112
57910.	172.62	.9425	.9793	1.0014	1.0864	1.0657	1.0276	1.1304	1.1876	1.2223	1.2160	1.2041
57917.	172.60	.9409	.9749	.9989	1.1031	1.0602	1.0755	1.1216	1.1676	1.2170	1.2071	1.2085
57924.	172.58	.9429	.9682	.9937	1.1561	1.0774	1.1201	1.1132	1.1577	1.2070	1.2076	1.2087
57931.	172.56	.9450	.9591	.9845	1.1722	1.0824	1.1318	1.1318	1.1681	1.1955	1.2116	1.2068
57937.	172.54	.9440	.9561	.9786	1.1318	1.0516	1.1199	1.1393	1.1693	1.1898	1.1977	1.2033
57944.	172.52	.9377	.9584	.9737	1.0873	1.0511	1.0907	1.1113	1.1599	1.1869	1.1777	1.1885
57951.	172.50	.9286	.9531	.9680	1.0815	1.0445	1.0768	1.0882	1.1534	1.1853	1.1772	1.1748
57957.	172.48	.9222	.9450	.9701	1.0907	1.0460	1.0915	1.0933	1.1541	1.1869	1.1835	1.1709
57964.	172.46	.9195	.9443	.9707	1.0679	1.0420	1.1034	1.0847	1.1577	1.1853	1.1879	1.1652
57971.	172.44	.9200	.9473	.9631	1.0634	1.0490	1.1001	1.0664	1.1493	1.1794	1.1900	1.1529
57978.	172.42	.9252	.9510	.9597	1.1202	1.0425	1.0806	1.0736	1.1324	1.1770	1.1745	1.1362
57984.	172.40	.9302	.9584	.9586	1.1744	1.0455	1.0471	1.0755	1.1264	1.1751	1.1493	1.1301
57991.	172.38	.9327	.9652	.9572	1.1724	1.0485	1.0377	1.0465	1.1348	1.1678	1.1362	1.1392
57998.	172.36	.9331	.9635	.9581	1.1349	1.0384	1.0654	1.0085	1.1457	1.1641	1.1360	1.1422
58005.	172.34	.9331	.9622	.9592	1.0941	1.0242	1.0613	.9899	1.1459	1.1681	1.1425	1.1236
58011.	172.32	.9347	.9649	.9615	1.0522	1.0323	1.0023	.9996	1.1437	1.1711	1.1512	1.1080
58018.	172.30	.9311	.9603	.9604	1.0348	1.0389	.9607	1.0085	1.1454	1.1686	1.1517	1.1063
58025.	172.28	.9236	.9517	.9574	1.0728	1.0349	.9906	1.0053	1.1430	1.1600	1.1520	1.1036
58031.	172.26	.9229	.9478	.9552	1.1093	1.0258	1.0507	1.0117	1.1379	1.1477	1.1567	1.0962
58038.	172.24	.9279	.9429	.9529	1.0870	1.0131	1.0649	1.0139	1.1394	1.1388	1.1449	1.0825
58045.	172.22	.9300	.9360	.9504	1.0936	1.0455	1.0367	.9894	1.1396	1.1388	1.1262	1.0606
58052.	172.20	.9311	.9415	.9516	1.1320	1.0511	1.0091	.9724	1.1317	1.1380	1.1241	1.0527
58058.	172.18	.9327	.9550	.9549	1.1140	1.0086	.9972	.9862	1.1237	1.1302	1.1247	1.0735
58065.	172.16	.9322	.9547	.9540	1.0889	.9964	1.0093	1.0002	1.1218	1.1335	1.1173	1.0954
58072.	172.14	.9295	.9503	.9480	1.0883	1.0328	1.0157	.9829	1.1319	1.1488	1.1136	1.0981
58079.	172.12	.9293	.9547	.9428	1.0608	1.0369	.9878	.9894	1.1348	1.1512	1.1186	1.0880
58085.	172.10	.9286	.9508	.9435	1.0015	1.0222	.9609	1.0330	1.1206	1.1431	1.1226	1.0751
58092.	172.08	.9256	.9422	.9459	.9702	.9893	.9584	1.0220	1.1155	1.1378	1.1194	1.0609
58099.	172.06	.9263	.9501	.9491	1.0041	.9807	.9642	.9805	1.1273	1.1445	1.1231	1.0546
58106.	172.04	.9284	.9566	.9513	1.0581	1.0136	.9521	.9781	1.1432	1.1541	1.1318	1.0652
58112.	172.02	.9263	.9478	.9471	1.0726	1.0086	.9371	1.0090	1.1440	1.1463	1.1283	1.0710

2. Cross Sections of First Order and Second Order Deconvolutions, 190-172 nm.

WAVENUMBER CM-1	WAVELENGTH NM	CROSS SECTION X E19, CM-2 FIRST ORDER (000)	(010)	SECOND ORDER (000)	(010)	(020)
52619.	189.98	.8425	4.0464	.8452	3.6497	2.8067
52624.	189.96	.8397	4.1100	.8423	3.7366	2.6419
52630.	189.94	.8410	4.1298	.8436	3.7562	2.6433
52635.	189.92	.8419	4.1564	.8445	3.7877	2.6084
52641.	189.90	.8431	4.1793	.8457	3.8153	2.5761
52646.	189.88	.8433	4.2051	.8458	3.8483	2.5246
52652.	189.86	.8433	4.2290	.8458	3.8802	2.4676
52658.	189.84	.8445	4.2359	.8470	3.8862	2.4747
52663.	189.82	.8461	4.2386	.8486	3.8878	2.4818
52669.	189.80	.8470	4.2420	.8494	3.8949	2.4556
52674.	189.78	.8481	4.2385	.8505	3.8929	2.4455
52680.	189.76	.8493	4.2327	.8517	3.8906	2.4208
52685.	189.74	.8503	4.2260	.8527	3.8887	2.3865
52691.	189.72	.8515	4.2170	.8538	3.8826	2.3666
52696.	189.70	.8525	4.2086	.8548	3.8779	2.3401
52702.	189.68	.8532	4.2102	.8554	3.8896	2.2683
52707.	189.66	.8543	4.2060	.8565	3.8900	2.2355
52713.	189.64	.8558	4.1894	.8581	3.8662	2.2870
52719.	189.62	.8561	4.1818	.8584	3.8554	2.3093
52724.	189.60	.8559	4.1815	.8582	3.8546	2.3135
52730.	189.58	.8561	4.1818	.8584	3.8563	2.3027
52735.	189.56	.8563	4.1867	.8585	3.8694	2.2457
52741.	189.54	.8562	4.1939	.8584	3.8850	2.1854
52746.	189.52	.8574	4.1881	.8596	3.8796	2.1830
52752.	189.50	.8593	4.1776	.8615	3.8635	2.2227
52758.	189.48	.8612	4.1710	.8634	3.8551	2.2357
52763.	189.46	.8633	4.1727	.8655	3.8608	2.2071
52769.	189.44	.8649	4.1666	.8671	3.8518	2.2269
52774.	189.42	.8673	4.1542	.8695	3.8337	2.2681
52780.	189.40	.8694	4.1535	.8716	3.8369	2.2404
52785.	189.38	.8712	4.1549	.8734	3.8439	2.2003
52791.	189.36	.8731	4.1483	.8752	3.8373	2.2000
52797.	189.34	.8742	4.1472	.8763	3.8419	2.1602
52802.	189.32	.8754	4.1462	.8775	3.8472	2.1161
52808.	189.30	.8763	4.1441	.8784	3.8489	2.0889
52813.	189.28	.8765	4.1388	.8786	3.8437	2.0882
52819.	189.26	.8761	4.1327	.8781	3.8391	2.0776
52824.	189.24	.8764	4.1267	.8785	3.8336	2.0744
52830.	189.22	.8778	4.1164	.8799	3.8230	2.0760
52836.	189.20	.8788	4.1048	.8809	3.8110	2.0789
52841.	189.18	.8789	4.0985	.8809	3.8046	2.0797
52847.	189.16	.8801	4.0905	.8822	3.7949	2.0914
52852.	189.14	.8818	4.0876	.8838	3.7943	2.0754
52858.	189.12	.8836	4.0794	.8857	3.7850	2.0831
52864.	189.10	.8851	4.0755	.8871	3.7822	2.0752
52869.	189.08	.8866	4.0749	.8887	3.7799	2.0871
52875.	189.06	.8879	4.0829	.8900	3.7906	2.0683
52880.	189.04	.8899	4.0884	.8919	3.7988	2.0485
52886.	189.02	.8911	4.0921	.8931	3.8053	2.0294
52892.	189.00	.8924	4.0905	.8944	3.8043	2.0250

WAVENUMBER CM-1	WAVELENGTH NM	CROSS SECTION X E19, CM-2 FIRST ORDER (000)	(010)	SECOND ORDER (000)	(010)	(020)
52897.	188.98	.8946	4.0843	.8966	3.7955	2.0429
52903.	188.96	.8969	4.0783	.8990	3.7860	2.0678
52908.	188.94	.8982	4.0806	.9003	3.7899	2.0568
52914.	188.92	.8994	4.0820	.9015	3.7933	2.0429
52920.	188.90	.9005	4.0825	.9026	3.7930	2.0484
52925.	188.88	.9021	4.0851	.9041	3.7974	2.0356
52931.	188.86	.9035	4.0891	.9055	3.8038	2.0190
52936.	188.84	.9053	4.0881	.9073	3.8039	2.0108
52942.	188.82	.9062	4.0915	.9082	3.8085	2.0024
52948.	188.80	.9071	4.0973	.9091	3.8134	2.0086
52953.	188.78	.9069	4.1147	.9089	3.8319	2.0009
52959.	188.76	.9078	4.1252	.9097	3.8433	1.9943
52964.	188.74	.9098	4.1275	.9117	3.8462	1.9905
52970.	188.72	.9117	4.1313	.9136	3.8527	1.9719
52976.	188.70	.9129	4.1400	.9148	3.8639	1.9534
52981.	188.68	.9137	4.1529	.9156	3.8803	1.9282
52987.	188.66	.9146	4.1618	.9165	3.8907	1.9185
52992.	188.64	.9155	4.1637	.9174	3.8888	1.9447
52998.	188.62	.9172	4.1489	.9191	3.8679	1.9884
53004.	188.60	.9189	4.1366	.9209	3.8517	2.0158
53009.	188.58	.9198	4.1400	.9217	3.8585	1.9918
53015.	188.56	.9201	4.1556	.9221	3.8787	1.9590
53021.	188.54	.9215	4.1651	.9234	3.8886	1.9566
53026.	188.52	.9227	4.1817	.9246	3.9058	1.9516
53032.	188.50	.9239	4.2022	.9258	3.9293	1.9313
53037.	188.48	.9247	4.2246	.9266	3.9551	1.9071
53043.	188.46	.9254	4.2454	.9273	3.9778	1.8932
53049.	188.44	.9271	4.2657	.9290	3.9975	1.8974
53054.	188.42	.9285	4.2897	.9304	4.0257	1.8680
53060.	188.40	.9298	4.3126	.9316	4.0532	1.8357
53066.	188.38	.9305	4.3326	.9323	4.0784	1.7991
53071.	188.36	.9312	4.3613	.9329	4.1165	1.7319
53077.	188.34	.9325	4.3843	.9342	4.1441	1.6996
53083.	188.32	.9344	4.3937	.9361	4.1531	1.7021
53088.	188.30	.9355	4.3997	.9371	4.1633	1.6731
53094.	188.28	.9364	4.3992	.9380	4.1636	1.6668
53099.	188.26	.9371	4.3984	.9387	4.1638	1.6602
53105.	188.24	.9393	4.3875	.9410	4.1494	1.6843
53111.	188.22	.9410	4.3807	.9426	4.1411	1.6948
53116.	188.20	.9421	4.3772	.9438	4.1391	1.6848
53122.	188.18	.9430	4.3767	.9447	4.1410	1.6673
53128.	188.16	.9437	4.3783	.9454	4.1418	1.6732
53133.	188.14	.9446	4.3793	.9463	4.1411	1.6856
53139.	188.12	.9460	4.3762	.9477	4.1372	1.6915
53145.	188.10	.9483	4.3709	.9500	4.1327	1.6856
53150.	188.08	.9499	4.3673	.9516	4.1314	1.6691
53156.	188.06	.9508	4.3651	.9525	4.1281	1.6775
53162.	188.04	.9515	4.3683	.9532	4.1350	1.6510
53167.	188.02	.9522	4.3707	.9538	4.1387	1.6418
53173.	188.00	.9533	4.3712	.9550	4.1384	1.6473

WAVENUMBER CM-1	WAVELENGTH NM	CROSS SECTION X E19, CM-2 FIRST ORDER (000)	(010)	SECOND ORDER (000)	(010)	(020)
53179.	187.98	.9545	4.3687	.9562	4.1331	1.6667
53184.	187.96	.9559	4.3678	.9575	4.1353	1.6450
53190.	187.94	.9571	4.3692	.9586	4.1437	1.5956
53196.	187.92	.9580	4.3711	.9595	4.1497	1.5662
53201.	187.90	.9586	4.3702	.9601	4.1485	1.5684
53207.	187.88	.9591	4.3692	.9606	4.1469	1.5726
53213.	187.86	.9608	4.3584	.9623	4.1353	1.5786
53218.	187.84	.9620	4.3416	.9636	4.1156	1.5986
53224.	187.82	.9628	4.3329	.9643	4.1108	1.5719
53230.	187.80	.9633	4.3256	.9649	4.1071	1.5458
53235.	187.78	.9634	4.3201	.9649	4.1030	1.5359
53241.	187.76	.9631	4.3181	.9646	4.1041	1.5146
53247.	187.74	.9630	4.3260	.9644	4.1245	1.4258
53252.	187.72	.9634	4.3216	.9647	4.1280	1.3702
53258.	187.70	.9646	4.3032	.9660	4.1037	1.4114
53264.	187.68	.9663	4.2845	.9678	4.0761	1.4751
53269.	187.66	.9678	4.2830	.9692	4.0780	1.4508
53275.	187.64	.9691	4.2782	.9705	4.0803	1.4001
53281.	187.62	.9711	4.2598	.9725	4.0604	1.4108
53286.	187.60	.9725	4.2504	.9739	4.0513	1.4086
53292.	187.58	.9744	4.2462	.9758	4.0472	1.4075
53298.	187.56	.9762	4.2475	.9776	4.0489	1.4051
53303.	187.54	.9778	4.2517	.9791	4.0561	1.3843
53309.	187.52	.9787	4.2536	.9800	4.0602	1.3683
53315.	187.50	.9796	4.2475	.9810	4.0501	1.3966
53320.	187.48	.9799	4.2471	.9813	4.0491	1.4010
53326.	187.46	.9796	4.2530	.9809	4.0587	1.3753
53332.	187.44	.9793	4.2599	.9806	4.0709	1.3369
53337.	187.42	.9795	4.2664	.9808	4.0842	1.2898
53343.	187.40	.9800	4.2686	.9812	4.0864	1.2892
53349.	187.38	.9818	4.2589	.9832	4.0701	1.3360
53355.	187.36	.9840	4.2519	.9853	4.0625	1.3401
53360.	187.34	.9858	4.2587	.9870	4.0805	1.2610
53366.	187.32	.9876	4.2624	.9888	4.0881	1.2334
53372.	187.30	.9901	4.2566	.9914	4.0791	1.2563
53377.	187.28	.9922	4.2511	.9934	4.0737	1.2546
53383.	187.26	.9928	4.2558	.9940	4.0878	1.1890
53389.	187.24	.9933	4.2635	.9944	4.1064	1.1116
53394.	187.22	.9935	4.2645	.9946	4.1120	1.0790
53400.	187.20	.9943	4.2504	.9954	4.0908	1.1291
53406.	187.18	.9960	4.2317	.9972	4.0612	1.2061
53412.	187.16	.9972	4.2243	.9984	4.0502	1.2315
53417.	187.14	.9981	4.2238	.9993	4.0484	1.2408
53423.	187.12	.9995	4.2222	1.0008	4.0462	1.2454
53429.	187.10	1.0007	4.2148	1.0020	4.0343	1.2774
53434.	187.08	1.0016	4.2198	1.0028	4.0438	1.2454
53440.	187.06	1.0028	4.2197	1.0040	4.0451	1.2351
53446.	187.04	1.0039	4.2162	1.0052	4.0355	1.2784
53452.	187.02	1.0044	4.2144	1.0057	4.0266	1.3288
53457.	187.00	1.0048	4.2236	1.0061	4.0381	1.3122

WAVENUMBER CM-1	WAVELENGTH NM	CROSS SECTION X E19, CM-2 FIRST ORDER (000)	(010)	SECOND ORDER (000)	(010)	(020)
53463.	186.98	1.0056	4.2310	1.0069	4.0492	1.2860
53469.	186.96	1.0065	4.2360	1.0078	4.0562	1.2718
53474.	186.94	1.0080	4.2265	1.0093	4.0396	1.3229
53480.	186.92	1.0089	4.2205	1.0103	4.0276	1.3645
53486.	186.90	1.0100	4.2249	1.0114	4.0307	1.3746
53492.	186.88	1.0112	4.2303	1.0125	4.0345	1.3852
53497.	186.86	1.0120	4.2408	1.0133	4.0494	1.3542
53503.	186.84	1.0128	4.2482	1.0142	4.0595	1.3347
53509.	186.82	1.0137	4.2571	1.0150	4.0717	1.3117
53514.	186.80	1.0131	4.2684	1.0144	4.0806	1.3289
53520.	186.78	1.0130	4.2818	1.0143	4.0923	1.3412
53526.	186.76	1.0134	4.2934	1.0148	4.1038	1.3416
53532.	186.74	1.0135	4.3134	1.0148	4.1306	1.2933
53537.	186.72	1.0141	4.3198	1.0154	4.1370	1.2931
53543.	186.70	1.0150	4.3232	1.0163	4.1372	1.3157
53549.	186.68	1.0166	4.3298	1.0179	4.1406	1.3385
53555.	186.66	1.0178	4.3527	1.0191	4.1691	1.2995
53560.	186.64	1.0202	4.3707	1.0215	4.1906	1.2740
53566.	186.62	1.0233	4.3759	1.0246	4.1913	1.3060
53572.	186.60	1.0272	4.3781	1.0286	4.1869	1.3523
53578.	186.58	1.0307	4.3941	1.0320	4.2048	1.3399
53583.	186.56	1.0347	4.4179	1.0359	4.2377	1.2744
53589.	186.54	1.0383	4.4317	1.0395	4.2547	1.2519
53595.	186.52	1.0407	4.4472	1.0419	4.2728	1.2338
53601.	186.50	1.0409	4.4824	1.0420	4.3236	1 1234
53606.	186.48	1.0402	4.5175	1.0412	4.3760	1.0013
53612.	186.46	1.0396	4.5343	1.0405	4.4012	.9418
53618.	186.44	1.0398	4.5345	1.0407	4.3995	.9554
53624.	186.42	1.0403	4.5256	1.0413	4.3844	.9995
53629.	186.40	1.0397	4.5224	1.0407	4.3790	1.0149
53635.	186.38	1.0382	4.5319	1.0391	4.3966	.9571
53641.	186.36	1.0378	4.5345	1.0387	4.4029	.9317
53647.	186.34	1.0378	4.5235	1.0388	4.3883	.9564
53652.	186.32	1.0383	4.5113	1.0393	4.3762	.9563
53658.	186.30	1.0384	4.5018	1.0393	4.3709	.9264
53664.	186.28	1.0385	4.4939	1.0393	4.3731	.8552
53670.	186.26	1.0386	4.4766	1.0394	4.3603	.8229
53675.	186.24	1.0393	4.4464	1.0402	4.3234	.8702
53681.	186.22	1.0400	4.4185	1.0409	4.2871	.9300
53687.	186.20	1.0415	4.3924	1.0425	4.2564	.9624
53693.	186.18	1.0421	4.3835	1.0430	4.2541	.9155
53698.	186.16	1.0421	4.3875	1.0429	4.2688	.8400
53704.	186.14	1.0425	4.3792	1.0433	4.2630	.8222
53710.	186.12	1.0433	4.3651	1.0442	4.2446	.8523
53716.	186.10	1.0445	4.3577	1.0453	4.2386	.8421
53722.	186.08	1.0452	4.3530	1.0460	4.2361	.8266
53727.	186.06	1.0469	4.3398	1.0478	4.2230	.8268
53733.	186.04	1.0484	4.3288	1.0493	4.2090	.8482
53739.	186.02	1.0484	4.3344	1.0492	4.2200	.8091
53745.	186.00	1.0484	4.3383	1.0491	4.2337	.7403

WAVENUMBER CM-1	WAVELENGTH NM	CROSS SECTION X E19, CM-2 FIRST ORDER (000)	(010)	SECOND ORDER (000)	(010)	(020)
53750.	185.98	1.0492	4.3241	1.0499	4.2203	.7349
53756.	185.96	1.0504	4.3049	1.0512	4.1984	.7534
53762.	185.94	1.0514	4.2957	1.0522	4.1861	.7754
53768.	185.92	1.0519	4.2978	1.0526	4.1927	.7437
53774.	185.90	1.0537	4.2968	1.0544	4.1982	.6978
53779.	185.88	1.0565	4.2865	1.0572	4.1878	.6983
53785.	185.86	1.0593	4.2683	1.0601	4.1649	.7319
53791.	185.84	1.0620	4.2531	1.0627	4.1484	.7405
53797.	185.82	1.0651	4.2408	1.0658	4.1372	.7334
53802.	185.80	1.0677	4.2319	1.0684	4.1290	.7279
53808.	185.78	1.0702	4.2246	1.0709	4.1233	.7166
53814.	185.76	1.0720	4.2259	1.0727	4.1318	.6653
53820.	185.74	1.0736	4.2317	1.0742	4.1436	.6232
53826.	185.72	1.0747	4.2306	1.0753	4.1431	.6190
53831.	185.70	1.0747	4.2306	1.0753	4.1456	.6012
53837.	185.68	1.0740	4.2353	1.0745	4.1566	.5568
53843.	185.66	1.0740	4.2274	1.0746	4.1481	.5611
53849.	185.64	1.0751	4.2095	1.0757	4.1228	.6136
53855.	185.62	1.0764	4.1920	1.0771	4.0981	.6643
53860.	185.60	1.0778	4.1872	1.0784	4.0898	.6891
53866.	185.58	1.0797	4.1839	1.0804	4.0831	.7131
53872.	185.56	1.0803	4.1917	1.0810	4.0918	.7069
53878.	185.54	1.0798	4.2038	1.0804	4.1083	.6759
53884.	185.52	1.0795	4.2068	1.0802	4.1104	.6819
53889.	185.50	1.0802	4.2051	1.0808	4.1060	.7014
53895.	185.48	1.0811	4.2110	1.0818	4.1157	.6744
53901.	185.46	1.0817	4.2188	1.0823	4.1253	.6616
53907.	185.44	1.0829	4.2123	1.0836	4.1098	.7254
53913.	185.42	1.0834	4.2080	1.0841	4.0980	.7788
53919.	185.40	1.0831	4.2149	1.0839	4.1059	.7715
53924.	185.38	1.0832	4.2254	1.0840	4.1193	.7511
53930.	185.36	1.0844	4.2268	1.0852	4.1164	.7816
53936.	185.34	1.0848	4.2336	1.0856	4.1219	.7903
53942.	185.32	1.0859	4.2445	1.0867	4.1381	.7531
53948.	185.30	1.0873	4.2549	1.0880	4.1547	.7091
53953.	185.28	1.0892	4.2650	1.0899	4.1685	.6831
53959.	185.26	1.0894	4.2876	1.0900	4.2002	.6187
53965.	185.24	1.0891	4.3095	1.0896	4.2372	.5112
53971.	185.22	1.0898	4.3032	1.0903	4.2323	.5014
53977.	185.20	1.0909	4.2821	1.0914	4.2016	.5699
53983.	185.18	1.0921	4.2653	1.0927	4.1731	.6520
53988.	185.16	1.0934	4.2588	1.0941	4.1586	.7091
53994.	185.14	1.0937	4.2640	1.0945	4.1580	.7502
54000.	185.12	1.0946	4.2745	1.0953	4.1650	.7747
54006.	185.10	1.0957	4.2878	1.0965	4.1758	.7922
54012.	185.08	1.0963	4.3196	1.0971	4.2166	.7291
54018.	185.06	1.0967	4.3558	1.0974	4.2586	.6883
54023.	185.04	1.0973	4.3932	1.0980	4.2994	.6640
54029.	185.02	1.0967	4.4538	1.0972	4.3804	.5190
54035.	185.00	1.0951	4.5180	1.0954	4.4694	.3443

WAVENUMBER CM-1	WAVELENGTH NM	CROSS SECTION X E19, CM-2 FIRST ORDER (000)	(010)	SECOND ORDER (000)	(010)	(020)
54041.	184.98	1.0934	4.5622	1.0936	4.5248	.2645
54047.	184.96	1.0930	4.5785	1.0933	4.5380	.2871
54053.	184.94	1.0935	4.5886	1.0938	4.5465	.2977
54059.	184.92	1.0938	4.5993	1.0941	4.5598	.2798
54064.	184.90	1.0937	4.6072	1.0940	4.5717	.2511
54070.	184.88	1.0944	4.6057	1.0947	4.5756	.2129
54076.	184.86	1.0949	4.6014	1.0951	4.5716	.2107
54082.	184.84	1.0957	4.5912	1.0959	4.5556	.2520
54088.	184.82	1.0969	4.5807	1.0972	4.5446	.2557
54094.	184.80	1.0983	4.5704	1.0986	4.5391	.2218
54099.	184.78	1.1006	4.5507	1.1008	4.5167	.2409
54105.	184.76	1.1030	4.5296	1.1032	4.4930	.2591
54111.	184.74	1.1047	4.5189	1.1049	4.4874	.2230
54117.	184.72	1.1061	4.5134	1.1063	4.4888	.1742
54123.	184.70	1.1078	4.5011	1.1080	4.4770	.1705
54129.	184.68	1.1093	4.4789	1.1095	4.4511	.1963
54135.	184.66	1.1097	4.4674	1.1098	4.4415	.1832
54140.	184.64	1.1090	4.4642	1.1091	4.4440	.1431
54146.	184.62	1.1090	4.4587	1.1091	4.4414	.1221
54152.	184.60	1.1094	4.4560	1.1095	4.4461	.0698
54158.	184.58	1.1102	4.4473	1.1102	4.4450	.0164
54164.	184.56	1.1111	4.4237	1.1112	4.4135	.0721
54170.	184.54	1.1118	4.3990	1.1119	4.3810	.1270
54176.	184.52	1.1120	4.3905	1.1121	4.3773	.0934
54182.	184.50	1.1128	4.3803	1.1129	4.3716	.0613
54187.	184.48	1.1131	4.3671	1.1132	4.3595	.0538
54193.	184.46	1.1141	4.3500	1.1142	4.3409	.0646
54199.	184.44	1.1149	4.3374	1.1150	4.3277	.0689
54205.	184.42	1.1157	4.3272	1.1158	4.3176	.0679
54211.	184.40	1.1165	4.3146	1.1166	4.3043	.0723
54217.	184.38	1.1168	4.3077	1.1168	4.2990	.0618
54223.	184.36	1.1176	4.2974	1.1176	4.2898	.0541
54229.	184.34	1.1182	4.2934	1.1182	4.2901	.0234
54234.	184.32	1.1197	4.2816	1.1197	4.2773	.0309
54240.	184.30	1.1212	4.2667	1.1213	4.2552	.0810
54246.	184.28	1.1222	4.2590	1.1223	4.2440	.1062
54252.	184.26	1.1216	4.2640	1.1217	4.2515	.0887
54258	184.24	1.1206	4.2740	1.1207	4.2686	.0383
54264.	184.22	1.1202	4.2862	1.1202	4.2862	0.
54270.	184.20	1.1202	4.2822	1.1202	4.2822	0.
54276.	184.18	1.1208	4.2590	1.1208	4.2573	.0118
54282.	184.16	1.1215	4.2304	1.1216	4.2121	.1289
54288.	184.14	1.1221	4.2224	1.1223	4.1988	.1669
54293.	184.12	1.1228	4.2271	1.1230	4.2050	.1569
54299.	184.10	1.1237	4.2250	1.1239	4.2007	.1719
54305.	184.08	1.1259	4.2133	1.1262	4.1806	.2310
54311.	184.06	1.1270	4.2193	1.1272	4.1907	.2020
54317.	184.04	1.1264	4.2441	1.1265	4.2289	.1072
54323.	184.02	1.1255	4.2685	1.1256	4.2634	.0364
54329.	184.00	1.1259	4.2785	1.1259	4.2744	.0292

WAVENUMBER CM-1	WAVELENGTH NM	CROSS SECTION X E19, CM-2 FIRST ORDER (000)	(010)	SECOND ORDER (000)	(010)	(020)
54335.	183.98	1.1270	4.2838	1.1271	4.2801	.0265
54341.	183.96	1.1290	4.2878	1.1290	4.2847	.0213
54347.	183.94	1.1313	4.2857	1.1314	4.2845	.0085
54352.	183.92	1.1337	4.2781	1.1338	4.2720	.0436
54358.	183.90	1.1367	4.2720	1.1368	4.2617	.0733
54364.	183.88	1.1392	4.2679	1.1393	4.2588	.0639
54370.	183.86	1.1404	4.2716	1.1404	4.2697	.0136
54376.	183.84	1.1413	4.2766	1.1413	4.2766	0.
54382.	183.82	1.1429	4.2817	1.1429	4.2817	0.
54388.	183.80	1.1442	4.2729	1.1442	4.2729	0.
54394.	183.78	1.1443	4.2690	1.1443	4.2690	0.
54400.	183.76	1.1443	4.2611	1.1443	4.2611	0.
54406.	183.74	1.1449	4.2538	1.1449	4.2507	.0220
54412.	183.72	1.1453	4.2511	1.1453	4.2453	.0407
54418.	183.70	1.1460	4.2503	1.1460	4.2503	0.
54423.	183.68	1.1469	4.2498	1.1469	4.2498	0.
54429.	183.66	1.1470	4.2603	1.1470	4.2603	0.
54435.	183.64	1.1466	4.2669	1.1466	4.2669	0.
54441.	183.62	1.1468	4.2593	1.1468	4.2593	0.
54447.	183.60	1.1469	4.2482	1.1470	4.2409	.0514
54453.	183.58	1.1458	4.2517	1.1459	4.2386	.0925
54459.	183.56	1.1439	4.2677	1.1439	4.2607	.0494
54465.	183.54	1.1429	4.2817	1.1429	4.2809	.0057
54471.	183.52	1.1418	4.2884	1.1418	4.2862	.0156
54477.	183.50	1.1406	4.2974	1.1407	4.2930	.0311
54483.	183.48	1.1399	4.3037	1.1399	4.2957	.0564
54489.	183.46	1.1389	4.3121	1.1390	4.2985	.0962
54495.	183.44	1.1375	4.3264	1.1376	4.3117	.1035
54501.	183.42	1.1354	4.3510	1.1354	4.3440	.0497
54507.	183.40	1.1343	4.3736	1.1343	4.3730	.0044
54512.	183.38	1.1338	4.3897	1.1338	4.3888	.0067
54518.	183.36	1.1341	4.4005	1.1342	4.3951	.0377
54524.	183.34	1.1357	4.4086	1.1357	4.4037	.0347
54530.	183.32	1.1390	4.4166	1.1390	4.4166	0.
54536.	183.30	1.1439	4.4111	1.1439	4.4089	.0156
54542.	183.28	1.1488	4.4017	1.1489	4.3935	.0581
54548.	183.26	1.1527	4.4007	1.1527	4.3953	.0381
54554.	183.24	1.1558	4.4091	1.1558	4.4091	0.
54560.	183.22	1.1592	4.4092	1.1592	4.4092	0.
54566.	183.20	1.1620	4.4044	1.1620	4.4044	0.
54572.	183.18	1.1643	4.4063	1.1643	4.4063	0.
54578.	183.16	1.1659	4.4106	1.1659	4.4106	0.
54584.	183.14	1.1649	4.4229	1.1649	4.4229	0.
54590.	183.12	1.1630	4.4311	1.1630	4.4311	0.
54596.	183.10	1.1626	4.4155	1.1626	4.4155	0.
54602.	183.08	1.1628	4.3926	1.1628	4.3926	0.
54608.	183.06	1.1616	4.3761	1.1616	4.3761	0.
54614.	183.04	1.1588	4.3720	1.1588	4.3720	0.
54620.	183.02	1.1572	4.3733	1.1572	4.3733	0.
54626.	183.00	1.1568	4.3665	1.1568	4.3665	0.

WAVENUMBER CM-1	WAVELENGTH NM	CROSS SECTION X E19, CM-2 FIRST ORDER (000)	(010)	SECOND ORDER (000)	(010)	(020)
54632.	182.98	1.1563	4.3483	1.1563	4.3483	0.
54638.	182.96	1.1561	4.3147	1.1561	4.3147	0.
54644.	182.94	1.1551	4.2833	1.1551	4.2833	0.
54650.	182.92	1.1551	4.2562	1.1551	4.2562	0.
54656.	182.90	1.1557	4.2377	1.1557	4.2377	0.
54662.	182.88	1.1557	4.2283	1.1557	4.2283	0.
54668.	182.86	1.1551	4.2347	1.1551	4.2347	0.
54673.	182.84	1.1556	4.2225	1.1556	4.2225	0.
54679.	182.82	1.1579	4.1965	1.1579	4.1965	0.
54685.	182.80	1.1593	4.1878	1.1593	4.1878	0.
54691.	182.78	1.1596	4.1842	1.1596	4.1842	0.
54697.	182.76	1.1599	4.1710	1.1599	4.1710	0.
54703.	182.74	1.1601	4.1641	1.1601	4.1641	0.
54709.	182.72	1.1607	4.1592	1.1607	4.1592	0.
54715.	182.70	1.1607	4.1513	1.1607	4.1513	0.
54721.	182.68	1.1605	4.1383	1.1605	4.1383	0.
54727.	182.66	1.1609	4.1268	1.1609	4.1268	0.
54733.	182.64	1.1610	4.1189	1.1610	4.1189	0.
54739.	182.62	1.1616	4.1093	1.1616	4.1093	0.
54745.	182.60	1.1620	4.1050	1.1620	4.1050	0.
54751.	182.58	1.1622	4.1020	1.1622	4.1020	0.
54757.	182.56	1.1629	4.0797	1.1629	4.0797	0.
54763.	182.54	1.1635	4.0518	1.1635	4.0518	0.
54769.	182.52	1.1626	4.0523	1.1626	4.0523	0.
54775.	182.50	1.1620	4.0541	1.1620	4.0541	0.
54781.	182.48	1.1626	4.0428	1.1626	4.0428	0.
54787.	182.46	1.1641	4.0294	1.1641	4.0294	0.
54793.	182.44	1.1653	4.0244	1.1653	4.0244	0.
54799.	182.42	1.1669	4.0192	1.1669	4.0192	0.
54805.	182.40	1.1676	4.0224	1.1676	4.0224	0.
54811.	182.38	1.1678	4.0242	1.1678	4.0242	0.
54817.	182.36	1.1690	4.0191	1.1690	4.0191	0.
54823.	182.34	1.1696	4.0215	1.1696	4.0215	0.
54829.	182.32	1.1696	4.0310	1.1696	4.0310	0.
54835.	182.30	1.1692	4.0321	1.1692	4.0321	0.
54841.	182.28	1.1705	4.0273	1.1705	4.0273	0.
54847.	182.26	1.1714	4.0308	1.1714	4.0308	0.
54853.	182.24	1.1718	4.0384	1.1718	4.0384	0.
54860.	182.22	1.1720	4.0474	1.1720	4.0474	0.
54866.	182.20	1.1733	4.0529	1.1733	4.0529	0.
54872.	182.18	1.1740	4.0617	1.1740	4.0617	0.
54878.	182.16	1.1743	4.0700	1.1743	4.0700	0.
54884.	182.14	1.1751	4.0653	1.1751	4.0653	0.
54890.	182.12	1.1753	4.0663	1.1753	4.0663	0.
54896.	182.10	1.1744	4.0861	1.1744	4.0861	0.
54902.	182.08	1.1736	4.1130	1.1736	4.1130	0.
54908.	182.06	1.1728	4.1287	1.1728	4.1287	0.
54914.	182.04	1.1708	4.1503	1.1708	4.1503	0.
54920.	182.02	1.1683	4.1737	1.1683	4.1737	0.
54926.	182.00	1.1660	4.1973	1.1660	4.1973	0.

WAVENUMBER CM-1	WAVELENGTH NM	CROSS SECTION X E19, CM-2 FIRST ORDER (000)	(010)	SECOND ORDER (000)	(010)	(020)
54932.	181.98	1.1647	4.2237	1.1647	4.2237	0.
54938.	181.96	1.1645	4.2329	1.1645	4.2329	0.
54944.	181.94	1.1640	4.2268	1.1640	4.2268	0.
54950.	181.92	1.1642	4.2055	1.1642	4.2055	0.
54956.	181.90	1.1655	4.1824	1.1655	4.1824	0.
54962.	181.88	1.1664	4.1842	1.1664	4.1842	0.
54968.	181.86	1.1667	4.2076	1.1667	4.2076	0.
54974.	181.84	1.1683	4.2087	1.1683	4.2087	0.
54980.	181.82	1.1714	4.1901	1.1714	4.1901	0.
54986.	181.80	1.1734	4.1956	1.1734	4.1956	0.
54992.	181.78	1.1744	4.2150	1.1744	4.2150	0.
54998.	181.76	1.1747	4.2401	1.1747	4.2401	0.
55004.	181.74	1.1761	4.2735	1.1761	4.2735	0.
55010.	181.72	1.1776	4.3049	1.1776	4.3049	0.
55017.	181.70	1.1772	4.3370	1.1772	4.3370	0.
55023.	181.68	1.1756	4.3638	1.1756	4.3638	0.
55029.	181.66	1.1735	4.3788	1.1735	4.3788	0.
55035.	181.64	1.1718	4.3935	1.1718	4.3935	0.
55041.	181.62	1.1705	4.4055	1.1705	4.4055	0.
55047.	181.60	1.1688	4.4196	1.1688	4.4196	0.
55053.	181.58	1.1672	4.4185	1.1672	4.4185	0.
55059.	181.56	1.1678	4.3753	1.1678	4.3753	0.
55065.	181.54	1.1697	4.3243	1.1697	4.3243	0.
55071.	181.52	1.1713	4.2926	1.1713	4.2926	0.
55077.	181.50	1.1718	4.2661	1.1718	4.2661	0.
55083.	181.48	1.1720	4.2393	1.1720	4.2393	0.
55089.	181.46	1.1725	4.2255	1.1725	4.2255	0.
55095.	181.44	1.1734	4.2171	1.1734	4.2171	0.
55101.	181.42	1.1743	4.1974	1.1743	4.1974	0.
55108.	181.40	1.1754	4.1724	1.1754	4.1724	0.
55114.	181.38	1.1767	4.1525	1.1767	4.1525	0.
55120.	181.36	1.1772	4.1443	1.1772	4.1443	0.
55126.	181.34	1.1763	4.1448	1.1763	4.1448	0.
55132.	181.32	1.1756	4.1416	1.1756	4.1416	0.
55138.	181.30	1.1757	4.1321	1.1757	4.1321	0.
55144.	181.28	1.1761	4.1096	1.1761	4.1096	0.
55150.	181.26	1.1760	4.0863	1.1760	4.0863	0.
55156.	181.24	1.1757	4.0756	1.1757	4.0756	0.
55162.	181.22	1.1753	4.0624	1.1753	4.0624	0.
55168.	181.20	1.1757	4.0397	1.1757	4.0397	0.
55174.	181.18	1.1763	4.0229	1.1763	4.0229	0.
55181.	181.16	1.1762	4.0093	1.1762	4.0093	0.
55187.	181.14	1.1754	3.9964	1.1754	3.9964	0.
55193.	181.12	1.1747	3.9971	1.1747	3.9971	0.
55199.	181.10	1.1751	3.9866	1.1751	3.9866	0.
55205.	181.08	1.1752	3.9716	1.1752	3.9716	0.
55211.	181.06	1.1753	3.9660	1.1753	3.9660	0.
55217.	181.04	1.1761	3.9574	1.1761	3.9574	0.
55223.	181.02	1.1763	3.9450	1.1763	3.9450	0.
55229.	181.00	1.1760	3.9437	1.1760	3.9437	0.

WAVENUMBER CM-1	WAVELENGTH NM	CROSS SECTION X E19, CM-2 FIRST ORDER (000)	(010)	SECOND ORDER (000)	(010)	(020)
55235.	180.98	1.1764	3.9387	1.1764	3.9387	0.
55241.	180.96	1.1762	3.9368	1.1762	3.9368	0.
55248.	180.94	1.1757	3.9466	1.1757	3.9466	0.
55254.	180.92	1.1752	3.9540	1.1752	3.9540	0.
55260.	180.90	1.1760	3.9437	1.1760	3.9437	0.
55266.	180.88	1.1758	3.9427	1.1758	3.9427	0.
55272.	180.86	1.1735	3.9592	1.1735	3.9592	0.
55278.	180.84	1.1704	3.9858	1.1704	3.9858	0.
55284.	180.82	1.1685	3.9948	1.1685	3.9948	0.
55290.	180.80	1.1683	3.9810	1.1683	3.9810	0.
55296.	180.78	1.1697	3.9579	1.1697	3.9579	0.
55303.	180.76	1.1711	3.9476	1.1711	3.9476	0.
55309.	180.74	1.1712	3.9612	1.1712	3.9612	0.
55315.	180.72	1.1691	4.0002	1.1691	4.0002	0.
55321.	180.70	1.1678	4.0305	1.1678	4.0305	0.
55327.	180.68	1.1681	4.0477	1.1681	4.0477	0.
55333.	180.66	1.1679	4.0800	1.1679	4.0800	0.
55339.	180.64	1.1670	4.1021	1.1670	4.1021	0.
55345.	180.62	1.1679	4.1016	1.1679	4.1016	0.
55352.	180.60	1.1690	4.1131	1.1690	4.1131	0.
55358.	180.58	1.1704	4.1426	1.1704	4.1426	0.
55364.	180.56	1.1710	4.1800	1.1710	4.1800	0.
55370.	180.54	1.1717	4.1816	1.1717	4.1816	0.
55376.	180.52	1.1729	4.1703	1.1729	4.1703	0.
55382.	180.50	1.1738	4.1713	1.1738	4.1713	0.
55388.	180.48	1.1760	4.1572	1.1760	4.1572	0.
55395.	180.46	1.1787	4.1277	1.1787	4.1277	0.
55401.	180.44	1.1797	4.1154	1.1797	4.1154	0.
55407.	180.42	1.1792	4.1211	1.1792	4.1211	0.
55413.	180.40	1.1788	4.1214	1.1788	4.1214	0.
55419.	180.38	1.1790	4.1161	1.1790	4.1161	0.
55425.	180.36	1.1807	4.1038	1.1807	4.1038	0.
55431.	180.34	1.1826	4.0972	1.1826	4.0972	0.
55438.	180.32	1.1825	4.1067	1.1825	4.1067	0.
55444.	180.30	1.1817	4.1209	1.1817	4.1209	0.
55450.	180.28	1.1812	4.1315	1.1812	4.1315	0.
55456.	180.26	1.1813	4.1451	1.1813	4.1451	0.
55462.	180.24	1.1816	4.1382	1.1816	4.1382	0.
55468.	180.22	1.1800	4.1301	1.1800	4.1301	0.
55474.	180.20	1.1778	4.1370	1.1778	4.1370	0.
55481.	180.18	1.1768	4.1454	1.1768	4.1454	0.
55487.	180.16	1.1765	4.1450	1.1765	4.1450	0.
55493.	180.14	1.1761	4.1461	1.1761	4.1461	0.
55499.	180.12	1.1749	4.1447	1.1749	4.1447	0.
55505.	180.10	1.1738	4.1187	1.1738	4.1187	0.
55511.	180.08	1.1737	4.0940	1.1737	4.0940	0.
55518.	180.06	1.1742	4.0913	1.1742	4.0913	0.
55524.	180.04	1.1753	4.0839	1.1753	4.0839	0.
55530.	180.02	1.1780	4.0577	1.1780	4.0577	0.
55536.	180.00	1.1824	4.0222	1.1824	4.0222	0.

WAVENUMBER CM-1	WAVELENGTH NM	CROSS SECTION X E19, CM-2 FIRST ORDER (000)	(010)	SECOND ORDER (000)	(010)	(020)
55542.	179.98	1.1867	4.0001	1.1867	4.0001	0.
55548.	179.96	1.1892	4.0086	1.1892	4.0086	0.
55555.	179.94	1.1903	4.0155	1.1903	4.0155	0.
55561.	179.92	1.1913	4.0055	1.1913	4.0055	0.
55567.	179.90	1.1922	4.0073	1.1922	4.0073	0.
55573.	179.88	1.1914	4.0215	1.1914	4.0215	0.
55579.	179.86	1.1889	4.0225	1.1889	4.0225	0.
55586.	179.84	1.1862	4.0147	1.1862	4.0147	0.
55592.	179.82	1.1834	4.0122	1.1834	4.0122	0.
55598.	179.80	1.1810	3.9950	1.1810	3.9950	0.
55604.	179.78	1.1795	3.9590	1.1795	3.9590	0.
55610.	179.76	1.1774	3.9319	1.1774	3.9319	0.
55616.	179.74	1.1746	3.9302	1.1746	3.9302	0.
55623.	179.72	1.1724	3.9277	1.1724	3.9277	0.
55629.	179.70	1.1703	3.9092	1.1703	3.9092	0.
55635.	179.68	1.1699	3.8857	1.1699	3.8857	0.
55641.	179.66	1.1718	3.8505	1.1718	3.8505	0.
55647.	179.64	1.1717	3.8089	1.1717	3.8089	0.
55654.	179.62	1.1694	3.7839	1.1694	3.7839	0.
55660.	179.60	1.1676	3.7731	1.1676	3.7731	0.
55666.	179.58	1.1680	3.7528	1.1680	3.7528	0.
55672.	179.56	1.1697	3.7326	1.1697	3.7326	0.
55678.	179.54	1.1705	3.7279	1.1705	3.7279	0.
55685.	179.52	1.1699	3.7152	1.1699	3.7152	0.
55691.	179.50	1.1697	3.6904	1.1697	3.6904	0.
55697.	179.48	1.1698	3.6793	1.1698	3.6793	0.
55703.	179.46	1.1696	3.6862	1.1696	3.6862	0.
55709.	179.44	1.1688	3.6964	1.1688	3.6964	0.
55716.	179.42	1.1682	3.6973	1.1682	3.6973	0.
55722.	179.40	1.1675	3.6886	1.1675	3.6886	0.
55728.	179.38	1.1681	3.6685	1.1681	3.6685	0.
55734.	179.36	1.1702	3.6351	1.1702	3.6351	0.
55740.	179.34	1.1715	3.6176	1.1715	3.6176	0.
55747.	179.32	1.1712	3.6268	1.1712	3.6268	0.
55753.	179.30	1.1706	3.6381	1.1706	3.6381	0.
55759.	179.28	1.1701	3.6446	1.1701	3.6446	0.
55765.	179.26	1.1696	3.6512	1.1696	3.6512	0.
55772.	179.24	1.1708	3.6399	1.1708	3.6399	0.
55778.	179.22	1.1723	3.6305	1.1723	3.6305	0.
55784.	179.20	1.1717	3.6472	1.1717	3.6472	0.
55790.	179.18	1.1711	3.6457	1.1711	3.6457	0.
55797.	179.16	1.1716	3.6320	1.1716	3.6320	0.
55803.	179.14	1.1718	3.6307	1.1718	3.6307	0.
55809.	179.12	1.1708	3.6422	1.1708	3.6422	0.
55815.	179.10	1.1696	3.6552	1.1696	3.6552	0.
55821.	179.08	1.1691	3.6570	1.1691	3.6570	0.
55828.	179.06	1.1684	3.6665	1.1684	3.6665	0.
55834.	179.04	1.1676	3.6862	1.1676	3.6862	0.
55840.	179.02	1.1662	3.7133	1.1662	3.7133	0.
55846.	179.00	1.1662	3.7117	1.1662	3.7117	0.

WAVENUMBER CM-1	WAVELENGTH NM	CROSS SECTION X E19, CM-2 FIRST ORDER (000)	(010)	SECOND ORDER (000)	(010)	(020)
55853.	178.98	1.1679	3.6930	1.1679	3.6930	0.
55859.	178.96	1.1683	3.7086	1.1683	3.7086	0.
55865.	178.94	1.1679	3.7328	1.1679	3.7328	0.
55871.	178.92	1.1673	3.7559	1.1673	3.7559	0.
55878.	178.90	1.1669	3.7699	1.1669	3.7699	0.
55884.	178.88	1.1669	3.7833	1.1669	3.7833	0.
55890.	178.86	1.1669	3.8010	1.1669	3.8010	0.
55896.	178.84	1.1669	3.8104	1.1669	3.8104	0.
55903.	178.82	1.1662	3.8256	1.1662	3.8256	0.
55909.	178.80	1.1640	3.8620	1.1640	3.8620	0.
55915.	178.78	1.1613	3.8764	1.1613	3.8764	0.
55921.	178.76	1.1599	3.8764	1.1599	3.8764	0.
55928.	178.74	1.1595	3.9085	1.1595	3.9085	0.
55934.	178.72	1.1595	3.9317	1.1595	3.9317	0.
55940.	178.70	1.1586	3.9306	1.1586	3.9306	0.
55946.	178.68	1.1586	3.9401	1.1586	3.9401	0.
55953.	178.66	1.1603	3.9509	1.1603	3.9509	0.
55959.	178.64	1.1619	3.9496	1.1619	3.9496	0.
55965.	178.62	1.1627	3.9585	1.1627	3.9585	0.
55971.	178.60	1.1641	3.9681	1.1641	3.9681	0.
55978.	178.58	1.1665	3.9581	1.1665	3.9581	0.
55984.	178.56	1.1681	3.9608	1.1681	3.9608	0.
55990.	178.54	1.1675	3.9760	1.1675	3.9760	0.
55997.	178.52	1.1661	3.9768	1.1661	3.9768	0.
56003.	178.50	1.1649	3.9594	1.1649	3.9594	0.
56009.	178.48	1.1626	3.9249	1.1626	3.9249	0.
56015.	178.46	1.1593	3.9099	1.1593	3.9099	0.
56022.	178.44	1.1570	3.8985	1.1570	3.8985	0.
56028.	178.42	1.1554	3.8688	1.1554	3.8688	0.
56034.	178.40	1.1541	3.8321	1.1541	3.8321	0.
56040.	178.38	1.1517	3.8142	1.1517	3.8142	0.
56047.	178.36	1.1488	3.7989	1.1488	3.7989	0.
56053.	178.34	1.1460	3.7836	1.1460	3.7836	0.
56059.	178.32	1.1421	3.7799	1.1421	3.7799	0.
56066.	178.30	1.1395	3.7593	1.1395	3.7593	0.
56072.	178.28	1.1394	3.7257	1.1394	3.7257	0.
56078.	178.26	1.1406	3.6857	1.1406	3.6857	0.
56084.	178.24	1.1404	3.6456	1.1404	3.6456	0.
56091.	178.22	1.1390	3.6122	1.1390	3.6122	0.
56097.	178.20	1.1389	3.5961	1.1389	3.5961	0.
56103.	178.18	1.1392	3.5837	1.1392	3.5837	0.
56110.	178.16	1.1383	3.5588	1.1383	3.5588	0.
56116.	178.14	1.1367	3.5290	1.1367	3.5290	0.
56122.	178.12	1.1345	3.5161	1.1345	3.5161	0.
56129.	178.10	1.1336	3.5103	1.1336	3.5103	0.
56135.	178.08	1.1336	3.5032	1.1336	3.5032	0.
56141.	178.06	1.1331	3.4771	1.1331	3.4771	0.
56148.	178.04	1.1319	3.4502	1.1319	3.4502	0.
56154.	178.02	1.1299	3.4558	1.1299	3.4558	0.
56160.	178.00	1.1285	3.4502	1.1285	3.4502	0.

WAVENUMBER CM-1	WAVELENGTH NM	CROSS SECTION X E19, CM-2 FIRST ORDER (000)	(010)	SECOND ORDER (000)	(010)	(020)
56166.	177.98	1.1285	3.4152	1.1285	3.4152	0.
56173.	177.96	1.1301	3.3963	1.1301	3.3963	0.
56179.	177.94	1.1314	3.3994	1.1314	3.3994	0.
56185.	177.92	1.1312	3.3913	1.1312	3.3913	0.
56192.	177.90	1.1306	3.3802	1.1306	3.3802	0.
56198.	177.88	1.1313	3.3873	1.1313	3.3873	0.
56204.	177.86	1.1337	3.3695	1.1337	3.3695	0.
56211.	177.84	1.1346	3.3482	1.1346	3.3482	0.
56217.	177.82	1.1345	3.3592	1.1345	3.3592	0.
56223.	177.80	1.1350	3.3686	1.1350	3.3686	0.
56230.	177.78	1.1356	3.3923	1.1356	3.3923	0.
56236.	177.76	1.1351	3.4261	1.1351	3.4261	0.
56242.	177.74	1.1340	3.4534	1.1340	3.4534	0.
56249.	177.72	1.1333	3.4837	1.1333	3.4837	0.
56255.	177.70	1.1342	3.4887	1.1342	3.4887	0.
56261.	177.68	1.1348	3.4742	1.1348	3.4742	0.
56268.	177.66	1.1346	3.4693	1.1346	3.4693	0.
56274.	177.64	1.1349	3.4569	1.1349	3.4569	0.
56280.	177.62	1.1360	3.4566	1.1360	3.4566	0.
56287.	177.60	1.1353	3.4956	1.1353	3.4956	0.
56293.	177.58	1.1336	3.5374	1.1336	3.5374	0.
56299.	177.56	1.1322	3.5700	1.1322	3.5700	0.
56306.	177.54	1.1312	3.6205	1.1312	3.6205	0.
56312.	177.52	1.1289	3.6895	1.1289	3.6895	0.
56318.	177.50	1.1269	3.7382	1.1269	3.7382	0.
56325.	177.48	1.1271	3.7679	1.1271	3.7679	0.
56331.	177.46	1.1280	3.8016	1.1280	3.8016	0.
56337.	177.44	1.1280	3.8287	1.1280	3.8287	0.
56344.	177.42	1.1265	3.8500	1.1265	3.8500	0.
56350.	177.40	1.1268	3.8519	1.1268	3.8519	0.
56356.	177.38	1.1275	3.8687	1.1275	3.8687	0.
56363.	177.36	1.1264	3.8953	1.1264	3.8953	0.
56369.	177.34	1.1248	3.9006	1.1248	3.9006	0.
56375.	177.32	1.1246	3.8892	1.1246	3.8892	0.
56382.	177.30	1.1243	3.8929	1.1243	3.8929	0.
56388.	177.28	1.1228	3.8784	1 1228	3.8784	0.
56395.	177.26	1.1219	3.8558	1.1219	3.8558	0.
56401.	177.24	1.1221	3.8544	1.1221	3.8544	0.
56407.	177.22	1.1232	3.8326	1.1232	3.8326	0.
56414.	177.20	1.1223	3.7981	1.1223	3.7981	0.
56420.	177.18	1.1206	3.7834	1.1206	3.7834	0.
56426.	177.16	1.1201	3.7812	1.1201	3.7812	0.
56433.	177.14	1.1210	3.7576	1.1210	3.7576	0.
56439.	177.12	1.1221	3.7270	1.1221	3.7270	0.
56446.	177.10	1.1223	3.7097	1.1223	3.7097	0.
56452.	177.08	1.1212	3.6997	1.1212	3.6997	0.
56458.	177.06	1.1206	3.6910	1.1206	3.6910	0.
56465.	177.04	1.1209	3.6786	1.1209	3.6786	0.
56471.	177.02	1.1221	3.6721	1.1221	3.6721	0.
56477.	177.00	1.1222	3.6650	1.1222	3.6650	0.

WAVENUMBER CM-1	WAVELENGTH NM	CROSS SECTION X E19, CM-2 FIRST ORDER (000)	(010)	SECOND ORDER (000)	(010)	(020)
56484.	176.98	1.1225	3.6478	1.1225	3.6478	0.
56490.	176.96	1.1246	3.6344	1.1246	3.6344	0.
56497.	176.94	1.1280	3.6097	1.1280	3.6097	0.
56503.	176.92	1.1296	3.5829	1.1296	3.5829	0.
56509.	176.90	1.1293	3.5594	1.1293	3.5594	0.
56516.	176.88	1.1294	3.5405	1.1294	3.5405	0.
56522.	176.86	1.1295	3.5326	1.1295	3.5326	0.
56529.	176.84	1.1296	3.5160	1.1296	3.5160	0.
56535.	176.82	1.1291	3.4883	1.1291	3.4883	0.
56541.	176.80	1.1275	3.4681	1.1275	3.4681	0.
56548.	176.78	1.1258	3.4478	1.1258	3.4478	0.
56554.	176.76	1.1242	3.4102	1.1242	3.4102	0.
56560.	176.74	1.1227	3.3725	1.1227	3.3725	0.
56567.	176.72	1.1207	3.3598	1.1207	3.3598	0.
56573.	176.70	1.1178	3.3509	1.1178	3.3509	0.
56580.	176.68	1.1154	3.3338	1.1154	3.3338	0.
56586.	176.66	1.1154	3.2979	1.1154	3.2979	0.
56593.	176.64	1.1139	3.2547	1.1139	3.2547	0.
56599.	176.62	1.1112	3.2316	1.1112	3.2316	0.
56605.	176.60	1.1095	3.2392	1.1095	3.2392	0.
56612.	176.58	1.1081	3.2297	1.1081	3.2297	0.
56618.	176.56	1.1053	3.2128	1.1053	3.2128	0.
56625.	176.54	1.1023	3.1941	1.1023	3.1941	0.
56631.	176.52	1.0998	3.1864	1.0998	3.1864	0.
56637.	176.50	1.0976	3.2006	1.0976	3.2006	0.
56644.	176.48	1.0946	3.2106	1.0946	3.2106	0.
56650.	176.46	1.0925	3.1995	1.0925	3.1995	0.
56657.	176.44	1.0922	3.1887	1.0922	3.1887	0.
56663.	176.42	1.0906	3.1940	1.0906	3.1940	0.
56670.	176.40	1.0874	3.1871	1.0874	3.1871	0.
56676.	176.38	1.0848	3.1689	1.0848	3.1689	0.
56682.	176.36	1.0849	3.1579	1.0849	3.1579	0.
56689.	176.34	1.0856	3.1531	1.0856	3.1531	0.
56695.	176.32	1.0850	3.1460	1.0850	3.1460	0.
56702.	176.30	1.0815	3.1594	1.0815	3.1594	0.
56708.	176.28	1.0805	3.1670	1.0805	3.1670	0.
56715.	176.26	1.0819	3.1512	1.0819	3.1512	0.
56721.	176.24	1.0829	3.1357	1.0829	3.1357	0.
56727.	176.22	1.0825	3.1439	1.0825	3.1439	0.
56734.	176.20	1.0828	3.1522	1.0828	3.1522	0.
56740.	176.18	1.0840	3.1576	1.0840	3.1576	0.
56747.	176.16	1.0844	3.1588	1.0844	3.1588	0.
56753.	176.14	1.0835	3.1594	1.0835	3.1594	0.
56760.	176.12	1.0823	3.1628	1.0823	3.1628	0.
56766.	176.10	1.0821	3.1721	1.0821	3.1721	0.
56772.	176.08	1.0825	3.1710	1.0825	3.1710	0.
56779.	176.06	1.0858	3.1589	1.0858	3.1589	0.
56785.	176.04	1.0915	3.1337	1.0916	3.1169	.1189
56792.	176.02	1.0925	3.1564	1.0925	3.1451	.0795
56798.	176.00	1.0910	3.2001	1.0910	3.2001	0.

WAVENUMBER CM-1	WAVELENGTH NM	CROSS SECTION X E19, CM-2 FIRST ORDER (000)	(010)	SECOND ORDER (000)	(010)	(020)
56805.	175.98	1.0901	3.2261	1.0901	3.2261	0.
56811.	175.96	1.0914	3.2268	1.0914	3.2268	0.
56818.	175.94	1.0949	3.2284	1.0949	3.2284	0.
56824.	175.92	1.0971	3.2398	1.0971	3.2398	0.
56831.	175.90	1.0979	3.2543	1.0979	3.2543	0.
56837.	175.88	1.0971	3.2708	1.0971	3.2708	0.
56844.	175.86	1.0964	3.2804	1.0964	3.2783	.0150
56850.	175.84	1.0964	3.2804	1.0965	3.2664	.0994
56856.	175.82	1.0967	3.2896	1.0968	3.2735	.1139
56863.	175.80	1.0965	3.3180	1.0965	3.3143	.0259
56869.	175.78	1.0947	3.3461	1.0947	3.3461	0.
56876.	175.76	1.0925	3.3667	1.0925	3.3667	0.
56882.	175.74	1.0905	3.3922	1.0905	3.3922	0.
56889.	175.72	1.0880	3.4195	1.0880	3.4195	0.
56895.	175.70	1.0848	3.4429	1.0848	3.4429	0.
56902.	175.68	1.0812	3.4752	1.0812	3.4752	0.
56908.	175.66	1.0789	3.5116	1.0789	3.5116	0.
56915.	175.64	1.0781	3.5163	1.0781	3.5163	0.
56921.	175.62	1.0753	3.5074	1.0753	3.5074	0.
56928.	175.60	1.0695	3.5078	1.0695	3.5078	0.
56934.	175.58	1.0648	3.4943	1.0648	3.4943	0.
56941.	175.56	1.0643	3.4340	1.0643	3.4340	0.
56947.	175.54	1.0657	3.3687	1.0657	3.3687	0.
56954.	175.52	1.0653	3.3237	1.0653	3.3237	0.
56960.	175.50	1.0618	3.3140	1.0618	3.3140	0.
56967.	175.48	1.0576	3.3242	1.0576	3.3242	0.
56973.	175.46	1.0553	3.2968	1.0553	3.2968	0.
56980.	175.44	1.0532	3.2594	1.0532	3.2594	0.
56986.	175.42	1.0525	3.2346	1.0525	3.2346	0.
56993.	175.40	1.0535	3.1960	1.0535	3.1960	0.
56999.	175.38	1.0544	3.1668	1.0544	3.1668	0.
57006.	175.36	1.0558	3.1325	1.0558	3.1325	0.
57012.	175.34	1.0578	3.0815	1.0578	3.0815	0.
57019.	175.32	1.0578	3.0528	1.0578	3.0528	0.
57025.	175.30	1.0527	3.0788	1.0527	3.0788	0.
57032.	175.28	1.0469	3.0942	1.0469	3.0942	0.
57038.	175.26	1.0442	3.0569	1.0442	3.0569	0.
57045.	175.24	1.0435	3.0322	1.0435	3.0322	0.
57051.	175.22	1.0438	3.0213	1.0438	3.0213	0.
57058.	175.20	1.0431	2.9879	1.0431	2.9879	0.
57064.	175.18	1.0412	2.9618	1.0412	2.9618	0.
57071.	175.16	1.0396	2.9631	1.0396	2.9631	0.
57077.	175.14	1.0373	2.9779	1.0373	2.9779	0.
57084.	175.12	1.0361	2.9686	1.0361	2.9686	0.
57090.	175.10	1.0364	2.9322	1.0364	2.9322	0.
57097.	175.08	1.0355	2.8962	1.0355	2.8962	0.
57103.	175.06	1.0347	2.8578	1.0347	2.8578	0.
57110.	175.04	1.0359	2.8194	1.0359	2.8194	0.
57116.	175.02	1.0368	2.8149	1.0368	2.8149	0.
57123.	175.00	1.0342	2.8286	1.0342	2.8286	0.

WAVENUMBER CM-1	WAVELENGTH NM	CROSS SECTION X E19, CM-2 FIRST ORDER (000)	(010)	SECOND ORDER (000)	(010)	(020)
57129.	174.98	1.0312	2.8259	1.0312	2.8259	0.
57136.	174.96	1.0310	2.7978	1.0310	2.7978	0.
57142.	174.94	1.0309	2.7801	1.0310	2.7787	.0099
57149.	174.92	1.0316	2.7777	1.0317	2.7629	.1045
57156.	174.90	1.0330	2.7683	1.0333	2.7359	.2289
57162.	174.88	1.0315	2.7585	1.0319	2.7083	.3554
57169.	174.86	1.0282	2.7642	1.0286	2.7079	.3985
57175.	174.84	1.0257	2.8138	1.0258	2.7926	.1501
57182.	174.82	1.0208	2.8758	1.0208	2.8758	0.
57188.	174.80	1.0188	2.8758	1.0188	2.8758	0.
57195.	174.78	1.0206	2.8421	1.0208	2.8103	.2252
57201.	174.76	1.0213	2.8469	1.0217	2.7914	.3929
57208.	174.74	1.0207	2.8837	1.0210	2.8383	.3206
57214.	174.72	1.0194	2.9155	1.0196	2.8847	.2183
57221.	174.70	1.0171	2.9464	1.0173	2.9214	.1769
57228.	174.68	1.0140	2.9912	1.0142	2.9666	.1742
57234.	174.66	1.0125	3.0197	1.0126	2.9954	.1719
57241.	174.64	1.0115	3.0289	1.0116	3.0134	.1100
57247.	174.62	1.0099	3.0263	1.0100	3.0064	.1406
57254.	174.60	1.0093	3.0081	1.0097	2.9496	.4139
57260.	174.58	1.0104	3.0110	1.0110	2.9305	.5697
57267.	174.56	1.0110	3.0578	1.0114	2.9969	.4308
57273.	174.54	1.0113	3.1123	1.0115	3.0808	.2230
57280.	174.52	1.0127	3.1355	1.0130	3.1032	.2287
57287.	174.50	1.0141	3.1356	1.0145	3.0786	.4031
57293.	174.48	1.0124	3.1582	1.0128	3.0907	.4772
57300.	174.46	1.0097	3.2115	1.0100	3.1604	.3620
57306.	174.44	1.0083	3.2689	1.0085	3.2430	.1835
57313.	174.42	1.0054	3.3300	1.0054	3.3300	0.
57319.	174.40	1.0032	3.3816	1.0032	3.3816	0.
57326.	174.38	1.0043	3.4020	1.0043	3.4020	0.
57333.	174.36	1.0081	3.3898	1.0081	3.3898	0.
57339.	174.34	1.0104	3.3574	1.0104	3.3574	0.
57346.	174.32	1.0104	3.3342	1.0104	3.3342	0.
57352.	174.30	1.0099	3.3297	1.0099	3.3297	0.
57359.	174.28	1.0093	3.3266	1.0093	3.3266	0.
57365.	174.26	1.0081	3.3252	1.0081	3.3252	0.
57372.	174.24	1.0074	3.3276	1.0074	3.3276	0.
57379.	174.22	1.0082	3.3079	1.0082	3.3079	0.
57385.	174.20	1.0104	3.2594	1.0104	3.2594	0.
57392.	174.18	1.0131	3.2331	1.0131	3.2331	0.
57398.	174.16	1.0146	3.2253	1.0146	3.2253	0.
57405.	174.14	1.0138	3.2084	1.0138	3.2084	0.
57412.	174.12	1.0133	3.2023	1.0133	3.2023	0.
57418.	174.10	1.0133	3.2118	1.0133	3.2118	0.
57425.	174.08	1.0130	3.2211	1.0130	3.2211	0.
57431.	174.06	1.0145	3.2037	1.0145	3.2037	0.
57438.	174.04	1.0177	3.1771	1.0177	3.1771	0.
57445.	174.02	1.0187	3.1576	1.0187	3.1576	0.
57451.	174.00	1.0186	3.1240	1.0186	3.1240	0.

WAVENUMBER CM-1	WAVELENGTH NM	CROSS SECTION X E19, CM-2 FIRST ORDER (000)	(010)	SECOND ORDER (000)	(010)	(020)
57458.	173.98	1.0166	3.1002	1.0166	3.1002	0.
57464.	173.96	1.0115	3.1149	1.0115	3.1149	0.
57471.	173.94	1.0080	3.1204	1.0080	3.1204	0.
57478.	173.92	1.0060	3.1149	1.0060	3.1149	0.
57484.	173.90	1.0025	3.1084	1.0025	3.1084	0.
57491.	173.88	.9986	3.0767	.9986	3.0767	0.
57497.	173.86	.9977	3.0064	.9977	3.0064	0.
57504.	173.84	.9963	2.9658	.9963	2.9658	0.
57511.	173.82	.9906	3.0021	.9906	3.0021	0.
57517.	173.80	.9837	3.0371	.9837	3.0371	0.
57524.	173.78	.9778	3.0294	.9778	3.0294	0.
57531.	173.76	.9748	3.0027	.9748	3.0027	0.
57537.	173.74	.9769	2.9336	.9769	2.9336	0.
57544.	173.72	.9793	2.8583	.9793	2.8583	0.
57550.	173.70	.9788	2.8561	.9788	2.8561	0.
57557.	173.68	.9791	2.8541	.9791	2.8541	0.
57564.	173.66	.9788	2.8306	.9788	2.8306	0.
57570.	173.64	.9778	2.8191	.9778	2.8191	0.
57577.	173.62	.9732	2.8480	.9732	2.8480	0.
57584.	173.60	.9690	2.8582	.9690	2.8582	0.
57590.	173.58	.9685	2.8361	.9685	2.8361	0.
57597.	173.56	.9685	2.8050	.9685	2.8050	0.
57603.	173.54	.9686	2.7541	.9686	2.7541	0.
57610.	173.52	.9704	2.7244	.9704	2.7244	0.
57617.	173.50	.9696	2.7402	.9696	2.7402	0.
57623.	173.48	.9660	2.7552	.9660	2.7552	0.
57630.	173.46	.9645	2.7415	.9645	2.7415	0.
57637.	173.44	.9654	2.7162	.9654	2.7162	0.
57643.	173.42	.9619	2.7328	.9619	2.7328	0.
57650.	173.40	.9595	2.7427	.9595	2.7427	0.
57657.	173.38	.9618	2.7096	.9618	2.7096	0.
57663.	173.36	.9644	2.6768	.9644	2.6768	0.
57670.	173.34	.9661	2.6621	.9661	2.6621	0.
57677.	173.32	.9670	2.6718	.9670	2.6718	0.
57683.	173.30	.9658	2.7008	.9658	2.7008	0.
57690.	173.28	.9625	2.7399	.9625	2.7399	0.
57697.	173.26	.9575	2.7738	.9575	2.7738	0.
57703.	173.24	.9526	2.7943	.9526	2.7943	0.
57710.	173.22	.9526	2.7521	.9526	2.7521	0.
57717.	173.20	.9581	2.6790	.9581	2.6790	0.
57723.	173.18	.9639	2.6825	.9639	2.6825	0.
57730.	173.16	.9653	2.7391	.9653	2.7391	0.
57737.	173.14	.9648	2.7450	.9648	2.7450	0.
57743.	173.12	.9661	2.7170	.9661	2.7170	0.
57750.	173.10	.9679	2.6968	.9679	2.6968	0.
57757.	173.08	.9653	2.7273	.9653	2.7273	0.
57763.	173.06	.9602	2.7818	.9602	2.7818	0.
57770.	173.04	.9590	2.8114	.9590	2.8114	0.
57777.	173.02	.9607	2.8699	.9607	2.8699	0.
57783.	173.00	.9605	2.9254	.9605	2.9254	0.

WAVENUMBER CM-1	WAVELENGTH NM	CROSS SECTION X E19, CM-2 FIRST ORDER (000)	(010)	SECOND ORDER (000)	(010)	(020)
57790.	172.98	.9607	2.9162	.9607	2.9162	0.
57797.	172.96	.9613	2.9097	.9613	2.9097	0.
57803.	172.94	.9598	2.8896	.9598	2.8896	0.
57810.	172.92	.9615	2.8494	.9615	2.8494	0.
57817.	172.90	.9642	2.9195	.9642	2.9195	0.
57823.	172.88	.9657	3.0271	.9657	3.0271	0.
57830.	172.86	.9697	2.9903	.9697	2.9903	0.
57837.	172.84	.9751	2.8740	.9751	2.8740	0.
57843.	172.82	.9736	2.8508	.9736	2.8508	0.
57850.	172.80	.9658	2.9173	.9658	2.9173	0.
57857.	172.78	.9603	2.9468	.9603	2.9468	0.
57864.	172.76	.9558	2.9383	.9558	2.9383	0.
57870.	172.74	.9492	2.9719	.9492	2.9719	0.
57877.	172.72	.9455	3.0298	.9455	3.0298	0.
57884.	172.70	.9444	3.0332	.9444	3.0332	0.
57890.	172.68	.9435	2.9534	.9435	2.9534	0.
57897.	172.66	.9410	2.8987	.9410	2.8987	0.
57904.	172.64	.9341	2.9862	.9341	2.9862	0.
57910.	172.62	.9272	3.0370	.9272	3.0370	0.
57917.	172.60	.9267	2.8899	.9267	2.8899	0.
57924.	172.58	.9294	2.7982	.9294	2.7982	0.
57931.	172.56	.9310	2.8662	.9310	2.8662	0.
57937.	172.54	.9299	2.8824	.9299	2.8824	0.
57944.	172.52	.9237	2.8506	.9237	2.8506	0.
57951.	172.50	.9145	2.8605	.9145	2.8605	0.
57957.	172.48	.9077	2.9091	.9077	2.9091	0.
57964.	172.46	.9046	2.9557	.9046	2.9557	0.
57971.	172.44	.9057	2.8860	.9057	2.8860	0.
57978.	172.42	.9121	2.7175	.9121	2.7175	0.
57984.	172.40	.9178	2.6365	.9178	2.6365	0.
57991.	172.38	.9199	2.6860	.9199	2.6860	0.
57998.	172.36	.9197	2.7694	.9197	2.7694	0.
58005.	172.34	.9197	2.7710	.9197	2.7710	0.
58011.	172.32	.9215	2.7429	.9215	2.7429	0.
58018.	172.30	.9176	2.7805	.9176	2.7805	0.
58025.	172.28	.9098	2.8120	.9098	2.8120	0.
58031.	172.26	.9094	2.7764	.9094	2.7764	0.
58038.	172.24	.9146	2.7547	.9146	2.7547	0.
58045.	172.22	.9168	2.7421	.9168	2.7421	0.
58052.	172.20	.9184	2.6723	.9184	2.6723	0.
58058.	172.18	.9206	2.5984	.9206	2.5984	0.
58065.	172.16	.9201	2.5868	.9201	2.5868	0.
58072.	172.14	.9167	2.6847	.9167	2.6847	0.
58079.	172.12	.9163	2.7089	.9163	2.7089	0.
58085.	172.10	.9164	2.6015	.9164	2.6015	0.
58092.	172.08	.9135	2.5814	.9135	2.5814	0.
58099.	172.06	.9136	2.6699	.9136	2.6699	0.
58106.	172.04	.9149	2.7813	.9149	2.7813	0.
58112.	172.02	.9126	2.8017	.9126	2.8017	0.
190.	.00	4.0381	.8435	3.6517	2.7340	52613.

REFERENCES

1. Leifson, S., Astrophys. J., 63, 73 (1926).
2. Dutta, A. K., Proc. Roy. Soc. (London), 38, 84 (1932).
3. Wulf, R. and E. H. Melvin, Phys. Rev. 39, 180 (1932).
4. Duncan, A. B. F., J. Chem. Phys., 4, 638 (1936).
5. Sen-Gupta, P. K., Nature, 136, 513 (19935).
6. Henry, L., Nature, 134, 498 (1934).
7. Sponer, H. and L. G. Bonner, J. Chem. Phys., 8, 33 (1940).
8. Nicolle, J. and b. Vodar, Comptes Rendus, 210, 142 (1940).
9. Romand, J. and J. Mayence, Comptes Rendus, 228, 998 (1949).
10. Zelikoff, M., K. Watanabe and E. C. Y. Inn, J. Chem. Phys., 21, 1643 (1953).
11. Thompson, B. A., P. Harteck and R. R. Reeves, J. Geophys. Res., 68, 6431 (1963).
12. Bates, D.R. and P. B. Hays, Planet, Space Sci., 15, 189 (1967).
13. Holliday, M. G. and B. G. Reuben, Far. Soc. Trans., 64, 1735 (1968).
14. Rabalais, J. W., J. M. McDonald, V. Scherr and S. P. McGlynn, Chem. Revs. 71, 73 (1971).
15. Monahan, K. M. and W. G. Walker, J. CHem Phys., 36, 1682 (1962).
16. Doering, J. P. and B. H. Mahan, J. Chem. Phys., 36, 1682 (1962).
17. Yamazaki, H. and R. J. Cvetanovic, J. Chem. Phys., 41, 3703 (1964).
18. Paraskevopoulos, G. and R. J. Cvetanovic, J. Amer. Chem. Soc., 91, 7572 (1969).
19. Paraskevopoulos, G., J. Chem. Phys., 52, 5821 (1970).
20. Preston, K. F. and R. F. Barr, J. Chem. Phys., 54, 3347 (1971).

21. Simonaitis, R., R. I. Greenberg and J. Heicklen, Int. J. Chem. Kinetics, 4, 497 (1972).

22. Davidson, J.A., C. J. Howard, H. I. Schiff and F. C. Fehsenfeld, J. Chem. Phys., (in press, 1979).

23. Adel, A., Astrophys. J., 88, 168 (1938).

24. Seeley, J. S. and J. T. Houghton, Infrared Phys., 1, 116 (1961).

25. Rank, D. H., A.F. Slomba, E. F. Gardner and T. A. Wiggins, J. Opt. Soc. Am., 52, 858 (1962).

26. Birkeland, G. W. and G. H. Shaw, J. Opt. Soc. Am., 49, 637 (1959).

27. Slobod, R. L. and M. F. Krough, J. Amer. Chem. Soc., 72, 1175 (1950).

28. Craig, H. and L. G. Gordon, Geochim. Cosmochim. Acta, 27, 949 (1963).

29. Schutz, K., C. Junge, R. Beck and B. Albrecht, J. Geophys. Res., 75, 2230 (1970).

30. Murcray, D. G., A. Goldman, F. H. Murcray, W. J. Williams, T. N. Brooks and D. P. Barker, Proceedings of Second Cloud Impact Assessment Program Con., Rep. DOT - TSC-OST-74-15, Nat. Tech. Inform. Ser., Springfield, VA (1972).

31. Ehhalt, D. H., N. Roper and E. H. Moore, J. Geophys. Res., 80, 1653 (1975).

32. Schmeltekopt, A. L., P. D. Goldan, W. R. Henderson, W. J. Harrop, T. L. Thompson, F. C. Fehsenfeld, H. I. Schiff, P. J. Crutzen, I.S.A. Isaken and E. E. Ferguson, Geophys. Res. Lett., 2, 393 (1975).

33. Ehhalt, D., L. E. Heidt, R. H. Lueb and N. Roper, Proc. Third Conf. on CIAP, 153 (1974).

34. Ehhalt, D., L. E. Heidt, R. H. Lueb and E. A. Marsell, J. Atm. Sci., 32, 163 (1975).

35. Pierotti, D. and R. A. Rasmussen, J. Geophys. Res., 82, 5823 (1977).

36. Delwiche, C. C., Sci. Amer., 223, 137 (1970).

37. Alexander, M., Introduction to Soil Microbiology, Wiley and Sons Inc., NY, 472 pp (1961).

38. Rassmussen, R. A. and D. Pierotti, Geophys. Res. Lett., 5, 353 (1978).

39. Cicerone, J. J., J. D. Shetter, D. H. Stedman, T. J. Kelley and S. C. Liu, J. Geophys. Res., 83, 3042 (1978).

40. Goldan, P. D., Y. A. Bush, F. C. Fehsenfeld, D. A. Albritton, P. J. Crutzen, A. L. Schmeltekopt and E. E. Fergusson, J. Geophys. Res., 83, 935 (1978).

41. Tyson, B. J., J. C. Arveson and D. O'Hara, Geophys. Res. Lett., 5, 535 (1978).

42. Pierotti, D. and R. Rasmussen, Geophys. Res. Lett. 2, 265 (1976).

43. Weiss, R. F. and H. Craig, Geophys. Res. Lett.., 3, 751 (1976).

44. Bolin, B. and E. Arrhenius, Ambio., 6, 96 (1977).

45. Crutzen, P. and D. Ehhalt, Ambio., 6, 112 (1977).

46. McElroy, M., S. Wofsky and Y. Yung, Phil. Trans. Roy. Soc., 277B, 159 (1977).

47. Cicerone, R. J., J. D. Shetter and S. C. Liu, Geophys. Res. Lett., 5, 173 (1978).

48. Hahn, J. and C. Junge, Z. Naturforsch, 32a, 190 (1977).

49. Hahn, J., Tellus, 26, 160 (1974).

50. Hahn, J., Meteorforsch. Ergenbrisse A, 16, 1 (1975).

51. McElroy, M. B., J. W. Elkins, S. C. Wolfsky and Y. L. Yung, Revs.. Geophys. Space Phys., 14, 143 (1976).

52. Liu, S. C., R. J. Cicerone, T. M. Donahue and W. L. Chameides, Geophys. Res. Lett., 3, 157 (1976).

53. Johnston, H. S., Proc. Nat. Acad. Sci., 69, 2369 (1972).

54. Crutzen, P. J., Quart. J. Roy. Meterol. Soc., 96, 320 (1971).

55. McElroy, M. B. and J. C. McConnell, J. Atm. Sci., 28, 1095 (1971).

56. Crutzen, P. J., Ambio, 3, 201 (1974).

57. Johnston, H. S., J. Geophys. Res., 82, 1767 (1977).

58. Sze, N. D. and H. Rice, Geophys. Res. Lett., 3, 343 (1976).

59. McElroy, M. B., Chemical Processes in the Solar System: A Kinetic Perspective, in MTP Int. Rev. of Sci., ed by D. Herschbach, Butterworths, London, (1976).

60. Crutzen, P. J., Geophys. Res. Lett., 3, 169 (1976).

61. Liu, S., R. Cicerone, T. Donahue and W. Chameides, Tellus, 29, 251 (1977).

62. Blackmer, A. M. and J. M. Bremmer, Geophys. Res. Lett., 3, 739 (1976).

63. Payne, W. J., Bacteriol. Rev., 37, 409 (1973).

64. World Meterol. Organiz. Symp. on the Geophys. Aspects and Consequences of Changes in the Compos. of the Stra., Toronto, June (1978) , proceedings.

65. Turco, R. P., R. C. Whitten, I. G. Poppoff and L. A. Capone, Nature, (in press), (1979).

66. Schutz, K., C. Junge, R. Beck and B. Albrecht, J. Geophys. Res., 75, 2230 (1970).

67. Johnston, H. S. and G. S. Selwyn, Geophys. Res. Lett., 2, 549 (1975), copyright by American Geophysical Union.

68. Junge, C. and J. Hahn, J. Geophys. Res., 76, 8143 (1971).

69. Leighton, P. A., Photochemistry of Air Pollution, pp. 12-13, Academic Press, N.Y. (1961).

70. Forsythe, W. E., Smithsonian Physical Tables, pp. 532-33, Ninth Revised Edition, Smithsonian Inst., Washington, DC, (1956).

71. Gough, T. E., R. E. Miller and G. Scoles, J. Chem. Phys., 69, 1588 (1978).

72. Ogawa, M., J. Chem. Phys., 54, 2550 (1971).

73. Shemansky, D. E., J. Chem. Phys., 56, 1582 (1972).

74. Johnston, H. S. and G. Whitten, Pure Appl. Geophys., 106, 1468 (1973).

75. Stedman, D. H., R. J. Cicerone, W. L. Chameides, and R. B. Harvey, J. Geophys. Res., 81, 2003 (1976).

76. Johnston, H. S., O. Serang and J. Podolske, submitted to J. Geophys. Res. (1978).

77. Selwyn, G. S., J. Podolske and H. S. Johnston, Geophys. Res. Lett., 4, 427 (1977), copyright by American Geophysical Union.

78. McEwan, M. J. and L. F. Phillips, Chemistry of the Atmosphere, John Wiley and Sons, N.Y., p 3 (1975).

78a. ibid, pp. 22.

79. Hudson, R. D., Can. J. Chem., 52, 1465 (1974).

80. Lassettre, E. N., A. Skerbele, M. A. Dillon and K. J. Ross, J. Chem. Phys., 48, 5066 (1966).

81. Hass, G. and J. E. Waylonis, J. Opt. Soc. Am., 51, 719 (1961).

82. Hall, J. F., J. Opt. Soc. Am., 47, 662 (1957).

83. Schroeder, H., Optica Acta, 9, 249 (1962).

84. Angel, D. W., W. R. Hunter and R. Tousey, J. Opt. Soc. Am., 51, 913 (1961).

85. Hass, G. and E. Ritter, J. Vac. Sci. Tech., 4, 71 (1967).

86. Cox, J. T., H. Hass and J. B. Ramsey, J. Physique, 25, 250 (1964).

87. Hall, J. F., J. Opt. Soc. Am., 46, 1013 (1956).

88. Hass, G. W. R. Hunter and R. Tousey, J. Opt. Soc. Am., 46, 1009 (1966).

89. Canfield, L. R., G. Hass and J. E. Waylonis, Appl. Optics, 5, 45 (1966).

90. Bradford, A. P., G. Hass, J. F. Ostantowski and A. R. Tuft, Appl. Optics, 8, 1183 (1969).

91. Hass, G. (private communication, 1976).

92a. Herzberg, G., Elect. Spectra and Elect. Struct. Diatomic Mol., vol. I, 2nd ed., Van Nostrand Reinhold, NY (1950).

92b. ibid, pp 391.

92c. ibid, pp 285.

93. Knauss, H. P. and S. S. Ballard, Phys. Rev., 48, 796 (1935).

94. Ackerman, M. and F. Biaume, J. Mol. Spect., 35, 73 (1970).

95. McQuarrie, D. A., Statistical Mechanics, Harper and Row, N.Y., p 130 (1976).

96a. Herzberg, G., Infrared and Raman Spectra, Vol. II, Van Nostrand Co., N.Y., pp 278 (1945).

96b. ibid, pp. 80.

97a. Herzberg, G., Elect. Spect. and Elect. Struct. Poly. Mol., Vol. III, Van Nostrand Reinhold Co., N.Y., pp 128 (1966).

97b. ibid, pp 137.

97c. ibid, pp 183.

97d. ibid, pp 172-176.

97e. ibid, pp 451.

97f. ibid, pp 442.

97g. ibid, pp 134.

97h. ibid, pp 132.

98. Herzberg, G., Disc. Far. Soc., 35, 7 (1963).

99. Herzberg, G. and H. C. Longuet-Higgins, Disc. Far. Soc., 35, 77 (1963).

100. Blue, R. W., PhD Thesis, Univ. of Calif., Berkeley (1932).

101. Weast, R. C., Handbook of Chemistry and Physics, 50th ed., Chemical Rubber Co., Ohio, pp E117 (1970).

102. Coleman, C. D., W. R. Bozeman and N. F. Maggers, Table of Wave-numbers, Nat. Bur. of Stand., Monograph 3, US Govt. Printing Office, Washington, D.C. (1960)

103. Price, W. C. and D. M. Simpson, Proc. Roy. Soc. (London), A169, 501 (1939).

104a. Fortune, P. J., D. G. Hopper, B. J. Rosenberg, W. B. England, G. Das, A. C. Wahl and T. O. Tiernan, ARL TR-75-0202, vol. II, Air Force Systems Command, June 1975.

104b. Krauss, M., D. G. Hopper, P. J. Fortune, A. C. Wahl and T. O. Tiernan, ARL TR-75-0202, Vol. I, Air Force Systems Command, June 1975. Available from the National Technical Inform. Serv., Springfield, VA 22151.

105. Flicker, W. M., O. A. Mosher and A. Kuppermann, J. Chem. Phys., 69, 3910 (1978).

106. Chutjian, A. and G. A. Segal, J. Chem. Phys., 57, 3069 (1972).

107. Innes, K., J. Mol. Spect., 42, 575 (1972).

108. Liehr, A. D. and C. V. Ballhausen, Phys. Rev., 106, 1161 (1957).

109. Albrecht, A. C., J. Chem. Phys., 33, 156, 169 (1960).

110. Satten, R. A. and E. Y. Wong, J. Chem. Phys., 43, 3025 (1965).

111. Lohr, L. L., J. Chem. Phys., 50, 4596 (1968).

112. Lohr, L. L., , J. Amer. Chem. Soc., 92, 2210 (1970).

113. Walsh, S. D., J. Chem. Soc., 2266 (1953).

114. Bradley, H. N., A. D. Edwards and J. R. Gilbert, J. Chem. Soc. (A), 326 (1971).

115. Portions of this section were in paper presented, Selwyn, G. S. and H. S. Johnston, "Temperature Effect of Nitrous Oxide Vibronic Structuring between 172 and 190 nm", Atmospheric Spectroscopy Conference, Opt. Soc. Am., Keystone, CO, Sept. 1978, in proceedings.

116. Bevington, P. R., Data Reduction and Error Analysis for the Physical Sciences, McGraw Hill, N.Y., pp 119 (1969).

117. Gardner, P. J. and M. Kasha, J. Chem. Phys., 50, 1543 (1969).

118. Orlandi, G. and W. Siebrand, J. Chem. Phys., 58, 4513 (1973).

119. Orlandi, G., Chem. Phys. Lett., 15, 465 (1972).

120. Lawetz, V., G. Orlandi and W. Siebrand, J. Chem. Phys., 56, 4058 (1972).

121. Wittel, K. and S. P. McGlynn, Chem. Revs., 77, 745 (1977).

122. Henneker, W. H., A. P. Penner, W. Siebrand and M. Z. Zgierski, J. Chem. Phys., 69, 1884 (1978).

123. Gregory, A. R., W. H. Henneker, W. Siebrand and M. Z. Zgierski, J. Chem. Phys., 65, 2071 (1976).

124. Dixon, R. N., J. Physique, C5, 147 (1971).

125. Lohr, L. L., J. Amer. Chem. Soc., 92, 2210 (1970).

126. Davidson, J. A., H. I. Schiff, G. E. Streit, C. J. Howard and A. L. Schmeltekopf, J. Chem. Phys., 67, 5021 (1977).

127. see for example, Erying, H., J. Walter and G. E. Kimball, Quantum Chemistry, John Wiley, N. Y., pp 326 (1944).

128. Grosso, R. P. and T. K. McCubbin, Jr., J. Mol. Spect., 13, 240 (1964).

129. Pliva, J., J. Mol. Spect., 12, 360 (1951).

FIGURE CAPTIONS

Figure 1 Optical arrangement of spectrometer, mirror housing and gas cell.

Figure 2 ——— results of Bates and Hays[12]

oooooo this study

------ approximate Rayleigh scattering of N_2O

Figure 3 Result of Sponer and Bonner, microphotometer tracing; C, 5 atmospheres N_2O; B, 1.5 atmospheres N_2O; A, vacuum baseline.

Figure 4 Shorter wavelength absorption of N_2O.

oooo this study

—— Bates and Hays[12]

Figure 5 Rate of N_2O destruction, j, vs altitude, Km.

—— this study

---- Bates and Hays[12]

Figure 6 Schematic drawing of the stainless steel cell.

Figure 7 Cross section, $cm^2 \times 10^{21}$ vs wavelength, nm, for five temperatures,

—— this work, Δ data points of Zelikoff et al[10]. Note the discontinuity at 210 nm due to two different "room temperatures." The estimated standard deviation of wavelength (± 0.04 nm) and cross section (± 2%) is indicated by the cross on the 263 K curve. Resolution 0.7 nm.

Figure 8 Absorption spectrum of N_2O from Zelikoff et al[10]. Note the bulges superimposed on the absorption continuum.

Figure 9 High resolution spectrum in the structured region. Cross section, $cm^2 \times 10^{19}$, vs wavelength, nm. Temperature = 302 K. Pressure is 44 torr N_2O. Resolution 0.075 nm. Compare the structuring observed here with Figure 8.

Figure 10 Relative rotational populations vs J quantum number for three different temperatures of N_2O.

Figure 11 Relative vibrational state population vs temperature, K, for N_2O.

Figure 12 In the vibronically induced case on the right, transitions are allowed; otherwise all transitions are parity forbidden.

Figure 13 Vibronically induced transitions from ν_2'' (0 or 1) in the ground electronic state to upper level vibrations of ν_2 in the upper state.

Figure 14 Quartz cell design.

Figure 15 Absorption spectrum of N_2O at 11 different temperatures. Axes in this and all following figures are cross section (CSN) $\times 10^{-19}$ cm^2 vs wavenumber, cm^{-1}. Temperatures are 151, 182, 196, 223, 243, 268, 301, 303, 372, 423 and 485 K.

Figure 16 Densitometer tracing of plate exposure on the 3m spectrograph, in the region of structuring of N_2O.

Figure 17 Results of first order deconvolution into the (000) and (010) state spectra. Axes are cross section (CSN) $\times 10^{-19}$ cm^2 vs wavenumbers, cm^{-1}, corrected for vacuum.

Figure 18 Comparison of observed spectra (data points) with convoluted spectra (solid lines) for every other temperature studied.

Figure 19 Results of second order iteration: deconvolution into (000), (010) corrected for higher order vibrations, and the contribution of the higher order vibrations.

Figure 20a 20b Comparison of observed spectra (data points) with the convoluted spectra using the results of Figure 19 (solid lines) for each temperature.

Figure 21 Top curve, the absorption spectrum at 151 K; middle curve, an energy-weighted Gaussian curve empirically fit to the data.

Figure 22 Difference spectrum at 151 K, formed by subtracting the "background absorption" from the observed spectrum. Solid vertical lines denote selected peaks. Downward arrows indicate the progression of 970 cm^{-1}. The difference spectrum is shown at each temperature in Figures 22a-k.

Figure 23 Histogram of frequency of occurrence of energy spacings between selected peaks vs energy in wavenumbers. Shadings indicate contribution of individual temperatures. Energy separations are in bins of 20 cm^{-1}. See text for details.

Figure 24 Difference spectrum at 485 K superimposed on the difference spectrum at 151 K. Note the presence of alternate features in the cold spectrum and the presence of consecutive features in the hot spectrum. Scaling is the same for both cases.

Figure 25 Difference spectrum at 485 K with the calculated peak positions and assignments of ν_2 "(0) and ν_2" (1) superimposed. ω_2 is presumed to be an odd integer.

Figure 26 Potential energy diagram in the ν_3 coordinate taken from Figure 8 of reference 106. In this figure the repulsive curve has been relabeled $^1\Delta$ in agreement with references 104a, b and 14.

Figure 27 Figure 26 has been altered to reflect the avoided crossing proposed in C_s symmetry. In parentheses the $C_{\infty v}$ states are shown. Note that the $^1A'$ state from $^1\Delta$ is unperturbed. The Franck-Condon region is shown by the two vertical lines.

Figure 28a $N^{15}NO$ at 148, 213, 301, 372, 442 and 503 K.

Figure 28b ^{15}NNO at 148, 213, 301, 372, 442 and 503 K.

Figure 28c $^{15}N^{15}NO$ at 148, 213, 301, 372, 442 and 503 K.

Figure 28d NNO at 148, 213, 301, 372, 442 and 503 K.

Figure 29a Superposition of first order deconvolution, NNO/$N^{15}NO$ (red-shifted).

Figure 29b Superposition of first order deconvolution, NNO/^{15}NNO (red-shifted).

Figure 29c Superposition of first order deconvolution, NNO/$^{15}N^{15}NO$ (red-shifted).

Figure 29d Superposition of first order deconvolution, $N^{15}NO$/^{15}NNO (red-shifted).

Figure 29e Superposition of first order deconvolution, $N^{15}NO/^{15}N^{15}NO$ (red-shifted).

Figure 29f Superposition of first order deconvolution, $^{15}NNO/^{15}N^{15}NO$ (red-shifted).

Figure 30a Result of Second Order Deconvolution for $N^{15}NO$.

Figure 30b Result of Second Order Deconvolution for ^{15}NNO.

Figure 30c Result of Second Order Deconvolution for $^{15}N^{15}NO$.

Figure 30d Result of Second Order Deconvolution for Unlabeled NNO.

Figure 31 Ultraviolet Absorption Spectrum of Contaminated Sample of 95% ^{15}NNO with Reference Beam Containing Equal Pressure of 99% Sample of ^{15}NNO.

Errata

Page No.		
viii	line 16	$^1\Delta \leftarrow X\,^1\Sigma^+$
23	line 2	$j = \sum_i \sigma_i(\lambda_i) I(y,z,\lambda_i)\Phi(\lambda_i)$
57	last word	than
60	4th line from bottom	to be distinguished from Σ^+).
65	4th line from bottom	asymmetric
66	4th line	$^1\Sigma^- \leftarrow {}^1\Sigma^+$
76	Equation	$\sum_I Y(I) = \sum_I Y(I-1)/4 + Y(I)/2 + Y(I+1)/4$
78	line 10	H_2: Lyman α,
78	line 13	OCS
101	(Table 5) last column, line 3	967

This report was done with support from the Department of Energy. Any conclusions or opinions expressed in this report represent solely those of the author(s) and not necessarily those of The Regents of the University of California, the Lawrence Berkeley Laboratory or the Department of Energy.

Reference to a company or product name does not imply approval or recommendation of the product by the University of California or the U.S. Department of Energy to the exclusion of others that may be suitable.

TECHNICAL INFORMATION DEPARTMENT
LAWRENCE BERKELEY LABORATORY
UNIVERSITY OF CALIFORNIA
BERKELEY, CALIFORNIA 94720